WADC TECHNICAL REPORT 59-744
VOLUME VII

INVESTIGATION OF FEASIBILITY OF UTILIZING AVAILABLE HEAT RESISTANT MATERIALS FOR HYPERSONIC LEADING EDGE APPLICATIONS

Volume VII—Oxidation Resistance of Bare and Coated Molybdenum Alloy and Graphite

Donald J. Powers
John A. Dickson
Joseph C. Conti
Frank M. Anthony

Bell Aerosystems Company

DECEMBER 1960

WRIGHT AIR DEVELOPMENT DIVISION

NOTICES

When Government drawings, specifications, or other data are used for any purpose other than in connection with a definitely related Government procurement operation, the United States Government thereby incurs no responsibility nor any obligation whatsoever; and the fact that the Government may have formulated, furnished, or in any way supplied the said drawings, specifications, or other data, is not to be regarded by implication or otherwise as in any manner licensing the holder or any other person or corporation, or conveying any rights or permission to manufacture, use, or sell any patented invention that may in any way be related thereto.

☆

Qualified requesters may obtain copies of this report from the Armed Services Technical Information Agency, (ASTIA), Arlington Hall Station, Arlington 12, Virginia.

☆

This report has been released to the Office of Technical Services, U. S. Department of Commerce, Washington 25, D. C., for sale to the general public.

☆

Copies of WADD Technical Reports and Technical Notes should not be returned to the Wright Air Development Division unless return is required by security considerations, contractual obligations, or notice on a specific document.

WADC TECHNICAL REPORT 59-744
VOLUME VII

INVESTIGATION OF FEASIBILITY OF UTILIZING AVAILABLE HEAT RESISTANT MATERIALS FOR HYPERSONIC LEADING EDGE APPLICATIONS

Volume VII—Oxidation Resistance of Bare and Coated Molybdenum Alloy and Graphite

Donald J. Powers
John A. Dickson
Joseph C. Conti
Frank M. Anthony

Bell Aerosystems Company

DECEMBER 1960

Materials Central
Contract No. AF 33(616)-6034
Project Nos. 7350 & 1368

WRIGHT AIR DEVELOPMENT DIVISION
AIR RESEARCH AND DEVELOPMENT COMMAND
UNITED STATES AIR FORCE
WRIGHT-PATTERSON AIR FORCE BASE, OHIO

409 -- May 1961 -- 24-1111

FOREWORD

This report was prepared by Bell Aircraft Corporation under USAF Contract No. AF 33(616)-6034.
This contract was initiated under Materials Laboratory Project No. 7350, "Ceramic and Cermet Materials", Task No. 73500, "Ceramic and Cermet Materials Development", and Aircraft Laboratory Project No. 1368, "Construction Techniques and Application of New Materials", Task No. 13719, "Re-entry Structures." The work was administered under the combined direction of the Materials Laboratory and the Aircraft Laboratory, Directorate of Advanced Systems Technology, Wright Air Development Division, with Mr. J. J. Krochmal, Lt. J. Latva and Mr. C. J. Cosenza acting as project engineers.

This report covers work conducted from July 1958 to July 1960.

This particular report, Volume VII, is one of a series which, when combined, constitute the final technical report on this contract. In total, this technical report contains:

Volume I	Summary
Volume II	Analytical Methods and Design Studies
Volume III	Screening Test Results and Selection of Materials
Volume IV	Thermal Properties of Molybdenum Alloy and Graphite
Volume V	Mechanical Properties of Bare and Coated Molybdenum Alloy
Volume VI	Determination and Design Application of Mechanical Properties of Bare and Coated Graphite
Volume VII	Oxidation Resistance of Bare and Coated Molybdenum Alloy and Graphite
Volume VIII	Tests of Molybdenum and Graphite Leading Edge Components
Volume IX	Applicability to Future Weapon Systems

Volumes I through VIII are unclassified while Volume IX is classified Secret.

In an effort of the type described here, so many people are involved that it becomes difficult to give adequate credit to everyone. The excellent cooperation of the Langley Research Center of NASA is gratefully acknowledged, and in particular the efforts of Mr. K. L. Wadlin, Head, Thermal Protection Section, Special Projects Branch, Structures Research Division; Mr. J. N. Kotanchik, Chief, Special Projects Branch, Structures Research Division; and Mr. R. R. Heldenfels, Chief, Structures Research Division. Additional arc plasma testing was conducted by the Plasmadyne Corporation under the supervision of Miss Shirley L. Grindle. The in-house testing was conducted under the supervision of Mr. Harry A. Pearl and Mr. John M. Nowak. The authors wish to express their gratitude to E. A. Dolega and F. A. Merrihew for their contributions and to Miss Marie Zachary for her faithful and accurate typing of the manuscript.

ABSTRACT

The purpose of this contract was to investigate the feasibility of utilizing available heat resistant materials in the fabrication of leading edges for hypersonic boost-glide vehicles. This particular volume presents the results of oxidation resistance tests of bare and coated 0.5% titanium alloy of molybdenum and ATJ graphite. Chromalloy W-2 and Durak MG coatings were evaluated on the molybdenum alloy while the ATJ graphite was coated by the National Carbon Company's siliconizing process.

Tests were conducted in five different facilities including three arc plasma jets. Specimen temperatures ranged from 2000F to 3400F. Test times ranged from approximately 1 minute to 4 hours.

Both uncoated materials reacted exothermically under oxidizing conditions. Surface recession was the major result of the high temperature exposure in the oxidizing environments. The surface recession was quite predictable and uniform; it was a function of specimen temperature and environmental pressure.

A high degree of failures were encountered on all coated specimens. The failures were dependent on time and temperature but there was considerable scatter in the results. For the coated molybdenum specimens the edges and corners were most prone to failure. Failures of the siliconized ATJ specimens were more or less randomly located over the surface area.

PUBLICATION REVIEW

This report has been reviewed and approved.

FOR THE COMMANDER:

W. G. RAMKE
Chief, Ceramics and Graphite Branch
Metals and Ceramics Laboratory
Materials Central

TABLE OF CONTENTS

TABLE OF CONTENTS (CONTINUED)

LIST OF TABLES

LIST OF TABLES (CONTINUED)

LIST OF ILLUSTRATIONS

LIST OF ILLUSTRATIONS (CONTINUED)

LIST OF ILLUSTRATIONS (CONTINUED)

LIST OF ILLUSTRATIONS (CONTINUED)

LIST OF ILLUSTRATIONS (CONTINUED)

LIST OF ILLUSTRATIONS (CONTINUED)

LIST OF ILLUSTRATIONS (CONTINUED)

I. INTRODUCTION

The scope of this study encompassed the many considerations required for the investigation of the feasibility of using available heat resistant materials for the leading edges of hypersonic vehicles. The boost-glide vehicle concept formed the basis for this work with the flight parameter W/SC_L ranging from 100 to 400. Manned and unmanned, reusable and expendable flight vehicles were considered with emphasis being placed on manned, reusable systems. For purposes of this study maximum temperatures were to range from 2500°F to 3000°F. Ablation and cooling techniques were excluded.

The objective of the study was to determine the feasibility of employing available materials for the desired application. This goal was achieved by describing available materials to the degree required for design purposes, by establishing suitable design methods, by considering the peculiarities of materials in design, by indicating approximate operating temperatures and flight trajectories possible when various existing materials were used for leading edges, and finally, by actual testing of two typical leading edge designs. Many secondary benefits resulted from this study, including a better mutual understanding of the problems confronting material suppliers and airframe designers, a definition of the shortcomings of existing materials for this application which should form a foundation for future material development, an advancement in design technology for brittle materials used for structural applications, and a definition of critical parameters which would require laboratory simulation prior to actual usage of leading edge elements.

This study was conducted in four essentially concurrent phases; they involved design, materials evaluation, fabrication and component testing. The design phase investigated trajectories for hypersonic venicles to establish a range of typical flight and environmental conditions. Design criteria required to insure structural integrity of heat resistant leading edges were investigated and tentatively established. Methods for the determination of temperature gradients and thermal stresses were established and adapted to automatic computing equipment. The effects of leading edge geometry, both external and internal, on temperatures, temperature gradients and thermal stresses were studied as well as attachment details for metallic and non-metallic leading edges and the effects of various restraints upon thermal stresses. The design phase culminated with the design of two leading edges, one using metallic and the other using non-metallic material; both types were tested.

The materials evaluation phase began with a literature review to obtain known physical and mechanical characteristics of refractory metals and non-metals supplemented by contacts with material suppliers. A preliminary experimental evaluation of a number of promising metals, non-metals and coatings was conducted in order to supply data not found in the literature and to provide consistent sets of material property data for use in making meaningful

Note: Manuscript copy released by the authors October 1960 for publication as a WADC Technical Report

comparisons. Based upon the results of the preliminary evaluations and upon fabrication considerations the single most promising metal, .5% titanium alloy of molybdenum, the single most promising non-metal, siliconized ATJ graphite, and the two most promising coatings were evaluated in detail to provide the material property data required for design purposes. The detailed evaluation of the selected non-metallic material included an investigation to establish relationships required for the design of components using brittle materials.

The fabrication phase included the preparation of most of the test specimens as well as the production of the final leading edge designs. Test specimens were produced by techniques and process procedures similar to those expected to be required in the manufacture of final leading edge components. Restriction of the manufacturing process in such a manner may preclude attainment of the maximum material properties which could be achieved by employing the optimum fabrication techniques for small test bars. It did, however, provide a means of correlating test results and analytical predictions, since the material properties of the components should be approximately the same as those determined from the test specimens. For example, ceramic materials generally exhibit higher thermal conductivity and higher strength when fabricating by hot pressing than when fabricated from slip casting. While simple test bars can be made by hot pressing it may be necessary to fabricate more complex shapes by slip casting and test results on hot pressed bars are of little or no value in defining the characteristics of the slip cast component.

The component testing phase included several items of study. Typical attachments for brittle components were tested to aid in the selection of suitable designs. Finally a metallic leading edge design and a non-metallic design were tested under partially simulated conditions.

In order to achieve maximum efficiency, of both time and cost, and to integrate more closely the materials and design problems, extensive subcontracting was employed during this study. All specimen and component fabrication was done by subcontractors having extensive experience with the materials and fabrication procedures required. Existing testing capabilities of organizations throughout the country were utilized to the fullest possible extent.

This particular volume presents the results of testing to determine the oxidation resistance of the more promising materials for hypersonic leading edge applications. The materials investigated included the 0.5% Ti molybdenum alloy in the bare condition and as protected by Chromalloy W-2 coating and by Chromizing Durak MG coating, and ATJ graphite in the bare condition and as protected by a siliconized coating applied by the National Carbon Company. These materials were selected as the result of preliminary evaluations reported in Volume III.

Three basic types of tests were conducted, those in flowing preheated air, those in an oxy-acetylene furnace, and those in arc plasma jets. The first two types of tests permitted evaluation of the materials for long periods of time. These tests were conducted at Bell Aircraft Corporation and are discussed in Sections II and III. During the flowing air testing it was not possible to evaluate the effects of reduced pressure or of the dissociated gas species that would be encountered during actual flight. Arc plasma tests were conducted,

therefore, wherein the anticipated environmental conditions expected in flight were more closely simulated at the expense of reduced test duration.

The majority of the arc plasma testing was conducted at the Langley Research Center of NASA in Arc Jets No. 10 and No. 20, which are operated by the Thermal Protection Section, Special Projects Branch, Structures Research Division. Operating times were limited by the equipment capability under the desired test conditions. Tests of five and ten minute durations were conducted at atmospheric pressure while tests at approximately 2 psia were run for slightly more than one minute. Additional arc plasma testing was conducted by the Plasmadyne Corporation, on a subcontract basis, for periods of approximately five minutes at a static pressure of about .70 psia. The arc plasma portion of the program is presented in Section IV.

Section V compares the results obtained from the tests in flowing air and in the arc plasmas. The conclusions reached as the result of the testing conducted and recommendations for future work are discussed in Section VI. And finally, the materials tested are described in Appendix I.

II. FLOWING AIR TESTS AT 2000F AND 2450F

A. DESCRIPTION OF EQUIPMENT

The equipment used for the oxidation tests at temperatures of 2000F and 2450F consisted of a test furnace and a preheat furnace, both heated by silicon carbide elements, flow meter, pressure gage, flow regulator, Brown potentiometer pyrometer, and the power supplies for the furnace elements. A zirconia nozzle was used to hold the test specimen in place and to direct the air flow over the specimen surfaces. Figure 1 is a schematic diagram of the assembled equipment. Figures 2, 3, and 4 are photographos of the equipment.

The test furnace used as the primary heating source for the flowing air contained a 2-3/4" diameter by 4' long alumina tube, filled with alumina rods and balls to improve heat transfer, sealed in the furnace. The zirconia specimen nozzle was fastened to the outlet of this tube. The preheat furnace also contained an alumina tube, 2-3/4" diameter by 4' long, filled with alumina rods and balls. This unit was used to preheat the flowing air which was then introduced into the main heating unit.

The regulating and measurement equipment, such as the flow meter, pressure gage, and flow regulator were positioned downstream of the preheater furnace, so that room temperature air was being metered and measured. Flow conditions were essentially the same as those employed previously, Section G of Volume III. However, during the present test series a higher mass velocity was employed as the upper limit of this variable, 5000 #/ft^{2}hr rather than 4000 #/ft^{2}hr. Reasons for the flow conditions are discussed in Appendix I of Volume III which also presents test Reynold's numbers. Platinum-platinum 10% rhodium thermocouples were used with the Brown potentiometer pyrometer to measure specimen temperatures.

The specimen geometry employed during this test series is shown in Figure 111. Because of its larger size, more representative data should be obtained than was available previously regarding oxidation of uncoated materials and oxidation resistance of coated materials.

B. TEST PROCEDURE

1. Identification of Specimens

The uncoated 0.5% Ti molybdenum alloy specimens, the uncoated ATJ graphite specimens, and the coated 0.5% Ti molybdenum alloy specimens were assigned Bell identification numbers to facilitate reference to individual specimens. The National Carbon Company's identification numbers were used for the siliconized ATJ graphite specimens. Bell identification numbers were assigned to all specimens in the artificially damaged materials part of the program.

2. Uncoated Materials

The uncoated 0.5% Ti molybdenum alloy and ATJ graphite specimens were tested in accordance with the schedules given in Table 1. On the basis of initial tests, the exposure times were slightly altered. These instances have been noted in the table.

Alumina pins were bonded in the end holes of the specimen to hold the specimen in place and to align it properly in the specimen nozzle. The platinum-platinum 10% rhodium thermocouple which measured specimen temperature was not bonded in the specimen, but was inserted after the specimen was installed in the nozzle. Thickness measurements were made on the untested bare materials along a line midway between the front and rear edges of the specimen. This line was chosen to give a nominal loss in thickness due to oxidation. Each specimen was weighed before testing with the end pins inserted.

Before testing, and instrumented coated specimen was placed in the nozzle to measure the test zone temperature. Using this data, the temperature increase due to exothermic reaction could be determined. The specimen was inserted into the nozzle with a pair of tongs, and the thermocouple was placed in the center thermocouple hole. Since no bonding agent could be used, the thermocouple was held in place by supporting its insulating tubing on ceramic resting points. Recording of exposure time commenced as soon as the specimen entered the specimen nozzle. Temperature readings were taken at regular intervals. After testing, the specimens were measured and their weights taken with the end pins in place.

3. Coated Materials

The coated specimens were tested in accordance with the schedule shown in Table 2. Alumina pins were bonded in the end holes of the specimen to hold the specimen in place and to align it properly in the nozzle. The platinum-platinum 10% rhodium thermocouples were bonded in the thermocouple holes. An alumina-silica cement (QF-180, Carborundum Company, Niagara Falls, New York) was used for the bonding. The thermocouple wires were electrically insulated with high purity alumina tubing.

The hot air flow was achieved and stabilized before the introduction of the test specimen. This flow was maintained during insertion of the specimen. Temperature readings were taken at 15-minute intervals during the test period.

The specimens were withdrawn from the nozzle at one-hour intervals and allowed to cool to 300F or lower. This procedure introduced a periodic thermal shock. The hot specimens were observed for dark spots which might indicate a coating failure and for effects due to thermal shock. The cooled specimens were observed for failures, color changes, and other changes in coating appearance.

Upon reaching a temperature of 300F or lower, the siliconized ATJ graphite specimens were lightly probed with a pick-like instrument to check for coating failures. Since a coating failure resulted in an undermining action as the graphite oxidized, the probing, which would break through the thin coating over the void, would quickly determine the integrity of each specimen, but would not damage the siliconized coating when no substrate oxidation had occurred.

The coated molybdenum alloy specimens were not probed during the test since failure areas were easily located by visual examination (dark spots, presence of a hole and molybdic oxide crystals) and the probe was more likely to damage the relatively thinner protective coating. After completion of testing, the coated molybdenum alloy specimens were lightly probed.

If failures were found before the four-hour test period was completed, the specimen was tested for another hour and inspected to determine the extent of deterioration of the failure point. Inspection was also made for additional failures. If the failure area had not oxidized too severely, the test was allowed to continue until the four-hour period was completed. When the oxidative attack appeared to be extensive, the testing of that specimen was terminated. During the test of the coated molybdenum alloy specimens, the air exit was observed for white smoke which would indicate a coating failure.

4. Artificially Damaged Specimens

The artificially damaged specimens were tested in accordance with the schedule shown in Table 3. Siliconized ATJ graphite, W-2 coated 0.5% Ti molybdenum alloy, and Durak MG coated 0.5% Ti molybdenum alloy specimens were intentionally damaged and were then tested to determine the extent to which the failure points would deteriorate when exposed to flowing air at high temperatures. The types of damage were designed to artificially simulate the effect of meteoroid impacts. Two hole sizes were selected on the basis of the discussions of Appendix II of Volume II. One was 0.07 inch in diameter and 0.04 inch deep, and the other was 0.01 inch in diameter and 0.007 inch deep. The 0.07 inch diameter hole was made with a #50 drill, while a standard Rockwell machine using a Braille tip with the 150 Kg load was used for the 0.01 inch diameter indentation. A crater of each size was made in the nose and one of each size on the skirt of each specimen. The craters were spaced so that the failure areas would not join during four hours of testing. Since the oxidation products from the nose areas would pass over the holes in the side of the specimen, an extra crater, either 0.07 inch diameter or 0.01 inch diameter, was made in the undamaged skirt of several specimens to ascertain the effects of these oxidation products. It might be expected that the gaseous products flowing over the skirt holes could either accelerate deterioration of the hole by their corrosiveness or furnish oxidation protection to the holes by displacement of the air flow. Figure 5 shows the location of the damaged areas on the test specimens including the location of the extra holes. Temperature measurements were taken at 15-minute intervals. The specimens were removed for visual examination at one-hour intervals. X-ray inspections were made before testing and at the completion of four hours of testing. No probing of the oxidized areas was performed until after the final X-ray inspection on the tested specimens. Measurements were taken of the hole diameter and hole depth for the damaged areas of all specimens after testing.

C. DISCUSSION OF TEST RESULTS

1. General

The results of the tests on uncoated materials indicate good repeatability in test results and a high degree of accuracy in equipment control. The test results given in Tables 4 and 5 show good continuity when specimens tested under the same conditions are compared. Of special significance where testing continuity is concerned are the columns "Weight Loss (gm/min.)". The data in these columns are direct measurements. No factors have been introduced which would multiply small errors into large errors. The "Weight Loss (gm/min.)" columns indicate good testing repeatability except for the 2000F, 5000 lbs/ ft^2-hr test (Specimens UM-1 and UM-8 in Table 4). In this case it was found that Specimen UM-8 was not fully inserted in the specimen nozzle during testing, resulting in lower temperature exposure.

The temperatures given in the "Average Specimen Temperature" columns are not of the reliability desired due to the method of thermocouple measurement. The thermocouples were not cemented in the thermocouple holes but were inserted in the holes and supported by resting their insulation sleeving on ceramic fixtures. Cement was not used since accurate weight data was required. During testing the forward wall of the thermocouple hole oxidized and in some cases the thermocouple may have lost contact with the specimen. This would result in an insulating layer of air around the thermocouple bead and a resultant recording of lower temperatures. However, since the temperature of the flowing air was checked with a coated control specimen before each series of tests, the uncoated oxidation specimens were exposed to the correct test temperature as long as the specimens were fully inserted in the nozzle. Regardless of the small errors introduced by the manner in which the thermocouples were installed, the oxidation results obtained are far more accurate than those obtained without actual measurement of specimen temperature.

The loss rate data for the uncoated materials calculated on weight loss data gives an average loss of material based on the entire surface area of each specimen. This computation includes the areas of excessive material loss (i.e. the nose areas). The direct measurements at midpoint of the specimens give an accurate loss per side for each specimen at the point measured but do not indicate variances over the flat surface, nose losses, or losses on the back which vary from the midpoint figure. The losses at the nose and the back were measured using the holes for the support pins as reference points. The losses at the nose areas represent the greatest encountered on each specimen. The losses at the back areas were about the same as for the sides.

All data for material loss in thickness are given in mils per hour. The actual duration of each test on the uncoated materials was from 3 minutes to 17 minutes. For computation of rate losses, the heat-up time was subtracted from the test time. The heat-up time was of the order of 1 minute to 1 minute 20 seconds. Therefore, a large factor was used in computing the losses on an hourly basis. Small errors in measurement due to irregularity in the specimen surfaces and difficulty in accurate comparison of reference holes result in large loss rate discrepancies when the several minutes of exposure is increased to an hourly rate. Additional errors are introduced by small variations in test procedure, such as difficulty in insertion of the specimen into the nozzle.

2. Uncoated 0.5% Ti Molybdenum Alloy

Table 4 presents weight loss data, thickness change data, and test condition data for the uncoated 0.5% Ti molybdenum alloy. The thickness loss rate is given in mils per hour per side. The loss rate data was determined in three ways: (1) derivation from weight loss data, (2) measurements at a line across the specimen midway between the nose and the back, (3) measurement from the support pins to the nose and to the back edges. The data from each method is given in the table. Figure 6 shows the uncoated 0.5% Ti molybdenum alloy specimens before testing and after testing at 2000F in flowing air. Figure 7 shows the uncoated specimens before testing and after testing at 2450F in flowing air. During oxidation the metal loss was greatest at the nose and varied somewhat over the remainder of the specimen; however, the specimens retained their original wedge configuration. The oxidation reaction of molybdenum is exothermic; therefore, the specimen temperature during exposure is considerably higher than the initial test zone temperature (see Table 4). The actual specimen temperature was used for all computations.

The oxidation data for the uncoated 0.5% Ti molybdenum alloy fit the Arrhenius rate equation

$$k = Ae^{-\frac{Q}{RT}}$$

where

- k = Loss rate of material, mils/hr/side, experimentally determined
- A = Constant, determined by the value of k
- e = Base of natural logarithm
- Q = Activation energy (cal/mol)
- R = Gas constant (cal/mol/K)
- T = Absolute temperature (K)

That is, the plots of log k vs. 1/T for the nose and side surfaces are straight lines. The plots of log k vs. 1/T for the nose and side surfaces are given in Figure 8. Figure 9 presents the plots of material loss rate vs. temperature. The plots in Figure 8 are described by the following Arrhenius rate equations with the constants determined.

$$\text{Nose: } k = 57 \times 10^4 \, e^{\frac{-23,860}{1.986T}}, \text{ mils/hr}$$

$$\text{Side: } k = 123 \times 10^4 \, e^{\frac{-29,500}{1.986T}}, \text{ mils/hr/side}$$

The values for Q are within the expected accuracy range (see page 222, Volume III). The different values for A in the equation above are due to the material loss rates at the nose and side and, also, to the variance in the values of Q.

3. Uncoated ATJ Graphite

Table 5 presents weight loss data, thickness change data, and test condition data for the uncoated ATJ graphite. The thickness loss rate is given in mils per hour per side and was determined in the same manner as is described for the uncoated molybdenum alloy. During oxidation the graphite loss at the nose was much greater than at the other surfaces. However, the specimens retained their wedge configuration. The oxidation reaction of graphite is exothermic. Therefore, the specimen temperature during the test exposure was considerably higher than the initial test zone temperature.

Figure 10 shows the uncoated ATJ graphite specimens before testing and after testing at 2000F in flowing air. Figure 11 shows the uncoated specimens before testing and after testing at 2450F in flowing air.

The oxidation data for the uncoated ATJ graphite fit the Arrhenius rate equation,

$$k = Ae^{-\frac{Q}{RT}}$$

That is, the plots of log k vs. 1/T for the nose and side surfaces are straight lines. Figure 12 shows the plots of log k vs. 1/T for the nose and side surfaces. Figures 13 and 14 are plots of material loss rate vs. temperature. The plots in Figure 12 are described by the following Arrhenius rate equations with the constants determined.

$$\text{Nose: } k = 176 \times 10^5 \, e^{\frac{-30,466}{1.986T}}, \text{ mils/hr}$$

$$\text{Side: } k = 64 \times 10^5 \, e^{\frac{-32,260}{1.986T}}, \text{ mils/hr/side}$$

4. W-2 Coated 0.5% Ti Molybdenum Alloy

Table 6 presents the test results and test condition data for the W-2 coated 0.5% Ti molybdenum alloy. Figure 15 shows a typical W-2 coated molybdenum alloy specimen before testing. Figures 16 and 17 show the W-2 coated specimens after testing at 2000F and 2450F. All three W-2 coated specimens withstood the 2000F test program without failure.

At 2450F, two of the six specimens tested, WM-5 and WM-9, showed failures. The WM-9 specimen, tested at a mass velocity of 500 lbs/ft^2-hr, developed one edge failure at a back corner during the third hour of testing. The test was

continued for the full four hours with no further failures. The one failure area did not show any signs of self-healing. The WM-5 specimen, tested at a mass velocity of 5000 lbs/ft^2-hr, developed one edge failure at a back corner during the first hour of testing. The specimen was tested for one additional hour, and the test was terminated. The failure area continued to oxidize during the second hour of exposure. No additional failures occurred. No smoking was observed during the exposure of specimens WM-5 and WM-9; however, a small amount of smoking was visible after the specimens were removed from the furnace and before they cooled. While the specimens were red hot, the failure areas were dark. A white crystalline deposit formed around the failure area of each specimen after cooling. In both cases the penetration of the coating was visually apparent. The coating layer over the failure void was very fragile and broke off with the slightest handling.

The W-2 coating provided excellent protection to the flat surfaces of the test specimens. However, as shown by the failures which did occur, the coating on edges and corners is questionable. It is possible that if the edges of the molybdenum alloy specimens had been rounded off to a larger radius the failures might not have occurred. The drawings required radii of 0.020 to 0.030 inch for all edges on the specimens. However, difficulties in attaining complete coating integrity on edges of these radii still exist. Consideration should be given to increased radius requirements.

The appearance of the W-2 coated 0.5% Ti molybdenum alloy before testing was a dull brownish-grey to a dull greenish-grey. There were often mottled areas over the surfaces of the specimens. As the specimens were tested, the nose areas gradually became shiny, with the color of the specimen darkening to a dark grey. At the completion of four hours of testing, the specimens exposed to a 2000F test temperature had a grey, shiny nose with dull, dark brownish-grey side surfaces. The specimens tested at 2400F attained a shiny grey appearance over their entire surfaces.

5. Durak MG Coated 0.5% Ti Molybdenum Alloy

Table 7 presents the test results and test condition data for the Durak MG coated 0.5% Ti molybdenum alloy. Figure 15 shows a typical Durak MG coated molybdenum alloy specimen before testing. Figures 18 and 19 show the Durak MG coated specimens after testing at 2000F and 2450F. The three specimens tested at 2000F failed. Specimens DM-C, tested at 500 lbs/ft^2-hr, and DM-A, tested at 5000 lbs/ft^2-hr, each developed one failure. Specimen DM-8, tested at 1500 lbs/ft^2-hr, developed three failures. As shown in Figures 18 and 19, all failures developed at the edges of the specimens.

At test temperatures of 2450F, four specimens failed while two completed the testing without failure. Both specimens tested at 5000 lbs/ft^2-hr, DM-D and DM-E, developed failures while one specimen tested at 500 lbs/ft^2-hr, DM-H, and one tested at 1500 lbs/ft^2-hr, DM-F, failed.

In all cases, except for specimen DM-A, the failed specimens were tested for the full four hours. The testing of specimen DM-A was terminated after the third hour. The Durak MG coating provided excellent protection to the

flat surfaces; however, the coating tends to be undependable on edges where relatively sharp corners might lower the integrity of the coating. As was discussed in Section II.C, larger radii at the edges might improve coating dependability.

No smoking was observed during the exposure of any of the specimens. Even when failed specimens were further tested, the amount of smoke produced was not enough to be visible at the test nozzle entrance. However, upon removal of the specimens from the furnace, the areas of failure produced visible smoke.

The Durak MG coated 0.5% Ti molybdenum alloy specimens were a dull grey-black before testing. All specimens became black during testing. The specimens tested at 2000F developed a shiny appearance at the nose area, while the specimens tested at 2400F became shiny over their entire surfaces.

6. Siliconized ATJ Graphite

Table 8 presents the test results and test condition data for the siliconized ATJ graphite. Figure 15 shows a typical siliconized ATJ graphite specimen before testing. Figures 20 and 21 show the specimens after testing at 2000F and 2450F.

At 2000F test temperature, seven specimens failed while one specimen, C-9, completed the test without failure. Multiple failures were developed by six of the seven failed specimens. One failed specimen, I-12, experienced only one failure. In most cases the majority of the failures occurred on one side of the test specimen. In each case this side is shown in the photographs. For example, specimen B-8 has numerous failure points on the side shown in Figure 20, yet on the opposite side only two small failure areas occurred. Specimen J-5, in Figure 21, has seven failure areas showing, while there are no failures on the opposite side.

At 2450F test temperature, three specimens failed while five specimens completed the test without failure (see Table 8). As with the 2000F test specimens, most of the failures occurred on the flat surfaces of the specimen with the majority of the failures on one side.

The preponderance of failures on one surface of a specimen may be due to variations in coating thickness over a specimen's entire surface, as was observed on mechanical property test specimens (see Volume VI). Even in cases where the weight increase of each of several specimens due to coating is the same, the variations in coating thickness may occur since localized areas may experience a very heavy coating buildup while other areas acquire a very thin covering. Orientation of the specimens during the siliconizing operation may also be a possibly important variable. However, this aspect could not be checked since orientation during processing was not recorded.

The National Carbon Company classified the siliconized ATJ graphite specimens in accordance with structural integrity based on X-ray examination (see Appendix I. The classification is as follows:

Grade A - Nearly perfect ATJ structure.

Grade B - Fair structure with minor specks, voids, or density gradients.

Grade C - Poor (mottled) structure - high density inclusions finely divided into a low density matrix.

Table 9 gives a tabulation of the siliconized ATJ graphite specimens with their appropriate National Carbon classifications and the results of the oxidation tests. This table also presents the weight gain due to coating application for each specimen.

There appears to be a correlation between the National Carbon X-ray classification of specimens and the coating failure of the specimens. The specimens with more uniform structure and density, and with less voids (Grade A, B) tended to be more resistant to oxidative failure. Six of seven Grade C specimens failed during testing while only four of nine Grade AB specimens failed. However, the small number of specimens and the failure of four of the higher grade specimens renders this part of the study inconclusive. There was no apparent correlation between weight increase due to the coating process and failure of the siliconized ATJ graphite specimens. Since all specimens were coated by the National Carbon Company under the same coating run, consideration need not be given to the particular coating run as a variable in this program.

7. Artificially Damaged Specimens - General

The damaged test specimens were not instrumented to accurately measure exothermic reactions. However, the extra holes placed in several specimens were located in close proximity to the thermocouple hole. Temperature measurements taken for these specimens indicated no discernible temperature increase due to exothermic reactions. It is probable that the exothermic reaction was very small due to the small damaged areas, and that any heat given off by the reaction was spread throughout the test specimen resulting in only a small temperature increase.

The oxidation of the damaged areas produced symmetrical, hemispherical shaped depressions. The normal failure areas encountered during the coating testing were of random shape.

Failures due to meteorite-type damage produced greater deterioration than the failures due to coating imperfections. This was probably due to the greater hole size and deeper penetration in the intentionally damaged specimens. The areas damaged with the #50 drill sustained greater oxidative deterioration during testing than the areas damaged by Rockwell penetration. However, the dimensions of the #50 drill damage areas before and after testing were not proportional to the dimensions of the Rockwell damage areas before and after

testing under the same test conditions. For example, the diameters of the diameters of the damaged areas before testing were 0.07 inch for the drill and 0.01 inch for the Rockwell. The diameters of the damaged areas of a typical damaged specimen, W-2 coated specimen E, after testing were 0.28 inch for the drilled damage and 0.22 inch for the Rockwell damage. The resultant proportion of initial and final diameters is off by a factor of 550%. This lack of proportionality exists for all damaged specimens tested. No correlation of net diameter change or depth change was evident in the test data.

The loss rate of material in the damaged specimens during testing is much less than the loss rate of material experienced by the uncoated materials during testing. Since both the damaged coated 0.5% Ti molybdenum alloy and damaged siliconized ATJ graphite experienced a similar loss of material (see Tables 10, 11, and 12), the oxidation losses of a typical damaged specimen can be used for a comparison of rate losses with uncoated materials. The depth of the side surface damage of a typical damaged specimen, siliconized ATJ graphite specimen #3, after testing was 0.19 inch for the drilled damage and 0.12 inch for the Rockwell damage over a test period of four hours. This gives a loss rate of 48 mils/hour (drill) and 30 mils/hour (Rockwell).

The uncoated 0.5% Ti molybdenum alloy specimens had side surface (midpoint) rate losses of material of from 96 mils/hour to 322 mils/hour. The uncoated ATJ graphite specimens had side surface (midpoint) rate losses of from 135 mils/hour to 620 mils/hour. It is apparent that the damaged areas of the damaged specimens experienced a much lower rate of material loss than the uncoated materials.

The differences in material losses between damaged specimens and uncoated specimensis even more pronounced at the nose areas. The nose losses of a typical damaged specimen, W-2 coated 0.5% Ti molybdenum alloy specimen D, are 0.22 inch for the drilled damage and 0.12 inch for the Rockwell damage. This gives a rate loss of 55 mils/hour (drill) and 30 mils/hour (Rockwell). The uncoated 0.5% Ti molybdenum alloy specimens had nose losses of from 197 mils/hour to 672 mils/hour. The uncoated ATJ graphite specimens had nose losses of from 750 mils/hour to 2820 mils/hour.

8. Artificially Damaged W-2 Coated 0.5% Ti Molybdenum Alloy

Table 10 presents the dimensions of the damages areas in the W-2 coated specimens after testing. Figure 22 presents graphical plots of the dimensions versus specimen temperature.

Figure 23 is a photograph showing side views of typical W-2 coated molybdenum specimens after testing at 2000F and 2450F in flowing air. A typical specimen which was tested but not probed is shown in this figure. The W-2 coating shell over the voids was very fragile and often collapsed upon slight impact or jarring of the specimen.

Figures 24 and 25 present oblique views of all of the damaged W-2 coated 0.5% Ti molybdenum alloy specimens tested. These views give a more comprehensive picture of the appearance of the specimens and the extent of damage

encountered. The coating over the voids was removed from all specimens prior to taking the photographs. The small holes visible at the bottom of some of the voids were caused by the oxidation partly uncovering the sides of the thermocouple holes.

9. Artificially Damaged Durak MG Coated 0.5% Ti Molybdenum Alloy

Table 11 presents the dimensions of the damaged areas in the Durak MG coated specimens after testing. Figure 26 presents plots of the dimensions versus specimen temperature.

The typical W-2 coated specimens shown in Figure 23 are representative of the side views of the damaged Durak MG coated specimens after testing. Figure 27 presents oblique views of all of the damaged Durak MG coated 0.5% Ti molybdenum alloy specimens. Some edge failures occurred during the testing as indicated on the photograph. The Durak MG coating is similar to the W-2 coating in its fragility when the base molybdenum alloy has oxidized away.

10. Artificially Damaged Siliconized ATJ Graphite

Table 12 presents the dimensions of the damaged areas in the siliconized ATJ graphite specimens after testing. Figure 28 presents plots of the dimensions versus specimen temperature.

Figure 29 is a photograph of typical damaged siliconized ATJ graphite specimens both before and after testing. A specimen which was tested but not probed for coating removal is also shown. This specimen is typical of the damaged specimens after testing with the coating still covering the void areas. The siliconized coating on the ATJ graphite specimens is thicker and stronger over void areas than the W-2 and Durak MG coatings on the 0.5% Ti molybdenum alloy.

Figures 30 and 31 present oblique views of all of the damaged siliconized ATJ graphite specimens tested. These views give a comprehensive picture of the damaged areas. The coating over the voids was removed before taking the photographs.

11. Extra Hole Damage in Coated Materials

Figure 32 shows typical extra hole damage after testing in damaged siliconized ATJ graphite and W-2 coated 0.5% Ti molybdenum alloy specimens. In each case the holes are marked as to type of damage so that proper comparison between regular holes and the extra holes can be made. Tables 10, 11, and 12 give the dimensions of the extra holes after testing. The extra holes experienced approximately the same extent of damage as the corresponding regular holes in the flat surfaces. This was true for all the extra holes tested. Therefore, it is concluded that in this test program the sweep of contaminant gases from the damaged areas in the nose had little or no effect on the deterioration rate of the damaged areas of the flat surfaces.

12. X-ray Inspection of Damaged Materials

Figure 33 shows X-ray photographs of typical damaged siliconized ATJ graphite and W-2 coated 0.5% Ti molybdenum alloy before testing. Figure 33 also shows X-ray photographs of typical damaged siliconized ATJ graphite and W-2 coated 0.5% Ti molybdenum alloy after testing. Photographs of Durak MG coated molybdenum specimens were omitted since their appearance is the same as that of the W-2 coated specimens. The drilled damage areas on the side surfaces of all the specimens are readily discernible both before and after testing. The drilled areas in the nose are very clear after testing; however, these areas are not very distinct before testing. The Rockwell damage is nearly invisible at all locations before testing. When the Rockwell indentation areas are known, the marks can sometimes be found on the X-ray film, but small failures whose existance is unknown would be difficult to identify. After testing, the Rockwell damage areas were usually visible on the X-ray film. However, in some of the X-ray photographs even these areas are not clearly visible. The X-ray films were exposed as follows:

Coated 0.5% Ti Molybdenum Alloy

Side Surfaces: 218 KV, 30 MAM, at a distance of 36 inches, AA film
Nose: 180 KV, 20 MAM, at a distance of 36 inches, aa film

Siliconized ATJ Graphite

40 KV, 8 MAM, at a distance of 36 inches, AA film

These settings were selected after a brief study of the X-ray quality as influenced by the process parameters.

The value of X-ray inspection for defects in coated materials must be investigated further. Coating failures which are discernible on X-ray plates can be located visually and, in some cases, failures which were readily apparent to the naked eye were not visible on X-ray plates. At the present time probing and visual inspection offer the most certain procedures to detect actual failures.

TABLE 1

TEST SCHEDULE FOR UNCOATED 0.5% TI MOLYBDENUM ALLOY

AND UNCOATED ATJ GRAPHITE

Mass Velocity (lbs/ft^2-hr)	Test Temperature °F	Exposure Period (Minutes)	Specimen
	Uncoated 0.5% Ti Molybdenum Alloy		
500	2000	15(1)	UM-2, UM-3
500	2450	15	UM-11, UM-12, UM-13
1500	2000	15	UM-9, UM-10
1500	2450	10	UM-6, UM-7
5000	2000	10(2)	UM-1, UM-8
5000	2450	8	UM-4, UM-5
	Uncoated ATJ Graphite		
500	2000	7	UG-8, UG-10
500	2450	5	UG-12, UG-13
1500	2000	5(3)	UG-1, UG-6
1500	2450	4	UG-9, UG-11
5000	2000	4	UG-2, UG-4
5000	2450	3	UG-5, UG-7

Note (1): Specimen UM-3 was tested for 17 minutes

(2): Specimen UM-1 was tested for 15 minutes

(3): Specimen UG-1 was tested for 18 minutes

TABLE 2

TEST SCHEDULE FOR COATED TEST SPECIMENS

Exposure consisted of four, one-hour cycles or failure, whichever was first

Material	Mass Velocity (lbs/ft^2-hr)	Test Temperature (F)	Test Specimens
W-2 coated 0.5% Ti Molybdenum Alloy	500	2000	WM-3
	500	2450	WM-8, WM-9
	1500	2000	WM-1
	1500	2450	WM-6, WM-7
	5000	2000	WM-2
	5000	2450	WM-4, WM-5
Durak MG coated 0.5% Ti Molybdenum Alloy	500	2000	DM-C
	500	2450	DM-H, DM-I
	1500	2000	DM-B
	1500	2450	DM-F, DM-G
	5000	2000	DM-A
	5000	2450	DM-D, DM-E
Siliconized ATJ Graphite	500	2000	C-9, I-12, J-5
	500	2450	F-6, N-6, G-4
	1500	2000	B-8, F-10, G-11
	1500	2450	K-4, K-5, I-2
	5000	2000	D-11, N-5
	5000	2450	C-2, C-12

TABLE 3

TEST SCHEDULE FOR ARTIFICIALLY DAMAGED SPECIMENS

Material	Mass Velocity (lbs/ft^2-hr)	Test Temperature (F)	Specimens
W-2 coated 0.5% Ti Molybdenum Alloy	500	2000	G, H
	500	2450	A, B
	5000	2000	E, F
	5000	2450	C, D
Durak MG coated 0.5% Ti Molybdenum Alloy	500	2000	III-C
	500	2450	I-A
	5000	2450	II-B
Siliconized ATJ Graphite	500	2000	7, 8
	500	2450	1, 2
	5000	2000	5, 6
	5000	2450	3, 4

TABLE 4

UNCOATED 0.5% TI MOLYBDENUM ALLOY

Specimen	Test Temp. (F)	Test Zone Temp. (F)	Average Specimen Temp. (F)	Mass Velocity (#/ft²-hr)	Test Time (Min.)	Time at Temp. (Min.)	Initial Weight (gms)	Final Weight (gms)	Weight Loss(1) (gm/min.)	Initial Thickness Midpoint (Inch)	Final Thickness Midpoint (Inch)	Rate of Loss(1) per Side-Midpoint (mils/hr)	Rate of Loss(1) per Side Based on Weight (mils/hr)	Rate of(1) Loss-Nose (mils/hr)	Rate of(1) Loss-Back Surface (mils/hr)
UM-2	2000	1940	2195	500	15	13.8	141.1550	103.5883	2.7421	.356	.296	131	140	241	88
UM-3	2000	1940	2377	500	17	15.8	141.6554	96.1864	2.8961	.359	.280	149	148	267	153
UM-9	2000	2035	2333	1500	15	13.8	140.9516	109.2267	2.3157	.356	.312	97	119	197	175
UM-10	2000	2025	2325	1500	15	13.8	141.3737	110.0898	2.2835	.357	.310	105	117	241	88
UM-13	2000	2035	2329	1500	15	13.8	139.5417	106.5855	2.4056	.355	.307	105	123	311	88
UM-1	2000	2000	2523	5000	15	13.8	141.5270	72.7898	5.0173	.358	.224	293	257	504	219
UM-8(2)	2000	2000	2326	5000	10	8.8	141.1129	114.9813	3.0036	.356	.316	138	154	414	207
UM-11	2450	2225	2324	500	15	13.8	140.5986	109.5298	2.2678	.355	.308	105	116	241	88
UM-12	2450	2225	2425	500	15	13.8	141.1960	108.2880	2.4020	.357	.313	96	123	197	131
UM-6	2450	2380	2579	1500	10	8.8	141.0785	106.3861	3.9876	.356	.304	179	204	379	241
UM-7	2450	2380	2574	1500	10	8.8	141.4290	101.1413	4.6305	.357	.294	221	237	586	241
UM-4	2450	2480	2562	5000	8	6.8	141.5990	102.7212	5.8026	.358	.292	275	297	672	313
UM-5	2450	2480	2686	5000	8	6.8	141.8428	104.1041	5.6326	.359	.286	322	289	627	224

Note (1): Weight loss and thickness loss is based on time at temperature. Heat-up time has been subtracted for data computation.

(2): Specimen slipped back in nozzle.

TABLE 5

TEST CONDITIONS AND TEST RESULTS FOR UNCOATED ATJ GRAPHITE

Specimen	Test Temp. (F)	Test Zone Temp. (F)	Average Specimen Temp. (F)	Mass Velocity (#/ft^2-hr)	Test Time (Min.)	Time at Temp. (Min.)	Initial Weight (gms)	Final Weight (gms)	Weight Loss(1) (gm/min.)	Initial Thickness Midpoint (Inch)	Final Thickness Midpoint (Inch)	Rate of Loss(1) per Side-Midpoint (mils/hr)	Rate of Loss(1) per Side Based on Weight (mils/hr)	Rate of(1) Loss-Nose (mils/hr)	Rate of(1) Loss-Back Surface (mils/hr)
UG-8	2000	1940	2316	500	7	6	24.7250	18.6330	1.0270	.352	.313	215	308	950	100
UG-10	2000	1940	2325	500	7	6	24.9686	18.8630	1.0176	.352	.317	200	302	1200	100
UG-6	2000	1990	2427	1500	5	4	24.3000	17.5365	1.6909	.351	.303	398	507	1425	225
UG-1	2000	1990	2563	1500	18	17	24.6980	3.1661	1.2666	---	---	---	380	---	---
UG-2	2000	1960	2519	5000	4	3	24.9540	17.3361	2.5383	.351	.304	590	762	2400	200
UG-4	2000	1960	2582	5000	4	3	24.1338	16.3763	2.5858	.352	.299	520	776	2800	300
UG-12	2450	2260	2406	500	5	4	24.4350	21.0859	0.8373	.354	.332	165	252	850	75
UG-13	2450	2260	2312	500	5	4	24.8200	21.7496	0.7676	.352	.333	135	2[illegible]	750	75
UG-9	2450	2345	2582	1500	4	3	25.0910	20.4908	1.5334	.352	.320	440	460	1425	75
UG-11	2450	2345	2596	1500	4	3	24.6796	19.8031	1.6255	.352	.324	420	488	1900	300
UG-5	2450	2480	2608	5000	3	2	24.1457	19.5579	2.2939	.351	.323	465	688	2400	300
UG-7	2450	2480	2645	5000	3	2	24.7817	19.9267	2.4275	.354	.321	520	728	2820	100

Note (1): Weight loss and thickness loss are based on time at temperature. For data computation, the heat-up time has been subtracted.

TABLE 6

TEST RESULTS FOR W-2 COATED 0.5% TI MOLYBDENUM ALLOY

Specimen	Nominal Specimen Temp (F)	Mass Velocity (lb/ft^2-hr)	Time To Failure	Time Total	Remarks
WM-3	2000	500	No Failure	4 Hrs	
WM-1	2000	1500	No Failure	4 Hrs	
WM-2	2000	5000	No Failure	4 Hrs	
WM-8	2450	500	No Failure	4 Hrs	
WM-9	2450	500	3 Hrs	4 Hrs	One Failure
WM-6	2450	1500	No Failure	4 Hrs	
WM-7	2450	1500	No Failure	4 Hrs	
WM-4	2450	5000	No Failure	4 Hrs	
WM-5	2450	5000	1 Hr	2 Hrs	One Failure. Test terminated at 2 hours since self-healing had not occurred and failure area was enlarging.

TABLE 7

TEST RESULTS FOR DURAK MG COATED 0.5% TI MOLYBDENUM ALLOY

Specimen	Nominal Specimen Temp (F)	Mass Velocity (lbs/ft^2-hr)	Time (Hours) To Failure	Time (Hours) Total	Remarks
DM-C	2000	500	3	4	One failure
DM-B	2000	1500	1	4	One failure at end of 1 hour exposure. Since failure area did not increase excessively during subsequent exposures, the 4-hour total was run. Two additional failures occurred. No smoke was observed.
DM-A	2000	5000	3	3	One failure
DM-H	2450	500	1	4	One failure
DM-I	2450	500	No failure	4	
DM-F	2450	1500	1	4	One failure
DM-G	2450	1500	No failure	4	
DM-D	2450	5000	4	4	Two failures
DM-E	2450	5000	1	4	One failure

TABLE 8

TEST RESULTS FOR COATED ATJ GRAPHITE

Specimen	Test Temp (F)	Mass Velocity (lbs/ft^2-hr)	Time (Hours) To Failure	Time (Hours) Total	Remarks
C-9	2000	500	No failure	5	One extra hour
I-12	2000	500	3	4	One failure
J-5	2000	500	1	2	Multiple failures
B-8	2000	1500	3	3	Multiple failures
F-10	2000	1500	4	4	Multiple failures
G-11	2000	1500	4	4	Multiple failures
D-11	2000	5000	3	4	Multiple failures
N-5	2000	5000	2	3	Multiple failures
F-6	2450	500	No failure	4	
N-6	2450	500	4	4	Multiple failures
G-4	2450	500	1	4	Two failures occurred during the first hour. Number of failures increased as test progressed.
K-4	2450	1500	No failure	4	
K-5	2450	1500	No failure	4	
I-2	2450	1500	No failure	4	
C-2	2450	5000	No failure	4	
C-12	2450	5000	4	4	One failure

TABLE 9

TEST RESULTS COMPARED WITH NATIONAL CARBON CLASSIFICATION

FOR SILICONIZED ATJ GRAPHITE

Specimen	Test Conditions		National Carbon Classification	Weight Increase Due to Coating (gms)	Test Results
	Temp. (F)	Flow (lbs/ft^2-hr)			
C-9	2000	500	AB	2.23	No failure
I-12	2000	500	AB	2.61	One failure
J-5	2000	500	C	1.64	Two failures
B-8	2000	1500	C	1.64	Multiple failures - on one surface
F-10	2000	1500	AB	2.33	Multiple failures - on one surface
G-11	2000	1500	AB	1.65	Multiple failures - on one surface
D-11	2000	5000	C	3.02	Multiple failures - on one surface
N-5	2000	5000	C	1.62	Multiple failures - both surfaces
F-6	2450	500	AB	1.56	No failure
N-6	2450	500	C	1.47	Multiple failures - on one side; one failure - other side
G-4	2450	500	C	1.82	Multiple failures - both sides
K-4	2450	1500	C	4.69	No failure
K-5	2450	1500	AB	1.75	No failure
I-2	2450	1500	AB	1.90	No failure
C-2	2450	5000	AB	2.31	No failure
C-12	2450	5000	AB	1.71	One failure

TABLE 10

DIMENSION OF DAMAGED AREAS OF DAMAGED W-2 COATED 0.5% TI MOLYBDENUM ALLOY AFTER TESTING

Specimen No.	Test Conditions			Dimensions of Damaged Areas (In.)											
				Nose				Side Surface				Side Surface(1)			
				Rockwell		Drill		Rockwell		Drill		Rockwell		Drill	
	Temp °F	Flow #/ft²-hr	Time Hr	Length(2)	Depth	Length(2)	Depth	Dia.	Depth	Dia.	Depth	Dia.	Depth	Dia.	Depth
G	2000	500	4	9/32	1/8	11/32	5/32	11/32	1/8	5/16	5/32			5/16	5/32
H	2000	500	4	1/4	1/8	5/16	5/32	7/32	3/32	9/32	1/8	3/16	1/16		
A	2450	500	4	3/16	1/8	1/2	1/4	7/32	1/8	9/32	1/8				
B	2450	500	4	7/32	1/8	5/16	5/32	7/32	1/8	9/32	1/8				
E	2000	5000	4	1/4	1/8	17/32	7/32	7/32	1/8	9/32	5/32	1/8	1/16		
F	2000	5000	4	7/32	3/32	1/2	3/16	3/16	3/32	11/32	5/32			9/32	5/32
C	2450	5000	4	3/16	1/8	9/16	11/32	1/4	5/32	13/32	3/16				
D	2450	5000	4	3/16	1/8	9/32	7/32	1/8	1/16	5/16	5/32			9/32	5/32

Note (1): This column is data for the extra holes

(2): Nose damage dimensions are given in length and depth only since the width of the nose is smaller than the extent of oxidation experienced. Length is measured along forward edge while depth is measured from front to rear.

TABLE 11

DIMENSIONS OF DAMAGED AREAS OF DAMAGED DURAK MG 0.5% TI MOLYBDENUM ALLOY AFTER TESTING

Specimen No.	Test Conditions: Temp °F	Test Conditions: Flow #/ft²-hr	Test Conditions: Time Hr	Dimensions of Damaged Areas (In.): Nose: Rockwell: Length(2)	Nose: Rockwell: Depth	Nose: Drill: Length(2)	Nose: Drill: Depth	Side Surface: Rockwell: Dia.	Side Surface: Rockwell: Depth	Side Surface: Drill: Dia.	Side Surface: Drill: Depth	Side Surface(1): Rockwell: Dia.	Side Surface(1): Rockwell: Depth	Side Surface(1): Drill: Dia.	Side Surface(1): Drill: Depth
III-C	2000	500	4	7/32	3/32	1/4	5/32	5/32	3/32	1/4	5/32			1/4	5/32
I-A	2450	500	4	3/4	11/32	3/4	11/32	5/16	5/32	1/2	7/32			1/2	7/32
II-B	2450	5000	4	3/8	7/32	5/8	3/8	7/32	1/8	7/16	3/16				

Note (1): This column is data for the extra holes.

(2): Nose damage dimensions are given in length and depth only, since the width of the nose is smaller than the extent of oxidation experienced. Length is measured along the forward edge while depth is measured from front to rear.

TABLE 12

DIMENSIONS OF DAMAGED AREAS OF DAMAGED SILICONIZED ATJ GRAPHITE AFTER TESTING

Specimen No.	Test Conditions: Temp °F	Test Conditions: Flow #/ft²-hr	Test Conditions: Time Hr	Dimensions of Damaged Areas (In.): Nose: Rockwell: Length(2)	Nose: Rockwell: Depth	Nose: Drill: Length(2)	Nose: Drill: Depth	Side Surface: Rockwell: Dia.	Side Surface: Rockwell: Depth	Side Surface: Drill: Dia.	Side Surface: Drill: Depth	Side Surface(1): Rockwell: Dia.	Side Surface(1): Rockwell: Depth	Side Surface(1): Drill: Dia.	Side Surface(1): Drill: Depth
7	2000	500	4	7/32	1/8	7/32	5/32	7/32	1/8	1/4	3/16			1/4	5/32
8	2000	500	4	7/32	1/8	7/32	3/16	3/16	3/32	1/4	5/32	3/16	3/32		
5	2000	5000	4	7/32	5/32	1/4	3/16	3/16	3/32	9/32	5/32	5/32	3/32		
6	2000	5000	4	7/32	5/32	1/4	3/16	7/32	1/8	11/32	5/32			5/16	5/32
1	2450	500	4	7/32	1/4	7/32	5/32	3/16	1/8	9/32	5/32				
2	2450	500	4	3/16	1/8	7/32	5/32	3/16	1/8	5/16	5/32			3/8	5/32
3	2450	5000	4	3/16	5/32	7/16	1/4	1/4	1/8	5/16	3/16				
4	2450	5000	4	1/4	3/16	3/4	11/32	1/4	5/32	1/2	1/4				

Note (1): This column is data for the extra holes.

(2): Nose damage dimensions are given in length and depth only since the width of the nose is smaller than the extent of oxidation experienced. Length is measured along the forward edge while depth is measured from front to rear.

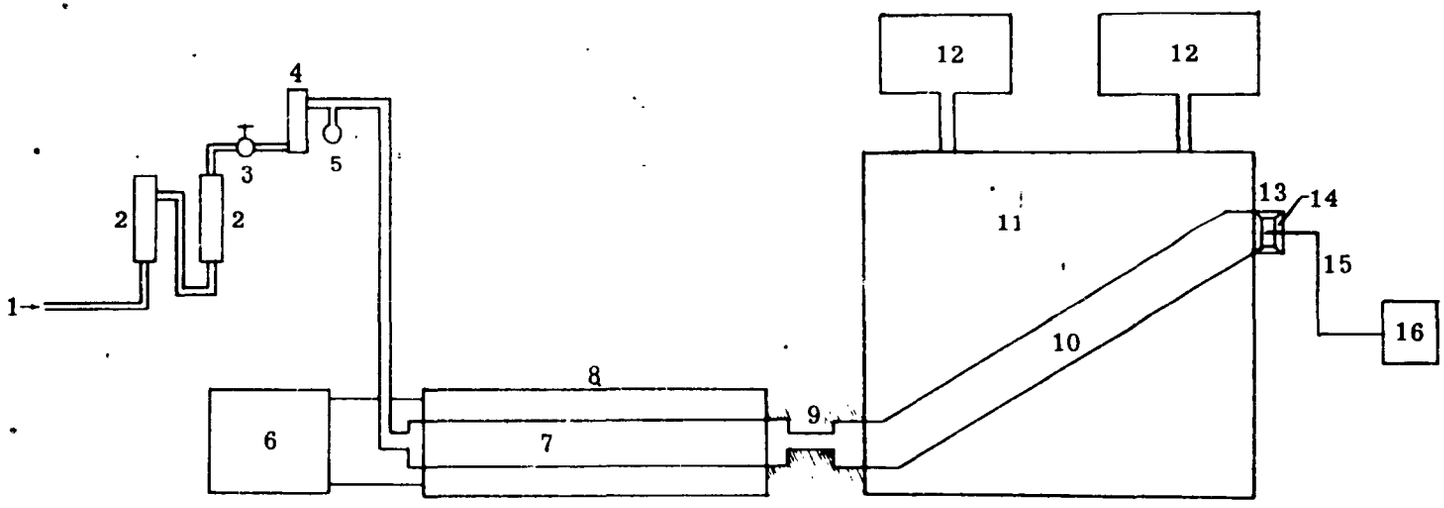

1. Plant Air Inlet
2. Dryers (Drying Agent-Molecular Sieve)
3. Pressure Regulators-Shutoff Valve
4. Flowrator
5. Pressure Gage
6. Motor Generator
7. Ceramic Tube
8. Preheat Furnace
9. Thermal Insulation
10. Ceramic Tube
11. Test Furnace
12. Transformers and Controllers
13. Zirconia Nozzle
14. Test Specimen
15. Thermocouple
16. Brown Potentiometer Pyrometer

FIGURE 1. SCHEMATIC OF OXIDATION TEST EQUIPMENT

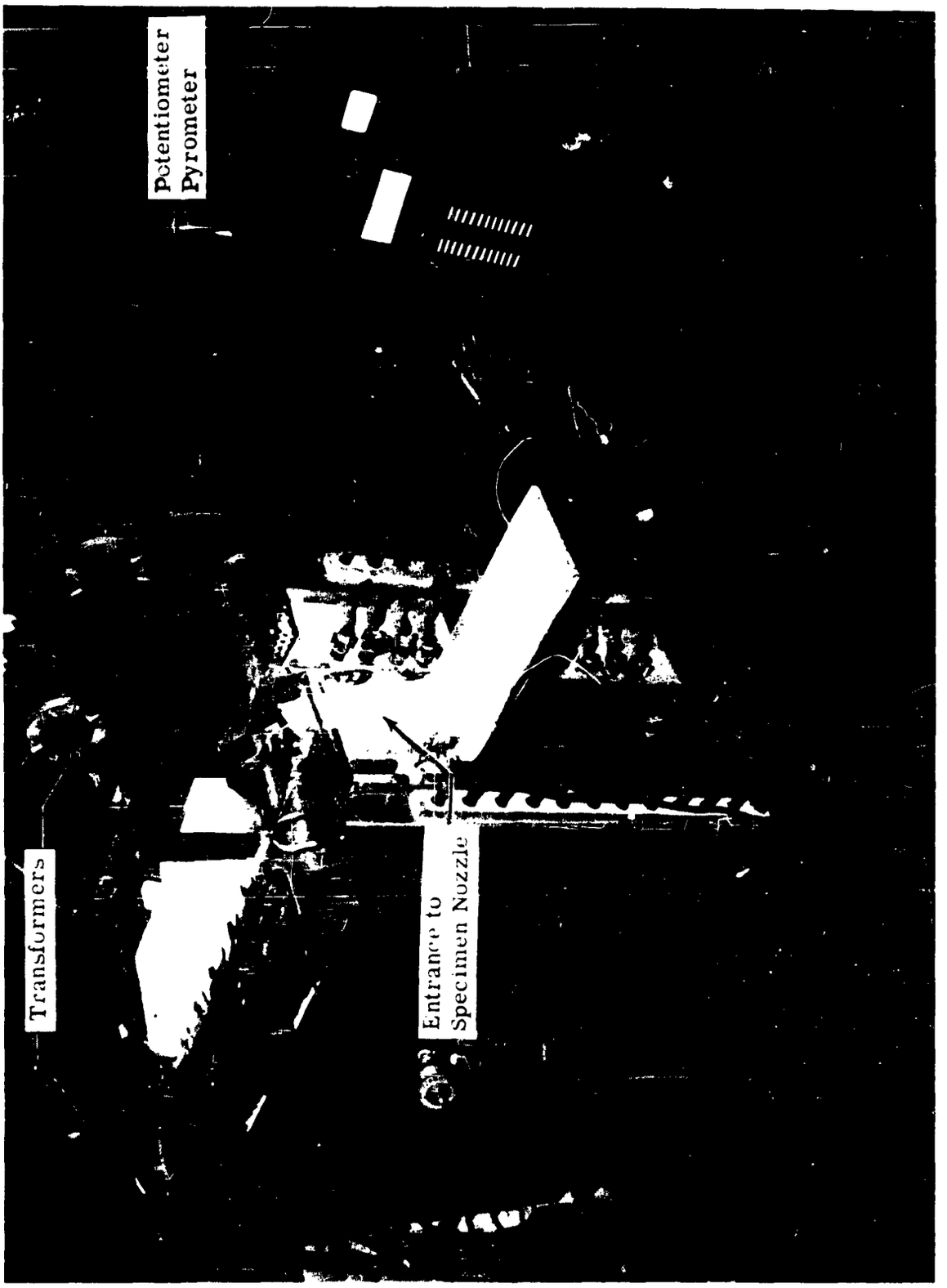

FIGURE 2. TEST FURNACE AND POTENTIOMETER PYROMETER

FIGURE 3. PREHEAT FURNACE

Air Drying and Metering

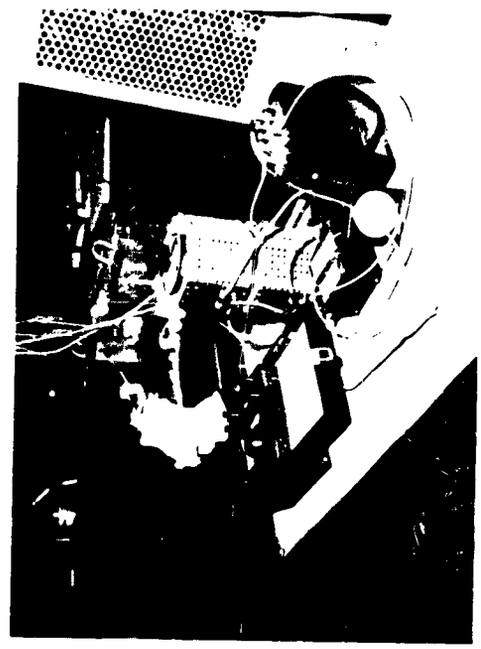

Controller for Platinum Furnace and Specimen Temperature Measuring

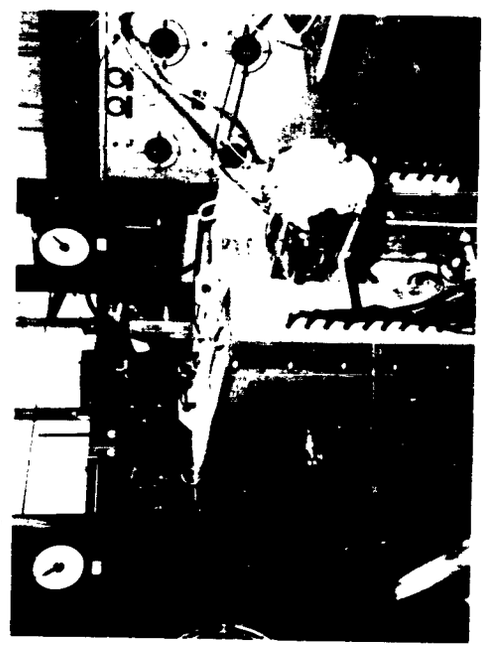

Preheat Furnace and Attached Tubular Platinum Furnace

FIGURE 4. AIR DRYING AND METERING EQUIPMENT

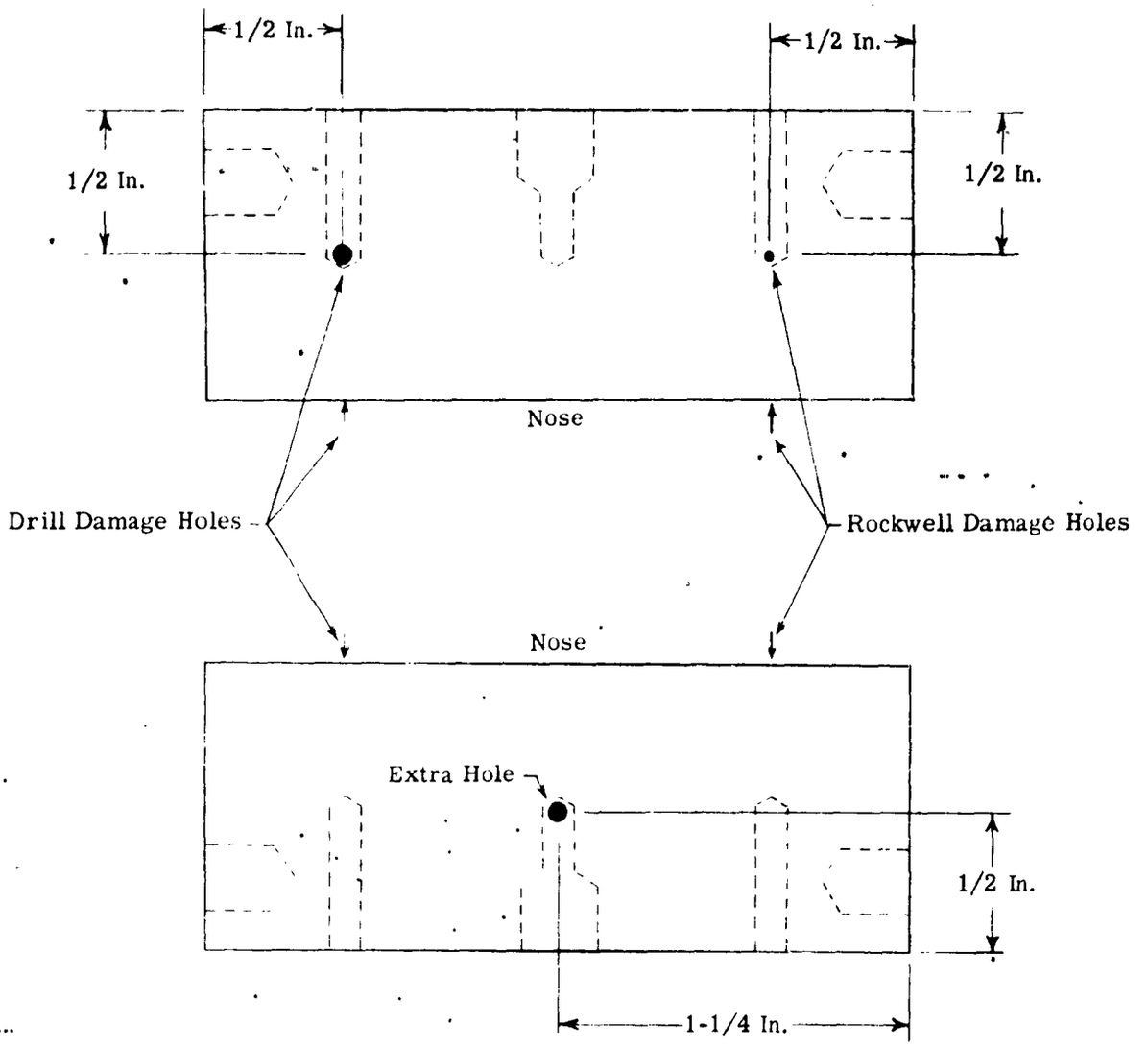

Note: Location Dimensions are Approximations

FIGURE 5. DIAGRAM OF DAMAGED COATED SPECIMENS SHOWING LOCATION OF REGULAR AND EXTRA HOLES

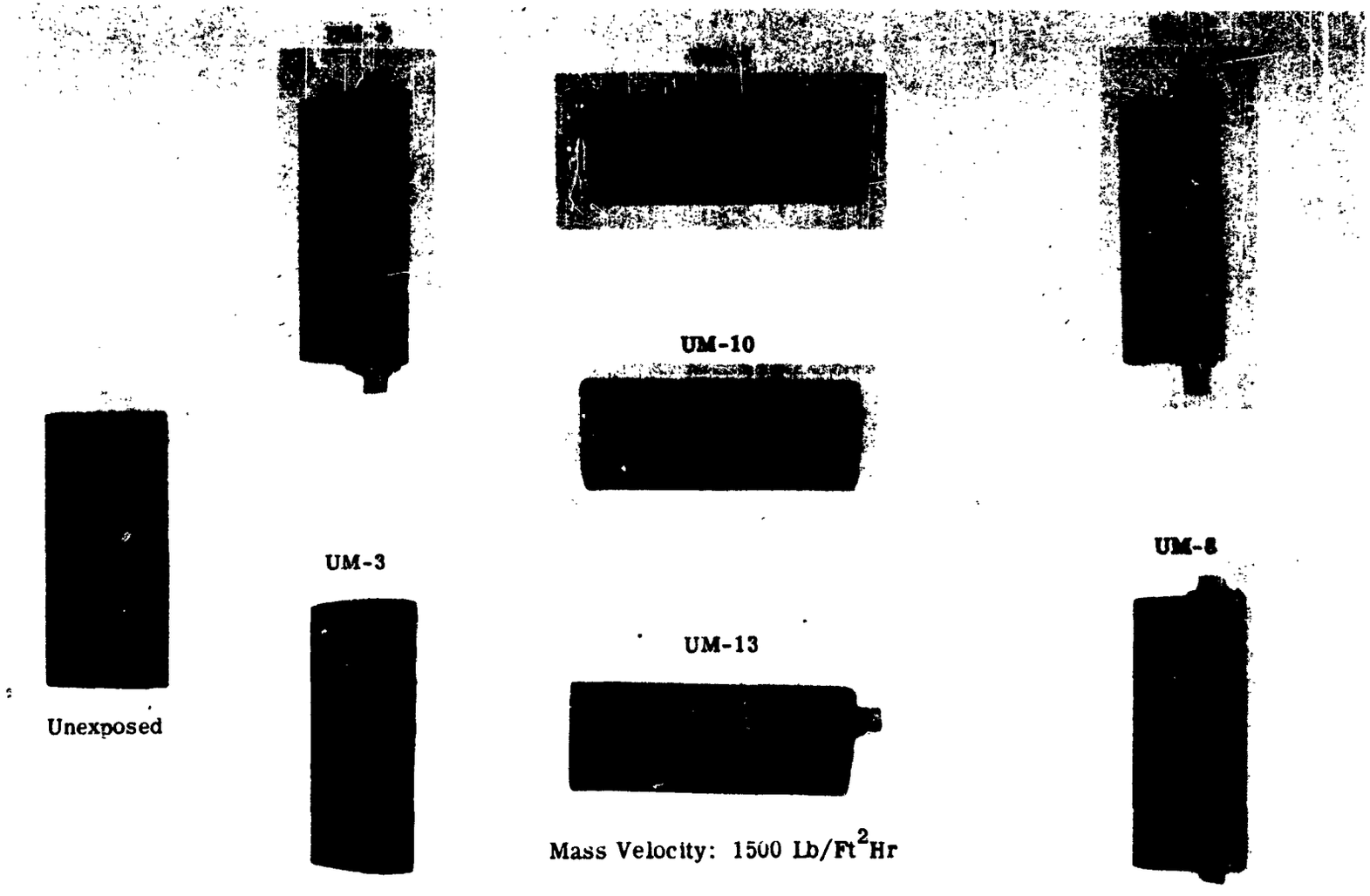

FIGURE 6. UNCOATED 0.5% TITANIUM MOLYBDENUM ALLOY OXIDATION SPECIMENS AFTER TESTING AT 2000°F IN FLOWING AIR

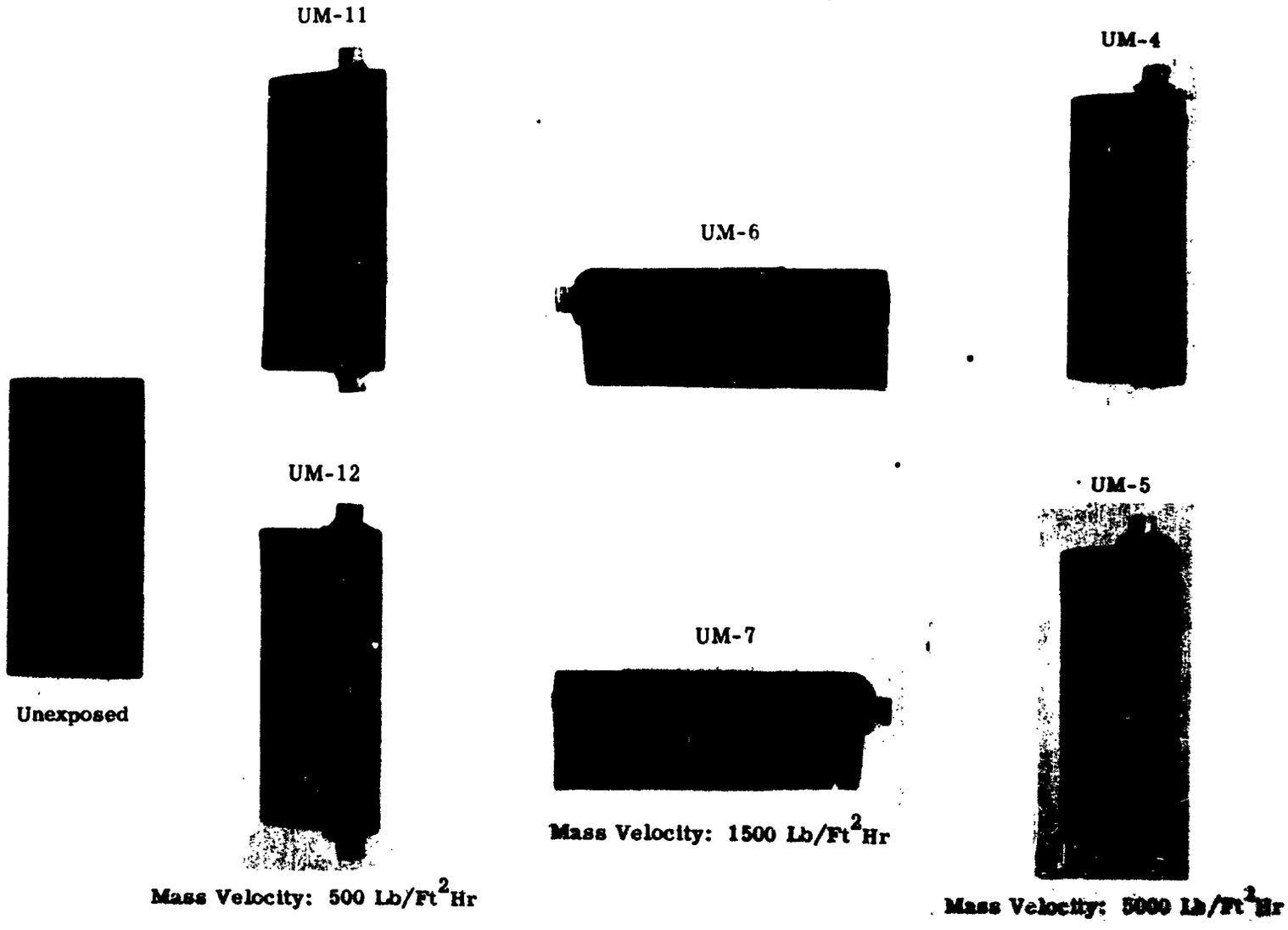

FIGURE 7. UNCOATED 0.5% TITANIUM MOLYBDENUM ALLOY OXIDATION SPECIMENS AFTER TESTING AT 2450°F IN FLOWING AIR

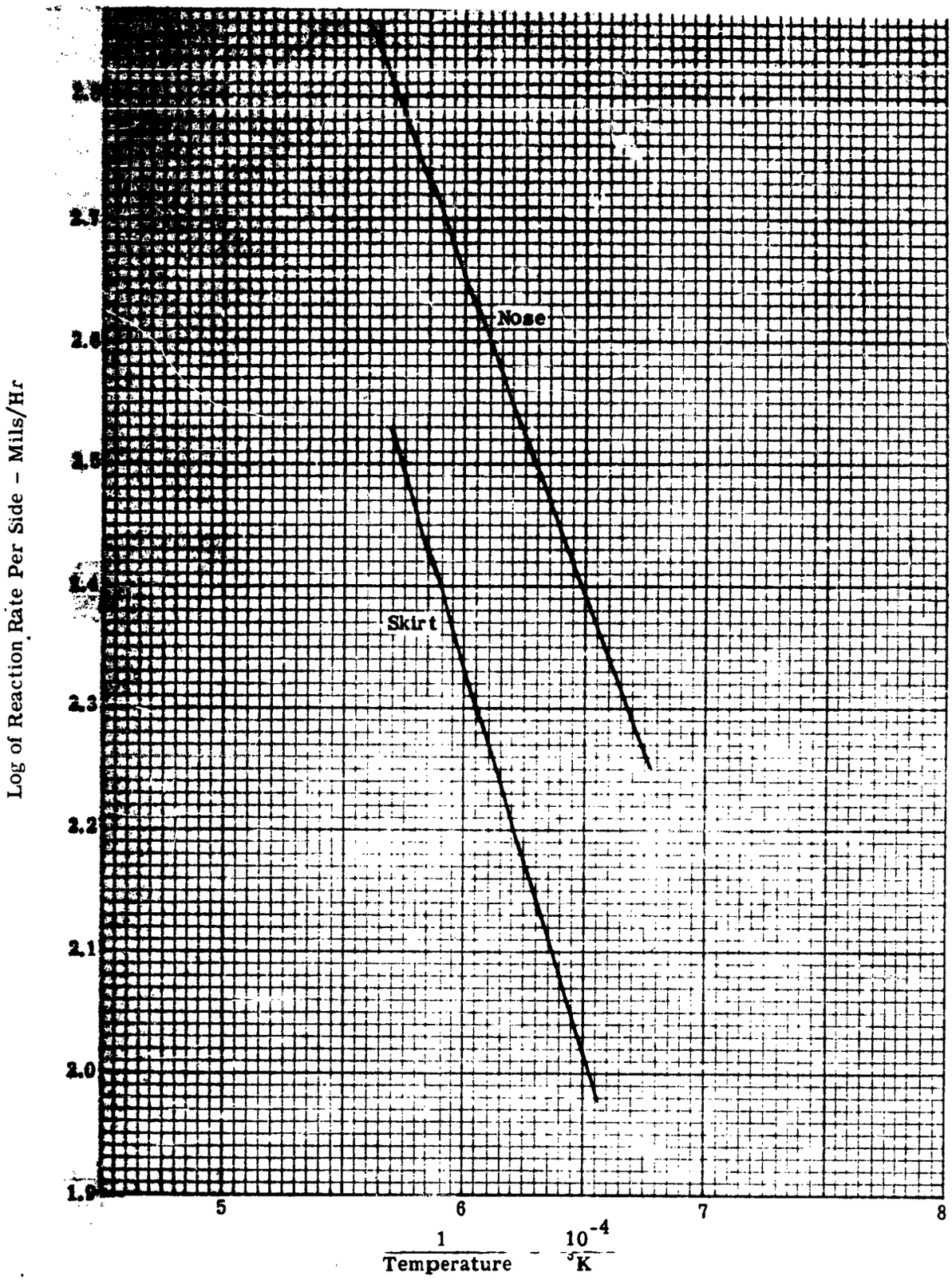

FIGURE 8. LOG OF SURFACE LOSS VS RECIPROCAL OF ABSOLUTE TEMPERATURE FOR UNCOATED 0.5% TITANIUM MOLYBDENUM ALLOY IN FLOWING AIR

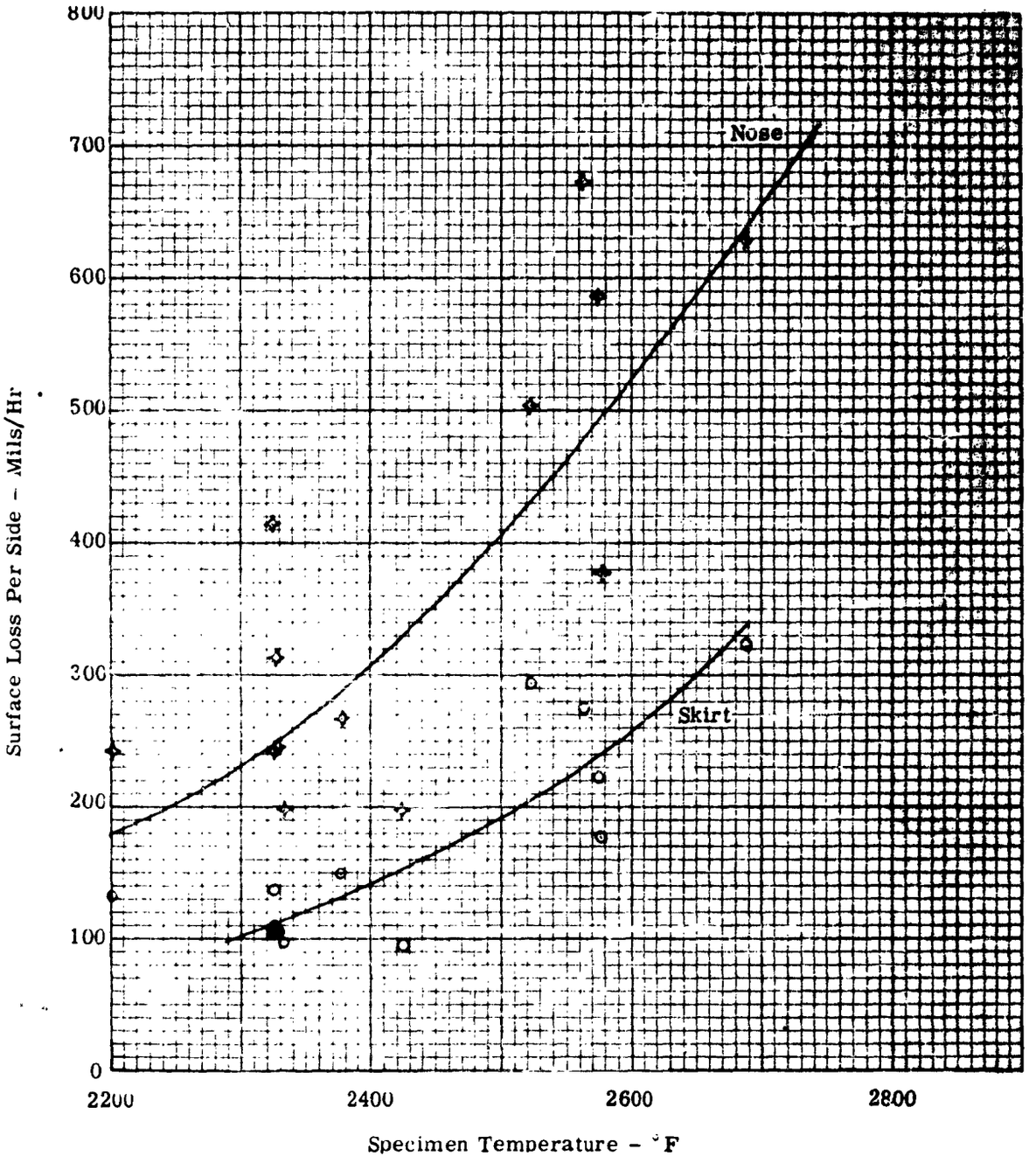

FIGURE 8. SURFACE LOSS FOR UNCOATED 0.5% TITANIUM MOLYBDENUM ALLOY IN FLOWING AIR

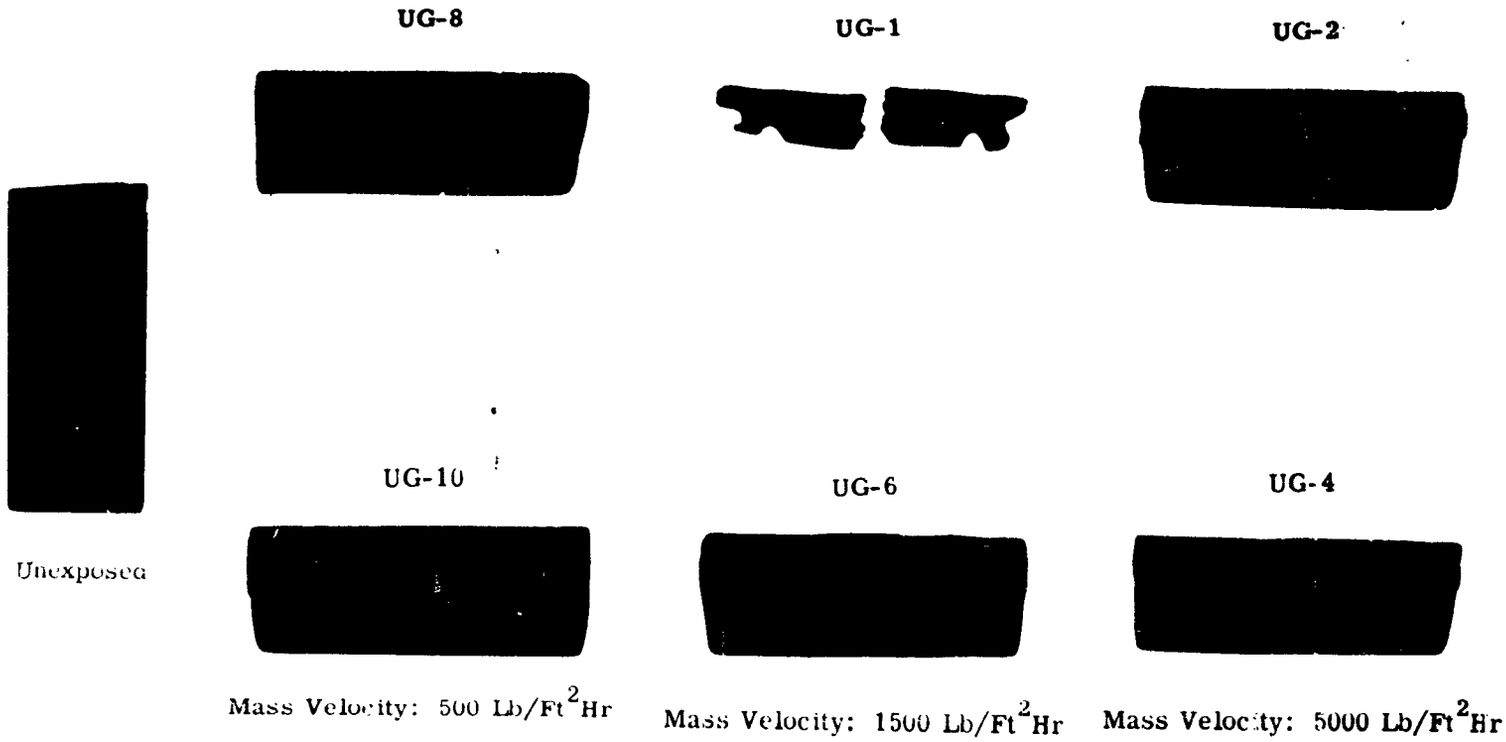

FIGURE 10. UNCOATED ATJ GRAPHITE OXIDATION SPECIMENS AFTER TESTING AT 2000°F IN FLOWING AIR

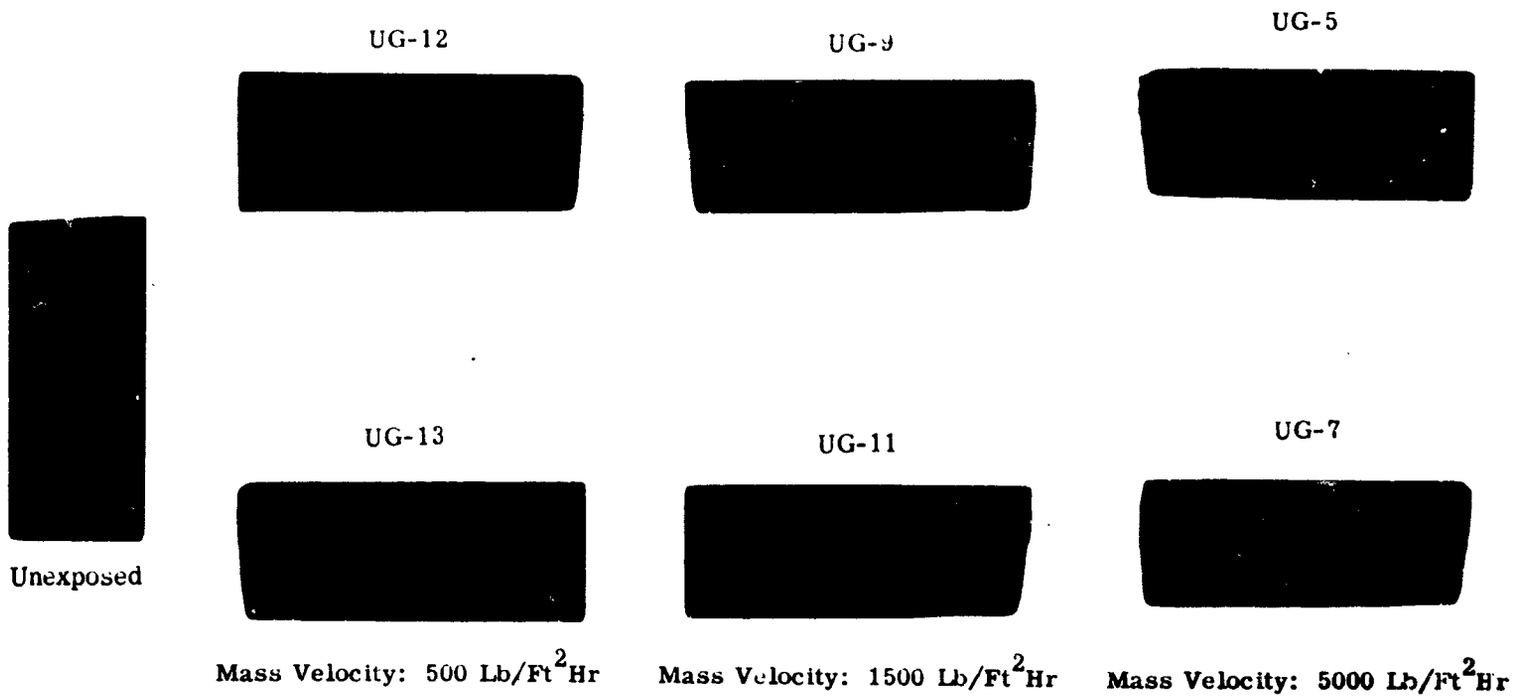

FIGURE 11. UNCOATED ATJ GRAPHITE OXIDATION SPECIMENS AFTER TESTING AT 2450°F IN FLOWING AIR

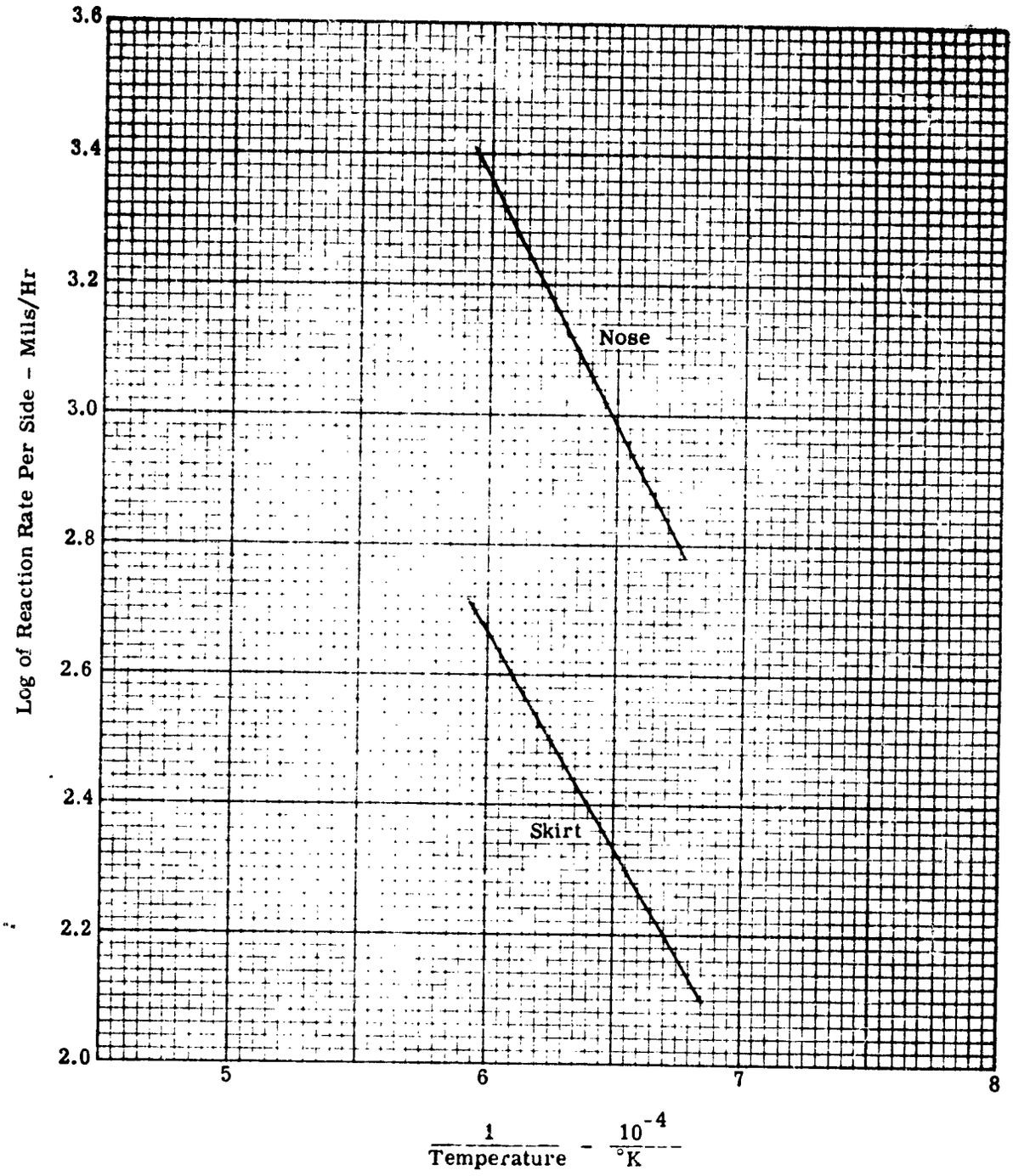

FIGURE 12. LOG OF SURFACE LOSS VS RECIPROCAL OF ABSOLUTE TEMPERATURE FOR UNCOATED ATJ GRAPHITE IN FLOWING AIR

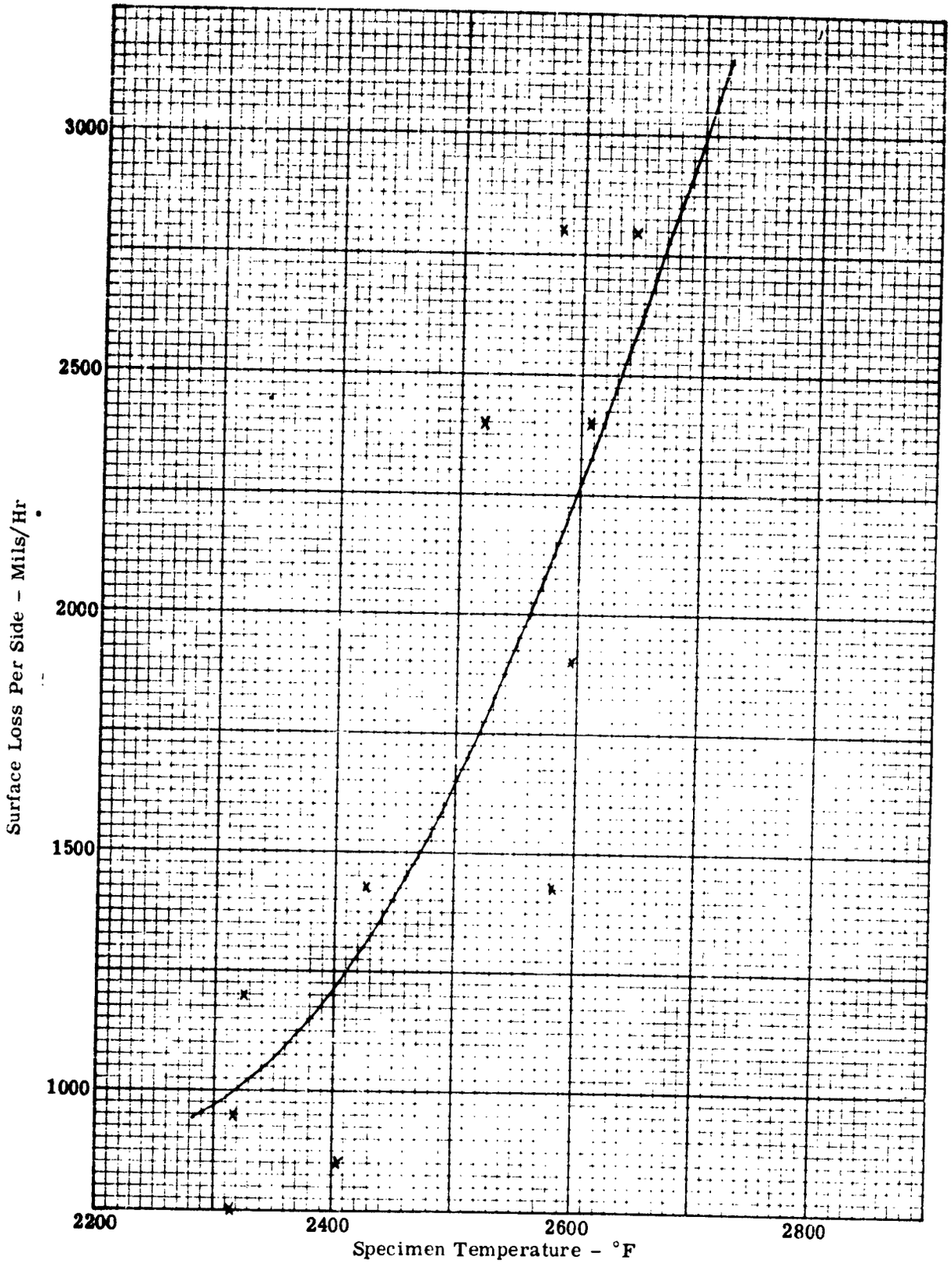

FIGURE 15. SURFACE LOSS AT NOSE FOR UNCOATED ATJ GRAPHITE IN FLOWING AIR

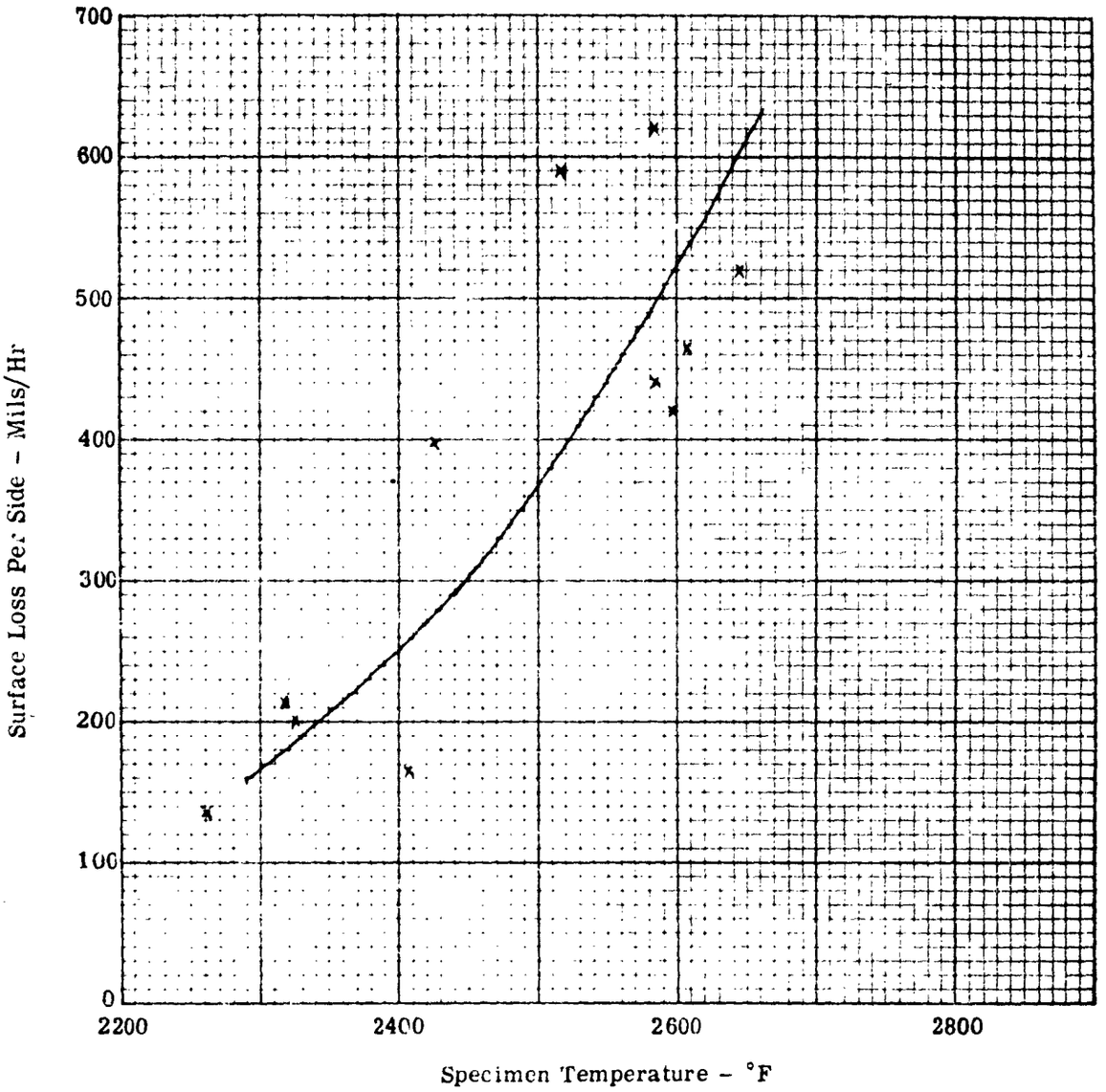

FIGURE 14. SURFACE LOSS AT SKIRT FOR UNCOATED ATJ GRAPHITE IN FLOWING AIR

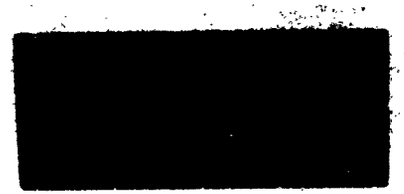

Siliconized ATJ Graphite

W-2 Coated 0.5% Titanium Molybdenum Alloy

Durak MG Coated 0.5% Titanium Molybdenum Alloy

FIGURE 15. TYPICAL COATED OXIDATION SPECIMENS BEFORE TESTING

WM-3

Mass Velocity: 500 Lb/Ft^2Hr

WM-1

Mass Velocity: 1500 Lb/Ft^2Hr

WM-2

Mass Velocity: 5000 Lb/Ft^2Hr

FIGURE 16. W-2 COATED 0.5% TITANIUM MOLYBDENUM ALLOY OXIDATION SPECIMENS AFTER TESTING AT 2000°F IN FLOWING AIR

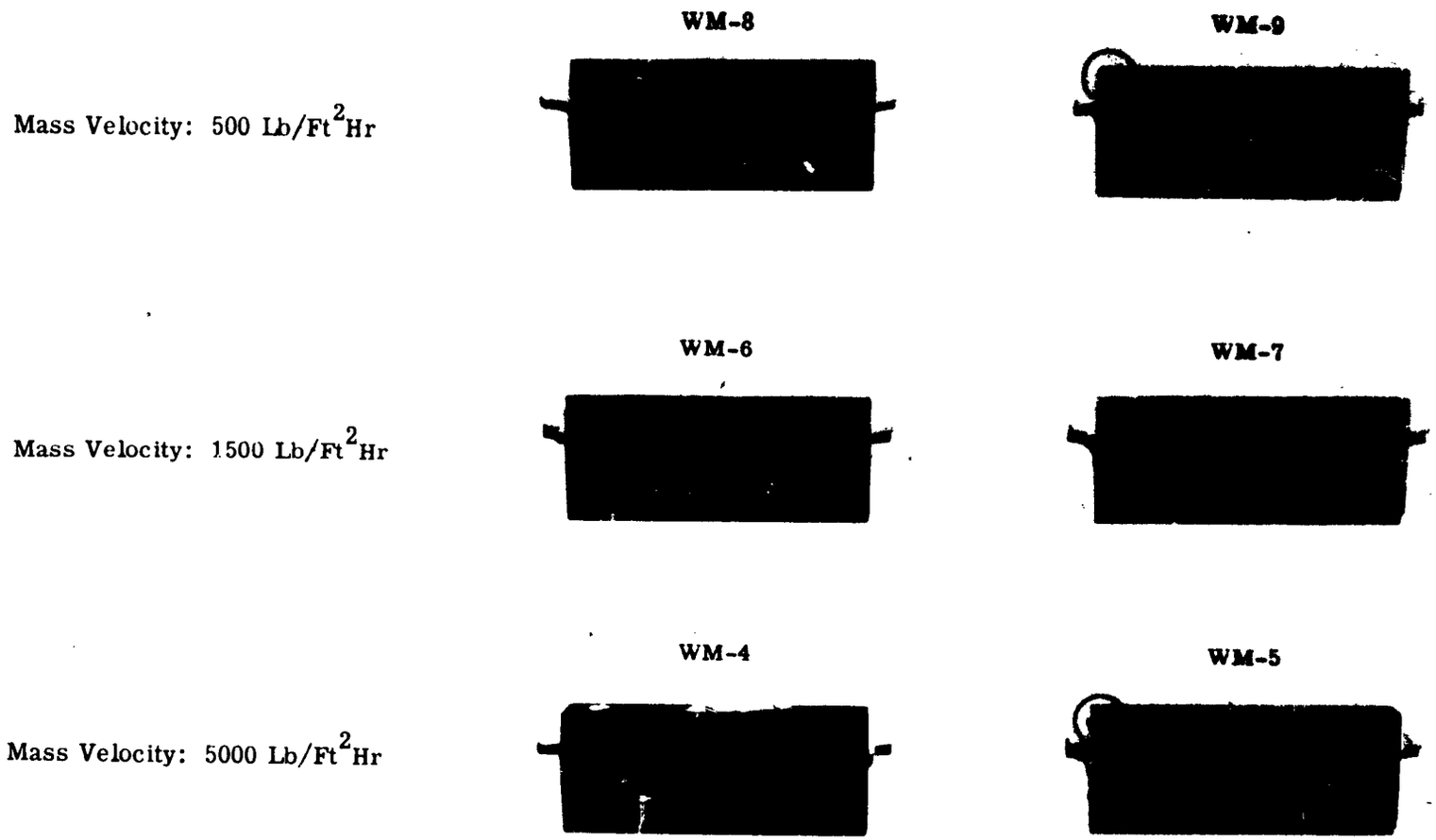

FIGURE 17. W-2 COATED 0.5% TITANIUM MOLYBDENUM ALLOY OXIDATION SPECIMENS AFTER TESTING AT 2450°F IN FLOWING AIR (FAILURES ENCIRCLED)

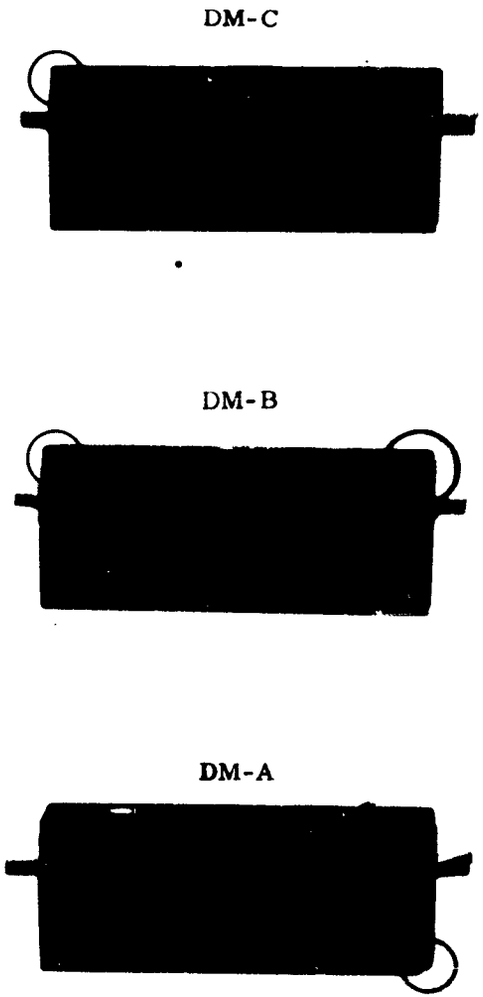

FIGURE 18. DURAK MG COATED 0.5% TITANIUM MOLYBDENUM ALLOY OXIDATION SPECIMENS AFTER TESTING AT 2000°F IN FLOWING AIR (FAILURES ENCIRCLED)

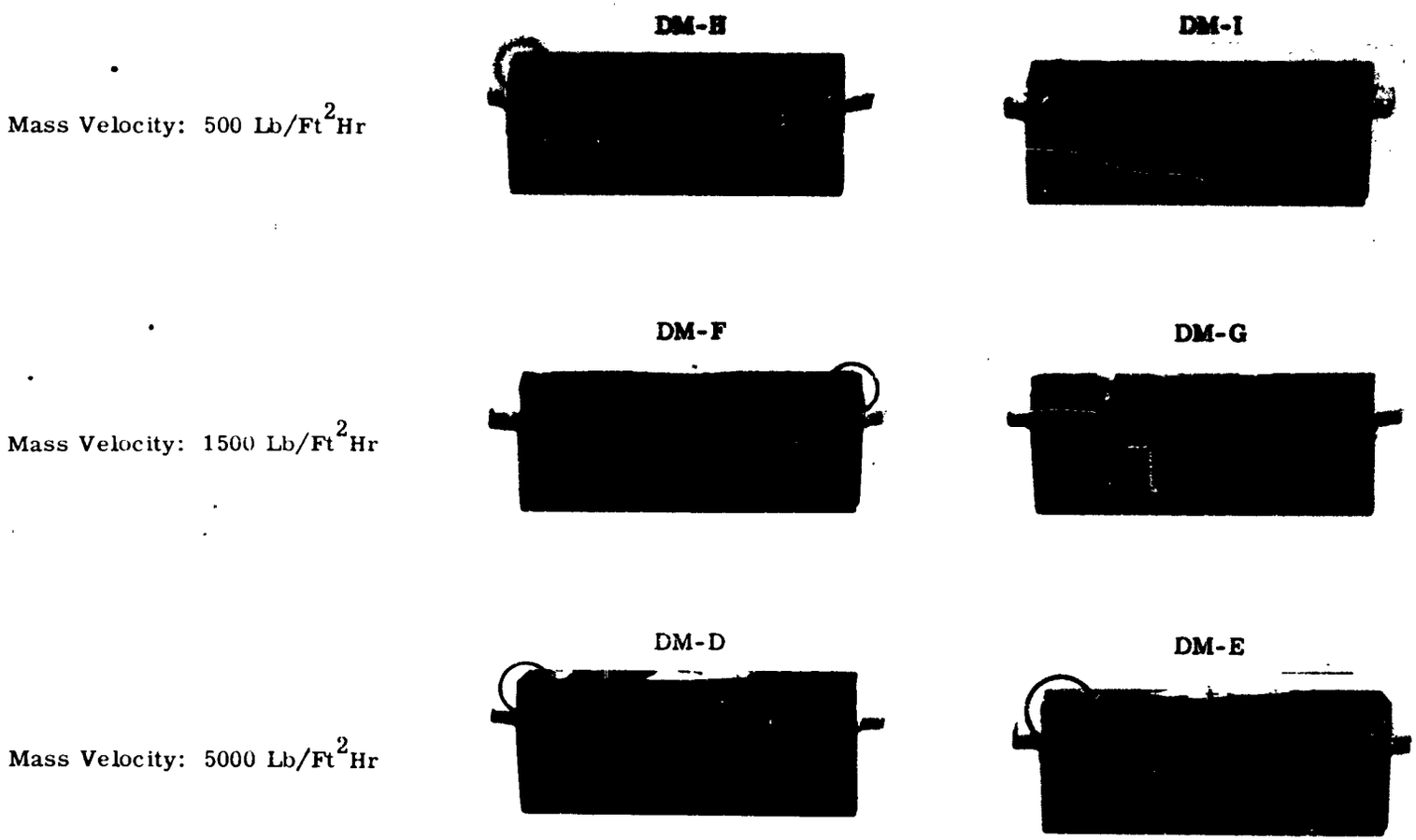

FIGURE 19. DURAK MG COATED 0.5% TITANIUM MOLYBDENUM ALLOY OXIDATION SPECIMENS AFTER TESTING AT 2450°F IN FLOWING AIR (FAILURES ENCIRCLED)

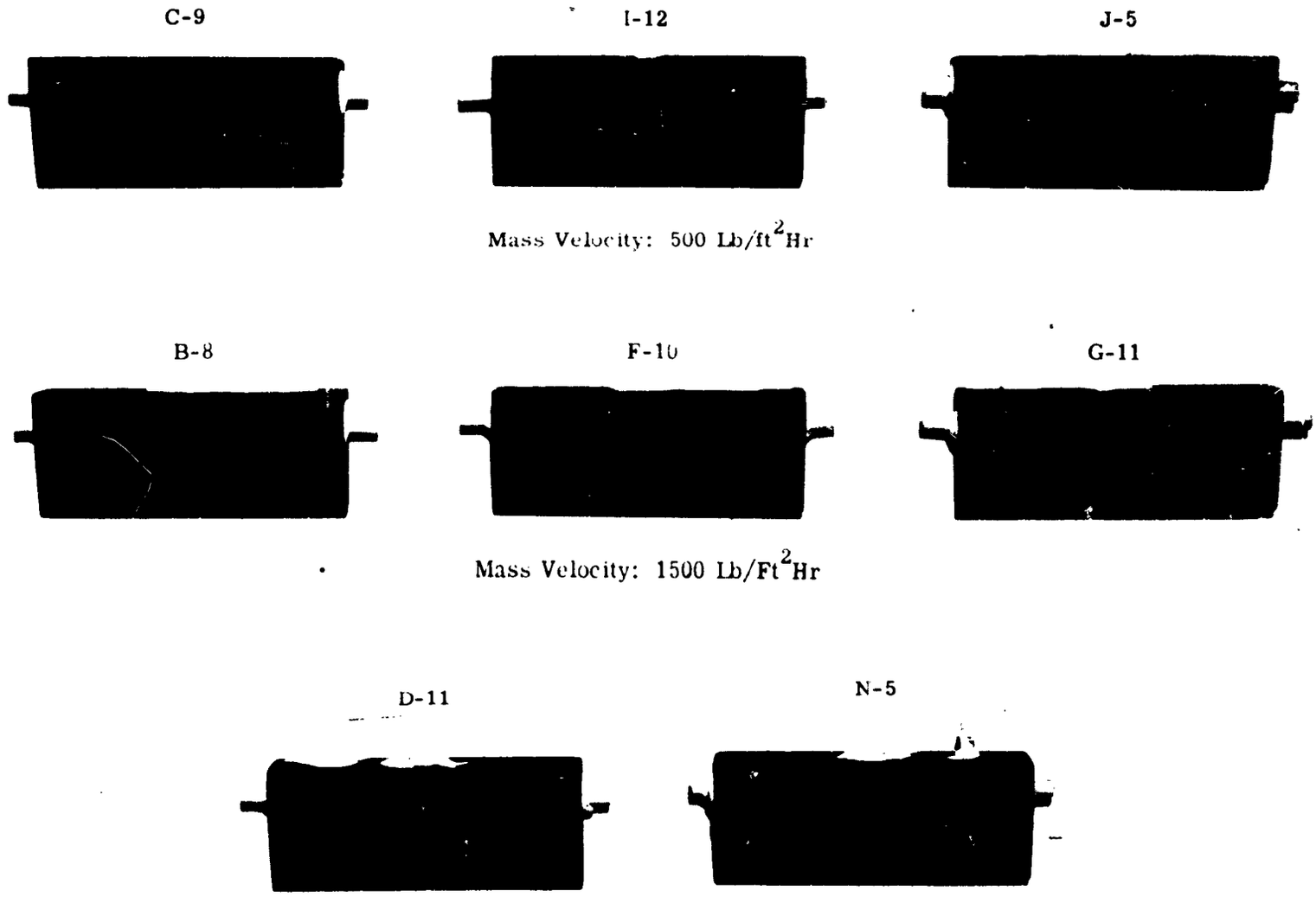

FIGURE 20. SILICONIZED ATJ GRAPHITE OXIDATION SPECIMENS AFTER TESTING AT 2000°F IN FLOWING AIR (FAILURES WHICH ARE DIFFICULT TO DETECT ON THE PHOTOGRAPH ARE ENCIRCLED)

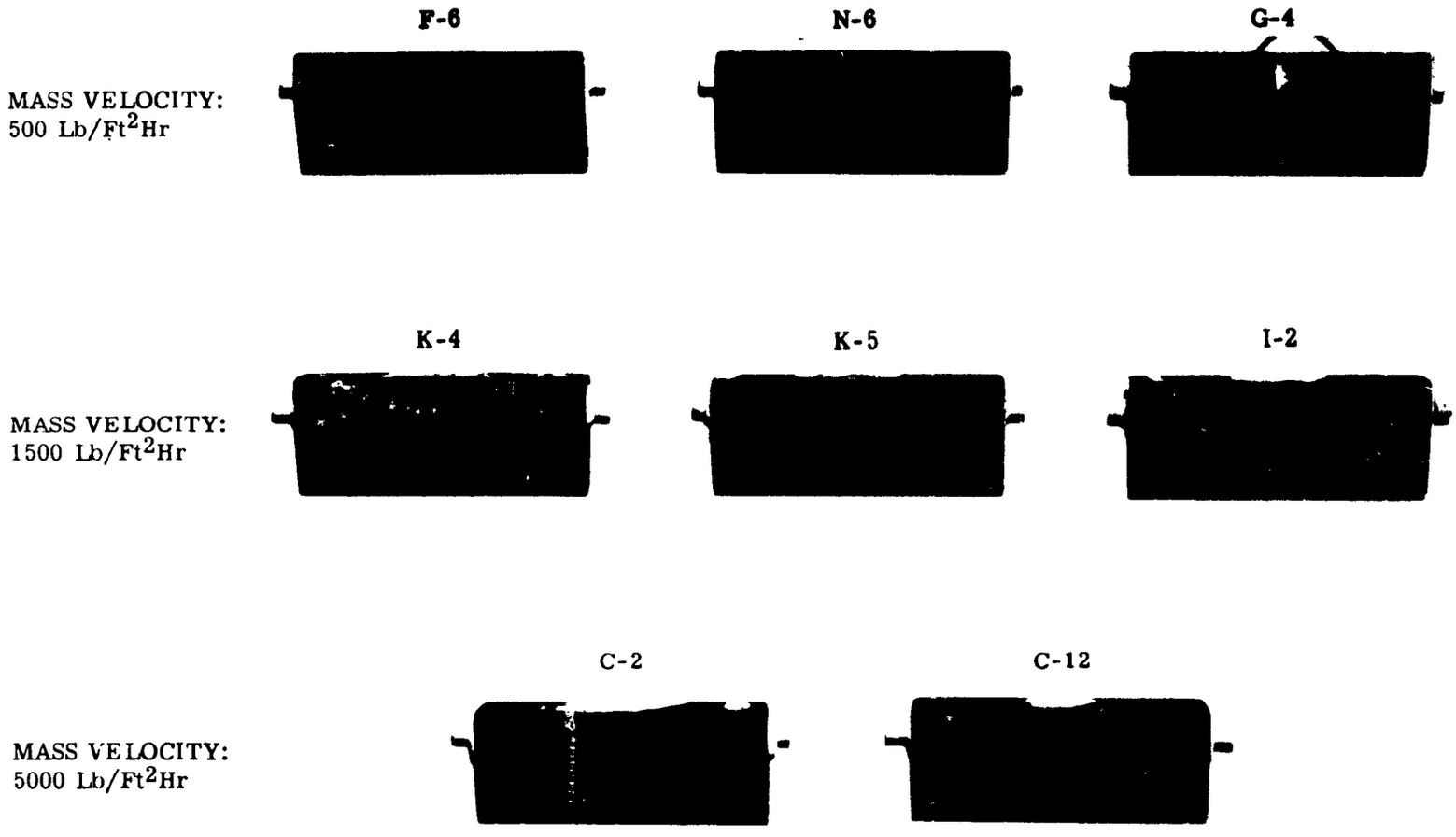

FIGURE 21. SILICONIZED ATJ GRAPHITE OXIDATION SPECIMENS AFTER TESTING AT 2450°F IN FLOWING AIR (FAILURES WHICH ARE DIFFICULT TO DETECT ON THE PHOTOGRAPH ARE ENCIRCLED)

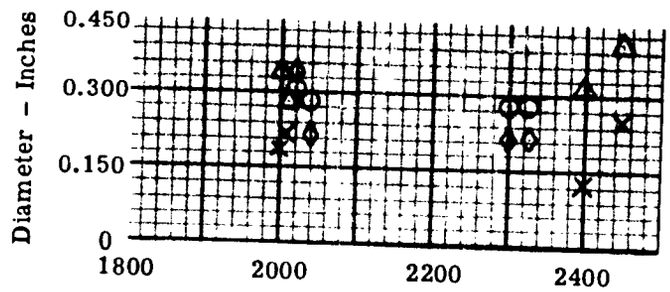

Diameters of Side Surface Areas

○ 500 Lb/Ft^{2}Hr, Drill
△ 5000 Lb/Ft^{2}Hr, Drill
◇ 500 Lb/Ft^{2}Hr, Rockwell
× 5000 Lb/Ft^{2}Hr, Rockwell

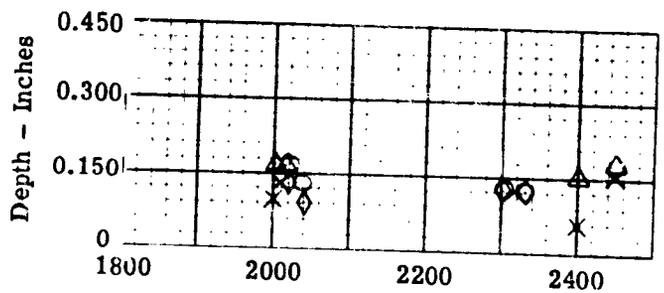

Depth of Side Surface Areas

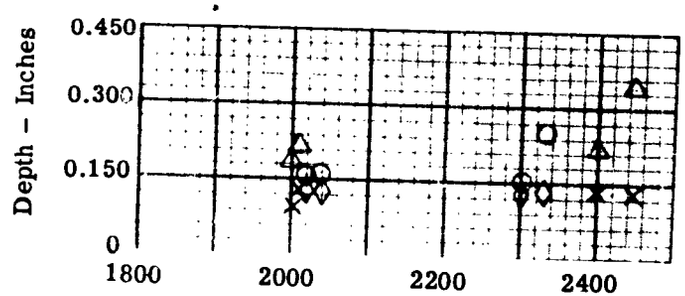

Depth of Nose Areas

FIGURE 22. DIMENSIONS OF DAMAGED AREAS IN W-2 COATED 0.5% TITANIUM MOLYBDENUM ALLOY SPECIMENS AFTER TESTING

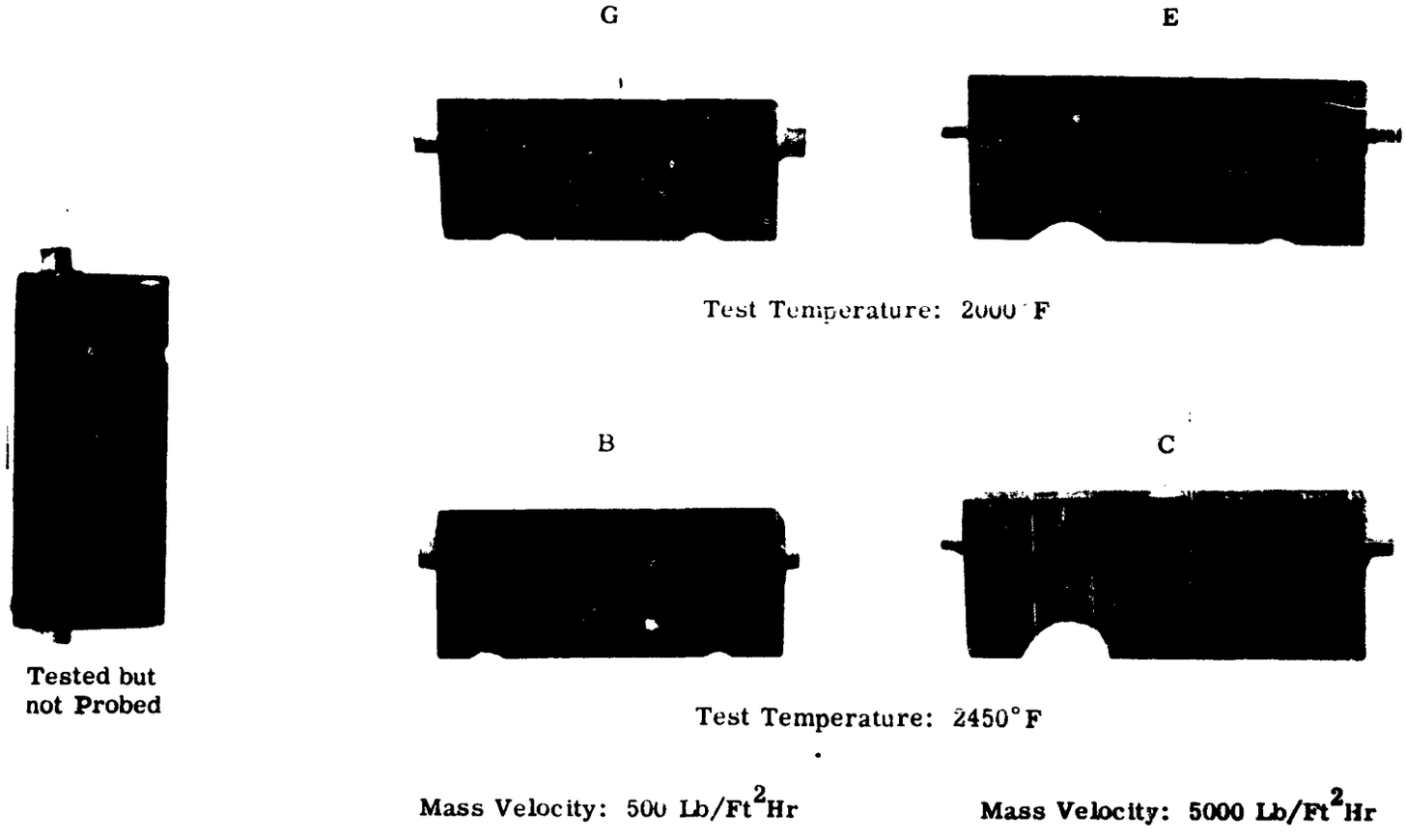

FIGURE 23. TYPICAL DAMAGED W-2 COATED 0.5% TITANIUM MOLYBDENUM ALLOY OXIDATION SPECIMENS AFTER TESTING IN FLOWING AIR

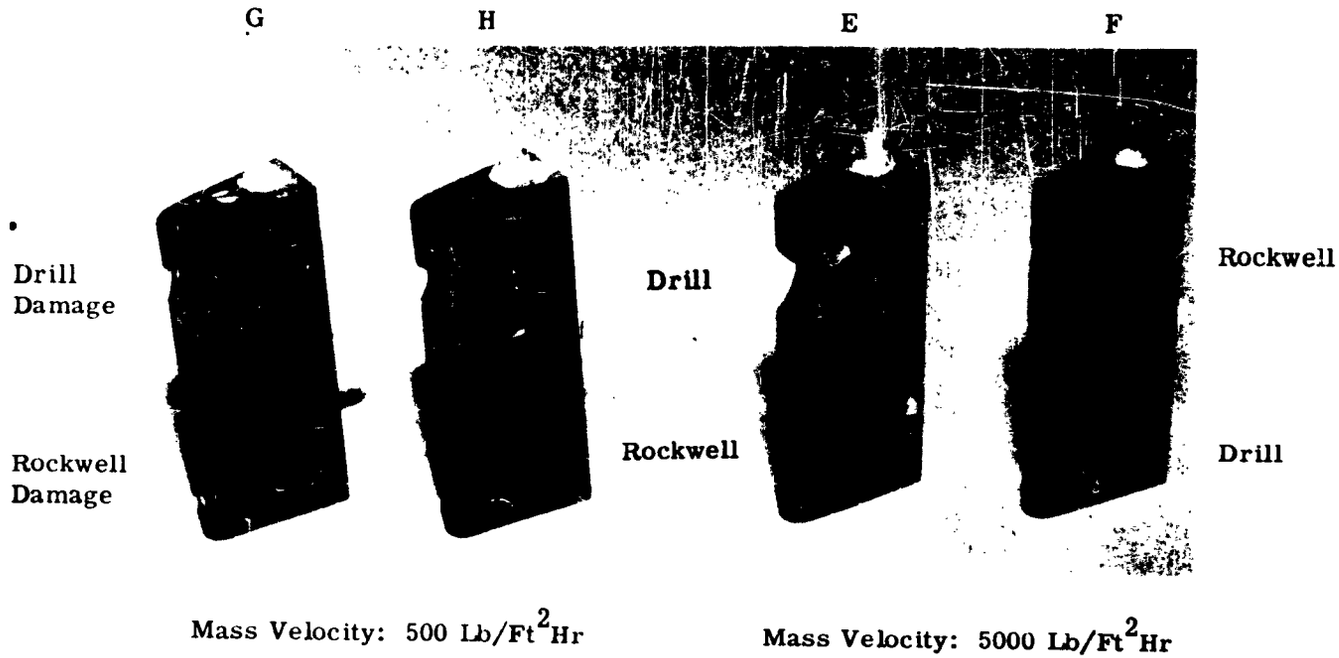

FIGURE 24. DAMAGED W-2 COATED 0.5% TITANIUM MOLYBDENUM ALLOY OXIDATION SPECIMENS AFTER TESTING AT 2000°F IN FLOWING AIR

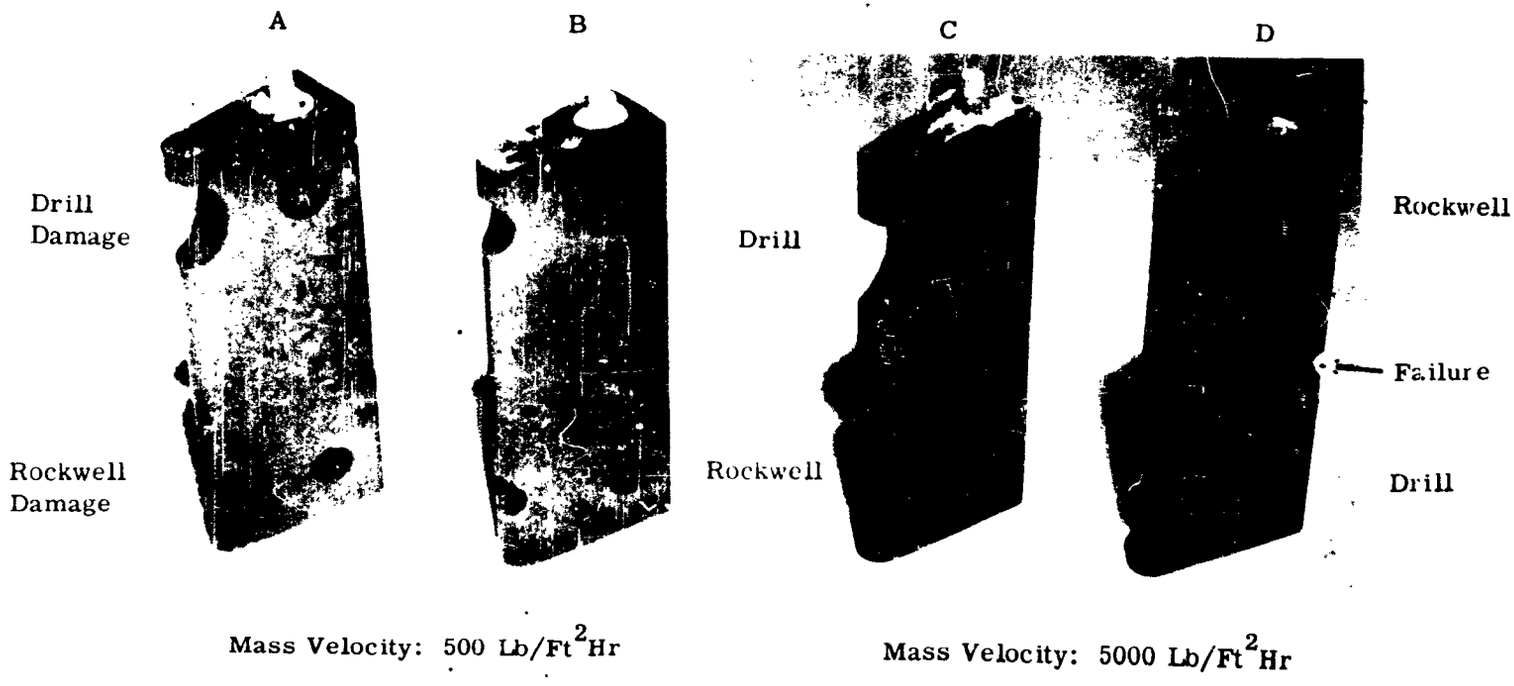

FIGURE 25. DAMAGED W-2 COATED 0.5% TITANIUM MOLYBDENUM ALLOY OXIDATION SPECIMENS AFTER TESTING AT 2450°F IN FLOWING AIR

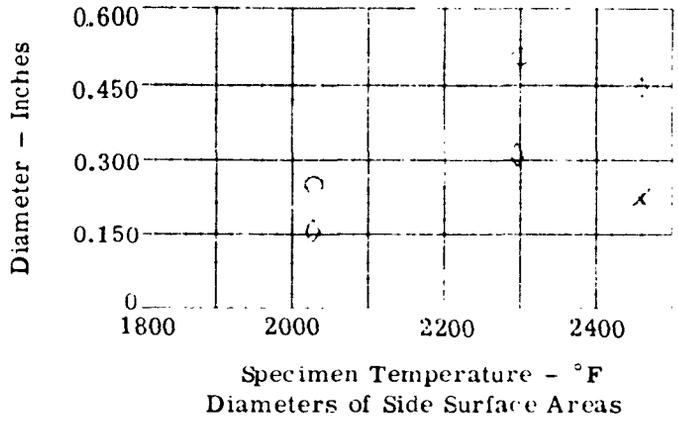

○ 500 Lb/Ft^{2}Hr, Drill
△ 5000 Lb/Ft^{2}Hr, Drill
◇ 500 Lb/Ft^{2}Hr, Rockwell
× 5000 Lb/Ft^{2}Hr, Rockwell

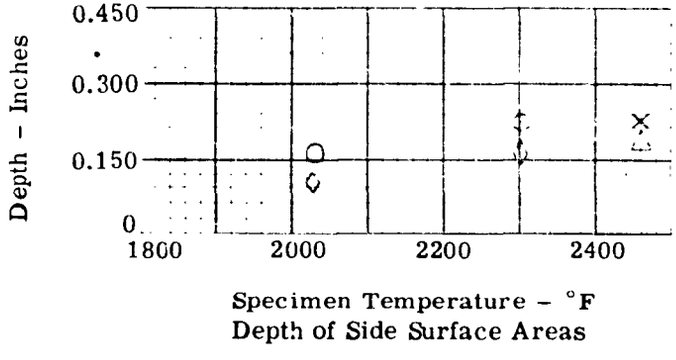

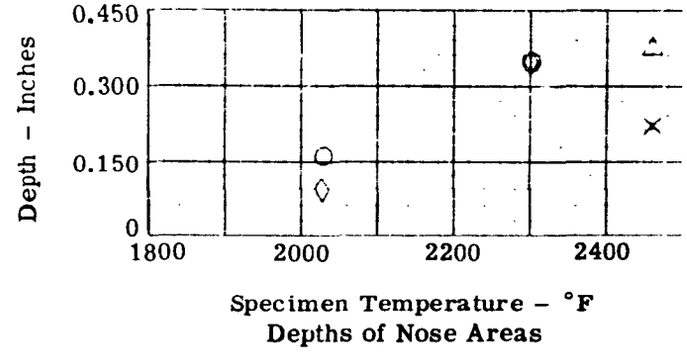

FIGURE 26. DIMENSIONS OF DAMAGED AREAS IN DURAK MG COATED 0.5% TITANIUM MOLYBDENUM ALLOY SPECIMENS AFTER TESTING

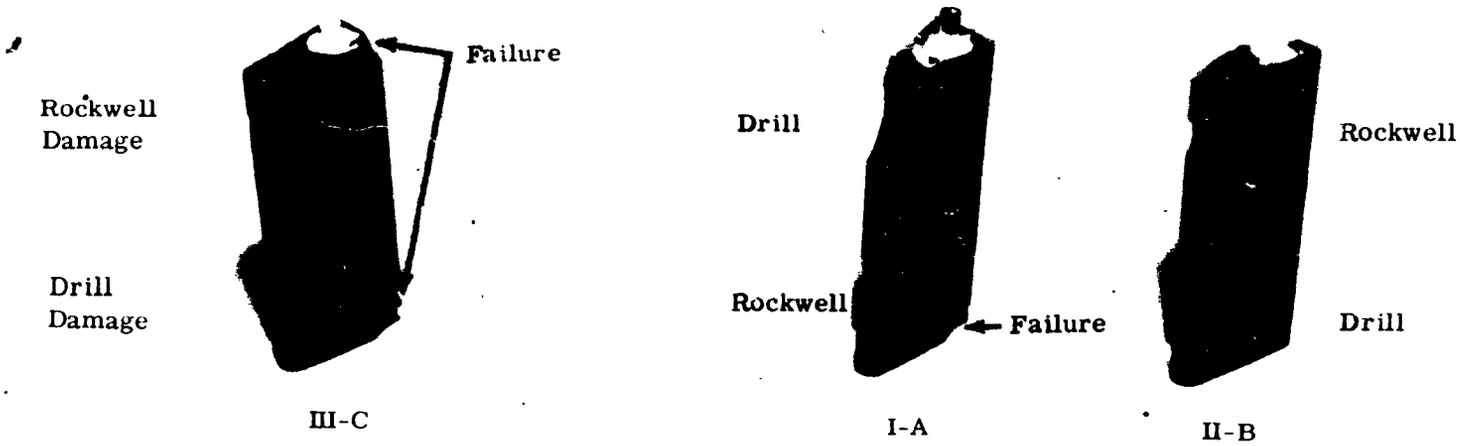

III-C

Mass Velocity: 500 Lb/Ft^{2}Hr

Test Temperature: 2000°F

I-A

Mass Velocity: 500 Lb/Ft^{2}Hr

II-B

Mass Velocity: 5000 Lb/Ft^{2}Hr

Test Temperature: 2450°F

FIGURE 27. DAMAGED DURAK MG COATED 0.5% TITANIUM MOLYBDENUM ALLOY OXIDATION SPECIMENS AFTER TESTING AT 2000°F AND 2450°F IN FLOWING AIR

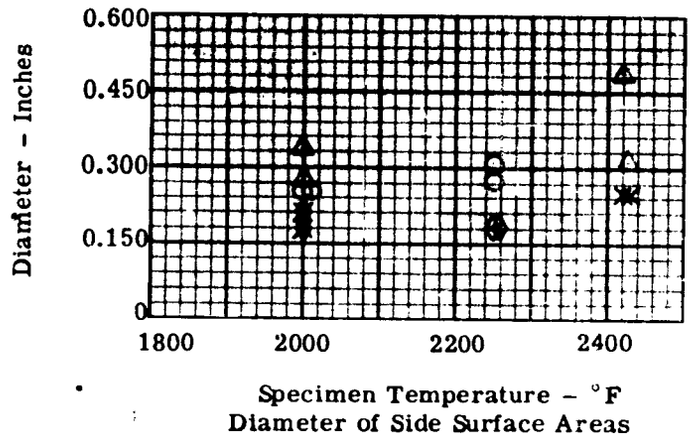

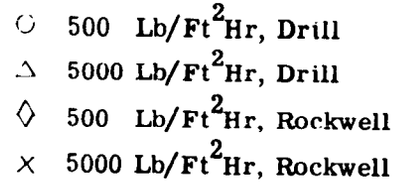

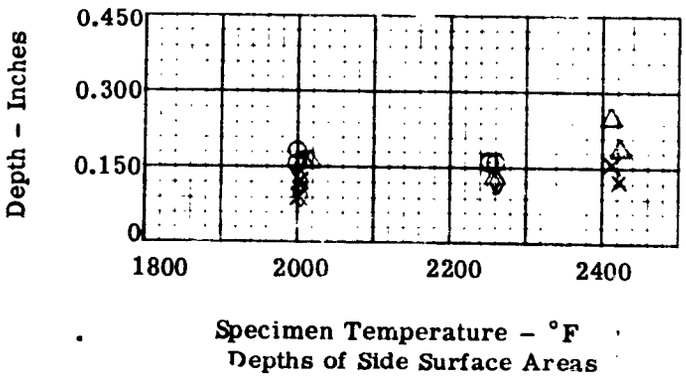

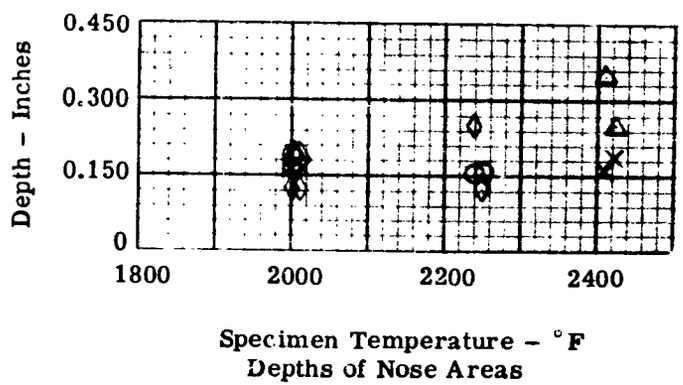

FIGURE 28. DIMENSIONS OF DAMAGED AREAS IN SILICONIZED ATJ GRAPHITE SPECIMENS AFTER TESTING

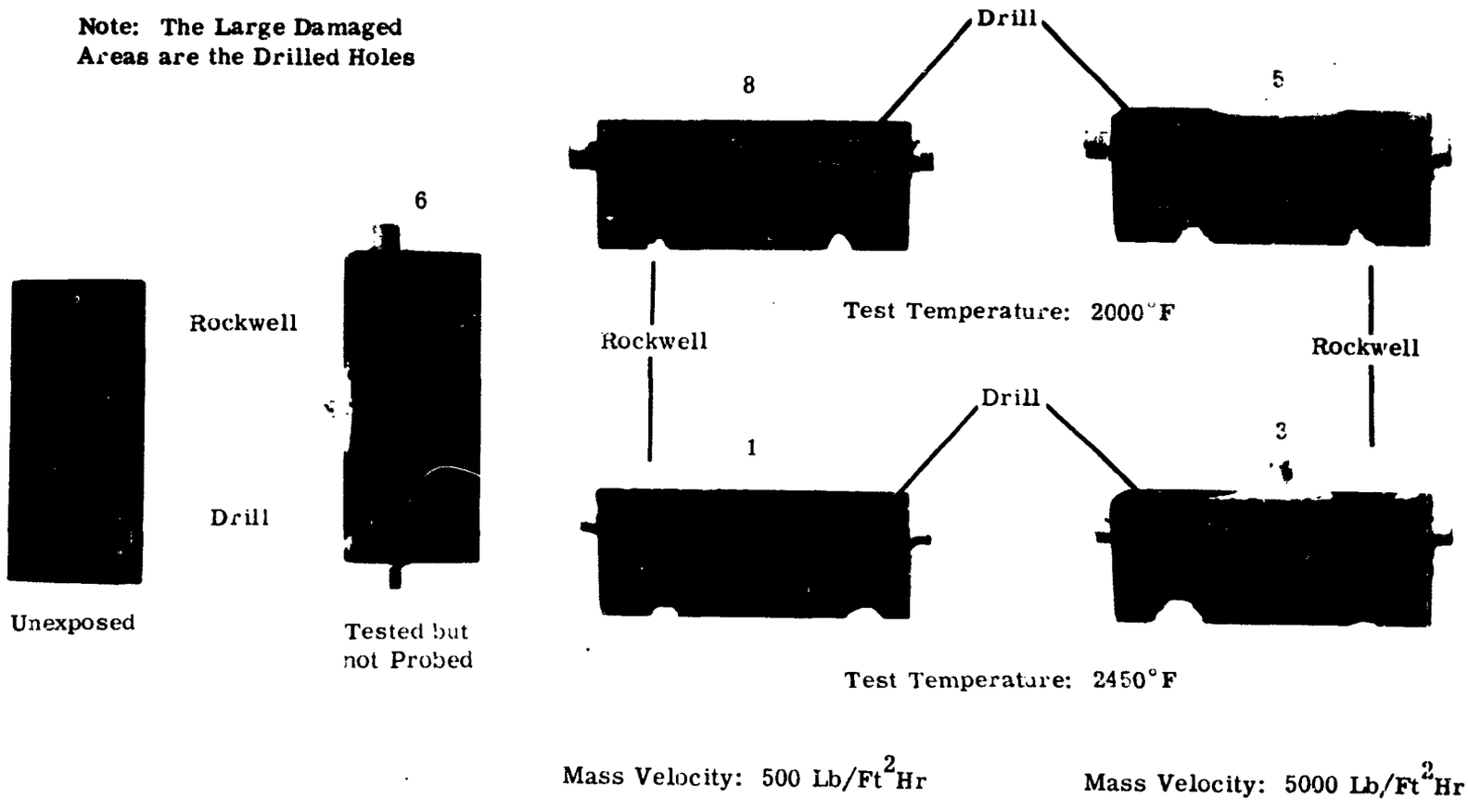

FIGURE 29. TYPICAL DAMAGED SILICONIZED ATJ GRAPHITE OXIDATION SPECIMENS BEFORE AND AFTER TESTING

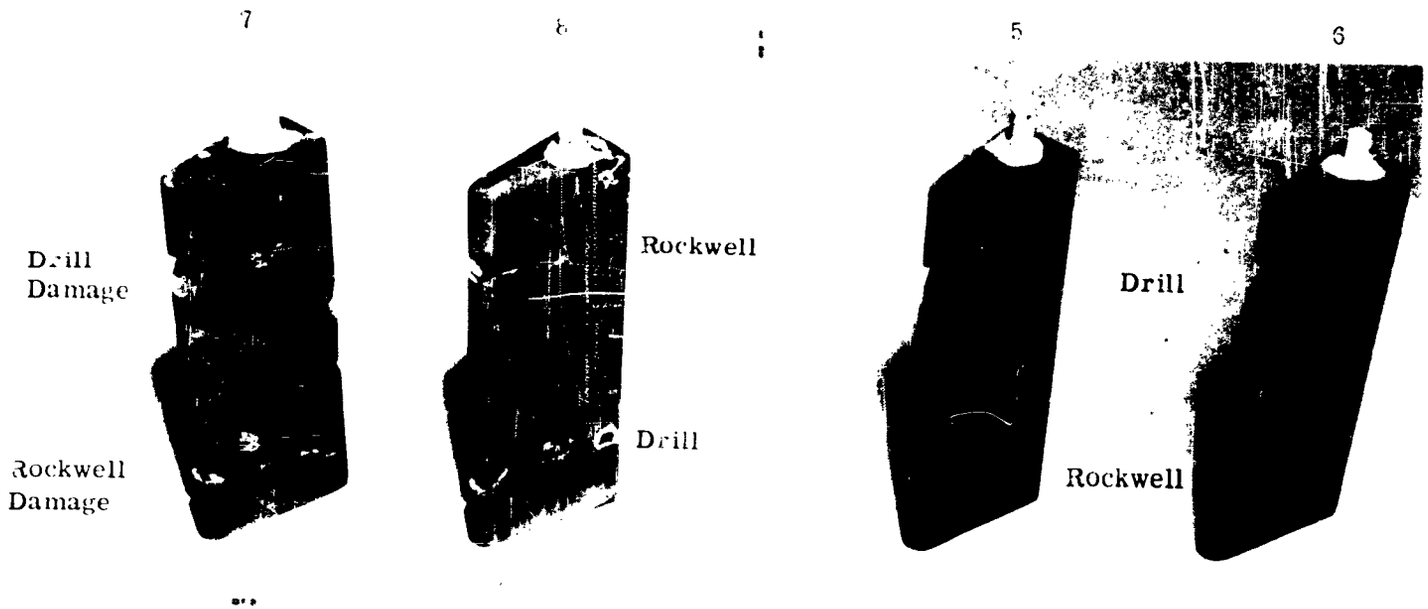

FIGURE 30. DAMAGED SILICONIZED ATJ GRAPHITE OXIDATION SPECIMENS AFTER TESTING AT 2000°F IN FLOWING AIR

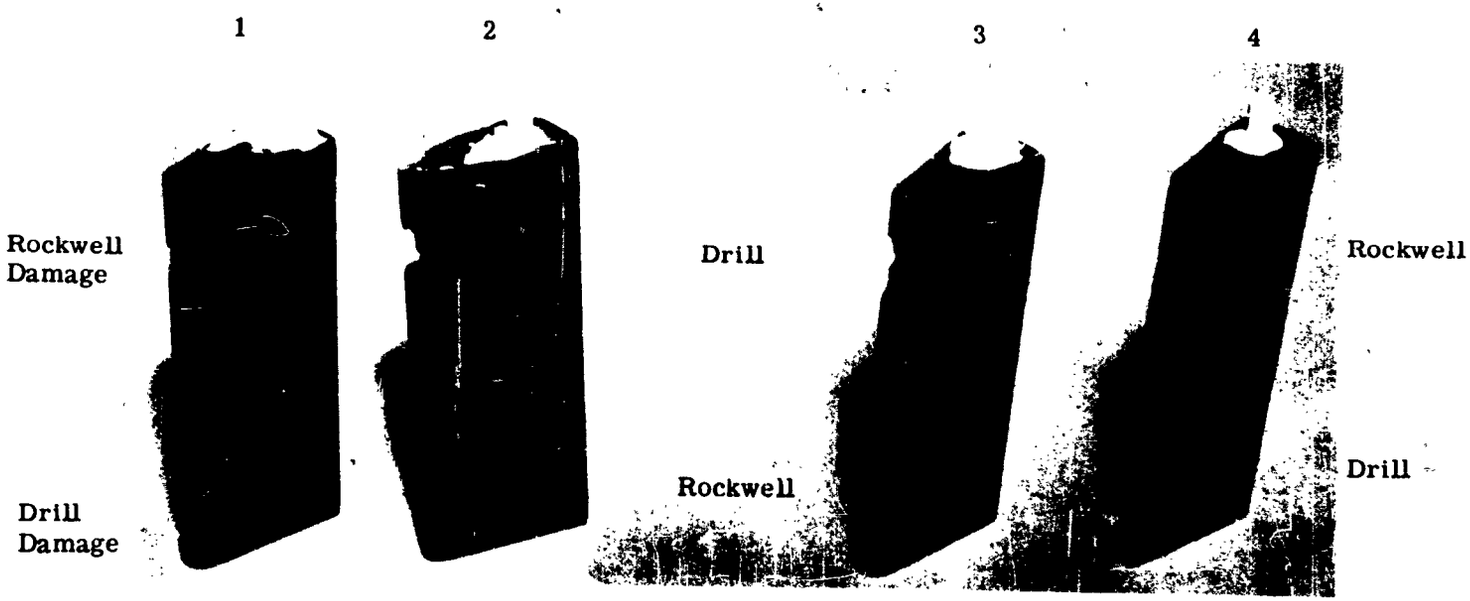

FIGURE 31. DAMAGED SILICONIZED ATJ GRAPHITE OXIDATION SPECIMENS AFTER TESTING AT 2450°F IN FLOWING AIR

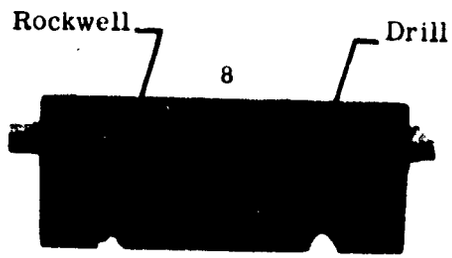

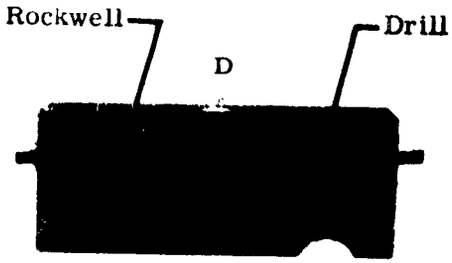

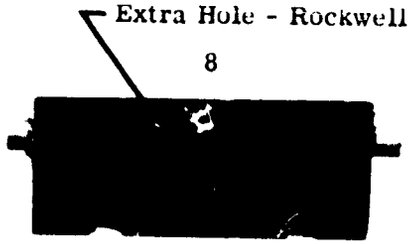

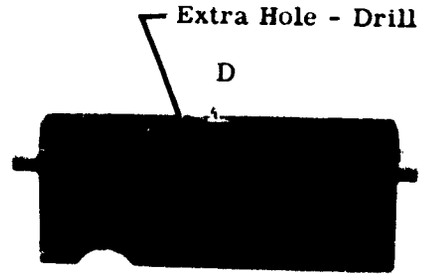

Test Temperature: 2000 F

Mass Velocity: 500 Lb/Ft^{2}Hr

Test Temperature: 2450F

MassVelocity: 5000 Lb/Ft^{2}Hr

FIGURE 32. EXTRA HOLE DAMAGE IN DAMAGED SILICONIZED ATJ GRAPHITE AND W-2 COATED 0.5% TITANIUM MOLYBDENUM ALLOY OXIDATION SPECIMENS AFTER TESTING

Before Testing

Test Temperature: 2450°F
Mass Velocity: 500 Lb/Ft^{2}Hr

W-2 Coated 0.5% Titanium Molybdenum Alloy

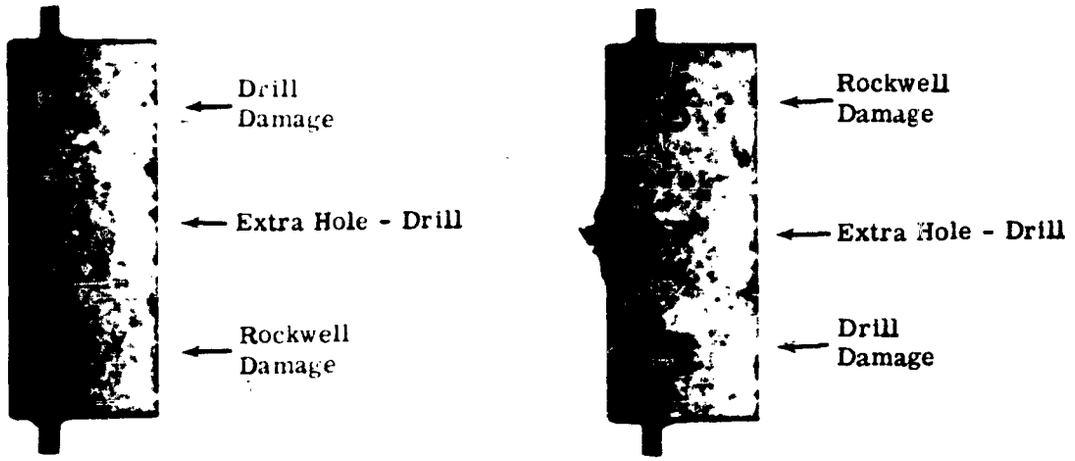

Before Testing

Test Temperature: 2000°F
Mass Velocity: 1500 Lb/Ft^{2}Hr

Siliconized ATJ Graphite

FIGURE 33. X-RAY OF TYPICAL DAMAGED SPECIMENS BEFORE AND AFTER TESTING

III. OXY-ACETYLENE TESTS AT 2750F AND 3000F

A. DESCRIPTION OF EQUIPMENT

The equipment used for this phase of the oxidation resistance evaluation consisted of: a small furnace heated by oxy-acetylene torches, a supply of oxygen and acetylene regulated to control flow rates and temperature, specimen support nozzles, an optical pryometer and Pt-Pt 10% rhodium thermocouples to measure specimen temperatures.

Figure 34 is an overall view of the test set-up. An interior view of the furnace showing one specimen in a mounted position is shown in Figure 35 The outside dimensions of the furnace were 13" diameter by 10" in height. The inside dimensions were 5" diameter and 7" deep. The outside shell was constructed of sheet steel. The shell was lined with stabilized zirconia and zircon. Two openings 180° from each other were provided for the oxy-acetylene torches. Standard oxy-acetylene torches with water cooled jackets at the torch tips were used. Liquid oxygen was procured in standard bottles and purchased to a purity of 99.5%. Liquid acetylene was procured in standard bottles and purchased to commercial purity.

The holding fixture for the leading edge specimens was fabricated from stabilized zirconia by the Titanium Alloy Division, National Lead Company. The overall dimension of the tubular element was 3-3/4" OD, 6" long with a 3/16" wall. Four 1/4" grooves, 1-1/4" deep were cut into the walls to receive the test specimen support pins. Tongs, nominally 5 feet in length fabricated with W-2 coated molybdenum, were used for inserting and removing the oxidation test specimens.

Specimen temperatures were measured by two methods. A Leeds and Northrup Model 8862-C with a range of 775 C to 2800 C was sighted into the central thermocouple hole in the rear of the specimen. In addition, a platinum-platinum 10% rhodium thermocouple, with suitable insulator sleeving, was installed in one of the outer thermocouple wells. Output from the thermocouple was supplied to a direct temperature reading potentiometer, Technique Associates, Inc., Model 4D. The optical pyrometer and the potentiometer were calibrated at frequent intervals.

B. TEST PROCEDURES

The specimens received from the vendors were prepared in the following manner to provide for support during test and to provide a means of determining specimen temperature by thermocouple readings. Zirconia rods were slightly beveled on a grinding wheel to fit into the specimen support holes drilled into the ends of the samples (see Figure 111 of Appendix I). These were cemented in place with alumina-silica cement (Carborundum Company, QF-180). A platinum-platinum 10% rhodium thermocouple with high purity alumina sleeving was inserted into one of the smaller holes on the back side of the specimens (see Figure

of Appendix I). The small hole was loosely packed with high purity (99%) alumina powder before the thermocouple was installed. The positioned thermocouple was bonded in place with alumina-silica cement.

The furnace temperature and oxidizing atmosphere were controlled by varying the ratio of oxygen and acetylene introduced into the furnace. One of the torches was used to burn the acetylene-oxygen combination, while to assure an oxidizing atmosphere the other torch was used to introduce oxygen only. Optical and thermocouple measurements were made on a dummy specimen positioned in the furnace to establish flow rates of combustibles required to achieve the desired test temperature. Temperature adjustments were made by increasing or decreasing the amount of acetylene used.

When the desired test temperature was attained the dummy specimens were replaced by the test specimens for the selected time exposure at temperature. Temperature readings were taken at selected intervals by both platinum-platinum 10% rhodium thermocouples and the optical pyrometer. All of the specimens except the Durak MG coated 0.5% titanium molybdenum alloy and the W-2 coated 0.5% titanium molybdenum alloy specimens tested at 3000F were exposed for one hour cycles at temperature with temperature readings taken every 15 minutes. The Durak MG and W-2 coated molybdenum samples exposed to 3000F had exposure cycles of 15 minutes. Temperature measurements in this case were recorded every 5 minutes.

Upon removal from the furnace the specimens were observed visually for dark spots, and in the case of the molybdenum samples, white oxide fumes. After allowing each specimen to cool to approximately 300F, its surfaces were probed with a pointed instrument to determine failures. Since the coatings tend to maintain their integrity in many cases even though failure has occurred, visual observations alone could not always reveal the location of the failures. Failures could usually be found at the locations where the dark spots were discerned during the cooling cycle. The dark spots are caused by the void areas under the coating which permit higher cooling rates for the coating in damaged regions than for the remainder of the sample.

Sketches were made of the samples after each exposure and cooling cycle, noting damaged areas, color changes and other pertinent information.

Samples which passed the first thermal cycle without a coating failure are returned to the oxy-acetylene furnace for another cycle. Table 13 is the test schedule for this phase of the oxidation testing. The number of specimens, test temperatures and exposure times are noted in this table.

C. DISCUSSION OF TEST RESULTS

The siliconized ATJ graphite samples exhibited the best resistance to the oxidation tests performed in the oxy-acetylene furnace at both 2750F and 3000F. The siliconized specimens withstood at least 4 one hour cycles at 2750F. Four of the five specimens tested at 2750F showed no apparent oxidation after the fourth cycle. The Durak MG coated 0.5% titanium molybdenum alloy specimens exhibited the least resistance at both test temperatures.

Test conditions in the oxy-acetylene furnace could not be accurately controlled. Since test temperature was controlled by regulating the flow of combustible gases, it was not possible to obtain a constant mass flow rate for all of the specimens tested. Gas was lost through the openings on the side of the furnace, through which the torches were introduced. From the gas flow rate measurements (both oxygen and acetylene) made hourly, assuming complete combustion, it was possible to calculate the theoretical excess of oxygen present. Mass flow rates presented in Table 14 are only approximate, however.

During each day of test, bare graphite samples were exposed to the air stream for approximately 5 minutes to assure that an oxidizing atmosphere existed. Weight measurements were made before and after exposure so that at least a qualitative indication of the oxidizing environment was obtained. Table 15 compiles the results of the proof tests run on the bare graphite samples.

Six of the 34 samples tested were not exposed to an oxidizing atmosphere as indicated by a calculated "0" lb/ft^2hr of excess oxygen in Table 14. Of these, five performed no better than the average of the others tested at the same temperature under oxidizing conditions. The sixth (siliconized ATJ specimen J-8) sample was tested immediately after one of the bare control graphite specimens was exposed. The bare graphite exposed (Sample No. 33) had a weight loss of 9.6% per minute after a 5 minute exposure. This would indicate that the test atmosphere should have revealed coating failures on specimen J-8).

1. Durak MG Coated 0.5% Titanium Molybdenum Alloy

The average life of 5 specimens when exposed to 2750F was slightly better than one hour. Three of the samples failed after one hour, one after two hours, and the fifth after 23 minutes. Figure 36 is a graphic presentation of the test results for this series of tests. Figure 37 is a photograph of the specimens after test. Specimen No. 2, which dropped into the furnace and was destroyed, is not shown in the photograph.

The average life of the 5 specimens when exposed to 3000F was slightly more than 15 minutes. Four of the 5 specimens withstood a 15 minute cycle, while the fifth withstood two 15 minute cycles. Figure 36 is a graphic presentation of the test results for this series of tests. Figure 37 is a photograph of the specimens after test.

Since the W-2 and Durak MG coatings being evaluated are supposed to be similar, it would be expected that the oxidation resistance afforded by the two coatings would be similar. This, however, is not borne out by the data obtained during the oxy-acetylene furnace tests performed. Figures 38 and 39 are close-up photographs comparing specimens with the different coatings after being exposed to approximately the same test conditions. The damage to the Durak MG specimens is by far much more severe than that exhibited by the W-2 coated specimens.

Nine of the ten Durak MG coated specimens which failed had failures at the edges. These failures tend to indicate a difficulty of the Durak MG coating in protecting edges despite the fact that the edges had been rounded slightly.

Durak MG specimen No. 4 shown in Figure 37 had several failures. This specimen was exposed for an hour after the original failures were noted. It is believed that the failures on the face of this specimen were caused by a reaction between the nickel plated steel tongs employed initially and the specimen coating. This is evidenced by the failures occurring in that portion of the specimen where the tongs gripped and by the abnormal discolorations and glazes present. The probable tong failure phenomenon was also present on several other specimens (W-2 coated 0.5% titanium molybdenum alloy specimens Numbers 2, 4 and 5). To eliminate this condition during subsequent testing, W-2 coated molybdenum alloy hooks were used for inserting and removing specimens from the furnace.

Durak MG specimen Numbers 5 and 10, as shown in Figure 37, appear to have extreme coating failures at the corners. The zirconia support pins on both of these specimens failed just prior to removal of the specimens from the furnace, causing the samples to fall to the furnace floor. The discolorations present may be due to the reaction of the specimens with the furnace floor.

2. W-2 Coated 0.5% Titanium Molybdenum Alloy

The average life of six specimens exposed to 2750F was slightly better than 1-1/2 hours. Two failed after 3 hours, two after 1 hour, and one specimen after 25 minutes. Figure 36 is a graphic presentation of the test results for this series of tests. Figure 40 is a photograph of the specimens after test.

The average life of five specimens exposed to 3000F was slightly better than two 15 minute cycles. Three specimens failed after three 15 minute cycles, one specimen failed after two 15 minute cycles and one specimen after one 15 minute cycle. Figure 36 is a graphic presentation of the test results for this series of tests. Figure 40 is a photograph of the specimens after test.

Most of the W-2 coated specimens did not have edge failures. Eight of the eleven specimens tested had failures on the 2-1/2" x 1" faces. Specimen No. 11 had a leading edge failure.

W-2 specimens Numbers 8, 9 and 10 shown in Figure 40 do not have the degree of glassy surface as the other specimens tested, including those tested at 2750F. According to the approximate calculations performed, specimens Numbers 8, 0 and 10 were exposed to the lowest mass flow rates.

3. Siliconized ATJ Graphite

The average life of seven specimens exposed to 2750F was greater than three 1 hour cycles. No average life has been estimated since three of the specimens were still satisfactory after four 1 hour cycles, the maximum test duration. Figure 36 is a graphic presentation of the test results for this series of tests. Figure 41 is a photograph of the specimens after test. Of the six specimens exposed at 3000F the average life was greater than 1.5 hours. Five specimens were failed at the first hour while one was still intact after four hours. Figure 36 presents the test results graphically while Figure 41 presents the specimens after testing.

The siliconized ATJ graphite specimens were examined by X-ray by the vendor before and after siliconizing. The samples were categorized as follows:

Grade A - nearly perfect ATJ structure

Grade B - fair structure with minor specks, voids, or density gradients

Grade C - poor (mottled) structure - high density inclusions, finely divided into a low density matrix

The specimen supplier likewise employed the following three methods of quality control in applying the siliconized coating: (1) visual inspection, (2) weight pickup, and (3) dimensional change.

As reported in Appendix III of Volume VI, National Carbon suggested that coating quality is reflected more by sample weight pickup per unit area than by other factors.

"For a given graphite density and structure, a correlation exists between weight pickup per unit area of coating and resistance of oxidation. As graphite structure changes, however, so does the weight pickup per unit area. A high density, low porosity graphite shows a lower weight increase per unit area than a low density graphite under the same coating conditions. The indications are, however, that a low density graphite showing a high weight pickup per unit area is inferior in oxidation resistance to a higher density graphite showing a lower weight increase."

Table 16 lists the X-ray grade for each of the specimens tested and the weight pickup of the specimens during the coating process. The limited number of samples tested precludes the drawing of definite conclusions regarding the effect of X-ray grade and weight pickup on oxidation resistance. Nothing can be said regarding X-ray classification. There is only the slightest evidence that with greater coating pickup there is greater oxidation resistance.

The after-test appearance of siliconized ATJ graphite specimens C-11 and E-6 differ from the other specimens tested at the same temperature (Figure 41 Specimen C-11 shows discoloration on both sides of the specimen. Specimen E-6 has discolorations and failures on only one face of the specimen. The failures noted on E-6 are a series of small pock marks.

4. Preliminary Evaluations

Several preliminary studies were undertaken in the oxy-acetylene furnace before the specimens were tested. The first was to duplicate as closely as possible the conditions present when a failure occurred with a W-2 coated 0.5% titanium molybdenum alloy sample, during an oxidation test at 2600F in the large graphite resistance furnace under controlled conditions. This was done to investigate the reason for the failure. A W-2 coated molybdenum 0.5% titanium alloy specimen was prepared for insertion into the oxy-acetylene furnace. The right side was the same as that used for the specimen which

failed and the left side with an experimental method that was being verified. The left side support pin was a 1/8" diameter high purity alumina rod bonded in place with an alumina silica cement (QF-180). The thermocouple for this side was pt-pt 10% rhodium in high purity alumina sleeving. The thermocouple bead was coated with a slurry made of high purity alumina powder and water before it was inserted into the hole on the backside of the specimen. The thermocouple was bonded in place with QF-180. The right side support pin was a zirconia rod bonded in place with QF-180. The thermocouple for this side was also pt-pt 10% rhodium but this time with thermocouple sleeving which according to the vendor can withstand 2800F. QF-180 was used to coat the thermocouple bead and bond the thermocouple in place. Into the large hole in the backside of the specimen was bonded a third pt-pt 10% rhodium thermocouple. The sleeving in this case was high purity alumina with an outer sleeving of zirconia. Bonding was with QF-180.

The sample was placed into the zirconia nozzle with the furnace temperature set to assure a specimen temperature of 2600F. After one hour the specimen was removed and visual observations made. A slight fluxing action had taken place at the tip of the 2800F thermocouple sleeving. No changes were noted in the specimen. At the end of the second hour of exposure, the slight fluxing of the 2800F thermocouple sleeving continued and a slight glaze formation was noted on the surfaces of the specimen. At the end of the third hour the 2800F sleeving failed completely, the coating in the area of the sleeving had also failed as evidenced by the oxidation of the molybdenum. Hairline cracks were noted on the specimen wherever the zirconia tubing came in contact with the coating. Figures 42 and 43 show the various surfaces of the W-2 coated specimen after test. As a result of this investigation, further testing in the oxy-acetylene furnace was performed with high purity alumina sleeving and thermocouple beads covered with a high purity alumina and water slurry.

The second study was to continue at higher temperatures the exothermic reaction experiments reported in Volume III and Section II of this volume. Uncoated molybdenum samples were thermocoupled and exposed to 2300F, 2600F, and 2985F for 4 minutes, 2-1/2 minutes, and 2 minutes, respectively. The exothermic oxidation reaction caused the specimen temperature to rise a minimum of 250F above the temperature of the furnace environment. Figure 44 is a graph of the recorded specimen temperature as a function of exposure time in the furnace.

The last preliminary study was conducted to determine the suitability of the equipment and methods for controlled flow conditions at 3000F using a Durak MG coated specimen. The specimen was prepared with high purity alumina support pins bonded with alumina-silica cement (QF-180) and had high purity alumina thermocouple sleeving.

After one hour at temperature, the specimen exhibited only a glaze formation on its outer surfaces. Half way during the second hour at 3000F smoke was detected from the furnace opening. Upon removal from the furnace at the end of the second hour, a coating failure was noted at the center of the specimen leading edge. Small black specks were also noted along the leading edge. At one corner it appeared that part of the zirconia nozzle had reacted with the Durak MG coating.

An additional five minute exposure in the furnace did not show an exothermic reaction due to continued oxidation, as evidenced by the following temperature readings:

Time Minutes	°F
0	Placed in Furnace
1	2890
2	2950
3	3000
4	3000
5	Removed from Furnace

After removal from the furnace, the specimen was re-examined. The small black specks noticed after the second hour of exposure had grown in dimension and several became points of failure. A scratch was made through the coating at a point 3/4 inch from the edge (Figure 42). The purpose of this was to see if on exposure the coating would self-heal and prevent oxidation. The specimen was exposed for 15 minutes to 3000F. Definite oxidation was noted with no apparent evidence of self healing. The small black specks continued to grow larger, with many more becoming points of failure.

TABLE 13

TEST SCHEDULE FOR OXIDATION TESTING

IN OXY-ACETYLENE FURNACE

Specimen	Number of Samples Tested Test Temperature(1) 2750 ± 50F	3000 ± 50F
Durak MG Coated Molybdenum (2)	5	5
W-2 Coated Molybdenum (2)	6	5
Siliconized ATJ Graphite (3)	7	6

Notes: 1. The samples exposed to 2750F and the siliconized ATJ exposed to 3000F were removed after 1 hour cycles, cooled to approximately 300F and then inspected. The Durak MG and W-2 coated molybdenum samples exposed to 3000F were removed after 15 minute intervals.

2. These samples were tested until a coating failure occurred.

3. These samples were run for four 1 hour cycles or to failure, whichever occurred first.

TABLE 14

CALCULATED MASS FLOW RATES

Specimen	Test Temperature	Mass Flow Rate #/ft^2-hr Total Gas Stream	Mass Flow Rate #/ft^2-hr Theoretically Calculated Excess Oxygen
Durak MG Coated Molybdenum			
Sample No. 2	2750	315	0
3	2750	218	56
4	2750	209	34
5	2750	169	43
6	3000	188	0
7	3000	188	0
9	3000	209	45
10	3000	218	71
11	2750	158	23
12	3000	198	110
W-2 Coated Molybdenum			
Sample No. 1	2750	212	58
2	2750	206	59
4	2750	206	59
5	2750	234	45
6	3000	203	56
7	3000	198	110
8	3000	173	91
9	3000	176	117
10	3000	132	30
11	2750	170	29
12	2750	180	33
Siliconized ATJ Graphite			
Sample No. H-2	2750	272	47
G-1	2750	272	47
J-3	2750	198	58
B-6	2750	192	52
C-11	2750	204	36
E-6	2750	201	33
H-6	2750	100	48
E-8	3000	197	85
C-6	3000	276	0
K-3	3000	194	18
J-8	3000	194	0
J-1	3000	268	0
E-2	3000	150	62

TABLE 15

PROOF TESTS ON OXIDIZING CONDITIONS

Bare Graphite Sample No.	Date Check Made	Time of Exposure Min.	Test Temperature* F	Percent Weight Loss Per Min.
32	1st day	5	2750	7.0
33	2nd day	5	3000	9.6
34	3rd day	5	3000	9.6
35	4th day	3	2750	4.2
39	5th day	3.5	2750	5.7

* Test temperature was determined using a dummy specimen. The actual temperature of the specimen was not measured. Because of the possible exothermic nature of the reaction the loss rates do not necessarily correspond to the indicated test temperatures. The purpose of this testing was to demonstrate the existence of oxidizing conditions.

TABLE 16

IDENTIFICATION OF SILICONIZED ATJ SPECIMENS

Specimen No.	X-ray Grade(1)	Weight Pickup (2) grams	Cycles to Failure
2750F			
H-2	AB	1.73	4+
G-1	AB	2.06	4+
J-3	AB	2.53	4+
B-6	AB	1.45	4
C-11	AB	1.55	2
E-6	AB	1.85	1
H-6	AB	1.92	2
3000F			
E-8	AB	1.72	1
C-6	C	1.70	1
K-3	AB	1.90	1
J-8	AB	2.46	4+
J-1	AB	2.28	1
E-2	C	1.49	1

Notes: 1. Definitions of the X-ray grades are:

A - nearly perfect ATJ structure

B - fair structure with minor specks, voids or density gradients

C - poor (mottled) structure - high density inclusions, finely divided in a low density matrix

2. All of the tested specimens were coated during National Carbon Run No. G-18.

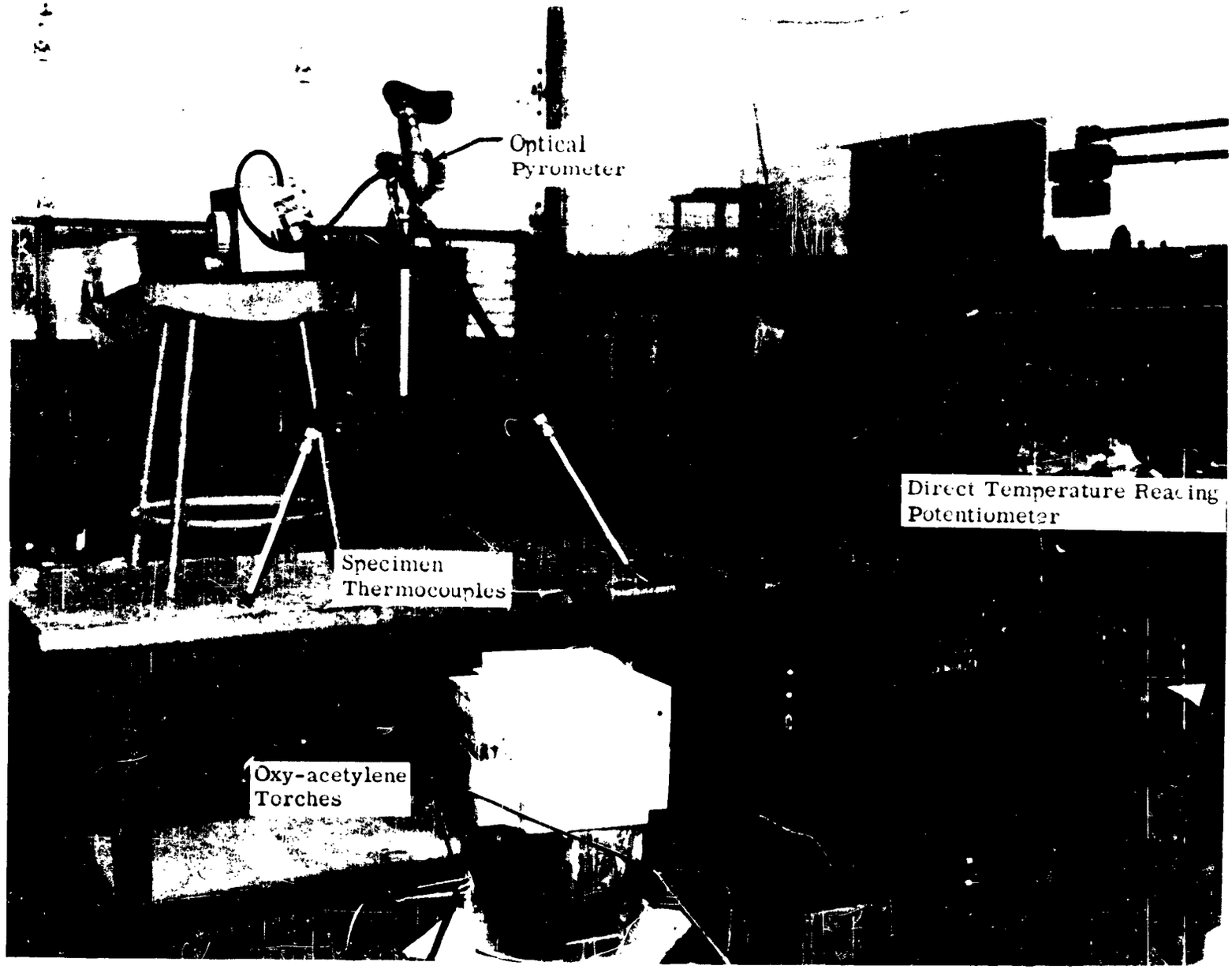

FIGURE 34. OVER-ALL VIEW OF OXY-ACETYLENE OXIDATION RESISTANCE TEST SETUP

FIGURE 35. INTERIOR VIEW OF OXY-ACETYLENE TEST FURNACE WITH ONE SPECIMEN IN PLACE

FIGURE 36. GRAPHIC PRESENTATION OF TEST RESULTS ON COATED SPECIMENS

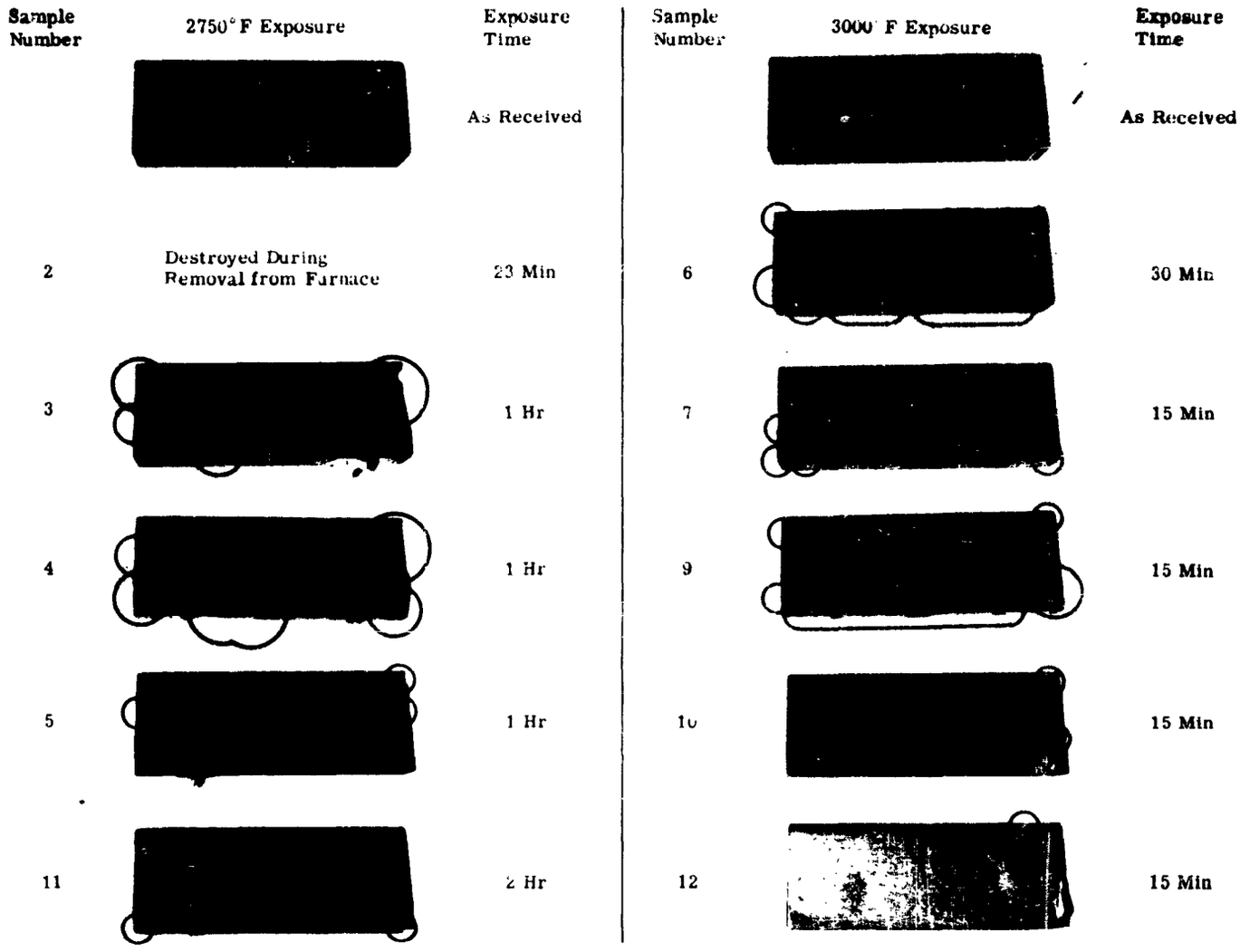

FIGURE 37. DURAK MG COATED MOLYBDENUM EXPOSED TO AN OXIDIZING ATMOSPHERE (FAILURES ENCIRCLED)

1 Hour
Exposure

Durak MG Sample No. 4

1 Hour
Exposure

W-2 Sample No. 2

FIGURE 38. CLOSEUP VIEW OF 0.5% TITANIUM MOLYBDENUM ALLOY COATED SAMPLES AFTER EXPOSURE TO 2750°F

FIGURE 39. CLOSEUP VIEW OF 0.5% TITANIUM MOL[illegible]BDENUM ALLOY COATED SAMPLES AFTER EXPOSURE TO 3000°F

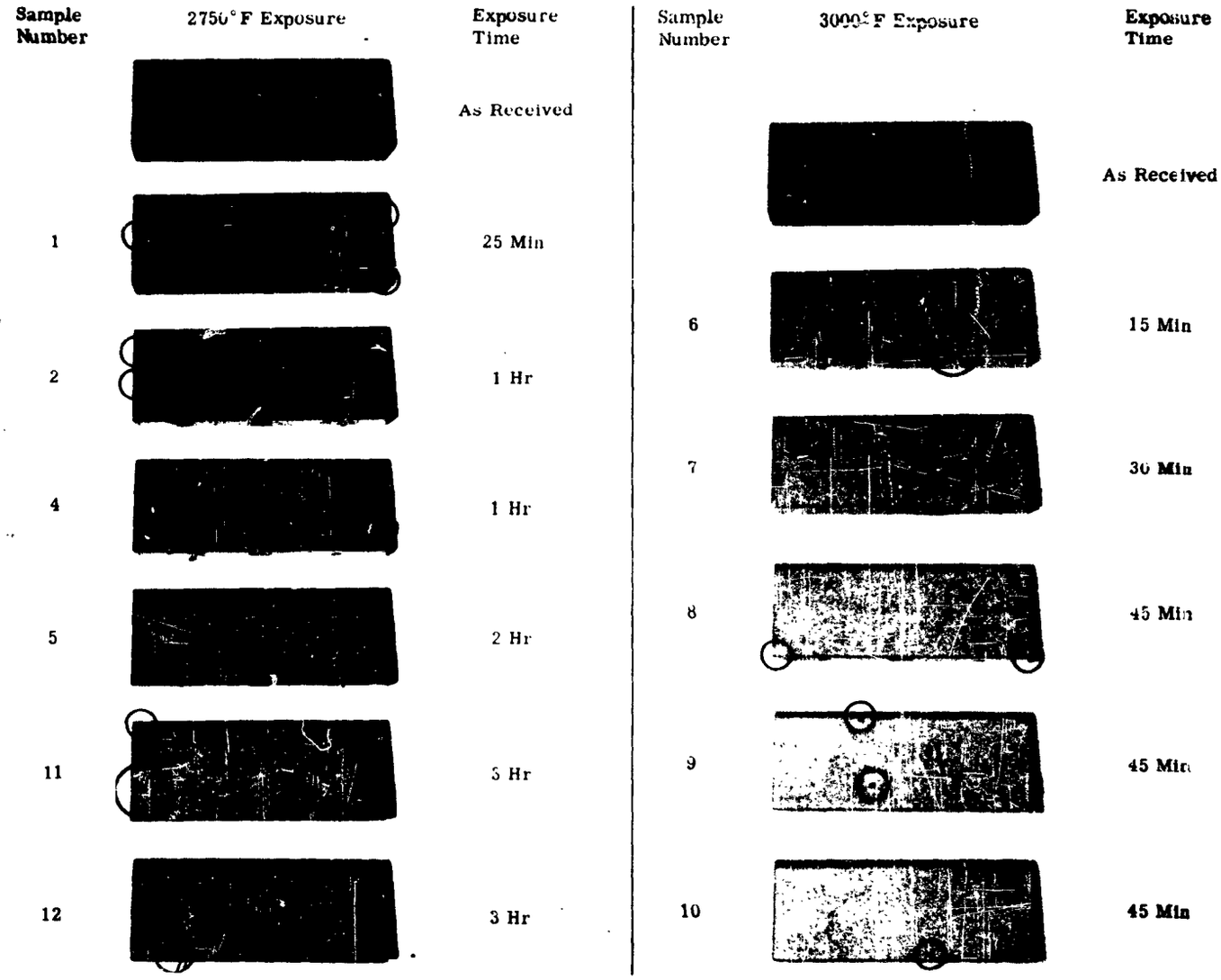

FIGURE 40. W-2 COATED MOLYBDENUM EXPOSED TO AN OXIDIZING ATMOSPHERE (FAILURES ENCIRCLED)

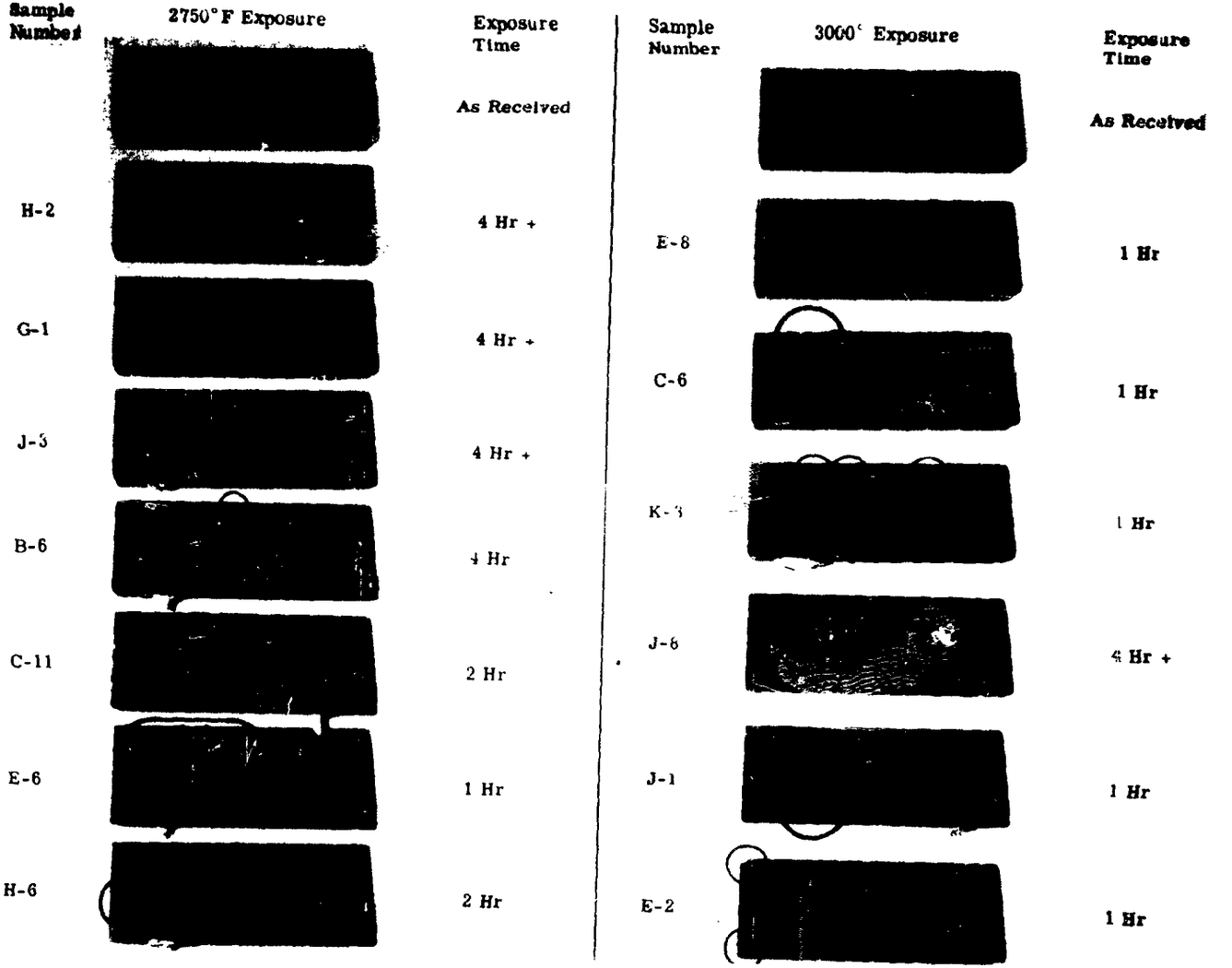

FIGURE 41. SILICONIZED ATJ COATED GRAPHITE EXPOSED TO OXIDIZING ATMOSPHERE (FAILURES ENCIRCLED)

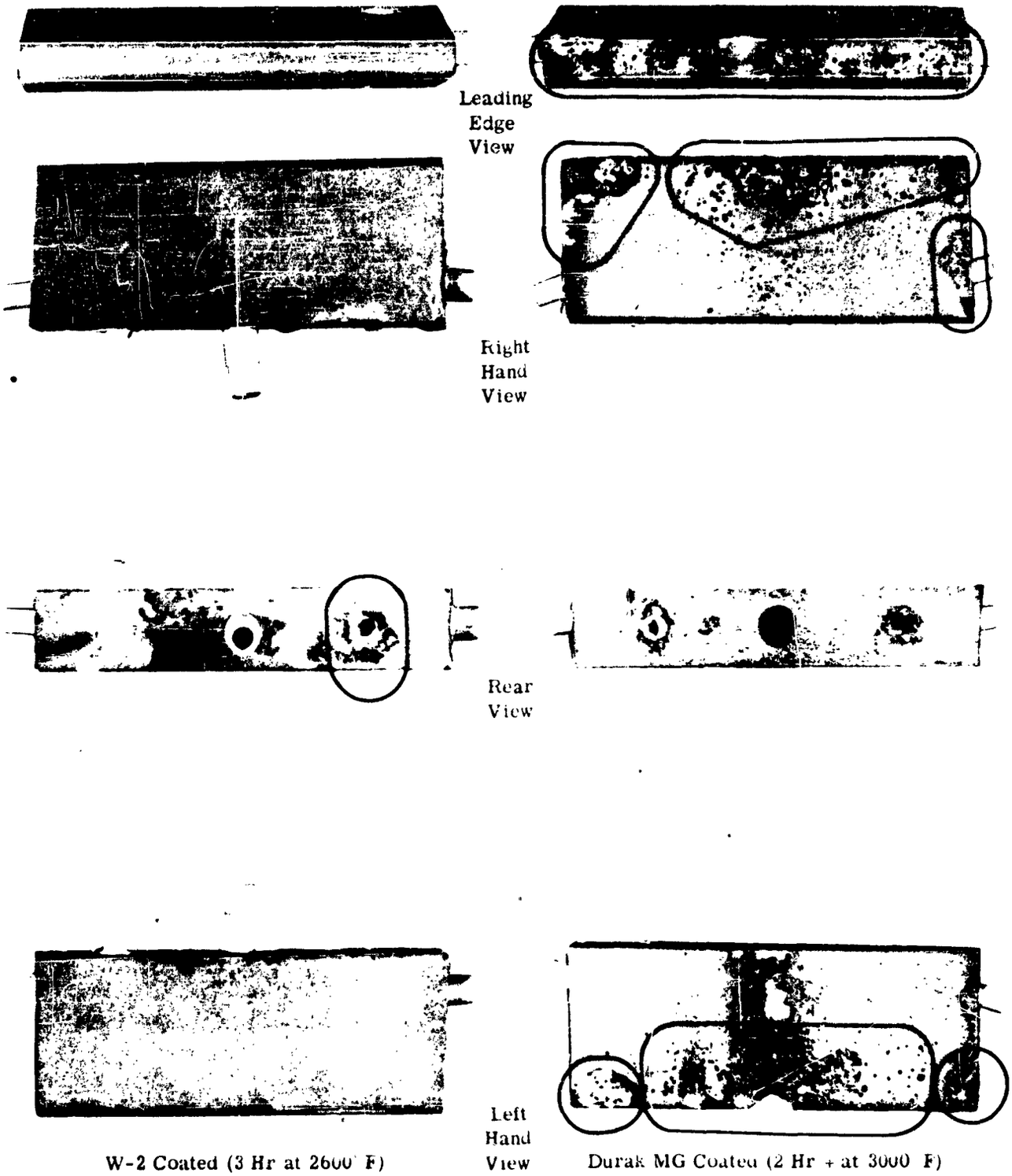

FIGURE 42. COATED MOLYBDENUM SPECIMENS AFTER TEST (FAILURES ENCIRCLED)

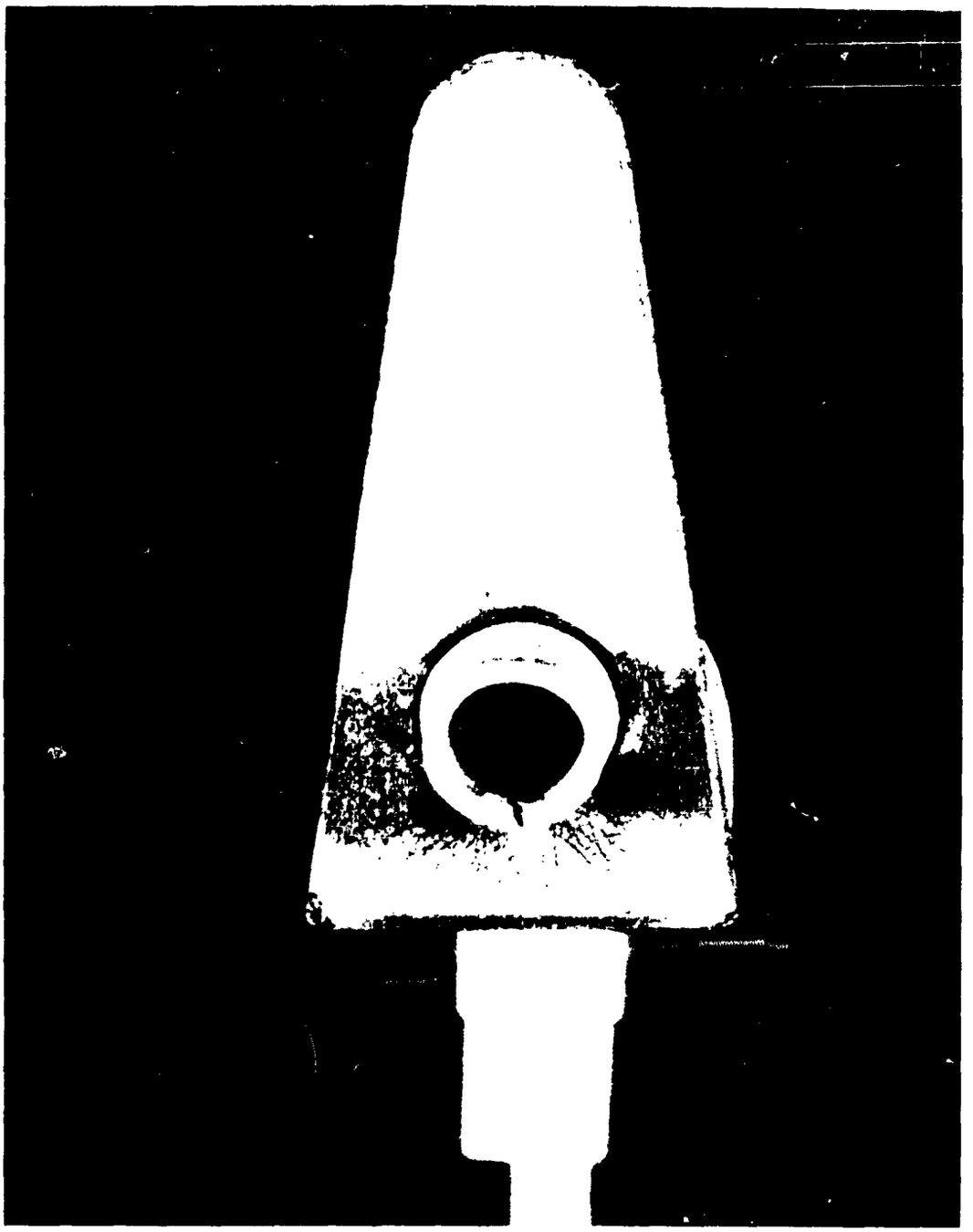

FIGURE 43. SIDE VIEW OF W-2 COATED MOLYBDENUM SPECIMEN SHOWING ZIRCONIA SUPPORTING ROD (AFTER 3 HOURS AT 2600°F)

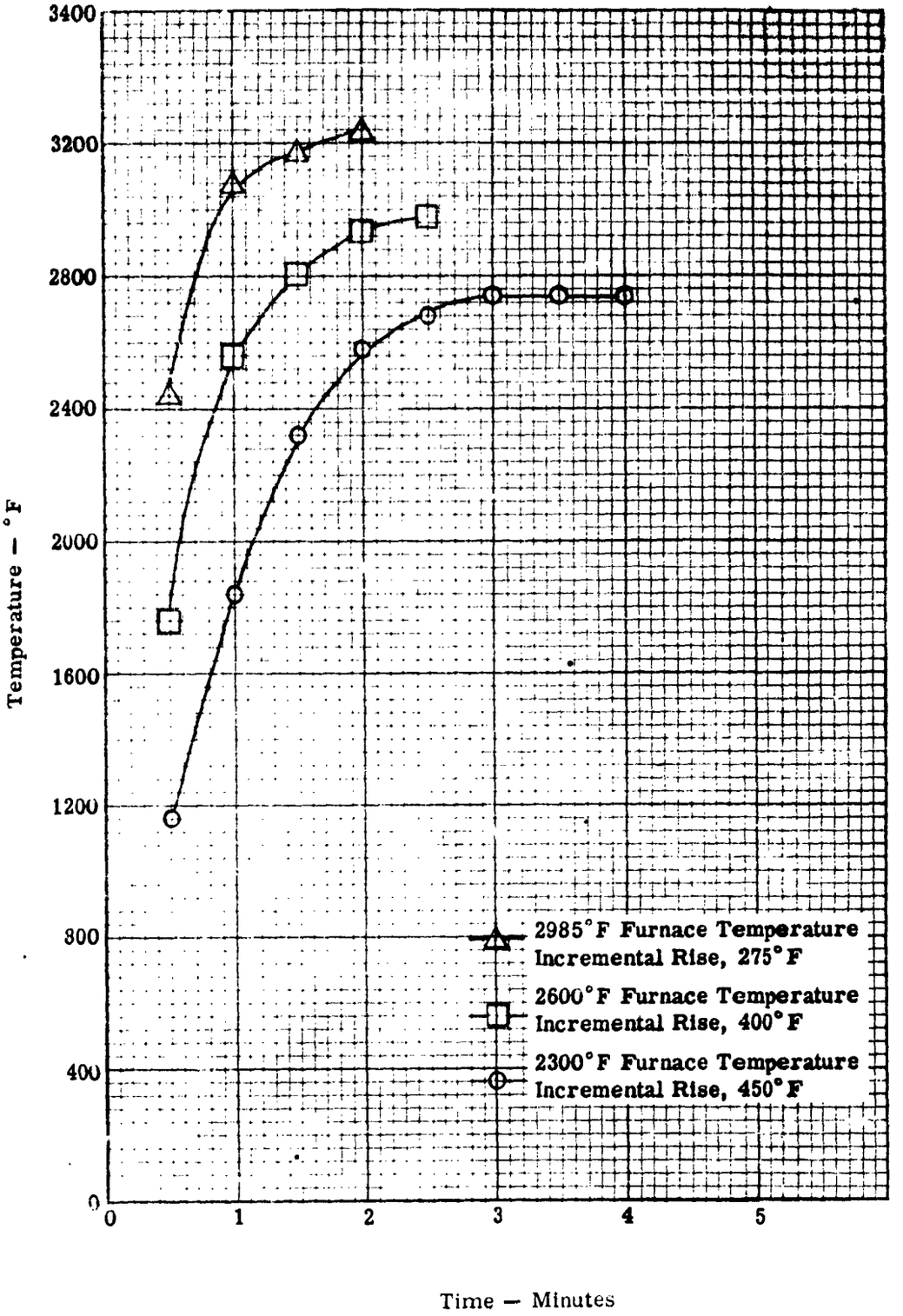

FIGURE 44. UNCOATED MOLYBDENUM SPECIMEN TEMPERATURE VS TIME OF EXPOSURE IN FURNACE

IV. ARC PLASMA TESTS

A. DESCRIPTION OF EQUIPMENT

For the arc plasma testing portion of this contract, three different arc jets were employed. Two are located at the Langley Research Center of NASA and are operated by the Structures Research Division; the third is located at the Plasmadyne Corporation. Descriptions of the facilities are presented in the following sub-sections.

1. NASA Langley Research Center Arc-Jet No. 20

Arc-Jet No. 20 is a vertical 1500 Kw AC arc jet which exhausts to the stmosphere; the chamber pressure is slightly above atmospheric. Air velocity is low subsonic, approximately 300 to 400 feet per second. It has a 6 inch diameter axisymmetric exit nozzle, made of graphite, and the arc chamber is a graphite cylinder of approximately 1 inch wall thickness. The arcing occurs phase-to-phase among 6 graphite electrodes of about 1.5 inches diameter, initially 18 inches long, equally spaced to form a circle. The electrodes are mounted in water-cooled holders, and extend through a perforated fused quartz plate, clearance between the electrodes and the holes in the plate provide 6 flow passages for air flowing toward the arc.

The arc chamber has an inside diameter of 18 inches. The arc is started by moving one pivoted electrode to make a short circuit contact with a neighboring electrode. After this contact has heated the 2 short-circuited electrodes for several seconds, an air cylinder rotates the pivoted electrode to its normal vertical position, and an arc is thereby created which spreads to the remaining 4 electrodes. The arc chamber is cooled by external coils containing circulating water which reduce radiation to the test cell walls and adjacent operating personnel.

A series of orifices and pressure pickups upstream of the jet are continuously monitored to insure a constant mass flow of air during any one test; they provide variable mass flow when it is desired to vary air temperature and heat transfer rate.

After passing over the test model, the jet exhausts into a duct which is slightly evacuated by an air ejector to take exhaust products out of the laboratory. The carbon content of Arc-Jet No. 20 is well below 5% by weight. The run time at high power (1500 Kw) is limited to 5 minutes by the capacity of the water cooling system in the power generating equipment. The reactor in the power circuit is a series of copper coils with air cores, and these coils contain circulating water for cooling. After 5 minutes of running, the water in the coils begins to boil, and operation of the arc must be terminated. Except for the cooling limitation, the run time at full power could be extended considerably; the air supply and electrode life is sufficient for times in excess of 5 minutes. By operating the arc at low power (600 Kw) the run time can be extended to 10 minutes, even with the cooling limitation.

The gas temperature at the nozzle exit of Arc-Jet No. 20 was measured spectrographically and found to be 9000°F for the 1500 Kw, 0.24 lb/sec mass flow condition. Measurements of gas temperature above the nozzle exit, at locations corresponding to specimen locations during test, could not be made spectrographically. A cooled gas pyrometer, described in NACA TN 4383, was used to measure gas temperature above the nozzle, but no satisfactory results were obtained. There are, therefore, no measured values for gas temperature at the specimen in Jet No. 20, nor at any location for other than the 1500 Kw, 0.24 lb/sec operating condition.

The test specimen is supported in the jet by a graphite wedge above the specimen, which is a continuation of the specimen contour, as well as two graphite wedges mounted alongside both the upper wedge and the specimen. A 1/32 inch thick layer of fibrequartz isolates the specimen from its supports. The specimen is attached to the adjacent supports by means of 2 graphite pins; the adjacent supports are, in turn, attached to the upper support wedge by 4 steel screws. Finally, the upper support wedge is suspended from a water-cooled sting, which can be raised or lowered by a hydraulic support column, so that the specimen height relative to the jet nozzle can be varied during a run although in the present tests the specimens were held to a fixed position throughout the run.

Figure 45 shows the specimen supported as described above. Figure 46 is a detail drawing of the specimen holder, and shows the passages through which the leads to the thermocouple, embedded in the specimen, were routed to the recorder. Table 17 summarizes the characteristics of Arc-Jet No. 20 applicable to the tests described in Section IV.C.

2. NASA Langley Research Center Arc-Jet No. 10

Arc-Jet No. 10 is a horizontal, variable power AC arc-tunnel which exhausts to a chamber evacuated by an air ejector; for the tests conducted in Jet No. 10 during this program, the chamber pressure was approximately 2.0 psia. The arc was operated at a power level of 1250 Kw, and the air velocity at the exit of the 6 inch diameter test section was approximately 1000 feet per second. The arc chamber is made of stainless steel, and has a graphite liner; it is 20 inches in diameter in the electrode region, tapering, through a subsonic nozzle, to the 6 inch test section diameter.

The electrodes are copper and are water-cooled. They are in the form of 6 concentric rings, 2 rings for each of the 3 phases, and arcing takes place phase-to-ground. Starting the arc is achieved by placing a thin copper wire across the electrodes to form a short circuit; by the time the wire has burned, the arc has been struck.

Arc-Jet No. 10 has a variable mass flow capability. The hot gas, after passing over the test specimen, exhausts through the air ejector to the atmosphere. The air supply for the air ejector which reduces the tunnel chamber pressure is the limiting factor as far as tunnel run time is concerned; it is the fact that only something over 1 minute of ejector air supply is available that limits the run time to somewhat over 1 minute. At atmospheric chamber pressure, Arc-Jet No. 10 can run for periods much greater than 1 minute.

The carbon content in Arc-Jet No. 10 is negligible; the gas temperature at the specimen is 7300°F, measured spectrographically.

Specimens tested in Arc-Jet No. 10 are supported in a manner similar to that described for specimens in Arc-Jet No. 20, although the wedge behind the specimen is shorter, and the sting does not require water cooling because of the short run times.

Figure 47 is a detail drawing of the specimen holder used in Arc-Jet No. 10. Table 18 summarizes the characteristics of Arc-Jet No. 10 applicable to the tests described in Section IV.C.

3. Plasmadyne Corporation Arc Tunnel

Plasmadyne Corporation's arc plasma tunnel is capable of simulating flight velocities in the atmosphere up to 25,000 feet per second and flight altitudes up to 300,000 feet, conditions which correspond to tunnel operating stagnation enthalpies up to 18,000 BTU per pound. Figure 48 shows this simulation range and includes the point corresponding to the conditions under which the tests described in this report were run. The simulation point is determined from conditions at the stagnation point of the specimen, behind the bow shock wave; specifically, the stagnation point pressure, p_o', and the stagnation enthalpy, h_T. These same values would exist behind the bow shock wave in flight, although the flight conditions that produce them would be different from the free stream conditions in the arc jet. That is, the free stream conditions in flight ahead of the shock wave, the free stream velocity, density, and pressure, are not duplicated in the tunnel, or in other words, the free flight Mach number is different from the tunnel Mach number. These facts concerning simulation should be borne in mind when data from Figure 48 is compared with data from Table 19.

The test chamber is a cylindrical pressure-tight tank, water-cooled, which is connected to a vacuum system. It contains several viewing ports, some offset, which permit both visual and photographic observation of the test specimen, and which allowed optical pyrometer readings to be made on both the leading edge radius and on points on the skirt of the specimen. Figure 49 shows the test chamber with the plasma head and nozzle attached.

The plasma generating system consists of the plasma head, a mixing chamber, and a nozzle; the system is shown schematically in Figure 50. The two electrodes are made of tungsten and are water-cooled; the arc strikes between them in the arc chamber. The working gas enters the arc chamber tangentially and is swirled through it into the hollow front electrode, then the mixing chamber, and finally issues from the nozzle into the test section, passing over the test specimen. Additional gas, either the same or different from that injected into the arc chamber, can be added through the radial holes located in the mixing chamber. In order to minimize oxidation of the electrodes when the test gas is air, nitrogen is injected into the arc chamber, and oxygen is added to the gas stream in the mixing chamber; this method was used for the tests described in this report.

The Mach number in the hot jet depends on gas type and stagnation temperature and pressure, as well as on the state of the gas, the nozzle contour, and the uniformity of the flow ahead of the nozzle. The particular nozzle used for these tests was designed to achieve a jet Mach number of 3.0 and a jet diameter of 3 inches.

Figure 50 includes schematic pressure taps at two locations in the gas flow path. The pressure measured by a wall tap in the mixing chamber, p_T, is both the static pressure in the mixing chamber and the stagnation pressure throughout the flow path. A wall tap at the nozzle exit measures the exit static pressure, p, less than p_T by an amount equal to the velocity head at the nozzle exit. A pitot tube at the nozzle exit would measure a third pressure, p_o', the pressure behind the shock wave caused by the presence of the pitot tube in the supersonic stream. p_o' is less than p_T by an amount equal to the loss across the shock wave. p_T, p and p_o' are included in Table 19; it should be noted that p_T is the pressure shown in Figure 48, representing stagnation pressure of the gas stream, but the stagnation pressure on the leading edge test specimen is p_o'.

For the present tests, the Plasmadyne arc tunnel was operated with a stagnation pressure, p_T, of 3.51 psia, a nozzle static pressure, p, of 0.068 psia, and a pitot pressure, p_o', of 0.68 psia.

The possible run duration in the Plasmadyne arc tunnel is in excess of 1 hour, since electrode erosion is very slight, the evacuation system is continuous, and cooling is available for both the test chamber, including the plasma generating system, and the instrumentation. The slight electrode erosion insures, in addition, an uncontaminated jet of plasma.

Gas temperature was not measured directly in the Plasmadyne arc tunnel. Calculations established that the gas approached a state of equilibrium, as shown by the comparison of measured and theoretical pressure ratios, Figure 51 and therefore a Mollier diagram for air provided a stagnation temperature for measured stagnation enthalpy and pressure conditions. Further gasdynamic calculations yielded a relative knowledge of gas temperature, density, and velocity, values of which are included in Table 19.

The test specimen was supported by a water-cooled graphite holder which positioned the specimen such that its spanwise axis was in a vertical plane. The holder, shown in Figure 52, was constructed by Plasmadyne personnel, and was designed for minimum interference with the leading edge specimens.

Table 19 summarizes the characteristics of the Plasmadyne Arc Tunnel applicable to the tests described in Section IV.C.

B. TEST PROCEDURE

1. General - NASA Langley Research Center

Twenty-four leading edge specimens, of the type described in Appendix I, were made available to the NASA Langley Research Center for testing in arc-jets. The 24 specimens included the following materials:

a. 6 bare ATJ graphite specimens
b. 6 siliconized ATJ graphite specimens
c. 4 bare molybdenum alloy specimens
d. 4 W-2 coated molybdenum alloy specimens
e. 4 Durak MG coated molybdenum alloy specimens

Five specimens, one of each material, was considered a set. In addition, trial samples of the same type as those listed above were supplied for preliminary runs in which specimen positioning and photographic and instrumentation techniques were established.

In view of the run times and gas conditions available in arc-jets Nos. 10 and 20, and realizing that a specimen in arc jet 10 might not reach the 3000°F surface temperature desired in all tests, during the limited tun time, it was decided to test only one set of specimens in arc-jet No. 10, the purpose being to determine the effect of reduced gas pressure on specimen behavior by comparing the condition of the set run in arc-jet No. 10 with a set run in arc-jet No. 20 for exactly the same time, except that a specimen which was unaffected during a 5 minute run in jet No. 20 was not run for 1 minute in jet No. 20, i.e., a material which showed no change during a 5 minute exposure was assumed to show no change during a 1 minute exposure, for the same conditions. Consequently, the following test program evolved, based on the need for the maximum amount of data for the number of available specimens, considering the arc-jet conditions available:

Number of Sets Run	Run Time	Arc Jet No.	Arc Power
1	5 minutes	20	1500 Kw
1	10 minutes	20	600 Kw
1	1+ minutes	10	1250 Kw
1, or part of 1, as needed	1+ minutes but equal to the time in arc-jet No. 10	20	600 Kw

Tests of all specimens were photographed in color; the film was exposed at the rate of 24 frames per second for the 1 and 5 minute runs, and at the rate of 12 frames per second for the 10 minute runs.

The specimen temperatures quoted later in Section C-2 are nominal values based on radiometer readings on the specimen leading edge and thermocouple readings obtained at a point within the specimen, half the specimen chord distance back from the leading edge. The radiometer data is based on emissivity values supplied by Bell Aircraft Corporation. The Barnes Engineering Company industrial recording pyrometer used during these tests is calibrated for certain emissivity values, and the calibrated values closest to those supplied by Bell were used in computing surface temperature, with the exception of bare molybdenum which, by trial, appeared to have a higher value of emissivity than the 0.3 specified by Bell.

The emissivity values supplied by Bell Aircraft Corporation were determined experimentally as part of this contract (see Volume IV); they were:

Bare ATJ graphite	0.75
Siliconized ATJ graphite	0.60
Bare molybdenum alloy	0.30
W-2 coated molybdenum alloy	0.60
Durak MG coated molybdenum alloy	0.60

2. NASA Langley Research Center Arc-Jet No. 20

The jet was calibrated for heating rate at specific specimen locations and jet power settings. Because of the many variables involved, it was necessary to locate the specimen by trial, for each material, in order to get the required 3000°F surface temperature. The approximate location could be established by the known heating rate data and the emissivity data, but accurate locations required trial runs.

The specimen temperature was measured in two ways: the interior temperature was measured by means of a platinum-platinum, 10% rhodium thermocouple located on the axis of symmetry of the specimen, 1/2 inch aft of the leading edge; the surface temperature at the stagnation region was measured by a Burns Engineering Company industrial recording pyrometer, Model No. R-4D1. In a number of runs, an optical pyrometer was used as a check on the stagnation region surface temperature. At equilibrium it was assumed that the internal temperature, as measured by the thermocouple, was within 100°F of the surface temperature, as measured by the radiometer; this value of temperature difference was based on an approximate analysis of the behavior of the specimen under combined conditions of conduction, convection, radiation, and re-radiation.

The specimen was photographed continuously throughout the entire test by two cameras at right angles, one recording the plan view, and the other the side view, providing a record of the specimen behavior during each test, on color film.

Each specimen was accurately weighed and measured before and after test, and changes were recorded. All pertinent arc jet parameters were recorded for each run, and the specimen surface temperature was continuously monitored. All specimens were returned to Bell Aircraft Corporation for final inspection.

3. NASA Langley Research Center Arc-Jet No. 10

The specimen location in Arc-Jet No. 10 was chosen to permit the specimen to be photographed through a window in the tunnel; the specimen location was not critical since, although the jet was calibrated for heating rate at the one position, the heating rate and gas temperature were essentially constant throughout the 6 inch diameter test section, 220 BTU/ft^2-sec and 7300°F, respectively. These values produced a maximum specimen surface temperature of approximately 3000°F, which was measured by means of a platinum-platinum 10% rhodium thermocouple only; the tunnel configuration made the use of a radiometer impractical. It was again assumed that at equilibrium, the thermocouple read 100°F less than the surface temperature.

The length of run was set by the predetermined capacity of the air ejector reservoir, approximately 80 seconds, 70 seconds of which comprised the actual time of exposure of the specimen to the hot gas stream. A run was started by turning on the air ejector to reduce the chamber pressure to 2.0 psia, after which the arc was turned on, with a low mass flow of air. After the arc stabilized, the mass flow of air was increased to the desired value, and upon stabilization of the mass flow, the specimen was placed in the hot gas stream by means of a system of pneumatically operated doors which fit the bottom of the tunnel test section.

Air mass flow, specimen temperature, and gas temperature were continuously monitored during each run, the last by means of a spectrograph, and each run was continuously photographed on color film.

Each specimen was accurately weighed and measured before and after test, and changes were recorded. All pertinent arc jet parameters were recorded for each run, and all specimens were returned to Bell Aircraft Corporation for final inspection.

4. Plasmadyne Corporation Arc Tunnel

Ten leading edge specimens of the type described in Appendix I were sent to Plasmadyne Corporation for arc jet testing, and included the following materials:

a. 2 Bare ATJ graphite specimens
b. 2 Siliconized ATJ graphite specimens
c. 2 Bare molybdenum alloy specimens
d. 2 W-2 coated molybdenum alloy specimens
e. 2 Durak MG coated molybdenum alloy specimens

Because of the limited funds available, Plasmadyne was requested to test all 10 specimens at the same tunnel operating point, with a run duration of five minutes each; with additional funds it would have been feasible to select a specific operating point for each material and to run the specimens which withstood the environment sufficiently well, for periods in excess of one hour.

The tunnel operating point was predicated on achieving a true temperature of 3000°F on the leading edge radius of a W-2 coated molybdenum alloy specimen.

The oxygen concentration in the gas mixture was based on providing a chemical composition at the specimen surface that would duplicate the composition at the vehicle surface during free flight, the free flight condition being that shown as the test point, Figure 48. The calculations which determined the required osygen concentration in the gas stream considered the fact that at the lower tunnel Mach number, the rate of diffusion of oxygen through the boundary layer would be different than the diffusion rate through the free flight, higher Mach number, boundary layer.* It was concluded that a free stream oxygen concentration of 10.8% by weight would provide the correct gas composition on the specimen surface, for the tunnel operating conditions (see Gas Flow Rate, Table 19). It has been found**, in fact, that beyond a concentration of 8% oxygen, a saturation condition is reached at which additional oxygen does not affect the oxidation rate. This saturation limit has been observed by Plasmadyne Corporation in laboratory tests where oxidation (not ignition) was of prime importance.

After establishing the operating conditions for the required test point, jet parameter data including stagnation enthalpy, pitot pressure, nozzle static and test section static pressures, mixing chamber pressure, and heat transfer rate, were measured. These data are included in Table 19 and are plotted in Figures 51 and 53. The particular flight altitude point simulated is shown on Figure 48, based, as previously stated, on conditions at the model stagnation point, behind the bow shock.

The stagnation enthalpy was determined by computing the amount of power remaining in the gas, assuming the only power loss was to the cooling water, and by measuring the gas flow rate. Previous experiments had shown that the power lost by radiation at the pressures being considered was extremely small. The power lost to the cooling water was determined from the cooling water flow rate and the measured temperature rise.

A water-cooled pitot tube, designed and developed at Plasmadyne, was used to obtain the stagnation point pressure on the surface of the specimen. The nozzle pressure taps, static and mixing chamber, are shown in Figure 50. The pitot, nozzle static, and mixing chamber pressures were read on Wallace & Tiernan absolute pressure gages. A hand-operated valve connected to the test chamber was used to balance the nozzle and test chamber static pressures to maintain a uniform jet with minimum shock or expansion waves. The Mach number plotted in Figure 51, was determined through the combination of pitot, static and total (mixing chamber) pressure measurements. As shown in Figure 51, the Mach number is 3.00, indicating the gas to be near equilibrium.

---

* Dennison, M. R. and Dooley, D. A., "Combustion in the Laminar Boundary Layer of Chemically Active Sublimators," Aeronutronics Systems Inc. Publication U-110, September 23, 1957.

** Personal communication with Dr. E. M. Kinderman, Stanford Research Institute.

The heat transfer rate to the stagnation point of the leading edge specimens was measured by a 5/8 inch diameter water cooled hemisphere calorimeter, designed and developed by Plasmadyne. The millivolt signal from this instrument was amplified (100X) and read on a Weston millivoltmeter. A radial survey was made using this instrument to establish the uniformity of the jet across the 2-1/2 inch specimens. The heat transfer distribution, plotted in Figure 53, shows an excellent degree of uniformity of the jet enthalpy distribution. Except for the outer region of cold boundary layer, the heat transfer rate was reasonably constant at approximately 396 BTU/ft^2-sec. This value represents the stagnation point heat flux sensed by the calorimeter, and must be adjusted to obtain the actual heat transfer rate experienced by the leading edge specimens, because: (1) the calorimeter is axially-symmetric whereas the specimen is two-dimensional, (2) the calorimeter is essentially cold wall whereas the specimen surface is about 3000°F, and (3) the calorimeter radius is 5/16 inch as compared with the 1/8 inch specimen radius.

The average value of heat transfer rate across the jet was taken as 360 BTU/ft^2-sec (see Figure 53) for the 2-1/2 inch specimen, as seen by the calorimeter. Using Lees' theory*, with equilibrium viscosity and a Prandtl Number of 0.75, the theoretical value of stagnation point heat flux was calculated to be 374 BTU/ft^2sec, which agrees fairly well with the experimentally determined values.

Since only one tunnel operating point was used for all 10 specimens, that is, the stagnation enthalpy and stagnation point heating rate was the same for each specimen, the surface temperature of the specimen was dependent on the emissivity of the specimen material. A Leeds and Northrup optical pyrometer was used for reading the apparent model surface temperatures, and corrections were made for the emissivity of each specimen and for the 1/2 inch Pyrex glass observation windows. At least one survey was made on the leading edge radius of each specimen, and in addition, temperature readings were taken at two different points 1/2 inch from the leading edge, on the skirt of the specimen.

Each specimen was weighed and measured before and after test, and changes were recorded. Where the chord dimension varied appreciably, measurements at three spanwise locations were made. Each test was continuously photographed on color film, with the film exposed at the rate of 12 frames per second. All specimens were returned to Bell Aircraft Corporation for final inspection.

---

* Lees, Lester, "Laminar Heat Transfer over Blunt Nosed Bodies in Hypersonic Flight," Jet Propulsion, Vol. 26, 1956.

C. TEST RESULTS

1. NASA Langley Research Center Tests

a. General

The gas temperature in Arc-Jet No. 10 was measured spectrographically and found to be 7300°F, as stated above in Section A.2. In addition, the gas temperature was essentially constant throughout the test section, so that 7300°F air passed over the test specimen.

Section A.1, in describing Arc-Jet No. 20, stated that measurements of gas temperature at points above the nozzle exit, corresponding to specimen locations during test, could not be made, either with a spectrograph or a cooled gas pyrometer. Furthermore, no gas temperature measurements could be made at other than 1500 Kw arc power, and 0.24 pounds per second air flow rate, so that no gas temperature information was available for the runs at arc powers other than 1500 Kw.

In the interest of presenting a complete data picture, the temperature situation in the free jet of Arc-Jet No. 20 has been estimated; oxidation behavior of major interest in these tests, and gas temperature implies gas composition. It should be clearly understood that all values quoted for gas temperature at the specimen in the NASA tests are the responsibility of the author, and not the responsibility of NASA Langley Research Center personnel.

Work done at Bell Aircraft Corporation concerning temperatures in the exhaust of turbo-jet engines has shown that the centerline temperature in a free jet is constant for a distance slightly exceeding 4 diameters of the exit nozzle. For NASA Langley Research Center Arc-Jet No. 20, therefore, it is assumed here that the 6 inch diameter nozzle exit produces a core whose temperature remains essentially constant for a distance of 24 inches above the nozzle exit, a distance within which all specimens were tested, and which has a diameter sufficient to envelop the leading edge specimens

The only measured value of gas temperature was the 9000°F temperature measured at the nozzle exit for 1500 Kw of arc power and a mass flow of gas of 0.24 pounds per second. For this combination of power and flow rate, then, the gas temperature was taken as constant, for all specimen locations, at 9000°F.

Other power-flow rate combinations were used to determine gas enthalpy, the variation being direct with arc power and inverse with mass flow rate, with the method including the assumption of constant arc efficiency. Temperatures corresponding to the calculated enthalpy values were then computed, considering real gas effects; these temperatures were also assumed to hold constant throughout the entire range of test specimen position.

The resulting gas temperature estimates are included in Tables 20, 21, 22, and 23; they are felt to be adequate to give an indication of the degree of dissociation of the gas flowing over the specimen, a quantity thought to be applicable to the consideration of specimen oxidation.

A fused quartz perforated plate fits over the 6 electrodes in NASA Langley Research Center's Arc-Jet No. 20. During some of the tests it is believed that quartz material from this plate was deposited on the specimen, and some of the weight gains shown later for the coated specimens may be due to either the deposited quartz or oxidation of the coating, or both. In the case of the bare specimens, the weight loss may have been retarded by deposit of the quartz. The presence of the rough, glass-like deposits also influences the change in chord measurement.

The difficulty in determining whether a weight or dimensional change was due to oxidation or a quartz deposit stems from the fact that in either case the foreign substance could be expected to be primarily silicon dioxide. It is believed that the roughness shown on most of the specimens after test in the NASA Arc-Jet No. 20, Figures 55 and 56, is deposited quartz from the jet; no such rough markings show on specimens tested in NASA Arc-Jet No. 10, Figure 57, or on those tested in the Plasmadyne arc tunnel, Figure 90.

The chord measurements applicable to the specimens tested at the NASA Langley Research Center are nominal values since, particularly after test, there is a slight spanwise variation in chord dimension.

As testing progressed at Langley Research Center it became necessary to add to the number of specimens contemplated under the program described in Section B.1, above, partly because some specimens did not receive their full exposure, and partly because additional specimens were made available. A net total of 25 specimens is therefore included in the results described later.

For comparison purposes, a specimen of each material was photographed before test, and the original appearance of the group of 5 specimens is shown in Figure 54. A typical group of specimens of each material is shown after nominal 5 and 10 minute runs in the atmospheric arc-jet and after nominal one minute runs in the arc tunnel in Figures 55, 56 and 57, respectively. Figure 58 shows all specimens, except trial specimens, which were tested at NASA Langley Research Center, compared with a set of specimens before test.

b. Bare ATJ Graphite Specimens

Five bare ATJ graphite specimens were tested, four at atmospheric pressure and one at a test section pressure of 2 psia. The maximum surface temperature-time history of these specimens during test is plotted in Figures 59 through 63. Table 20 shows that all specimens sustained a considerable loss of material, particularly specimens No. 25 and 29. Maximum surface temperature ranged from 3000°F to 3200°F, for all five specimens; gas temperature was higher in the atmospheric jet than in the arc tunnel, an estimated 9000°F to 10,000°F in the former, and 7300°F in the latter.

All bare and siliconized ATJ graphite specimens tested at NASA Langley Research Center were photographed after test, with a bare and coated specimen present for comparison, and are shown, with their designations, in Figure 64.

c. Siliconized ATJ Graphite Specimens

Six siliconized ATJ graphite specimens were tested, 5 at atmospheric pressure, and 1 at reduced gas pressure. The applicable test data is summarized in Table 21, and Figures 65 through 70 show a maximum surface temperature-time history for each specimen during test.

All 5 specimens subjected to the atmospheric pressure gas stream, for times ranging from 300 to 600 seconds, showed slight weight increases, although the chord dimension decreased in two cases. The maximum surface temperature was approximately 3000°F during all 5 runs, while the estimated gas temperature variation of 8000°F to 10,000°F indicates the relative dissociation of the gas stream.

The specimen subjected to 7300°F, 2.0 psia gas, showed a small weight loss, although no decrease in chord dimension could be measured. All 6 coated graphite specimens were inspected under a magnification of 30 X, and the following remarks are applicable:

Specimen I-7 - Some glazing but no failure of the coating.

Specimen I-8 - Some glazing but no failure of the coating.

Specimen D-12 - One corner of the leading edge was rounded and holes existed in the leading edge along the stagnation line. A glassy substance had filled the holes and had somewhat rebuilt the rounded corner. This specimen was heated at Bell Aircraft Corporation for 1 hour at a temperature of 2000°F in an air atmosphere to see if any change would occur, indicating either that the coating had healed itself, or that it had failed in the arc jet and the damage was extended by exposure in the furnace. This exposure indicated that the coating had failed during exposure to the arc jet, since probing resulted in the uncovering of large areas of oxidized graphite. The specimen after probing is pictured in Figure 71.

Specimen F-7 - Specimen glazed, but no coating failure.

Specimen D-8 - Corner of leading edge marked but no penetration of the coating.

Specimen G-3 - Color of stagnation region lighter than further aft, but no coating failure.

d. Bare Molybdenum Alloy Specimens

Seven bare molybdenum alloy specimens were tested, 5 at atmospheric pressure, and 2 at a test section pressure of 2.0 psia. The maximum specimen surface temperature range was 3000°F to 3300°F, with a 7300°F gas temperature under reduced pressure conditions, and estimated gas temperatures in the atmospheric jet of from 9000°F to 10,000°F.

All specimens showed a weight loss due to exposure to the arc jet, but the percent losses were in general less than those for bare graphite, for similar operating conditions.

The test results for the bare molybdenum specimens are summarized in Table 22. The maximum specimen surface temperature-time histories are plotted in Figures 72 through 78, and Figure 79 shows all bare and coated molybdenum alloy specimens after test, with their designations, and with a bare and coated specimen for comparison.

e. Coated Molybdenum Alloy Specimens

Three W-2 coated molybdenum alloy specimens were tested, 2 at atmospheric pressure and 1 at reduced pressure. In all 3 cases the maximum surface temperature ranged from 3100°F to 3200°F, and the gas temperature was 7300°F or greater. The test results, summarized in Table 23, show no significant weight or dimensional changes in the specimens after exposure to the hot gas stream. Figures 80, 81, and 82 give the maximum specimen surface temperature-time histories for the W-2 coated molybdenum alloy specimens.

A 30 X magnification of the W-2 coated specimens after test produced the following observations:

Specimen E - Specimen glazed but no failure of the coating.

Specimen H - Specimen glazed and crazing of the coating evident. Ten pinholes distributed across the stagnation region.

Specimen F - No damage.

Four Durak MG coated molybdenum alloy specimens were tested, 3 at atmospheric pressure and 1 at reduced pressure. Maximum surface temperatures for all 4 specimens ranged from 3000°F to 3100°F, and gas temperature was 7300°F in the arc tunnel, and estimated to be 9000°F to 10,000°F in the atmospheric jet.

Table 23 summarizes the test results and shows no significant weight or dimensional changes in the specimens after exposure to the hot gas stream. The specimen maximum surface temperature-time histories are plotted in Figures 83 through 86.

Inspection of the Durak MG coated specimens after test, using a magnification of 30X, provided the following information:

Specimen D - Specimen glazed, but no coating failure.

Specimen A - Glazed appearance, 3 corner failures and numerous pinholes along the stagnation region. This specimen was sectioned in two places. Figure 87 is a 250X view showing that penetration began but did not go through the diffusion region of the coating. Figure 88 magnified 100X, shows another portion of the cross section where penetration extends through the coating.

Specimen B - Specimen glazed; the stagnation region had 10 holes from 1/16 inch to 1/8 inch in diameter and over 30 pinholes; there were, in addition, 3 corner failures.

Specimen C - No damage.

2. Plasmadyne Corporation Tests

a. General

The nozzle used for this series of tests had experienced considerable running time and had suffered some erosion; the scheduling of these tests did not permit time for fabricating a new nozzle. The erosion of the nozzle chamber caused minor shock waves in the plasma jet, the boundaries of which produced higher surface temperatures on the specimens where the shock boundary intersected the specimen, than at points on the specimen which were exposed to the undisturbed flow. The reason for the higher surface temperature at this intersection is the increased density of the gas, which increases its heat transfer coefficient. The increased heat transfer rate at the intersection points was particularly noticeable on the bare graphite specimens, and somewhat less so on the molybdenum, as can be seen in Figures 90, 93 and 98.

The effect of the shock wave on the test specimens indicates that a more complete heat flux survey would show localized peaks at about a 0.65 jet radius, rather than the smooth distribution shown in Figure 53.

Since the effect of the shock waves was quite pronounced on the bare graphite specimens, three temperature surveys were made continuously on the leading edge, one at the center (spanwise) and one each at the two intersection points of the shock waves. Chord change measurements were taken at these same three points for both the bare graphite and the bare molybdenum alloy specimens.

A general view of the behavior of all the specimens under the conditions imposed by the arc-jet can be obtained from the comparison of weight loss rate for a stagnation enthalpy of 6800 BTU/lb, Figure 89. Figure 90 shows all specimens after the Plasmadyne tests, and all test data is summarized in Table 24. Table 19 includes characteristics of the Plasmadyne arc tunnel and should be referred to in conjunction with Table 24.

The run time for all specimens was 5 minutes at a stagnation enthalpy of 6800 BTU/lb, a stagnation pressure on the specimen surface of 0.68 psia, and a gas stagnation temperature at the specimen stagnation point of 9210°F.

b. Bare ATJ Graphite Specimens

The 2 bare ATJ graphite specimens experienced the highest percentage loss in weight of any of the 5 material types tested, and the second highest weight loss rate, as shown in Table 24 and Figure 89, respectively.

Specimen 6 has a maximum surface temperature of from 2600°F to 2900°F, depending on spanwise location, as seen in Figure 91, and Specimen 7 had a variation of 2600°F to 2750°F, Figure 92.

Figure 89 indicates a weight loss rate for both bare graphite specimens of about 1.0 grams per minute, and Table 24 shows a percentage weight loss of about 21%, and a chord reduction of up to 26%.

Figure 93 is a photograph including the bare ATJ graphite specimens after test; note the effect of the shock wave boundary.

c. Siliconized ATJ Graphite Specimens

The 2 siliconized graphite specimens suffered no apparent damage, but showed a gross weight loss of 0.1 to 0.2%, Table 24, and a weight loss rate of from 0.007 to 0.010 grams per minute, Figure 89. There was no measurable change in chord dimension.

Specimen N-7 had a maximum specimen surface temperature of 2600°F to 2700°F depending on location, as seen in Figure 94, as did Specimen L-3, whose temperature history is given in Figure 95.

The siliconized ATJ graphite specimens are pictured in Figure 93 after test.

d. Bare Molybdenum Alloy Specimens

The 2 bare molybdenum alloy specimens exhibited the second highest percentage weight loss of all 5 materials tested, and the highest rate of weight loss. Table 24 shows the former to be 6 to 7%, and the latter is about 1.8 grams per minute, Figure 89. The decrease in chord dimension ranged from 1 to 4%.

The maximum surface temperature for both specimens was approximately 3400°F, although the validity of the temperature measurement in this case is questionable because of the presence of a bright "halo" of molybdenum trioxide enveloping the entire specimen, which may have affected the optical pyrometer readings. Temperatures as measured are given in Figures 96 and 97.

The appearance of the bare molybdenum alloy specimens after test can be observed in Figure 98; the effect of the shock wave is noticeable.

e. Coated Molybdenum Alloy Specimens

The 2 W-2 coated and the 2 Durak MG coated molybdenum alloy specimens had no appreciable weight loss and no measurable decrease in chord dimension, as summarized in Table 24. All 4 specimens sustained a maximum surface temperature of 3000°F, including the points of shock intersection, as shown in Figures 99 through 102. Figure 98 is a photograph which includes the 4 coated specimens after test. The pitted region on the leading edge of Specimen W-2 indicates a coating failure. Figure 103 is an enlarged view of Specimen W-2, and Figure 104 is a further enlargement of the area of failure.

Except for Specimen W-2, the rate of weight loss for the coated molybdenum alloy was extremely low, as shown in Figure 89 ; 0.004 grams per minute, or less.

TABLE 17

CHARACTERISTICS OF THE NASA LANGLEY RESEARCH CENTER
6 INCH SUBSONIC ARC JET (JET NO. 20)
AS MEASURED FOR TESTS OF THE BELL LEADING EDGE SPECIMENS

Arc Power	500 to 1600 Kw
Jet Diameter	6 inches
Air Flow Rate	0.08 to 0.24 #/second
Height of Specimen Above Nozzle Exit	0 to 36 inches
Maximum Running Time:	
1. High Power	5 minutes
2. Low Power	10 minutes
Heating Rates:	
1. Leading Edge Specimen Stagnation Point	50 to 320 BTU/ft^2-sec
2. Leading Edge Specimen Skirt	15 to 90 BTU/ft^2-sec
Gas Stagnation Temperature	
1. At Nozzle Exit	9000°F
2. At Locations Above Nozzle	Could not be measured
Jet Static Pressure	Atmospheric

TABLE 18

CHARACTERISTICS OF THE NASA LANGLEY RESEARCH CENTER
6 INCH SUBSONIC ARC TUNNEL (JET NO. 10)
AS MEASURED FOR TESTS OF THE BELL LEADING EDGE SPECIMENS

Arc Power	1250 Kw
Tunnel Section Size	6 inch diameter
Air Flow Rate	0.082 #/second
Maximum Running Time	80 seconds
Heating Rates:	
1. Leading Edge Specimen Stagnation Point	220 BTU/ft^2-sec
2. Leading Edge Specimen Skirt	80 BTU/ft^2-sec
3. 3/8 inch Diameter Flat-Face Water Calorimeter	180 BTU/ft^2-sec
Gas Stagnation Temperature	7300°F
Tunnel Section Static Pressure	2 psia

TABLE 19

CHARACTERISTICS OF THE PLASMADYNE ARC TUNNEL

Stagnation Enthalpy - h_T	6800 BTU/#
Stagnation Point Heat Flux to 5/8 inch Diameter Water Cooled Calorimeter - $\dot{q}_s$	396 BTU/ft^2-sec
Nozzle Static Pressure - P	0.068 psia
Pitot Pressure - P_o' (Stagnation pressure on specimen surface)	0.68 psia
Stagnation Pressure - P_T (Pressure in plenum chamber)	3.51 psia
Nozzle Mach Number - M	3
Jet Diameter - d	3 inches
Arc Power Input - P	200 Kw
Gas Flow Rate - $\dot{m}$	0.013 #/sec N_2 0.00137 #/sec O_2
Free Stream Gas Properties*	
Gas Density -	2.20 x 10^{-5} #/ft^3
Gas Velocity - V	12,300 ft/sec
Gas Temperature - T	6600°F
Stagnation Values at Model Stagnation Point*	
Gas Density -	1.37 x 10^{-4} #/ft^3
Gas Temperature - T	9210°F

* Based on Mollier Chart for Equilibrium Air.
All other values listed are experimental measurements.

TABLE 20

TEST RESULTS OF BARE ATJ GRAPHITE SPECIMENS RUN IN NASA LANGLEY RESEARCH CENTER ARC JETS

Specimen Designation	Exposure Time Seconds	Arc Power Kw	Gas Temperature at Specimen °F	Mass Velocity ρV #/Ft^2-Hr	Max. Specimen Surface Temperature °F	Heating Rate at Specimen Stagnation Point BTU/Ft^2-Sec	Specimen Weight, Grams			Chord Dimension, Inches			Remarks
							Before	After	% Change	Before	After	% Change	
6 Inch Subsonic Atmospheric Arc Jet (Jet No. 20)													
43	135	1600	9440*	4400	3200	230	23.89	15.75	-34.1	--	--	--	Thermocouple failed at 80 seconds. Test terminated because of excessive temperature.
25	300	1500	9090*	4400	3200	210	23.56	10.14	-57.1	0.995	0.660	-33.7	
29	519	635	10,160*	1467	3100	170	23.93	6.96	-71.0	0.991	0.537	-45.8	Specimen holder failed at 519 seconds.
24	76	600	9990*	1467	3000	170	23.67	20.58	-13.1	0.993	0.937	- 5.6	
6 Inch Subsonic Arc Tunnel - Test Section Pressure - 2.0 psia (Jet No. 10)													
22	76	1215	7300	1504	3100	220	22.54	19.32	-14.3	0.992	0.932	-6.0	Thermocouple failed at 55 seconds

* Estimated by the author, not measured by NASA personnel.

TABLE VI

TEST RESULTS OF SILICONIZED ATJ GRAPHITE SPECIMENS RUN IN NASA LANGLEY RESEARCH CENTER ARC JETS

Specimen Designation	Exposure Time Seconds	Arc Power Kw	Gas Temperature at Specimen °F	Mass Velocity ρV #/Ft²-Hr	Max. Specimen Surface Temperature °F	Heating Rate at Specimen Stagnation Point BTU/Ft²-Sec	Specimen Weight, Grams			Chord Dimension, Inches			Remarks
							Before	After	% Change	Before	After	% Change	
6 Inch Subsonic Atmospheric Arc Jet (Jet No. 20)													
I-7	300	1520	9180*	4400	3000	190	24.59	24.75	0.7	0.998	0.995	-0.3	
I-8	300	1620-1120	9460-7290*	4400	3000	210	25.14	25.34	0.8	0.994	0.998	0.4	
D-22	483	635	10,160*	1467	2900	170	24.44	24.58	0.6	0.998	1.005	0.7	Test terminated at 483 seconds because of failure of specimen holder, coating failed.
F-7	520	636	6000*	2200	2800	170	24.72	24.77	0.2	0.999	0.995	-0.4	Test terminated at 520 seconds because of failure of specimen holder.
D-8	600	624	10,150*	1467	3000	170	24.59	24.71	0.5	0.997	1.001	0.4	
6 Inch Subsonic Arc Tunnel - Test Section Pressure - 2.0 psia (Jet No. 10)													
G-3	72	1265	7300	1504	3000	220	24.94	24.86	-0.3	0.995	0.995	0	Thermocouple failed at 48 seconds.

* Estimated by the author, not measured by NASA personnel.

TABLE

TEST RESULTS OF RARE MOLYBDENUM ALLOY SPECIMENS RUN IN NASA LANGLEY RESEARCH CENTER ARC JETS

Specimen Designation	Exposure Time Seconds	Arc Power Kw	Gas Temperature at Specimen °F	Mass Velocity ρV #/Ft²-Hr	Max. Specimen Surface Temperature °F	Heating Rate at Specimen Stagnation Point BTU/Ft²-Sec	Specimen Weight, Grams Before	After	% Change	Chord Dimension, Inches Before	After	% Change	Remarks
6 Inch Subsonic Atmospheric Arc Jet (Jet No. 20)													
Trial 11	188	1480	9000*	[illegible]	3000	230	122.80	96.10	-21.8	--	--	--	Previously run 300 seconds in Jet No. 20. Test terminated because of excessive temperature - specimen had moved.
Trial 2	301	1480	9000*	4400	3000	160	138.80	118.80	-14.4	--	--	--	
Trial 3	207	1500	9000*	4400	3000	210	138.53	120.56	-12.9	--	--	--	
21 J	600	620	10,050*	1467	3000	170	140.10	102.02	-27.2	0.999	0.885	-11.4	
K	70	624	10,150*	1467	3000	170	140.65	133.00	-5.4	0.955	0.936	-2.0	Arc shut off.
6 Inch Subsonic Arc Tunnel - Test Section Pressure - 2.0 psia (Jet No. 10)													
L	38	1265	7300	1504	3000	220	139.78	138.81	-0.7	0.999	0.997	-0.2	Arc shut off - equipment failure.
I	69	1230	7300	1504	3100	220	140.24	136.81	-2.4	--	--	--	Thermocouple failed at 44 seconds.

* Estimated by the author, not measured by NASA personnel.

TABLE 23

TEST RESULTS OF COATED MOLYBDENUM ALLOY SPECIMENS RUN IN NASA LANGLEY RESEARCH CENTER ARC JETS

Specimen Designation	Exposure Time Seconds	Arc Power Kw	Gas Temperature at Specimen °F	Mass Velocity ρV #/Ft²-Hr	Max. Specimen Surface Temperature °F	Heating Rate at Specimen Stagnation Point BTU/Ft²-Sec	Specimen Weight, Grams			Chord Dimension, Inches			Remarks
							Before	After	% Change	Before	After	% Change	
6 Inch Subsonic Atmospheric Arc Jet (Jet No. 20)													
CHROMALLOY W-2 COATING													
E	29[illegible]	141[illegible]	8720*	4400	3000	210	137.53	137.70	0.1	0.994	1.015	2.1	
H	60[illegible]	60[illegible]	9990*	1467	3200	170	138.02	139.07	0.8	0.998	*0.995	-0.3	Coating failed
CHROMIZING DURAK MG COATING													
D	142	1560	9260*	4400	3100	210	138.40	138.41	Negl.	0.997	0.999	0.2	Test terminated at 142 seconds because of failure of specimen holder.
A	300	1500	9090*	4400	3130	210	140.09	140.05	Negl.	0.997	1.004	0.7	Coating failed
B	570	630	10,150*	1467	3000	170	139.40	139.20	-0.2	0.999	1.009	1.0	Test terminated at 570 seconds because specimen began to drop; coating failed.
6 Inch Subsonic Arc Tunnel - Test Section Pressure - 2.0 psia (Jet No. 10)													
CHROMALLOY W-2 COATING													
F	71	1245	7300	1504	3100	220	140.75	140.80	Negl.	0.999	0.999	0	Thermocouple failed at 40 seconds.
CHROMIZING DURAK MG COATING													
C	71	1265	7300	1504	3000	220	140.52	140.54	Negl.	1.000	1.009	0.9	Thermocouple failed at 30 seconds.

* Estimated by the author, not measured by NASA personnel.

TABLE 24

TEST RESULTS OF SPECIMENS RUN IN PLASMADYNE CORPORATION ARC TUNNEL

Specimen Designation	Exposure Time Seconds	Arc Power Kw	Gas Temperature at Specimen °F	Mass Velocity ρV #/Ft²-Hr	Max. Specimen Surface Temperature °F	Heating Rate at Specimen Stagnation Point BTU/Ft²-Sec	Specimen Weight, Grams			Chord Dimension, Inches			Remarks
							Before	After	% Change	Before	After	% Change	
BARE ATJ GRAPHITE													
6	300	200	9210	950	2900	350	23.870	18.690	-21.7	.997	.756	-24.2	
										.997	.956	-4.1	
										.997	.735	-26.3	
7	300	200	9210	950	2750	352	23.580	18.760	-20.5	.996	.800	-19.7	
										.996	.960	-3.6	
										.996	.820	-17.5	
SILICONIZED ATJ GRAPHITE													
N-7	300	200	9210	950	2650	354	26.000	25.965	-0.1	.996	.996	0	
L-3	300	200	9210	950	2650	354	24.660	24.610	-0.2	.995	.995	0	
BARE MOLYBDENUM ALLOY													
4	300	200	9210	950	3450	342	139.960	130.790	-6.5	.999	.988	-1.1	Bright glow enveloped specimen; temperature readings may be too high.
										.999	.965	-3.4	
										.999	.958	-4.1	
5	300	200	9210	950	3400	342	140.365	130.935	-6.7	.995	.990	-0.5	Bright glow enveloped specimen; temperature readings may be too high.
										.995	.976	-1.9	
										.995	.926	-6.9	
W-2 COATED MOLYBDENUM ALLOY													
W-2	300	200	9210	950	3000	348	138.220	138.080	-0.1	.995	.995	0	Pitting of coating on leading edge of specimen; coating failed.
8	300	200	9210	950	3000	348	138.540	138.528	Negl.	.995	.995	0	
DURAK MG COATED MOLYBDENUM ALLOY													
2	300	200	9210	950	3000	348	139.000	138.980	Negl.	.998	.998	0	
3	300	200	9210	950	3000	348	138.870	138.850	Negl.	.996	.996	0	

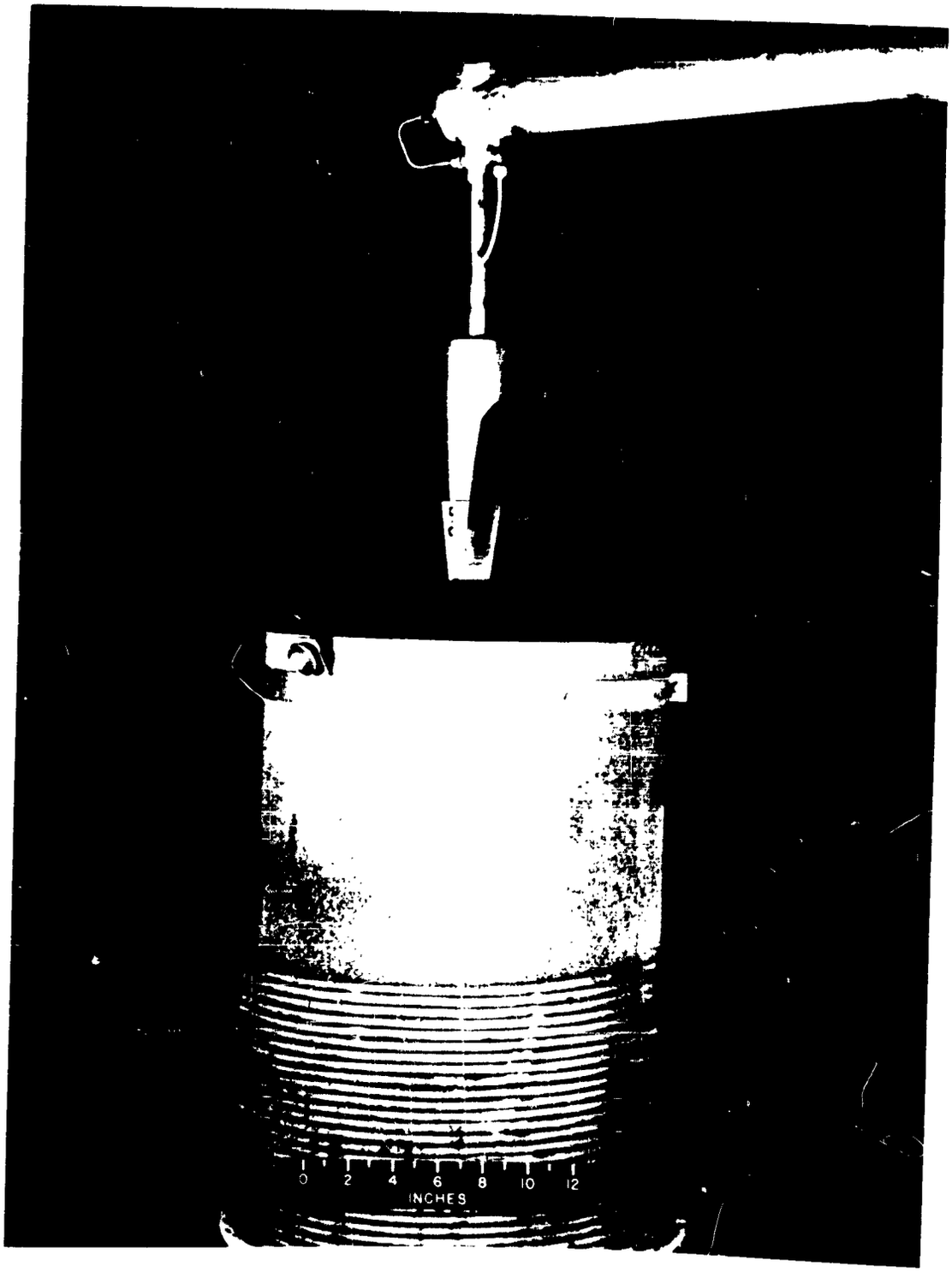

FIGURE 45. A LEADING EDGE SPECIMEN POSITIONED OVER NASA LANGLEY RESEARCH CENTER ARC JET NO. 20

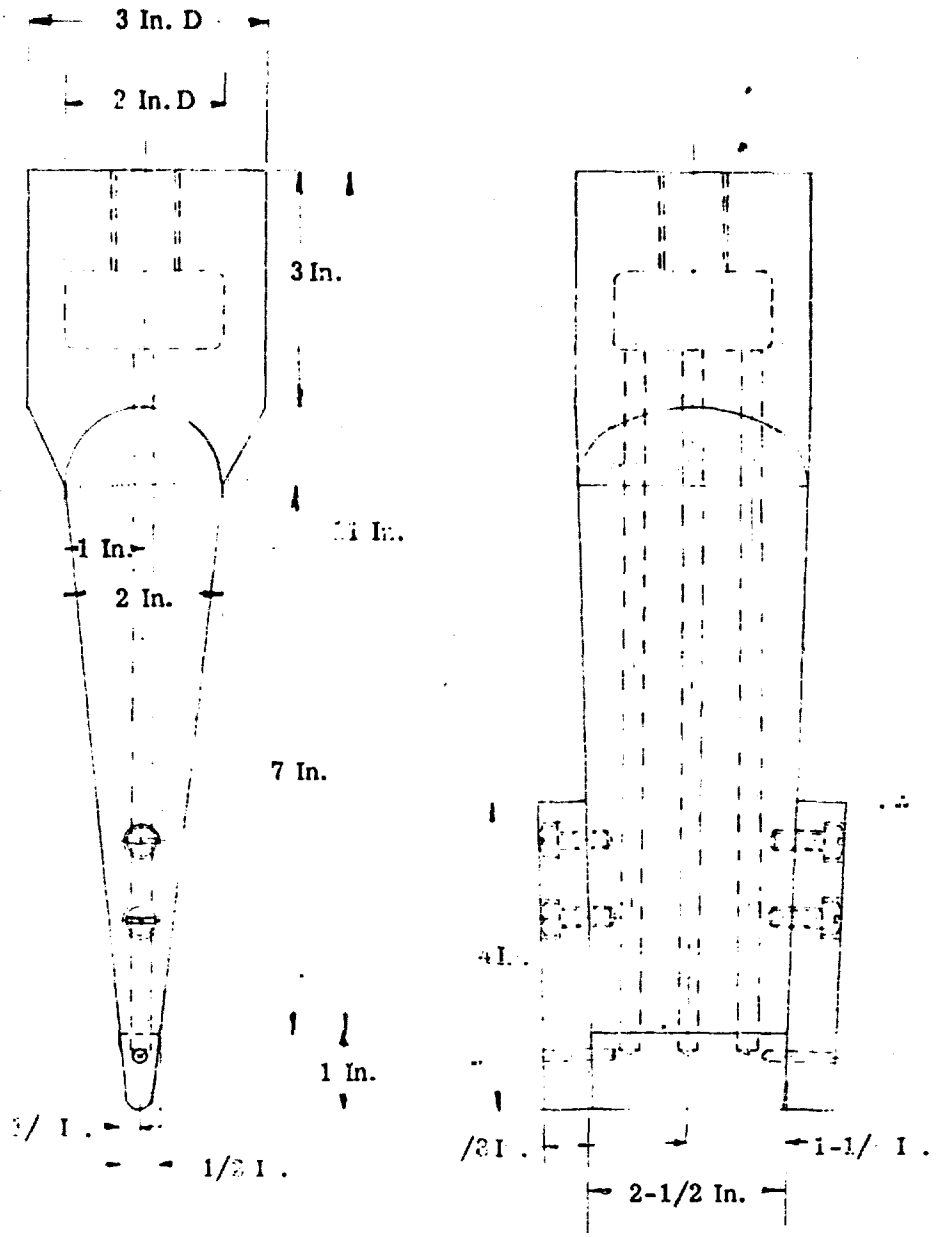

FIGURE 46. SPECIMEN HOLDER FOR NASA LANGLEY RESEARCH CENTER ARC JET NO. 20

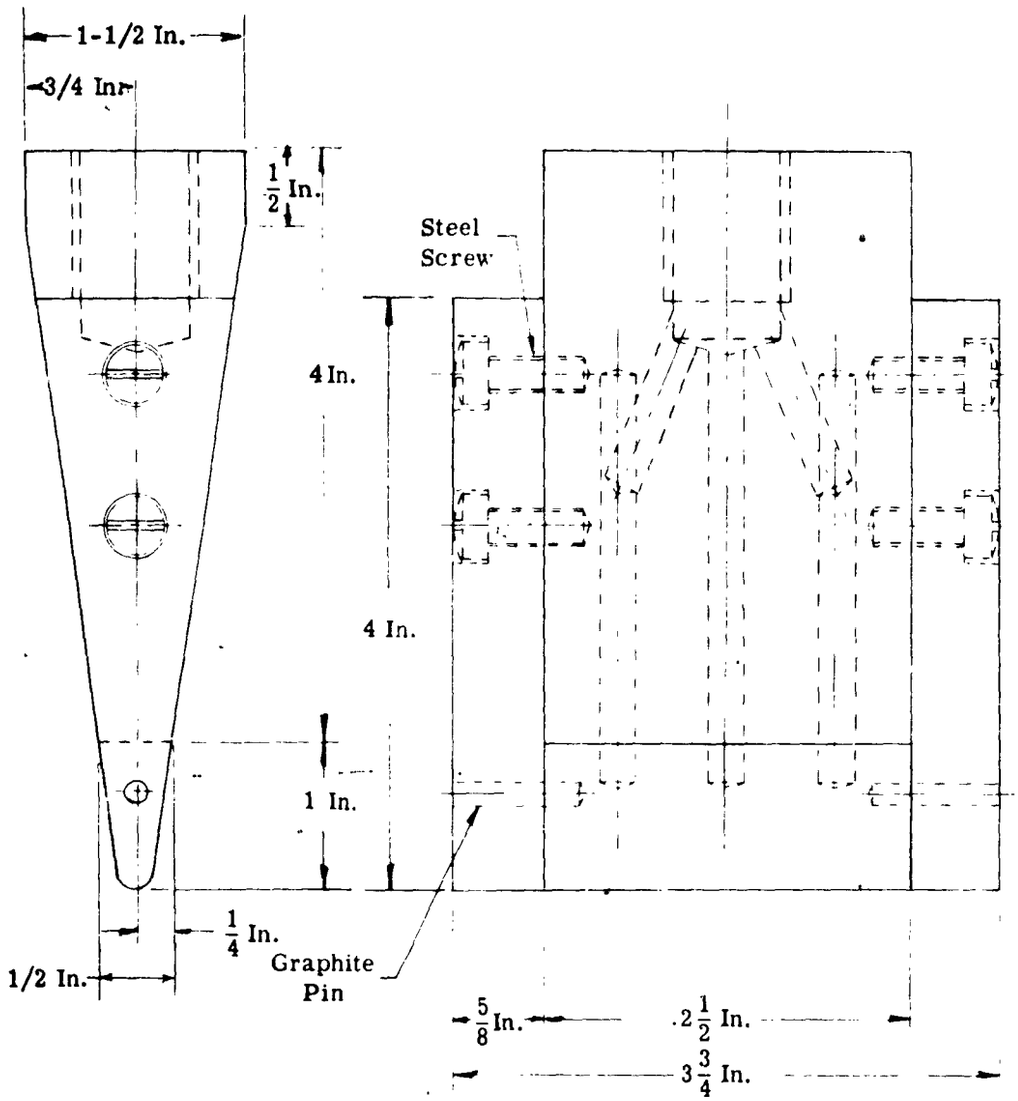

FIGURE 47. SPECIMEN HOLDER FOR NASA LANGLEY RESEARCH CENTER ARC JET NO. 10

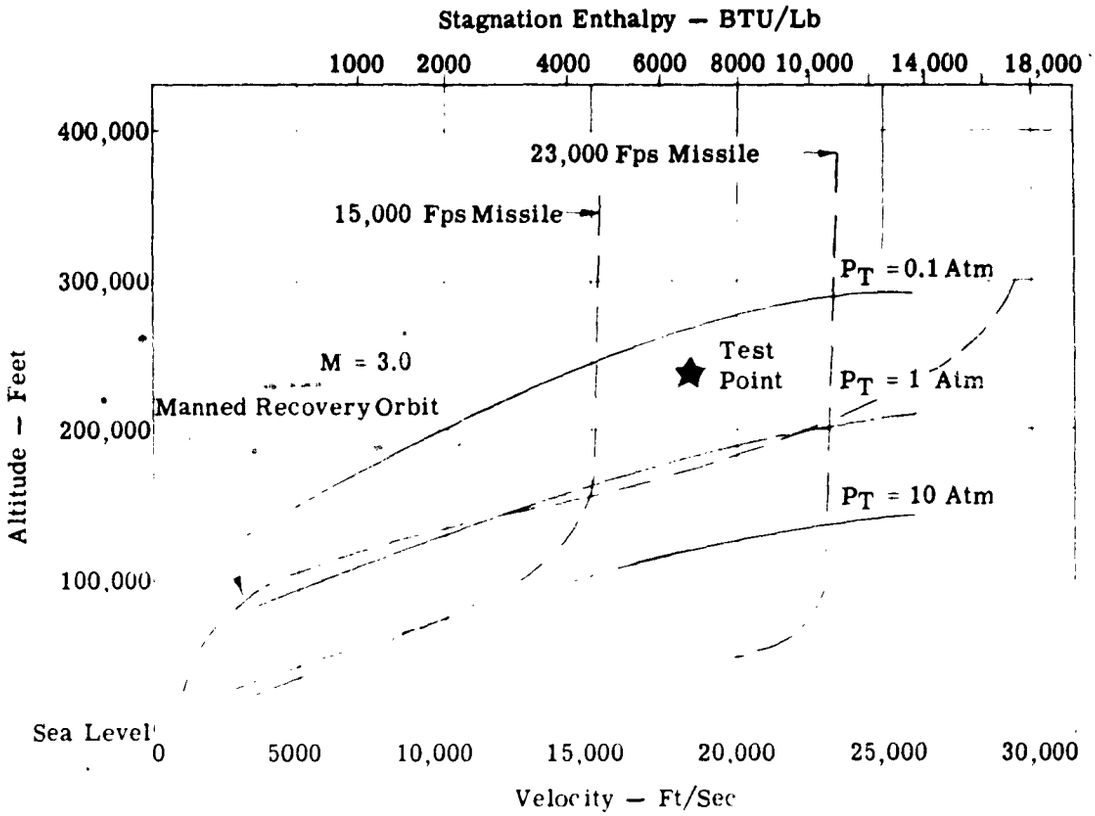

FIGURE 48. HEAT TRANSFER SIMULATION TUNNEL CAPABILITIES FOR M= 3.0, PLASMADYNE CORPORATION

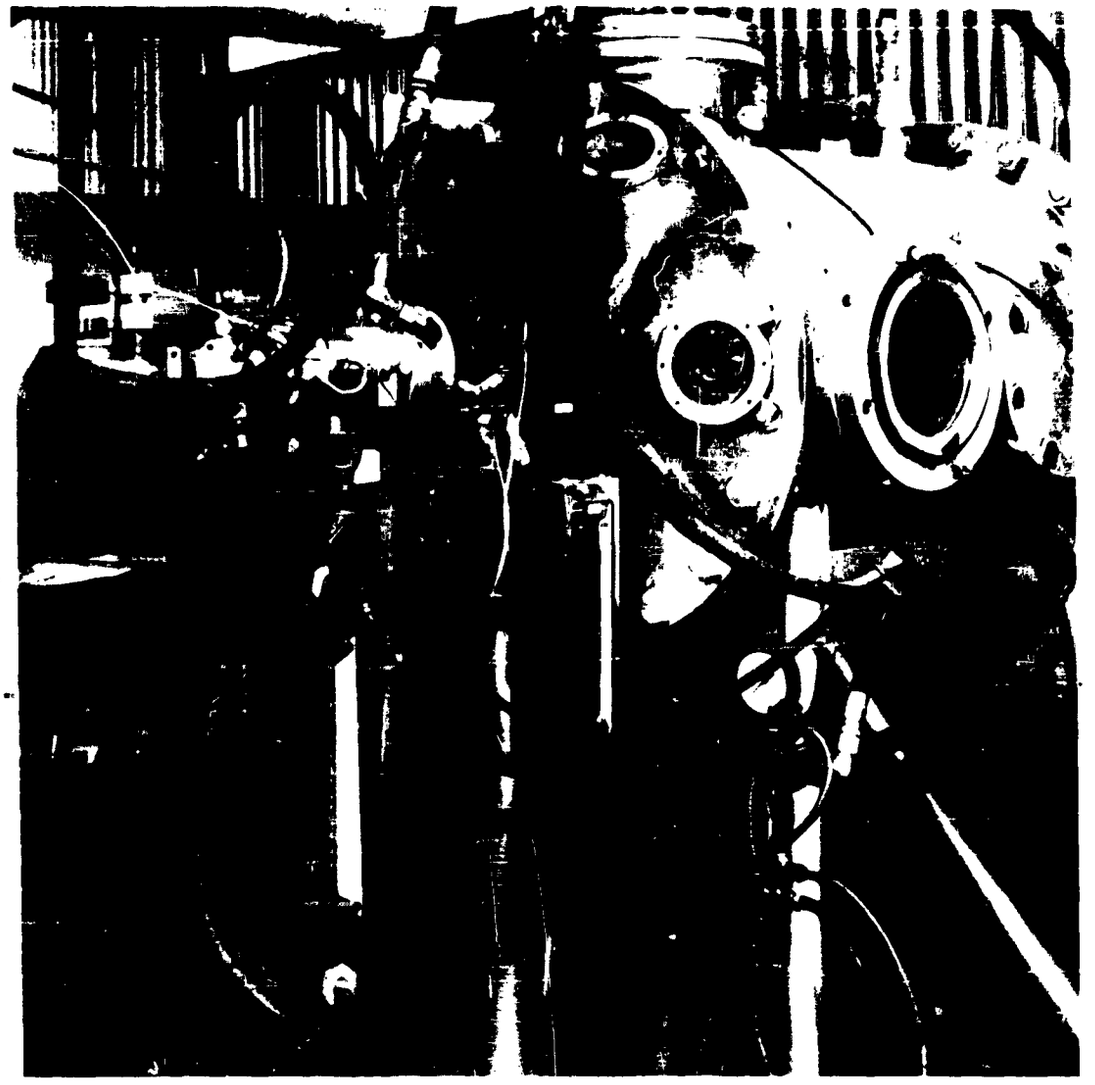

FIGURE 49. THE PLASMADYNE CORPORATION ARC TUNNEL TEST CHAMBER WITH PLASMA HEAD AND NOZZLE ATTACHED

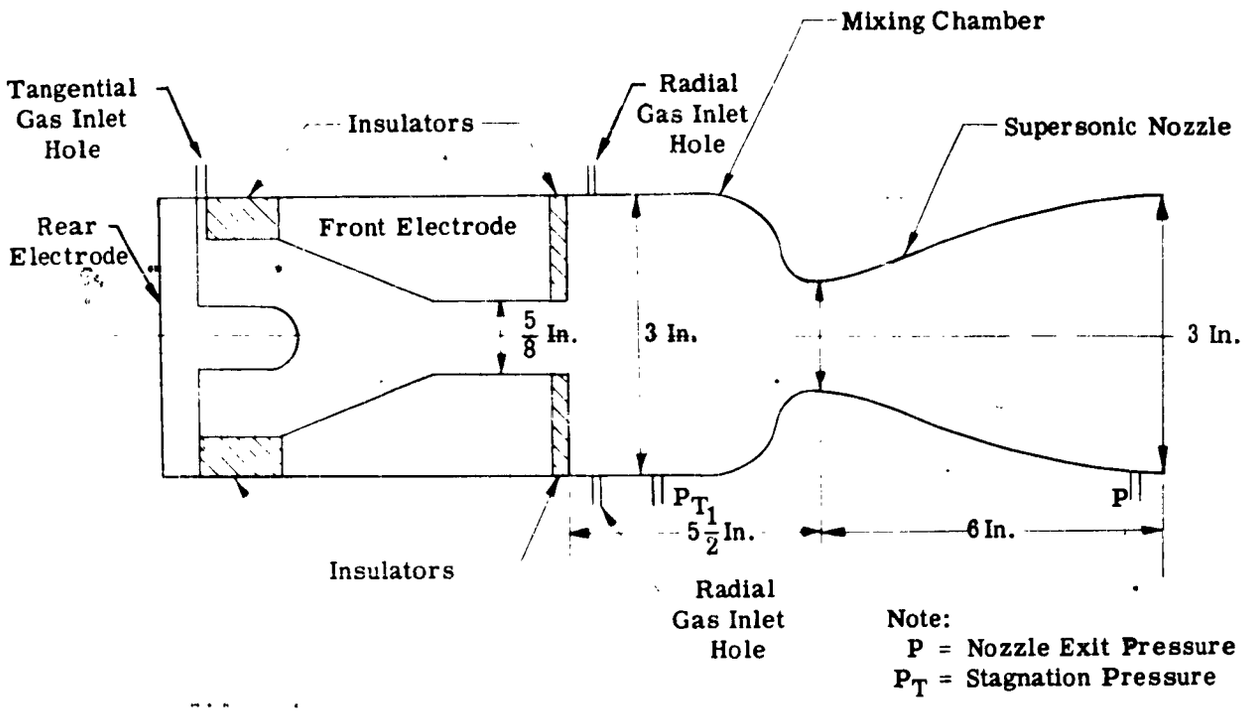

FIGURE 50. SCHEMATIC DRAWING OF PLASMA HEAD, MIXING CHAMBER, AND NOZZLE, PLASMADYNE CORPORATION

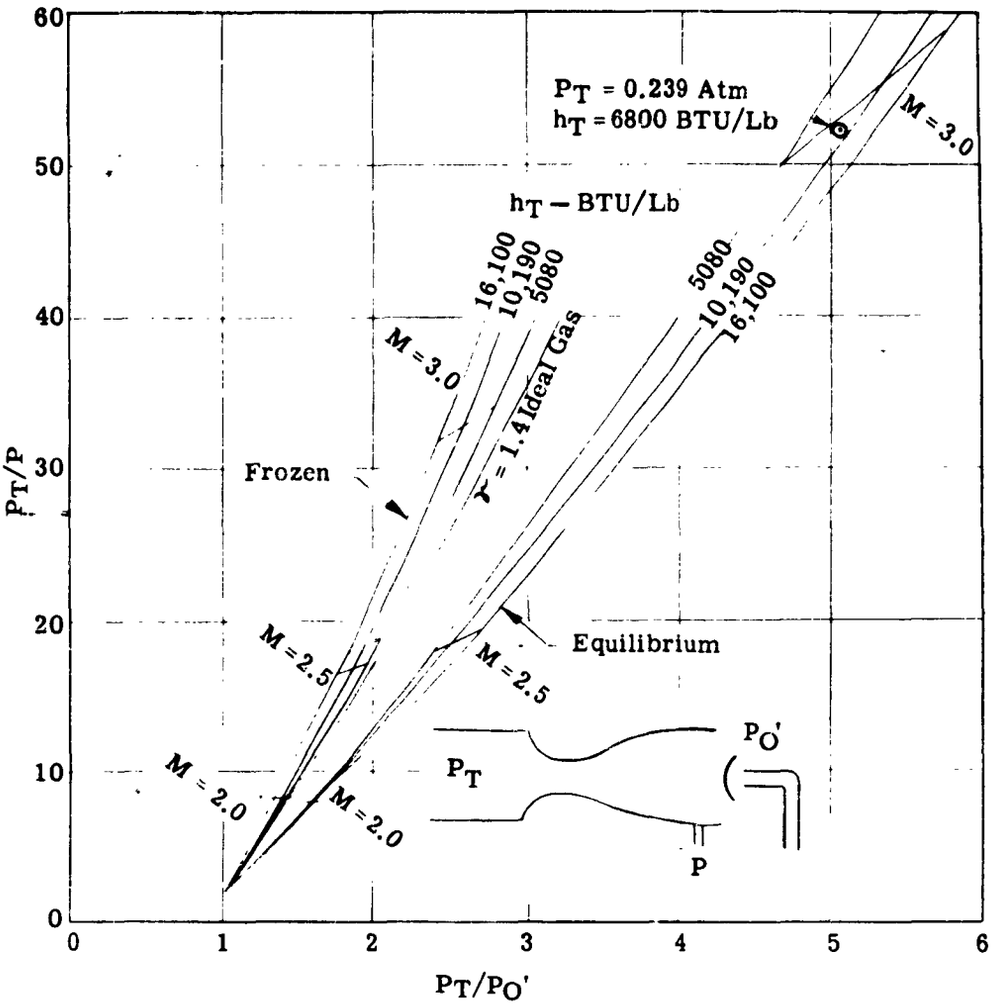

FIGURE 51. A COMPARISON OF THE MEASURED AND THEORETICAL STATIC PRESSURE RATIO AS A FUNCTION OF PITOT PRESSURE RATIO, PLASMADYNE CORPORATION

FIGURE 52. SPECIMEN HOLDER ASSEMBLY USED IN PLASMADYNE CORPORATION TESTS

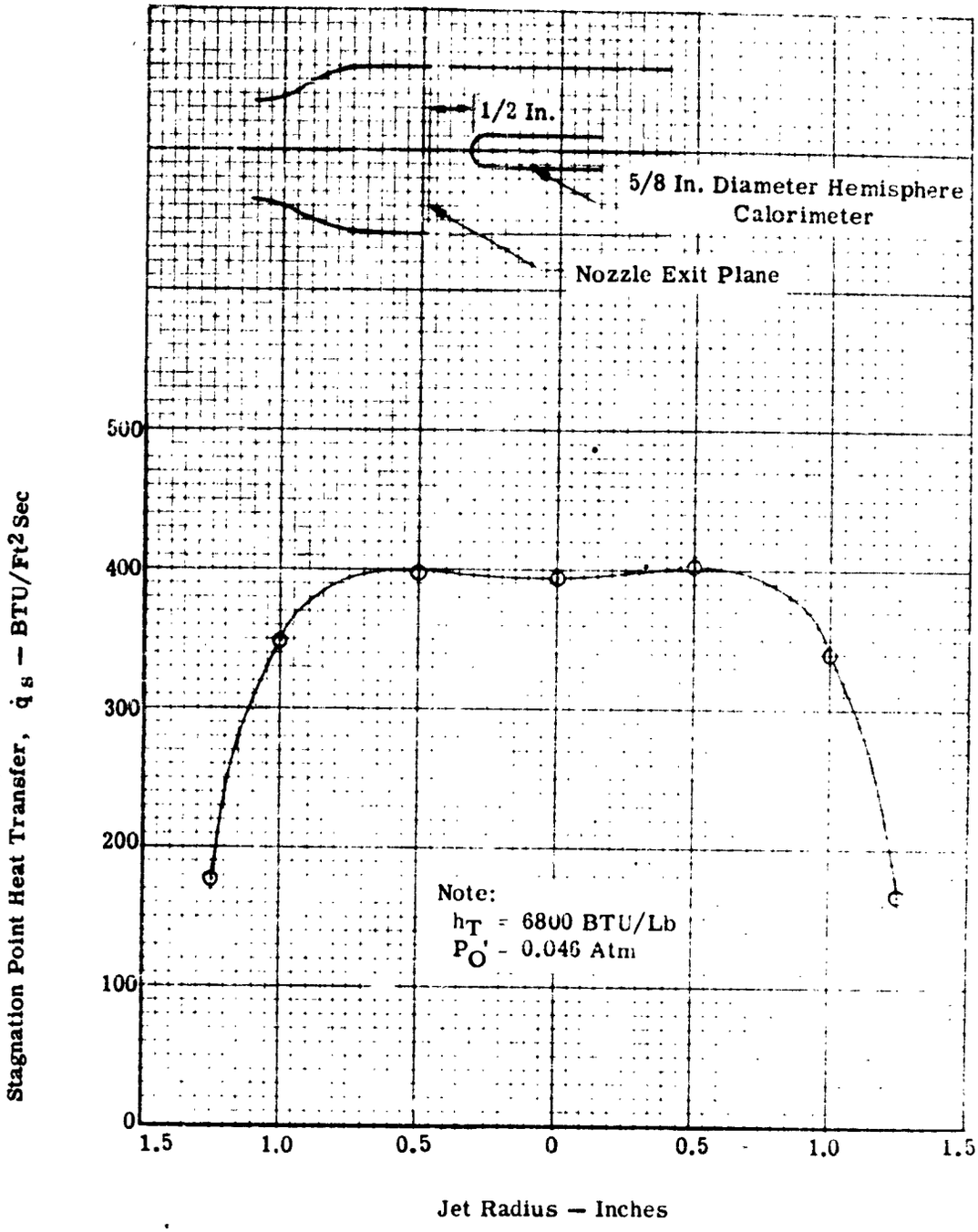

FIGURE 53. RADIAL SURVEY OF STAGNATION POINT HEAT TRANSFER RATE, PLASMADYNE CORPORATION

FIGURE 54. TYPICAL LEADING EDGE SPECIMENS BEFORE TEST

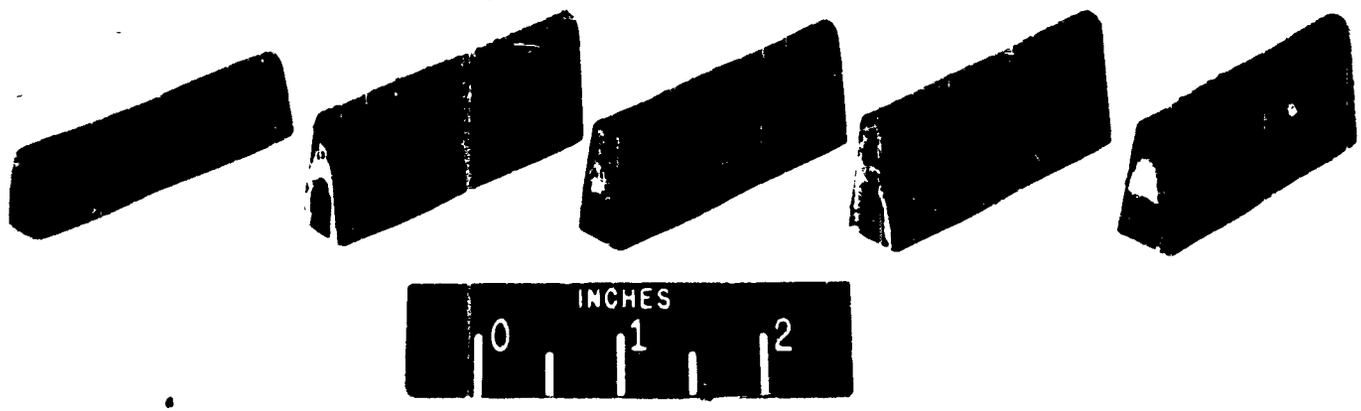

FIGURE 55. TYPICAL LEADING EDGE SPECIMENS AFTER NOMINAL 5-MINUTE TESTS IN NASA LANGLEY RESEARCH CENTER ARC JET NO. 20

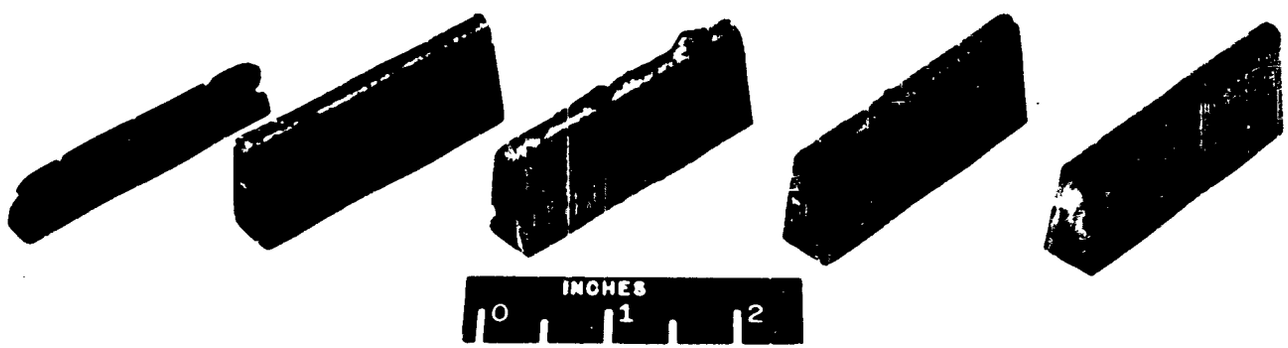

Bare Graphite | Siliconized Graphite | Bare Molybdenum | Durak Coated Molybdenum | W-2 Coated Molybdenum

FIGURE 56. TYPICAL LEADING EDGE SPECIMENS AFTER NOMINAL 10-MINUTE TEST IN NASA LANGLEY RESEARCH CENTER ARC JET NO. 20

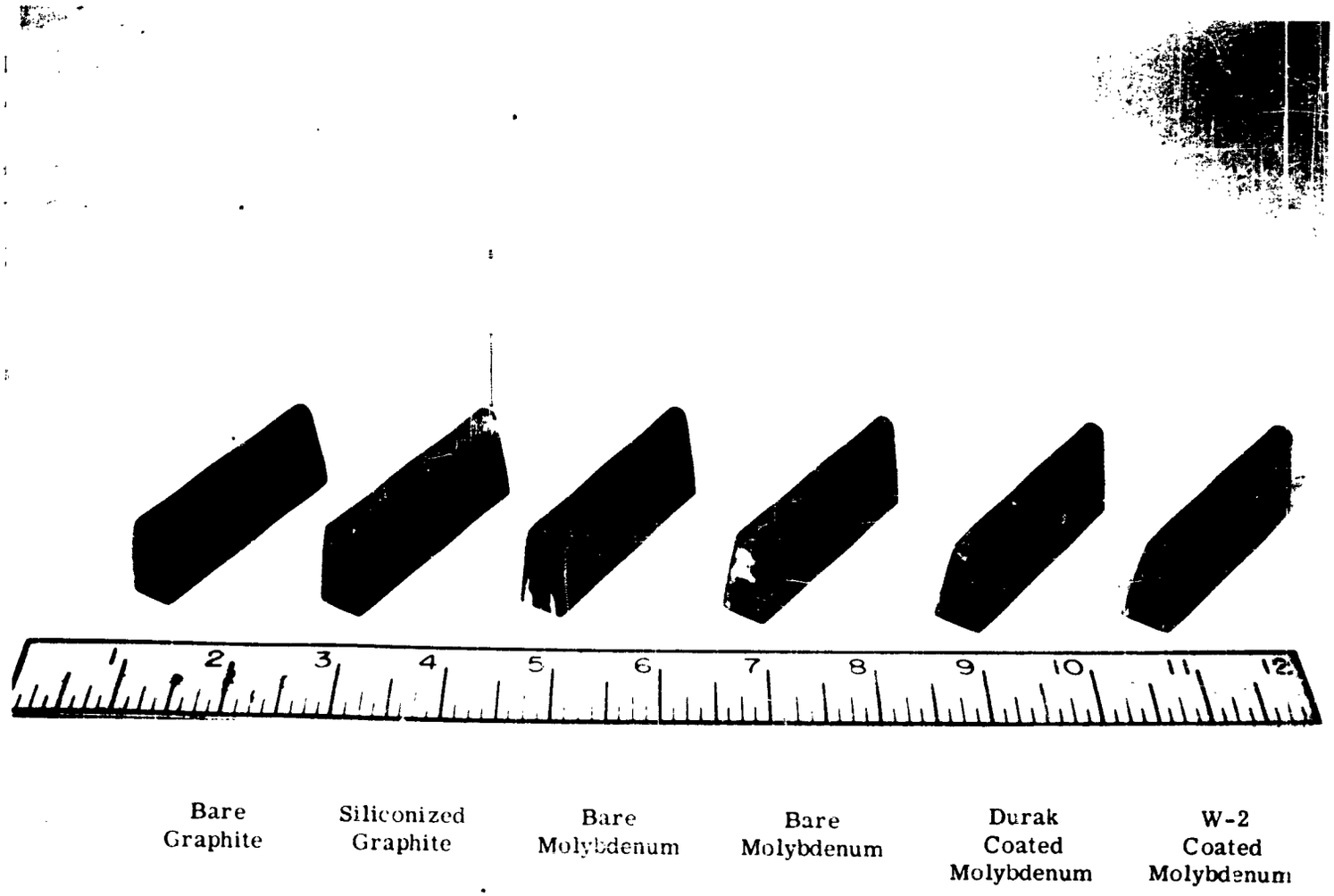

FIGURE 57. TYPICAL LEADING EDGE SPECIMENS AFTER NOMINAL 1-MINUTE TESTS IN NASA LANGLEY RESEARCH CENTER ARC TUNNEL (ARC JET NO. 10)

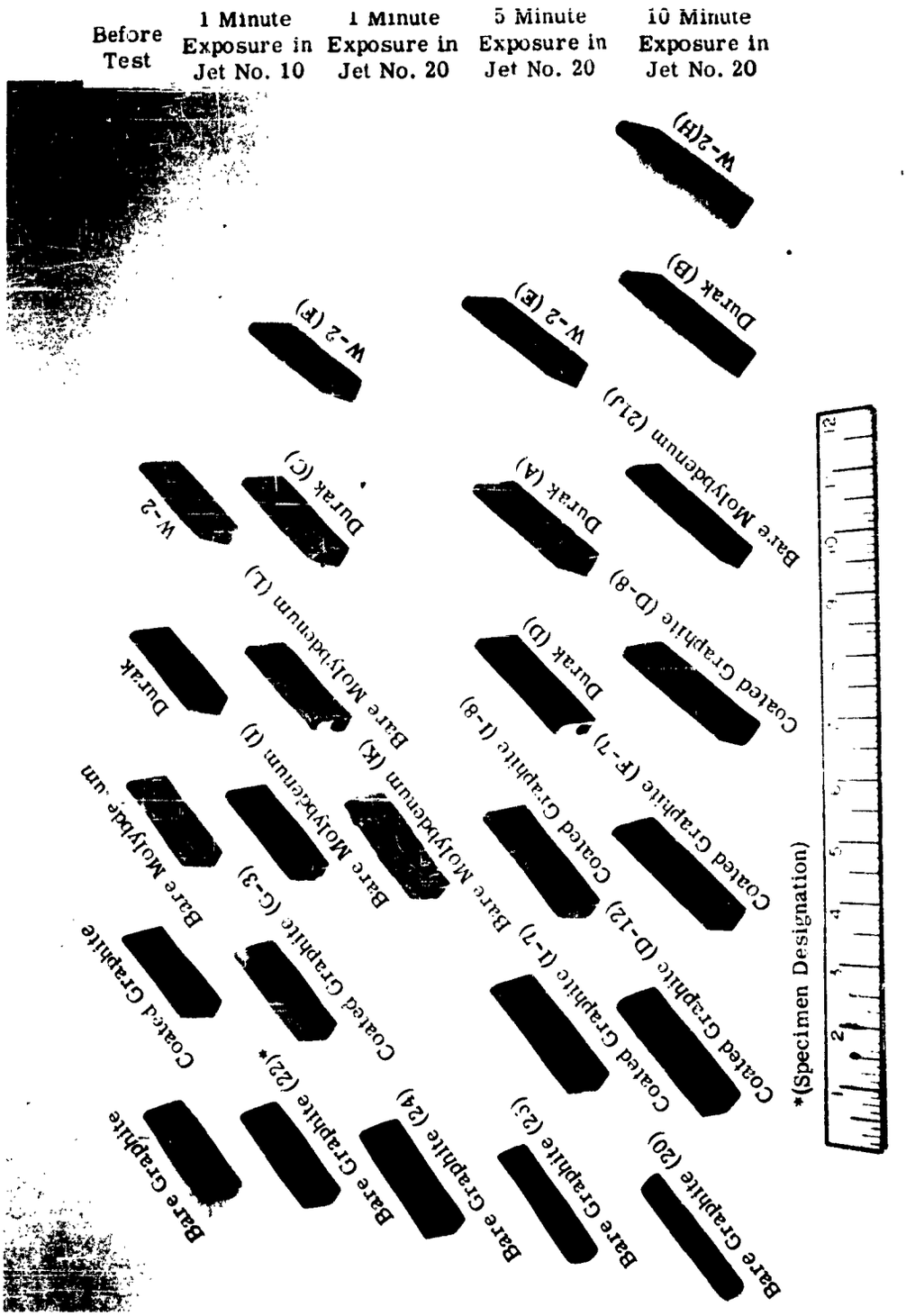

FIGURE 58. ALL SPECIMENS TESTED IN NASA LANGLEY RESEARCH CENTER ARC JETS

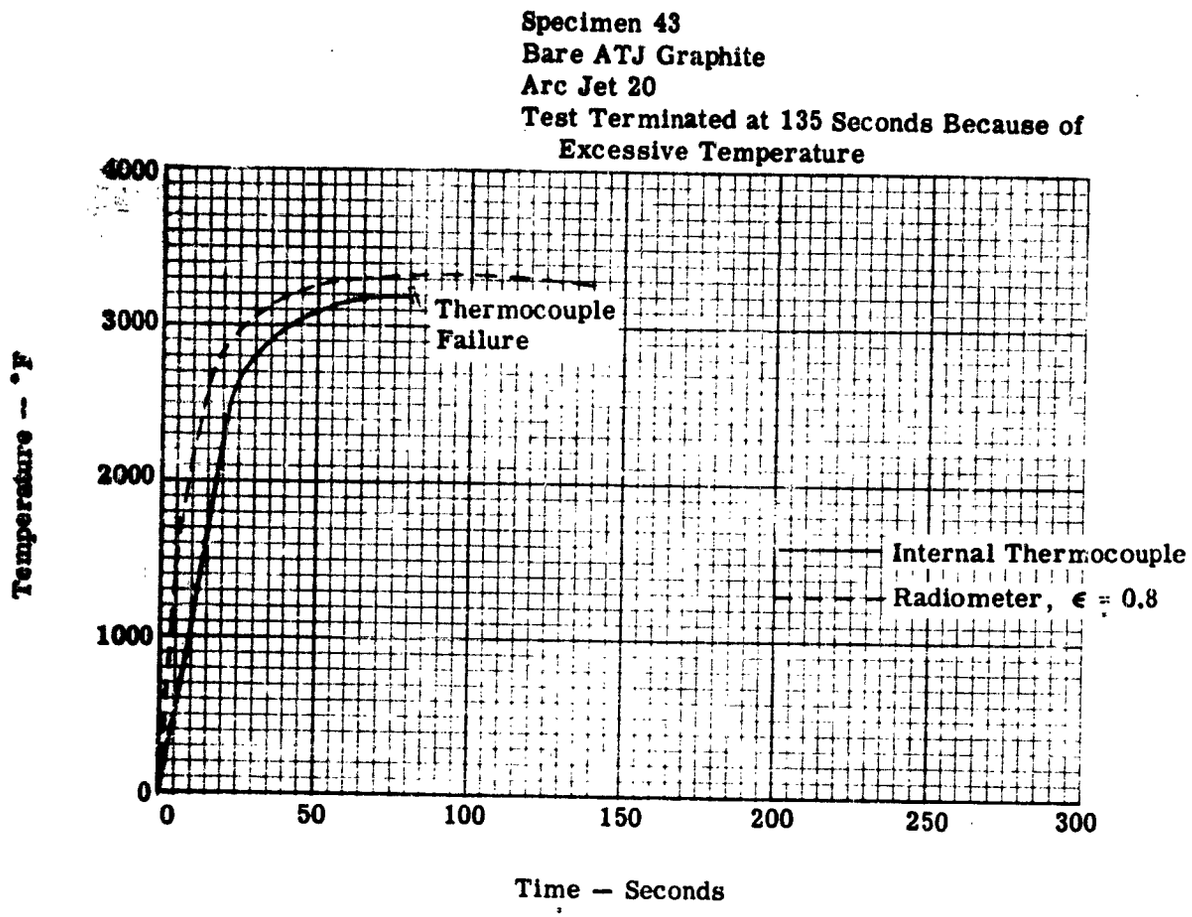

FIGURE 59. SPECIMEN 43 TEMPERATURE VS TIME, NASA LANGLEY RESEARCH CENTER

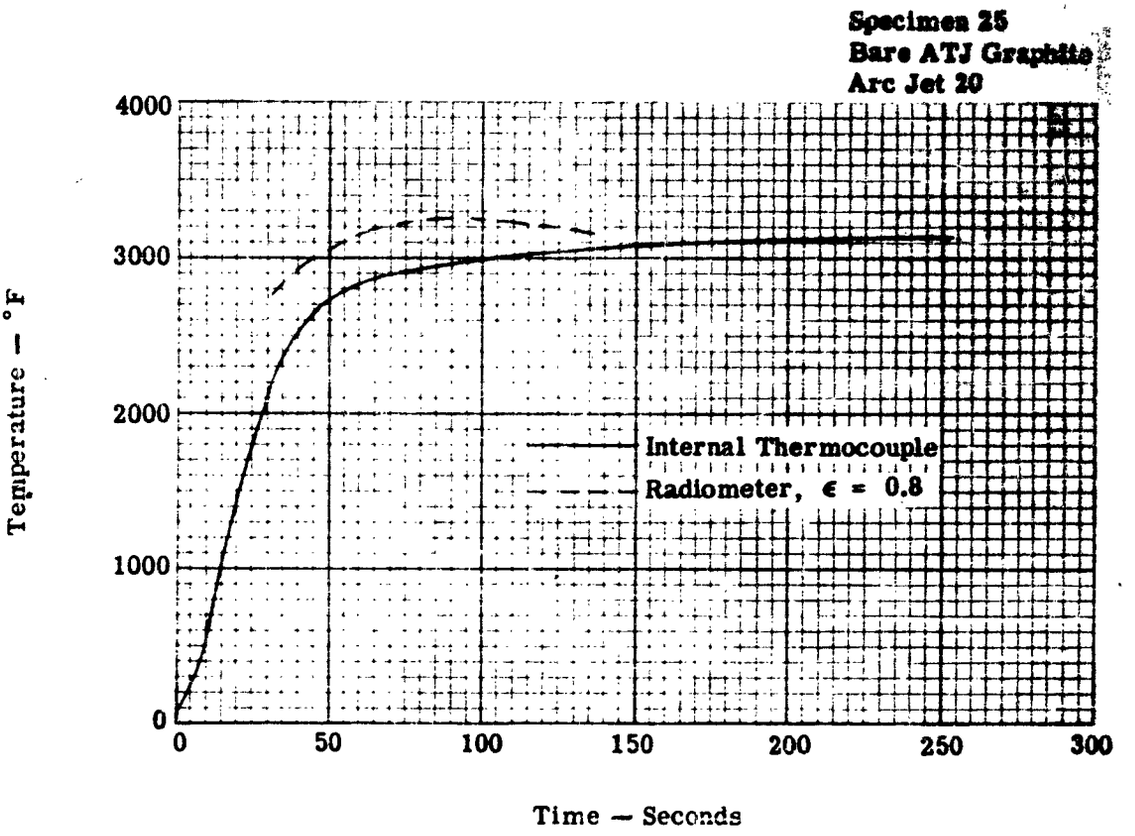

FIGURE 60. SPECIMEN 25 TEMPERATURE VS TIME, NASA LANGLEY RESEARCH CENTER

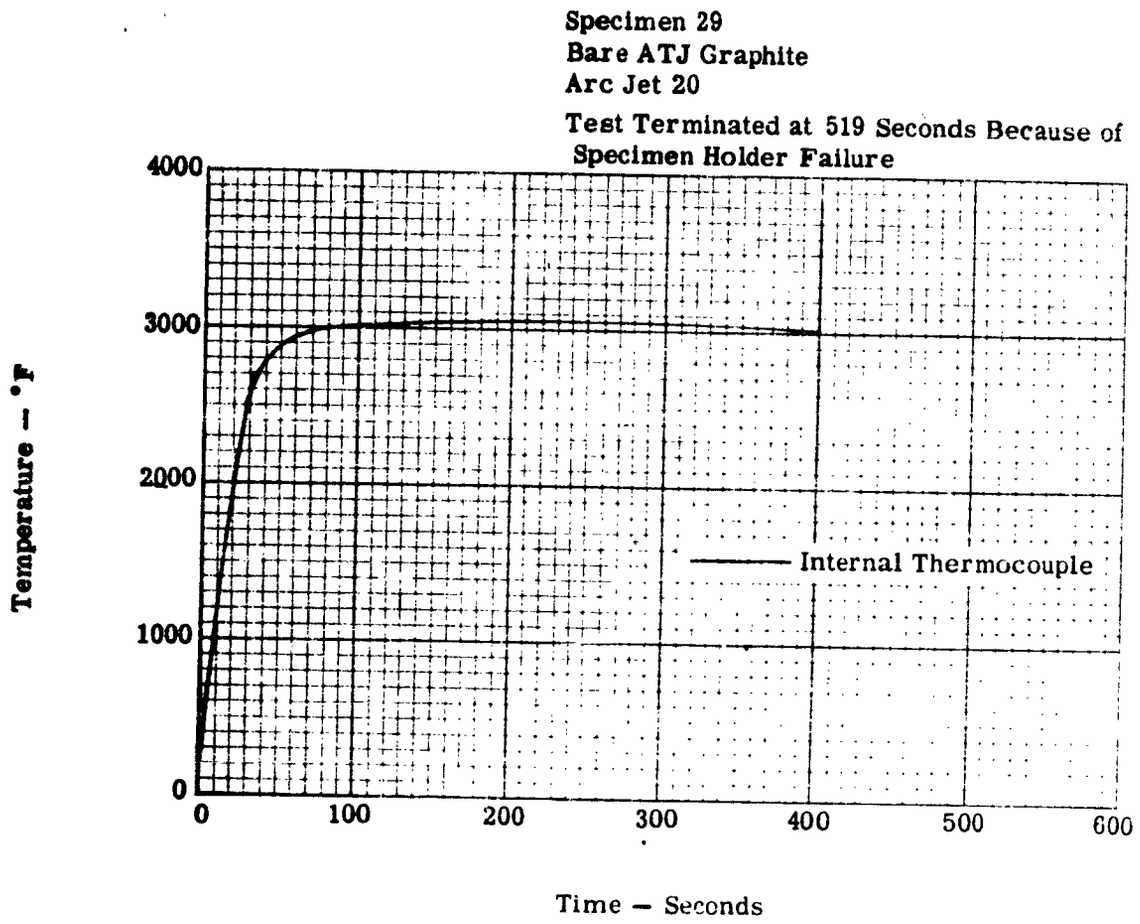

FIGURE 61. SPECIMEN 29 TEMPERATURE VS TIME, NASA LANGLEY RESEARCH CENTER.

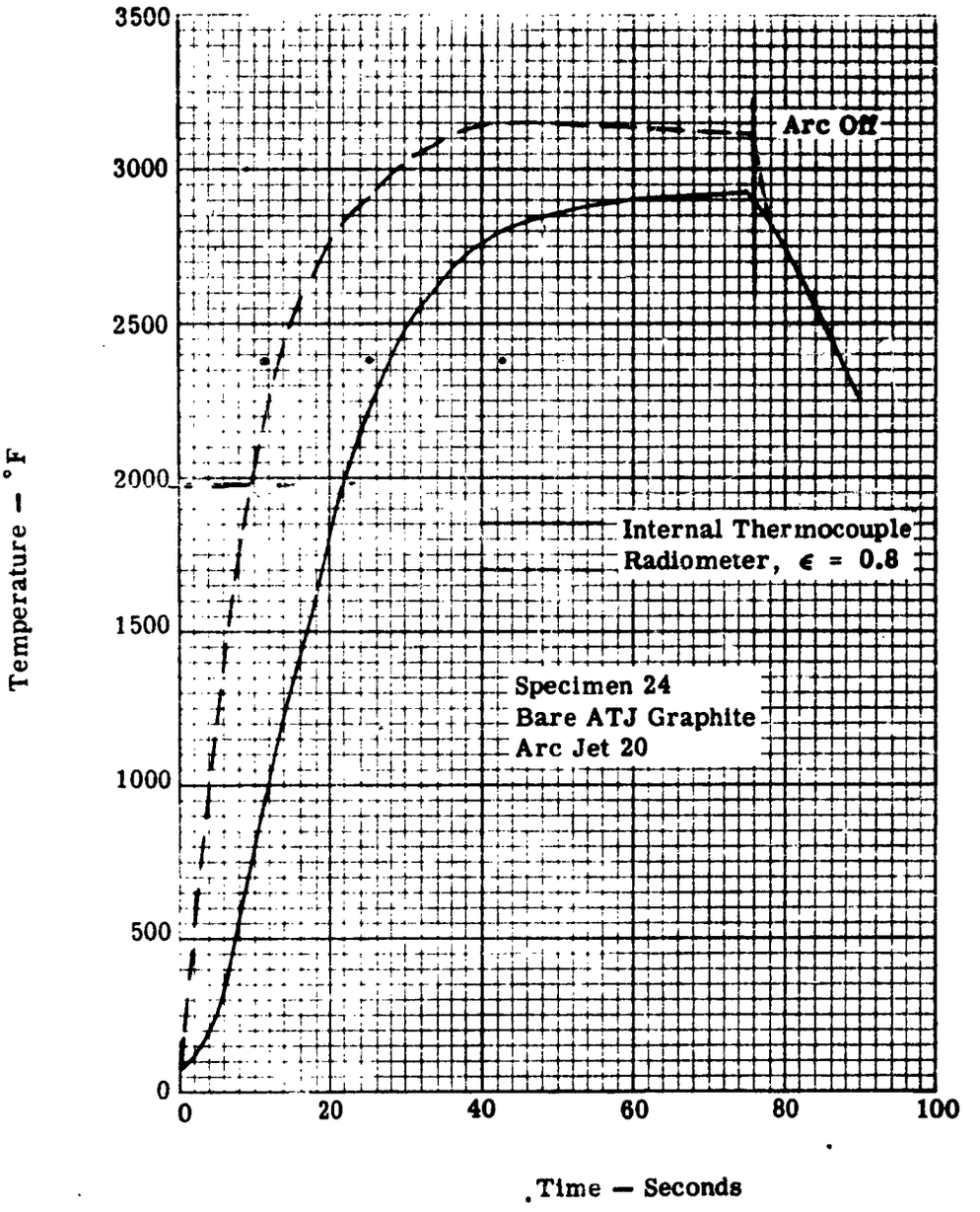

FIGURE 62. SPECIMEN 24 TEMPERATURE VS TIME, NASA LANGLEY RESEARCH CENTER

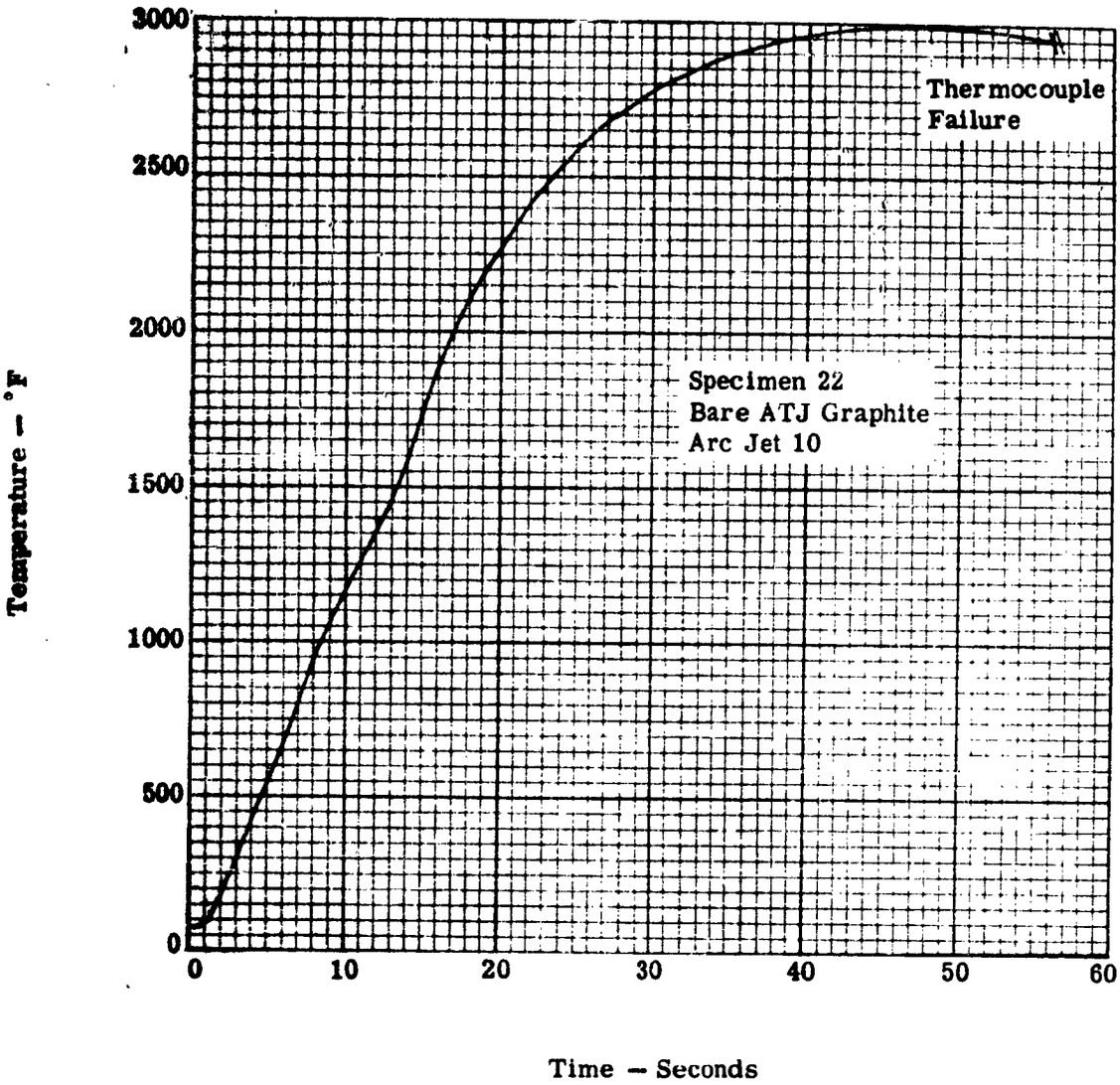

FIGURE 63. SPECIMEN 22 INTERNAL TEMPERATURE VS TIME, NASA LANGLEY RESEARCH CENTER

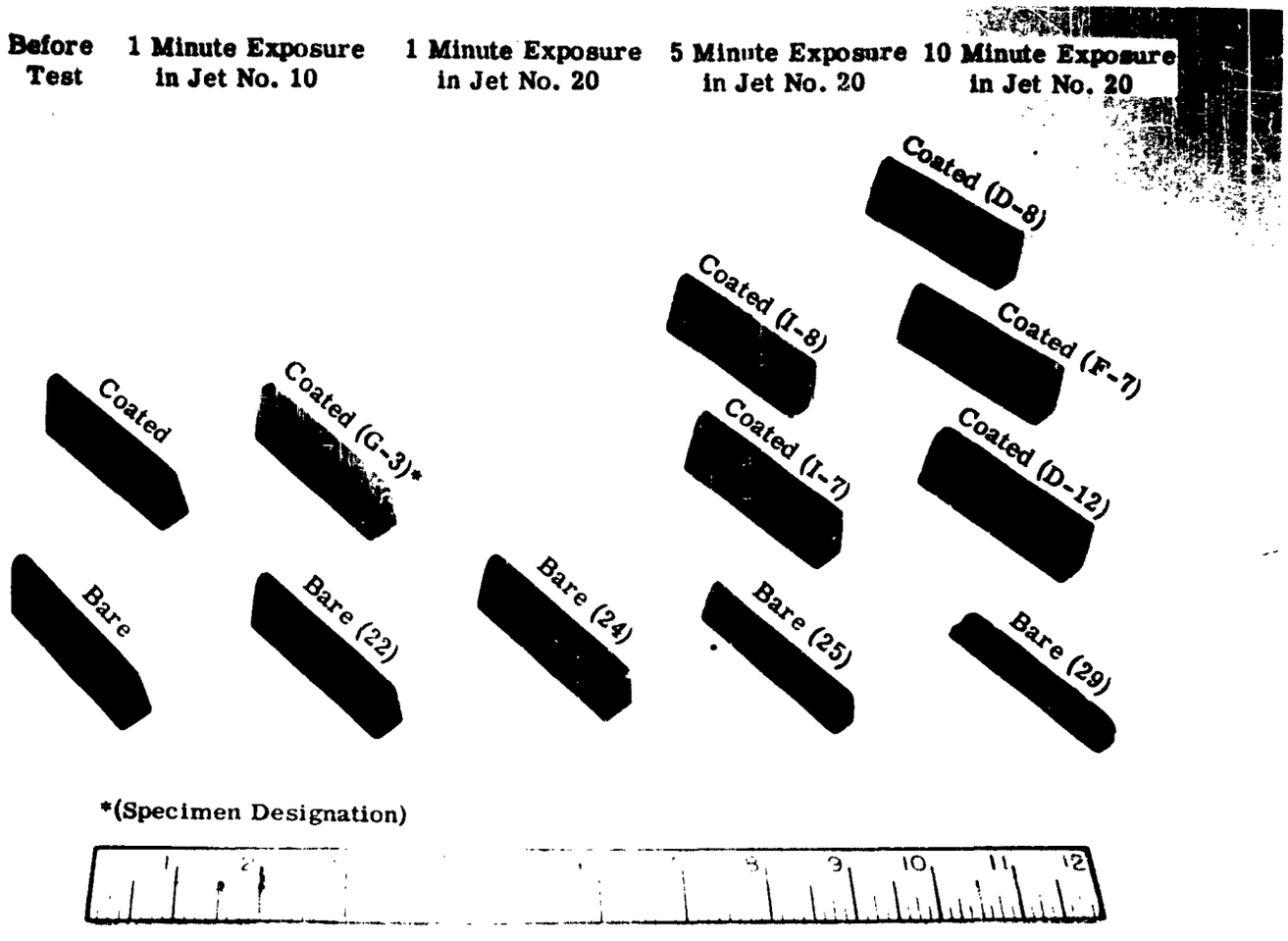

FIGURE 64. ALL BARE AND SILICONIZED ATJ GRAPHITE LEADING EDGE SPECIMENS TESTED IN NASA LANGLEY RESEARCH CENTER ARC JETS

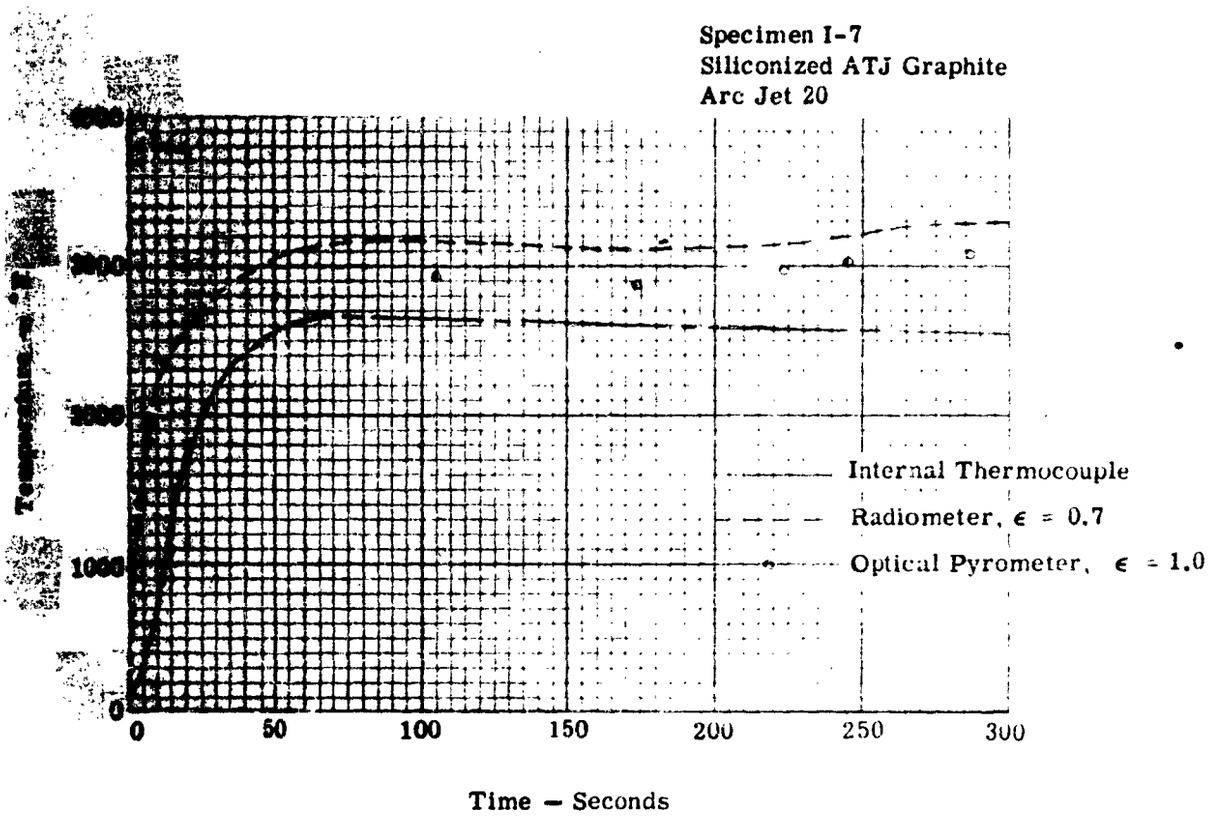

FIGURE 65. SPECIMEN I-7 TEMPERATURE VS TIME, NASA LANGLEY RESEARCH CENTER

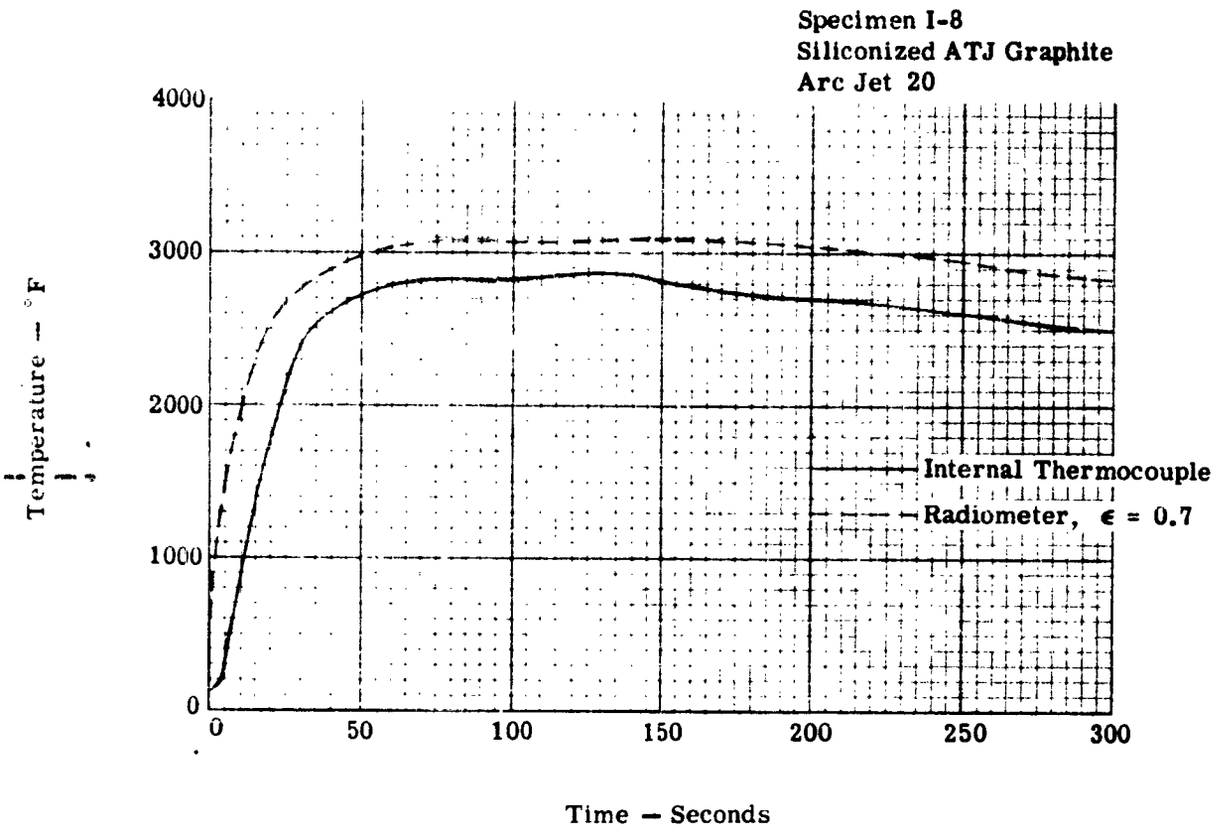

FIGURE 66. SPECIMEN I-8 TEMPERATURE VS TIME, NASA LANGLEY RESEARCH CENTER

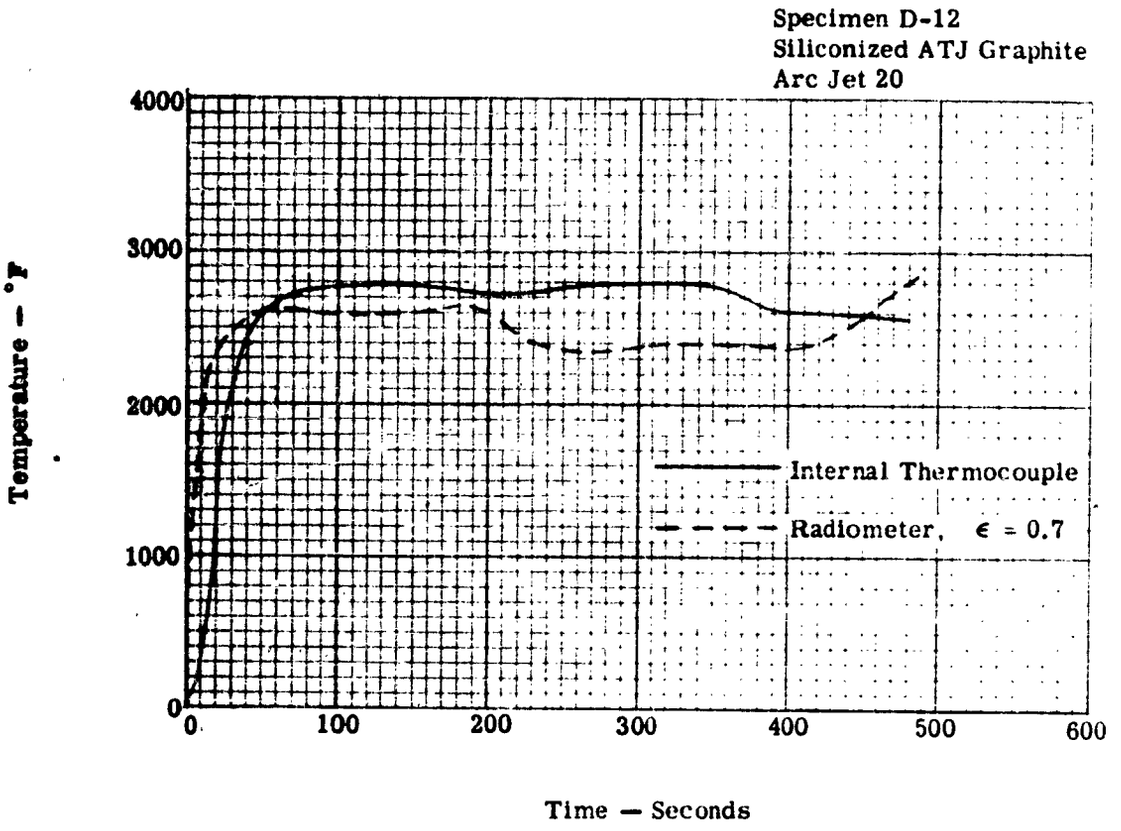

FIGURE 67. SPECIMEN D-12 TEMPERATURE VS TIME, NASA LANGLEY RESEARCH CENTER

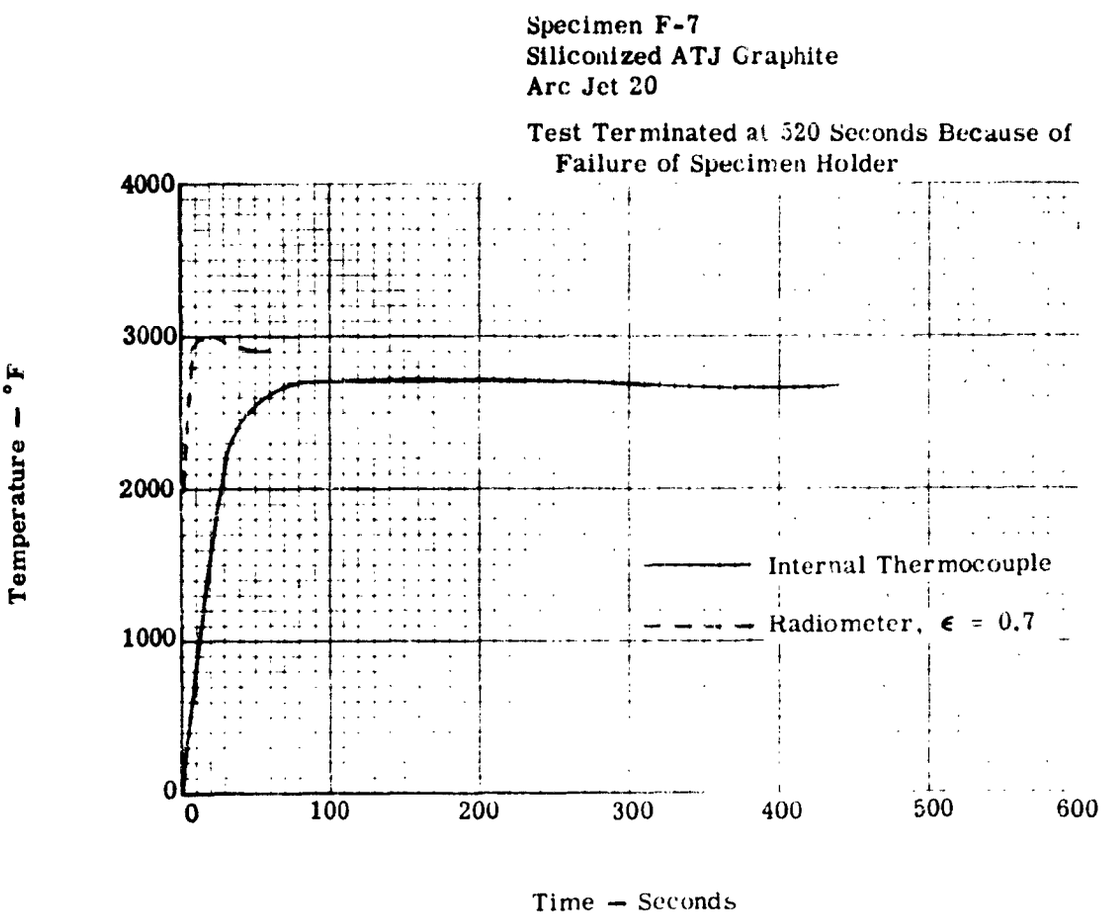

FIGURE 68. SPECIMEN F-7 TEMPERATURE VS TIME, NASA LANGLEY RESEARCH CENTER

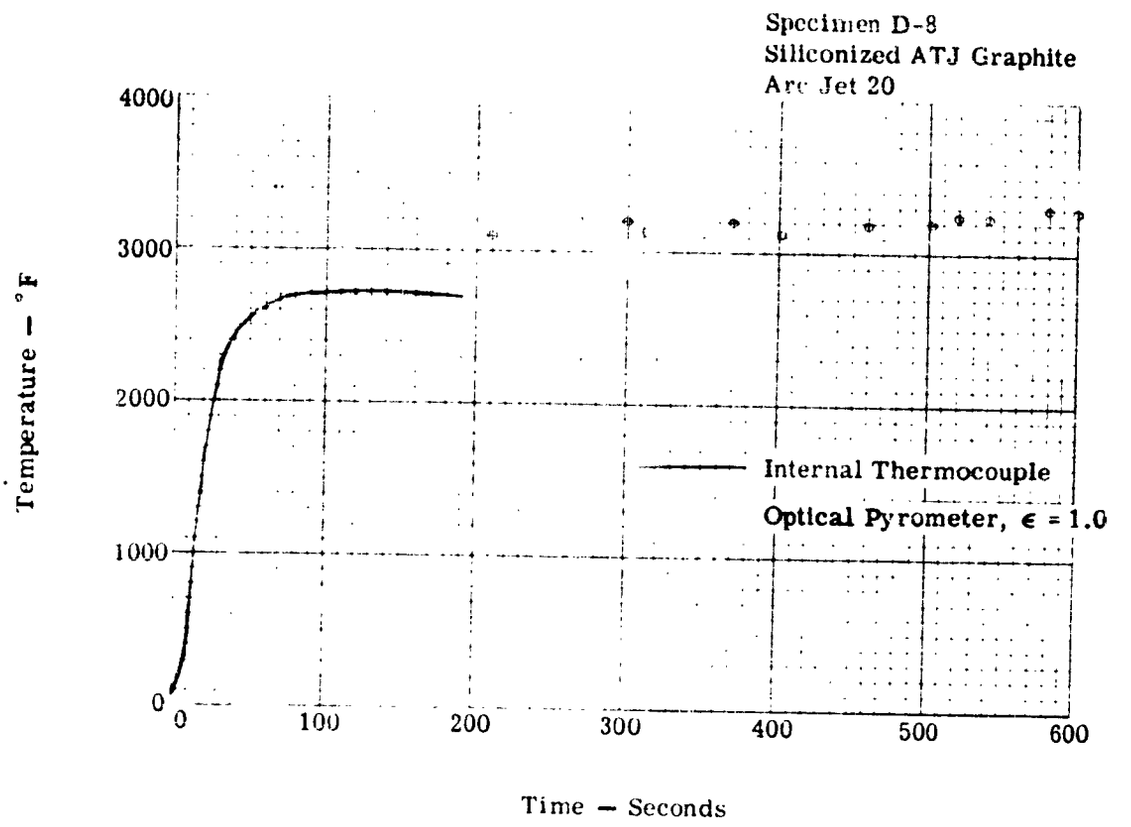

FIGURE 69. SPECIMEN D-8 TEMPERATURE VS TIME, NASA LANGLEY RESEARCH CENTER

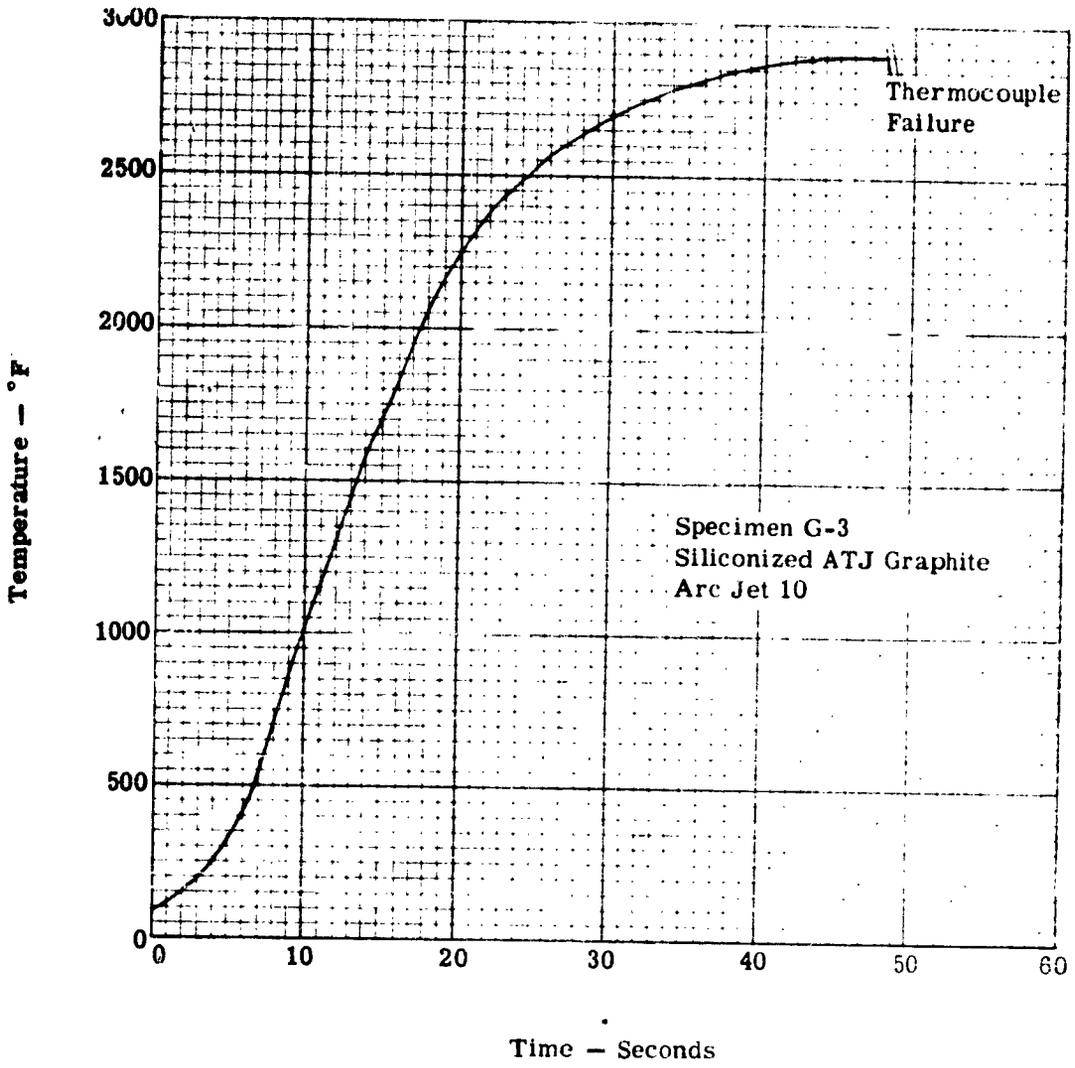

FIGURE 70. SPECIMEN G-3 INTERNAL TEMPERATURE VS TIME NASA LANGLEY RESEARCH CENTER

FIGURE 71. SPECIMEN D-12 AFTER PROBING, FOLLOWING AN EXPOSURE OF ONE HOUR AT 2000°F IN AN AIR ATMOSPHERE, IN ADDITION TO EXPOSURE IN NASA JET NO. 20 FOR 483 SECONDS

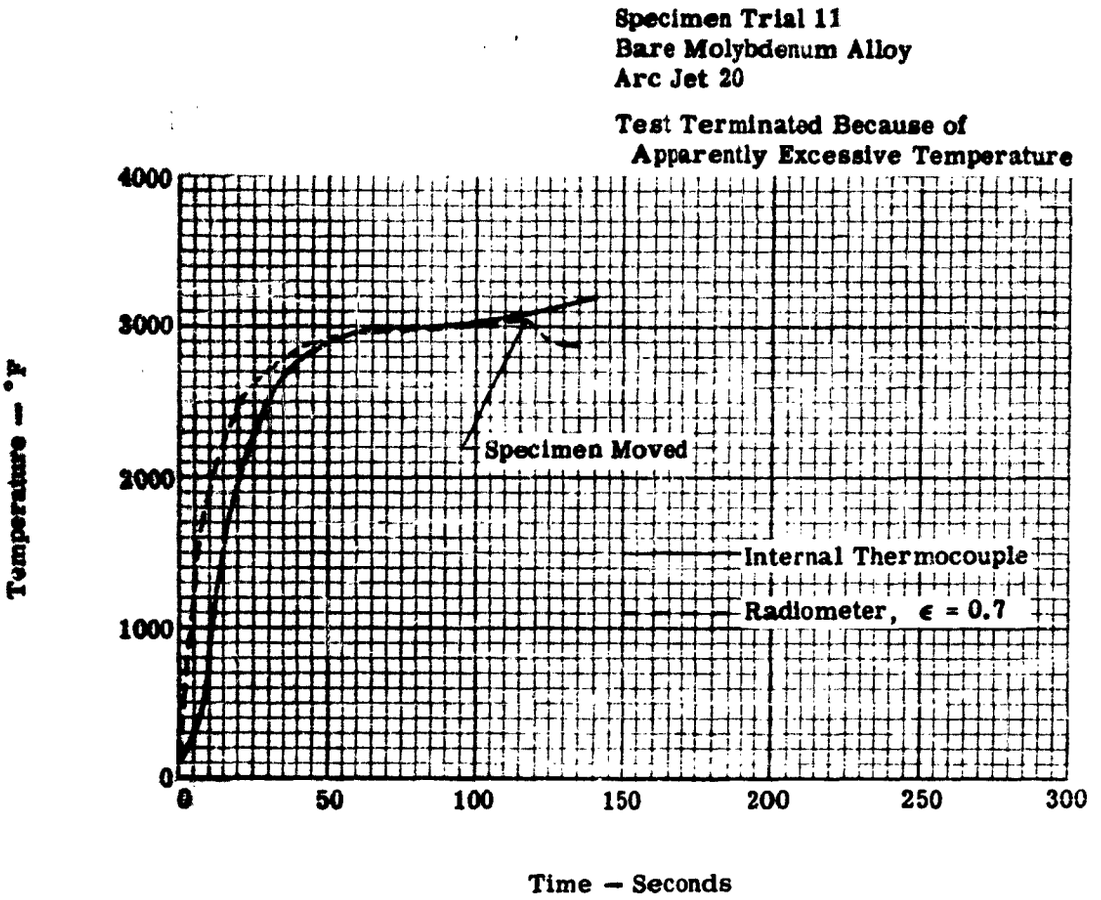

FIGURE 72. SPECIMEN TRIAL 11 TEMPERATURE VS TIME, NASA LANGLEY RESEARCH CENTER

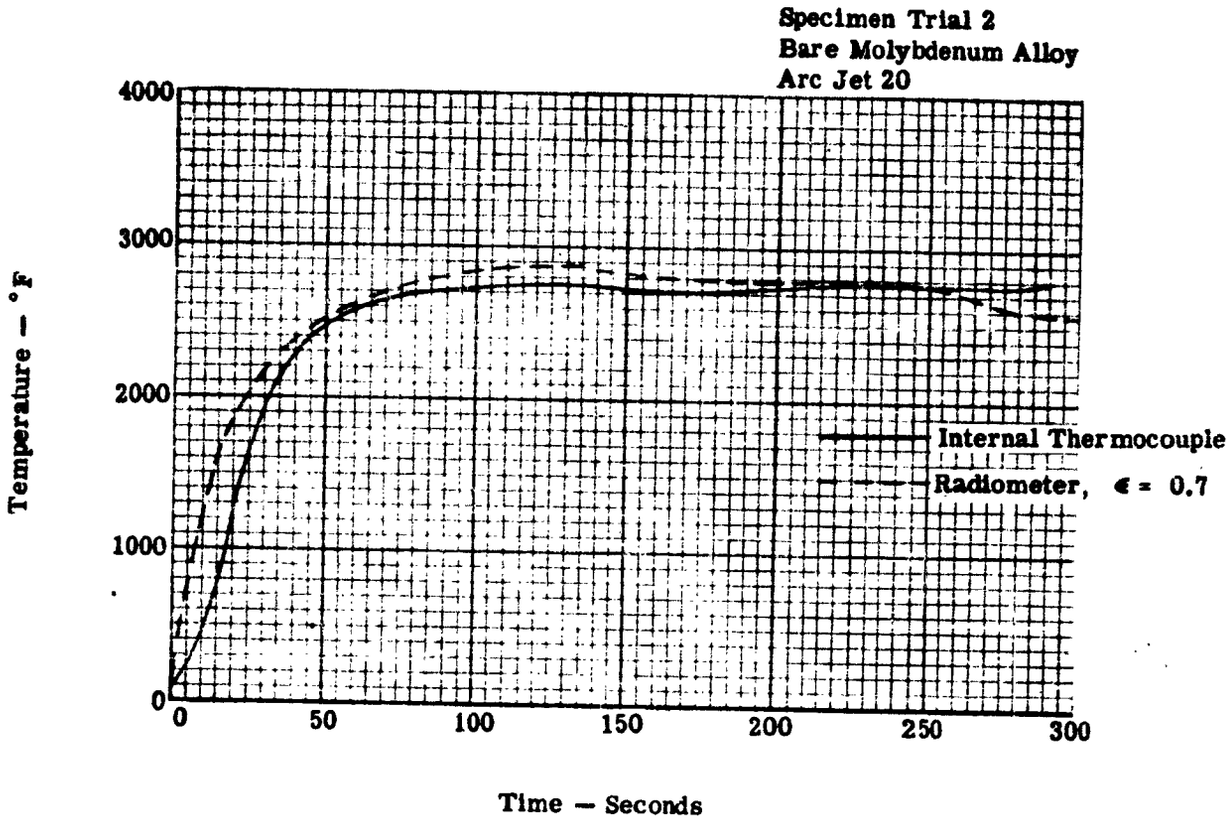

FIGURE 73. SPECIMEN TRIAL 2 TEMPERATURE VS TIME, NASA LANGLEY RESEARCH CENTER

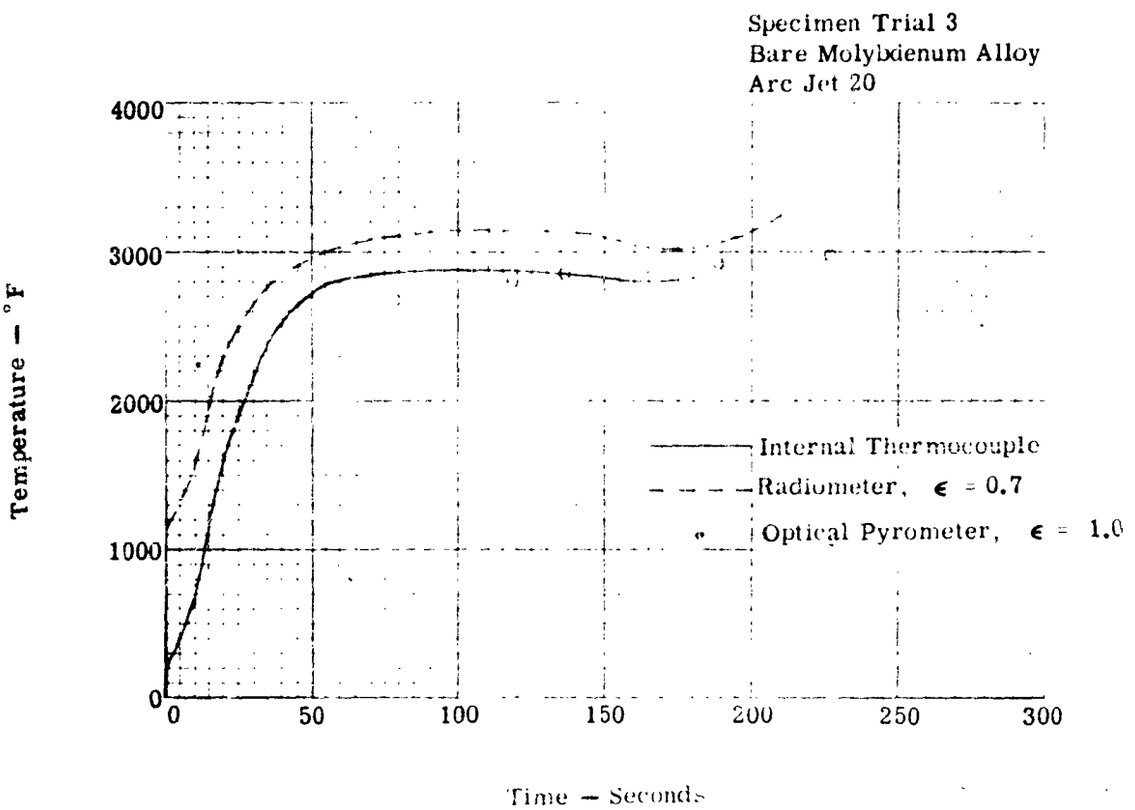

FIGURE 74. SPECIMEN TRIAL 3 TEMPERATURE VS TIME, NASA LANGLEY RESEARCH CENTER

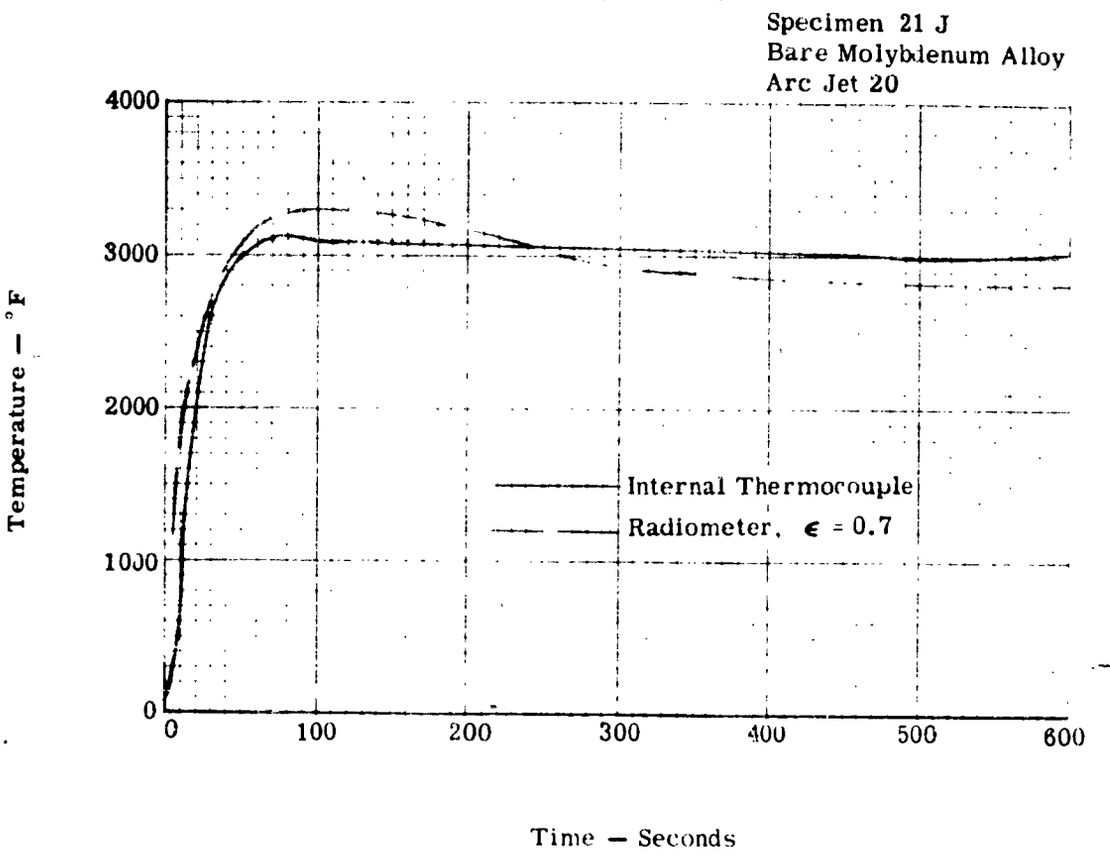

FIGURE 75. SPECIMEN 21J TEMPERATURE VS TIME, NASA LANGLEY RESEARCH CENTER

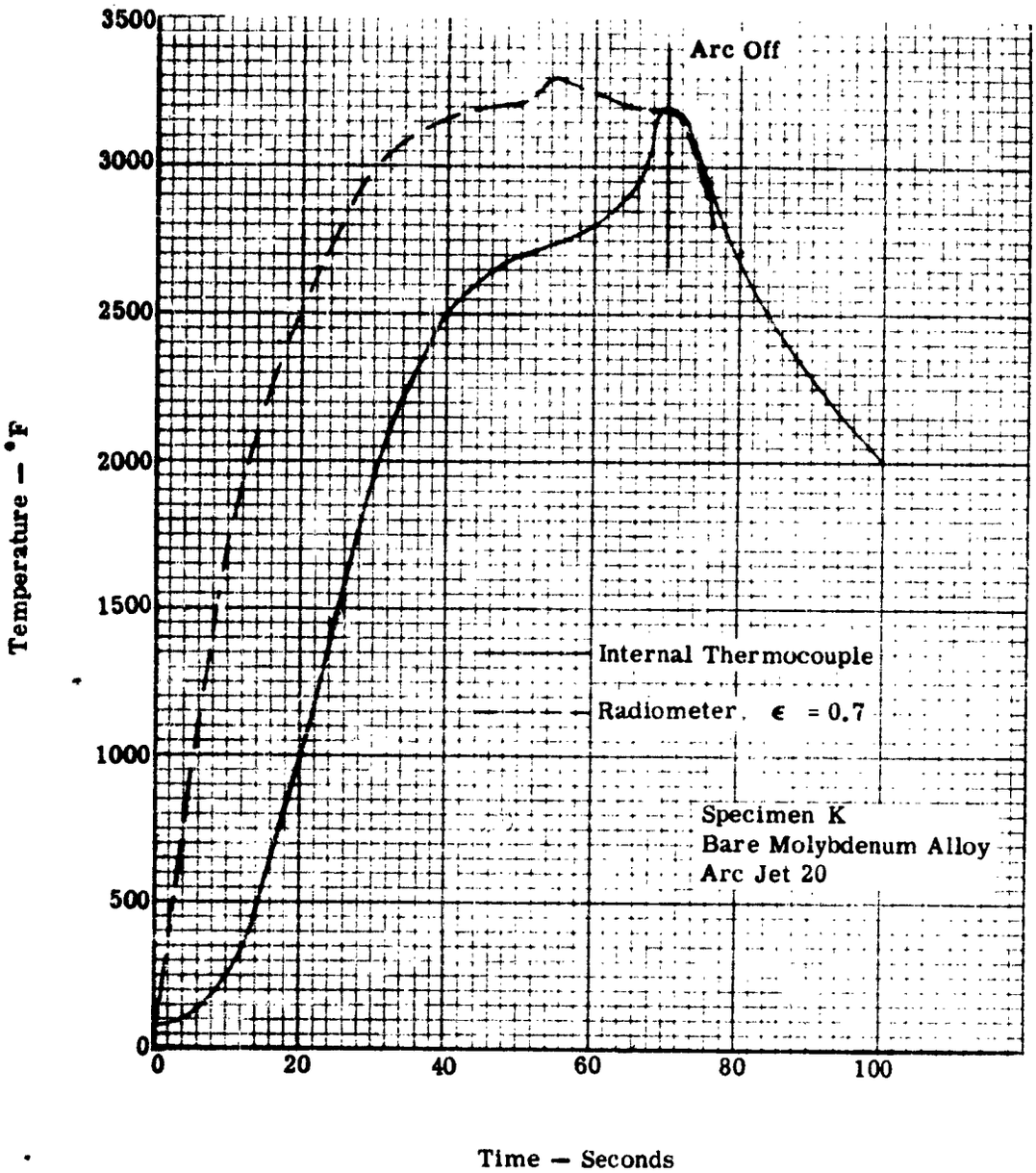

FIGURE 76. SPECIMEN K TEMPERATURE VS TIME, NASA LANGLEY RESEARCH CENTER

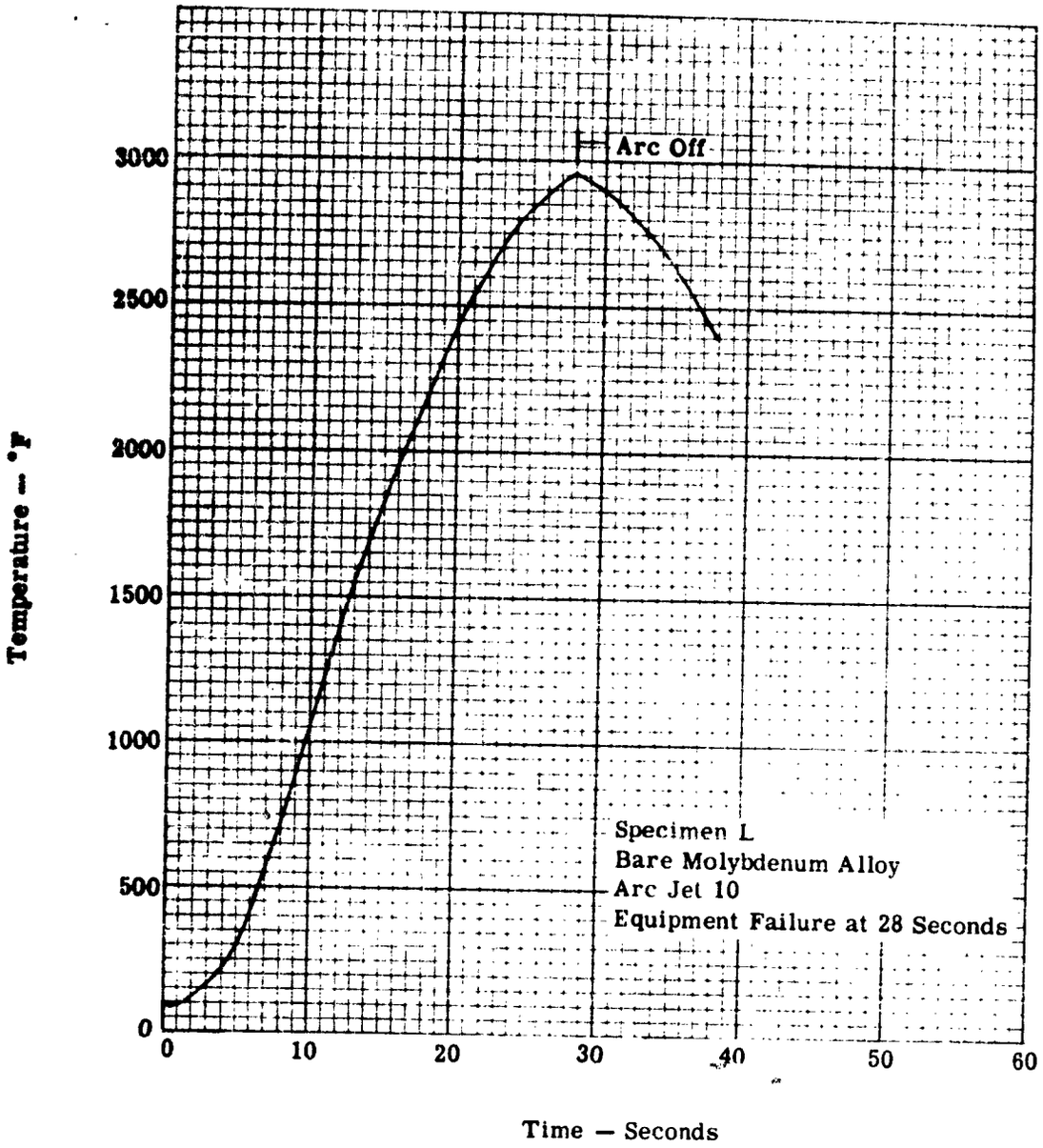

FIGURE 77. SPECIMEN L INTERNAL TEMPERATURE VS TIME, NASA LANGLEY RESEARCH CENTER

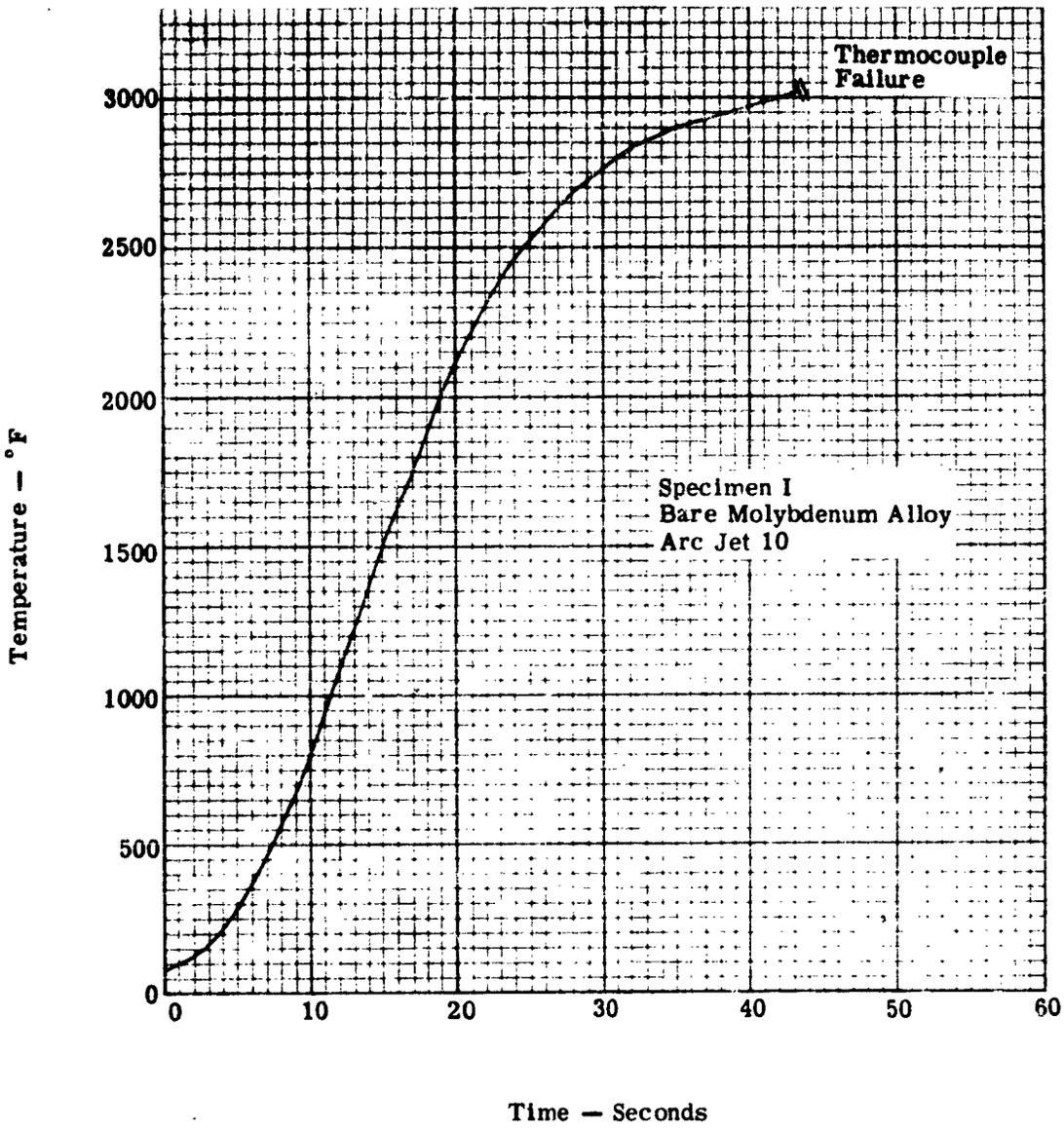

FIGURE 78. SPECIMEN I INTERNAL TEMPERATURE VS TIME, NASA LANGLEY RESEARCH CENTER

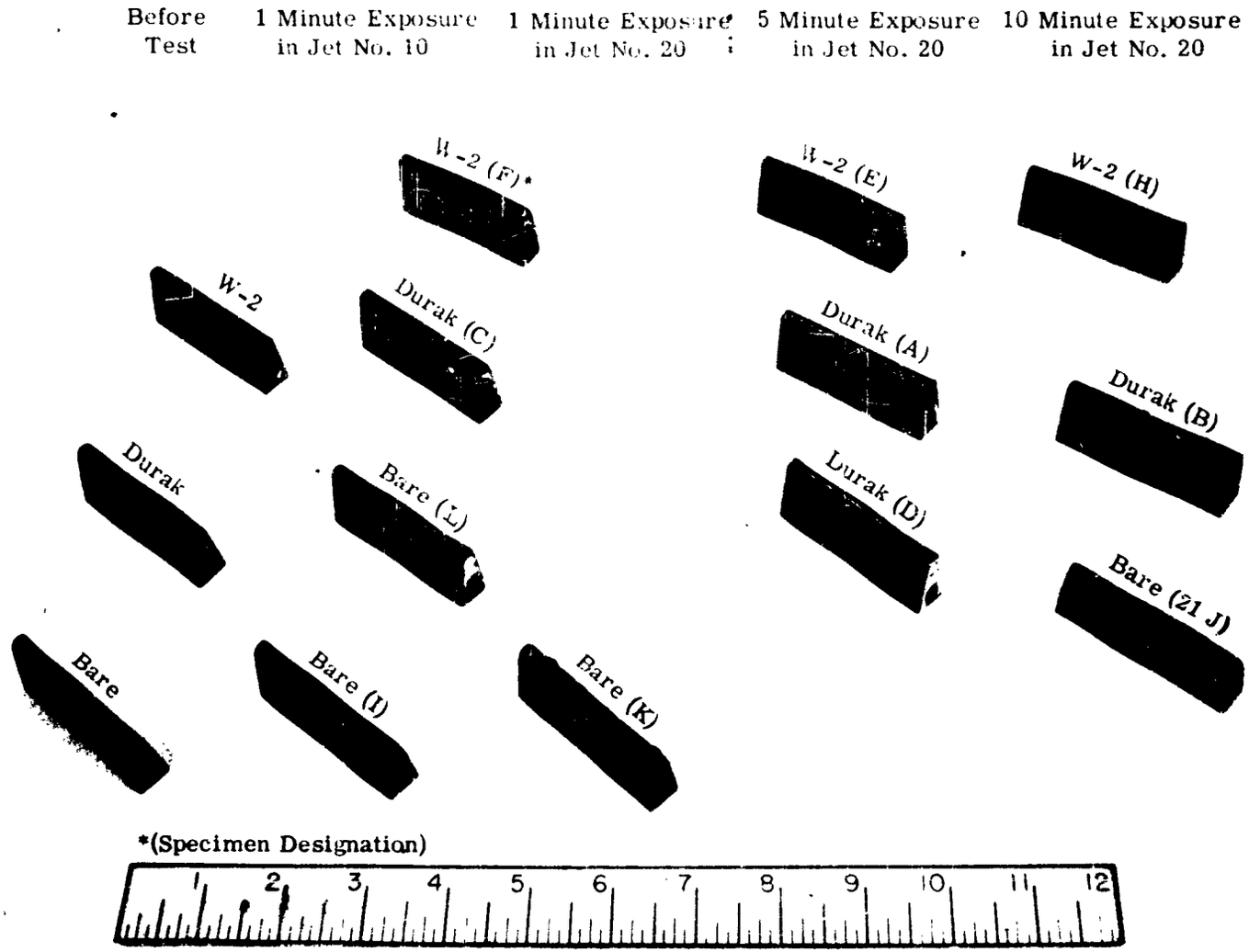

FIGURE 79. ALL BARE, W-2 COATED, AND DURAK MG COATED MOLYBDENUM ALLOY LEADING EDGE SPECIMENS TESTED IN NASA LANGLEY RESEARCH CENTER ARC JETS

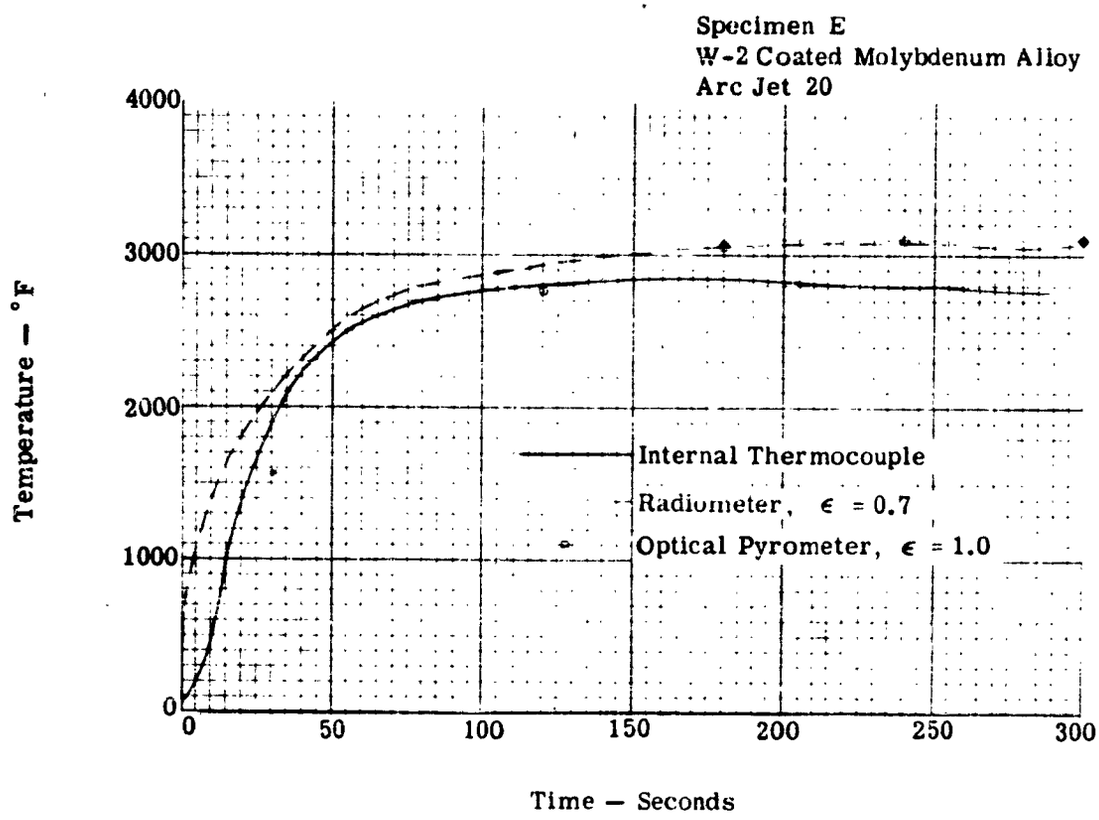

FIGURE 80. SPECIMEN E TEMPERATURE VS TIME, NASA LANGLEY RESEARCH CENTER

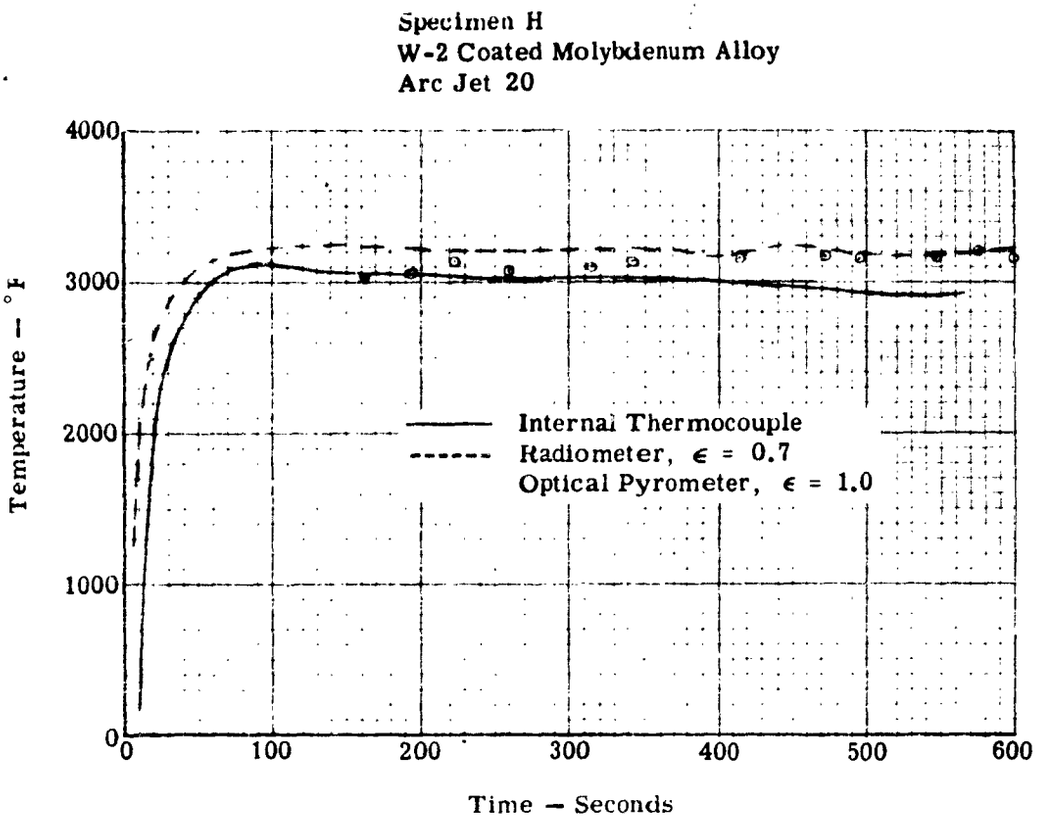

FIGURE 81. SPECIMEN H TEMPERATURE VS TIME, NASA LANGLEY RESEARCH CENTER

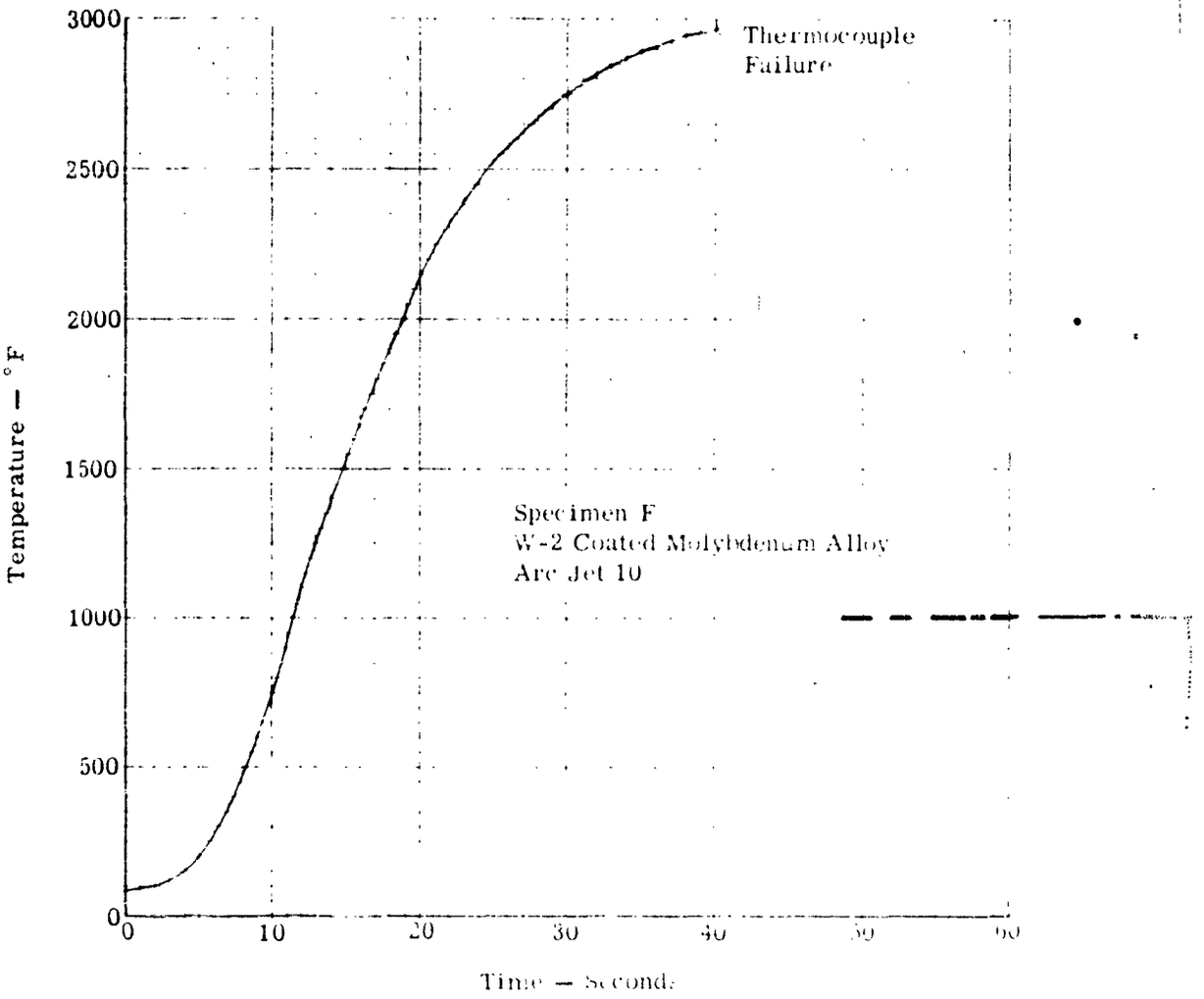

FIGURE 82. SPECIMEN F INTERNAL TEMPERATURE VS TIME, NASA LANGLEY RESEARCH CENTER

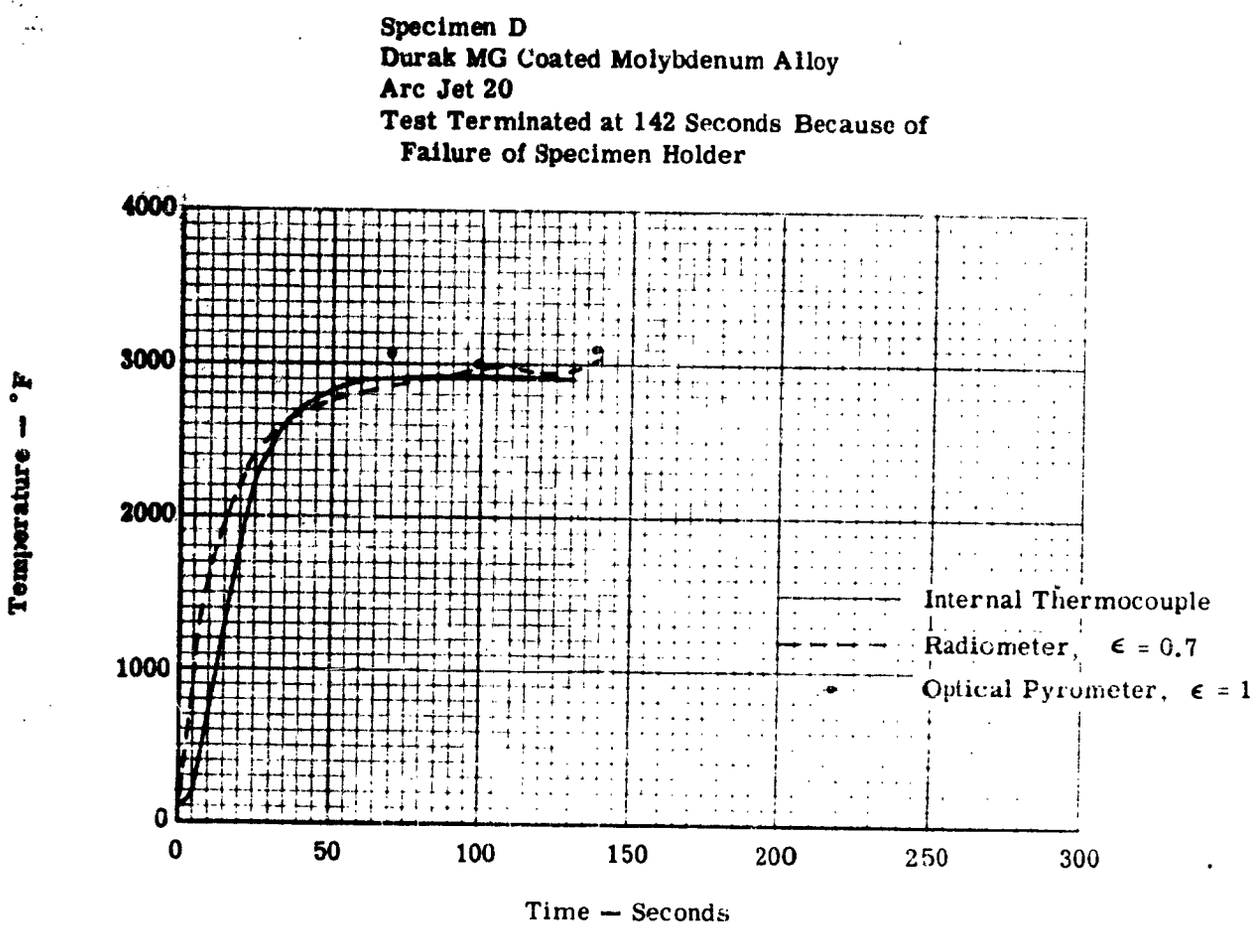

FIGURE 83. SPECIMEN D TEMPERATURE VS TIME, NASA LANGLEY RESEARCH CENTER

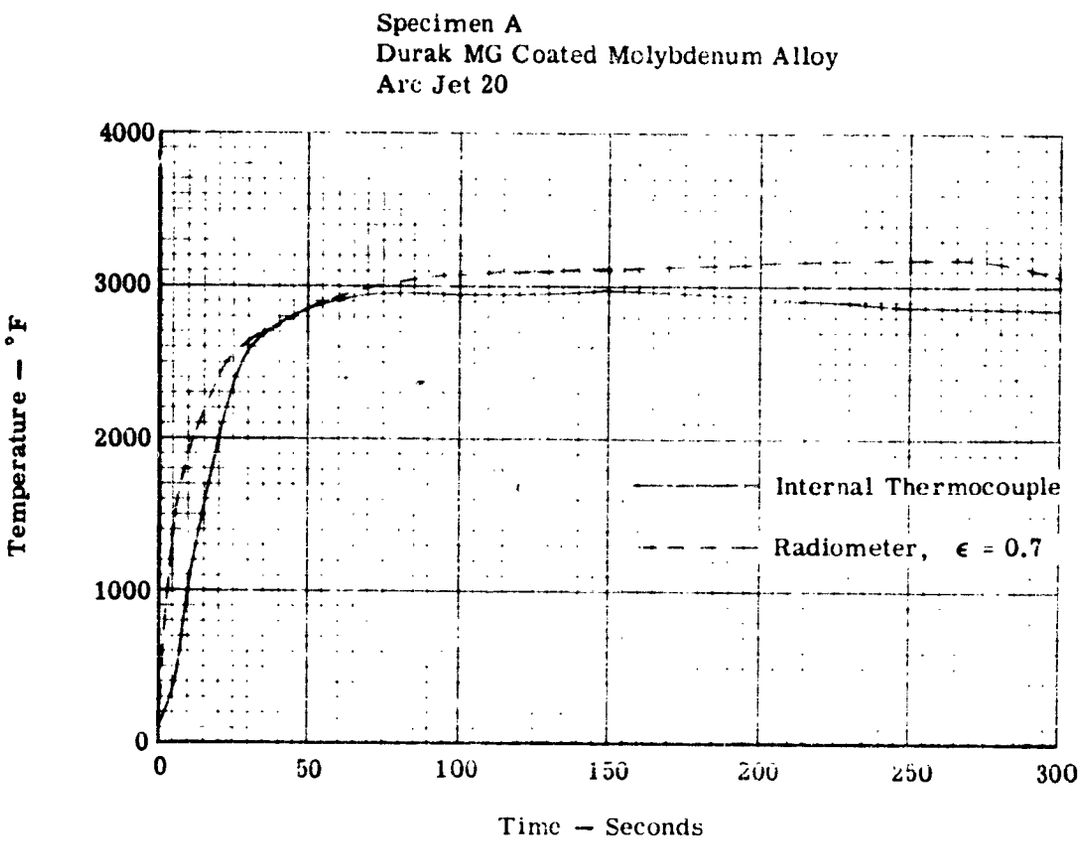

FIGURE 84. SPECIMEN A TEMPERATURE VS TIME, NASA LANGLEY RESEARCH CENTER

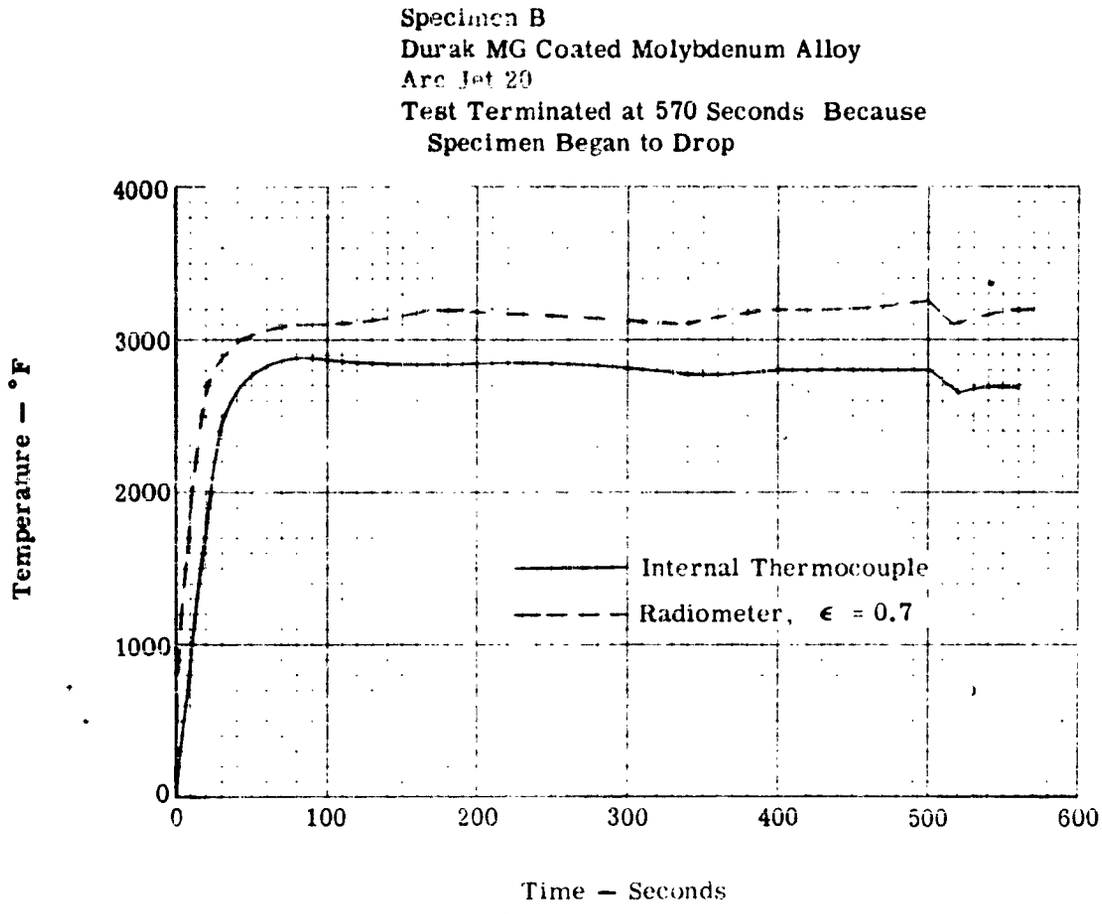

FIGURE 85. SPECIMEN B TEMPERATURE VS TIME, NASA LANGLEY RESEARCH CENTER

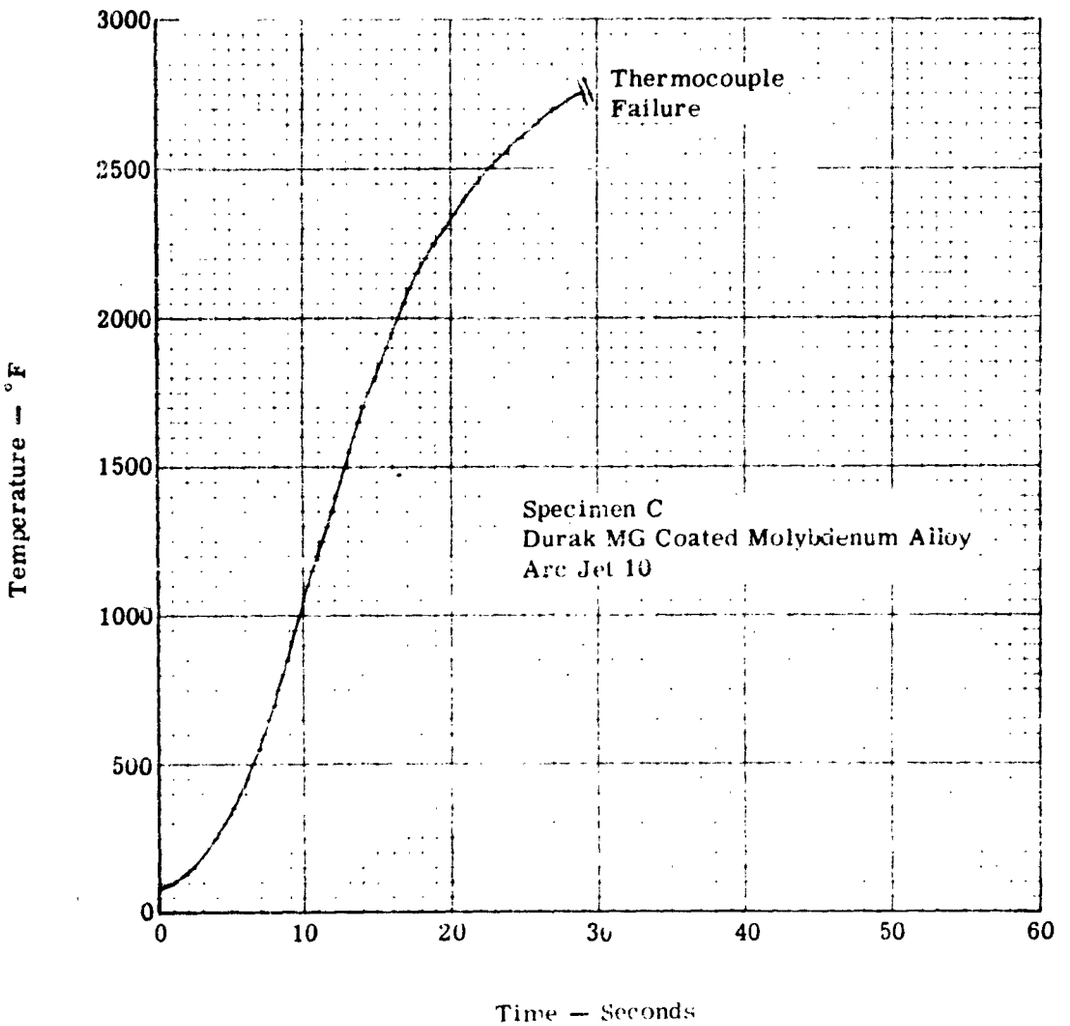

FIGURE 86. SPECIMEN C INTERNAL TEMPERATURE VS TIME, NASA LANGLEY RESEARCH CENTER

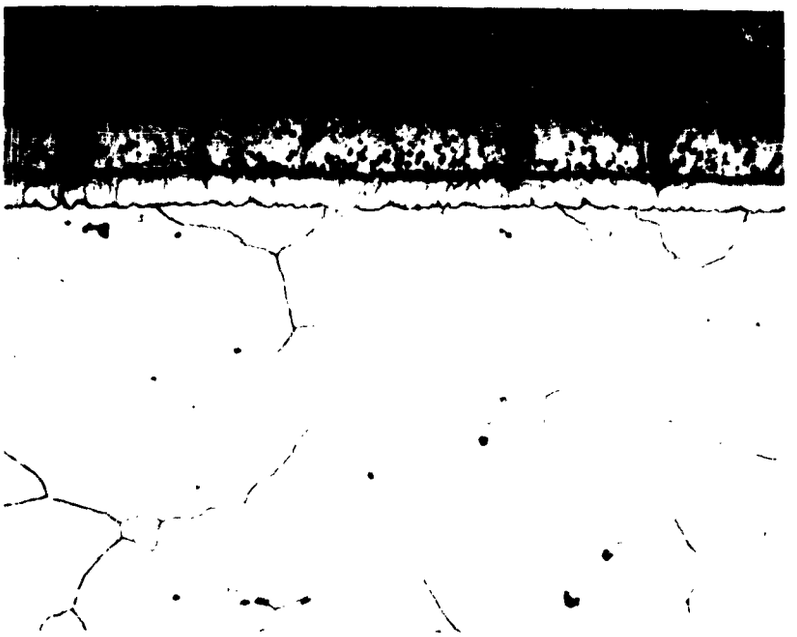

FIGURE 87. 250X PHOTOMICROGRAPH OF A SECTION OF SPECIMEN A SHOWING THE DIFFUSION LAYER OF THE DURAK MG COATING HAS NOT BEEN PENETRATED

FIGURE 88. 100X PHOTOMICROGRAPH OF A SECTION OF SPECIMEN A SHOWING COMPLETE PENETRATION OF THE DURAK MG COATING

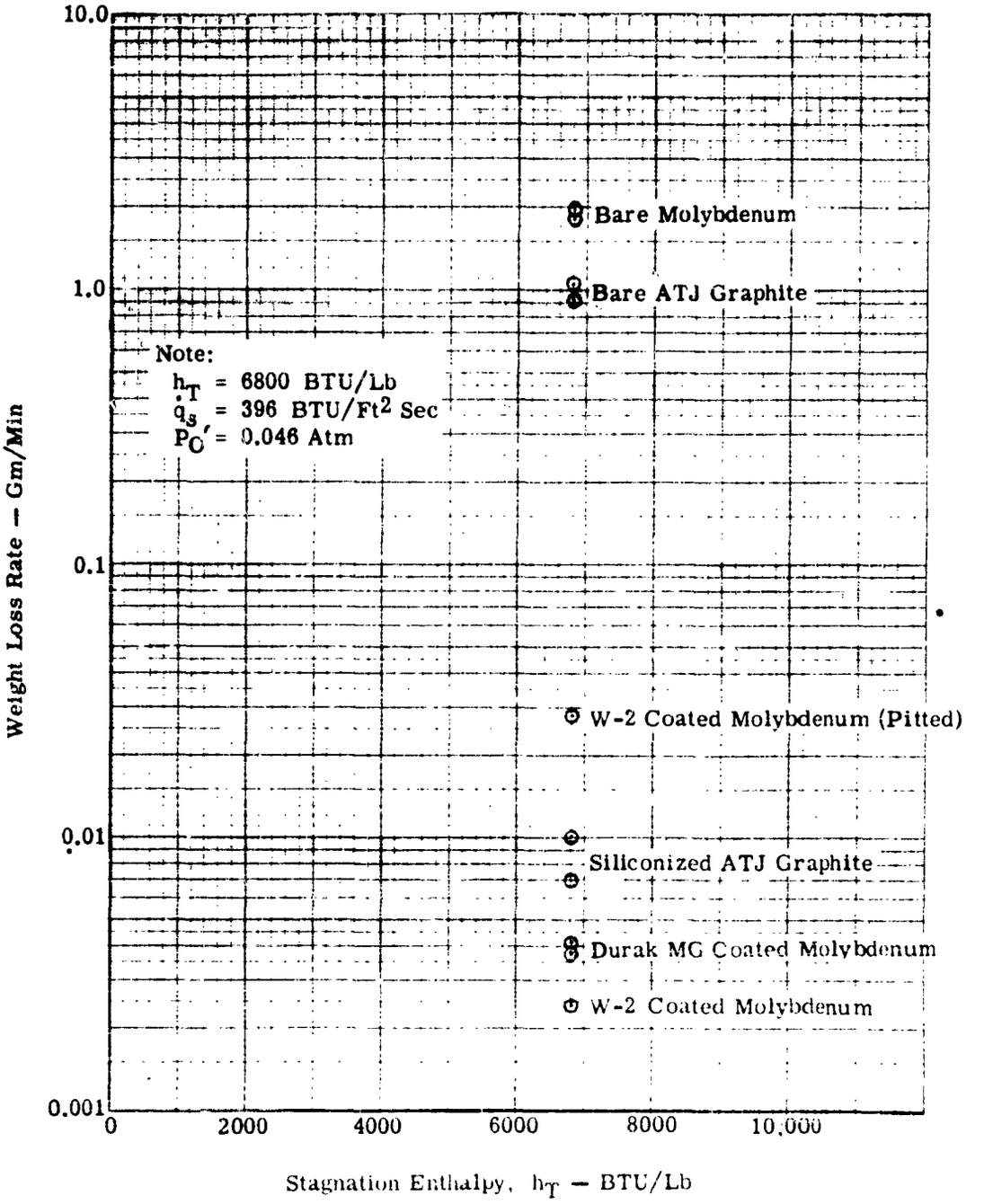

FIGURE 89. WEIGHT LOSS RATE VS STAGNATION ENTHALPY, PLASMADYNE CORPORATION

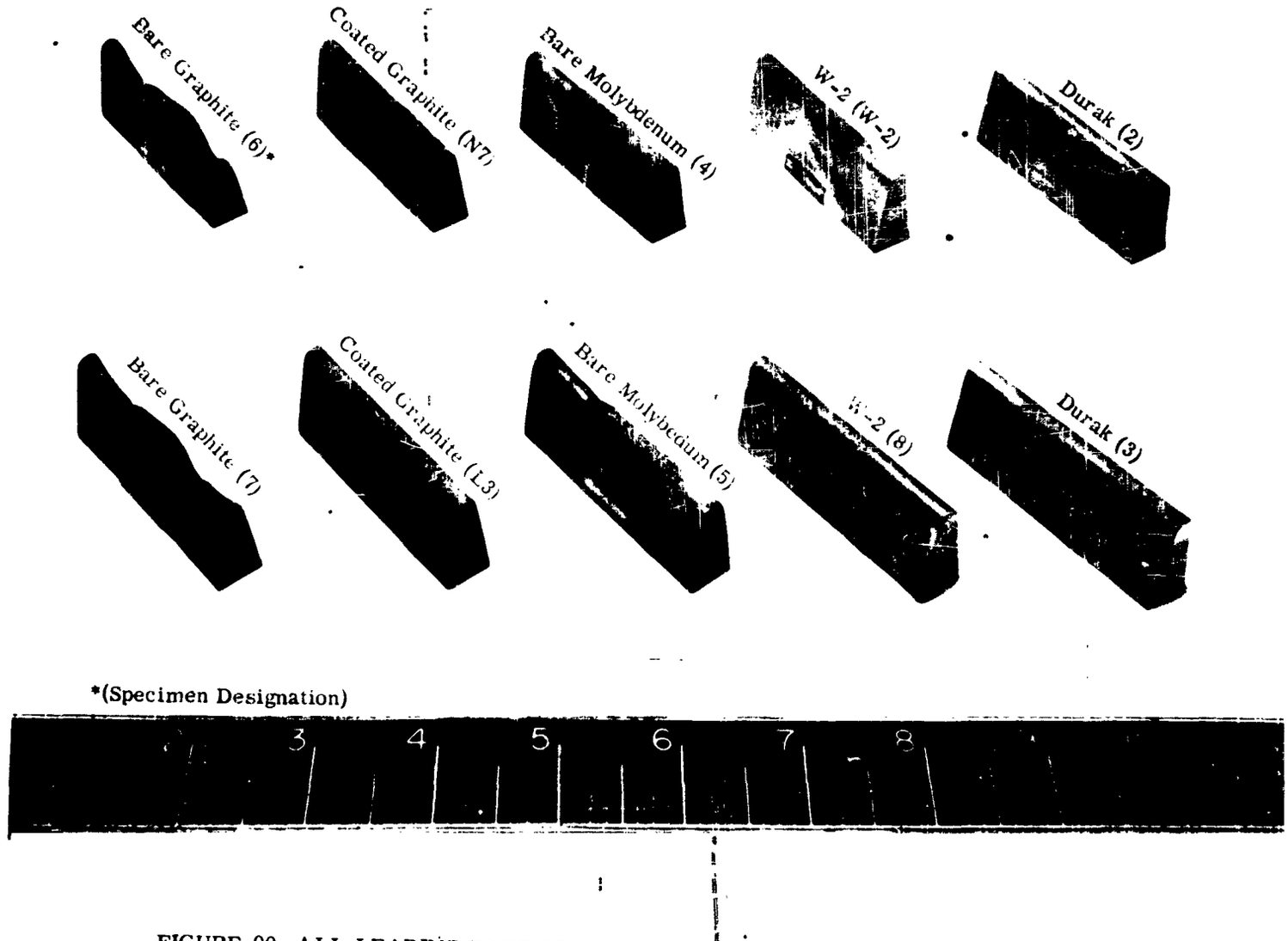

FIGURE 90. ALL LEADING EDGE SPECIMENS TESTED AT PLASMADYNE CORPORATION

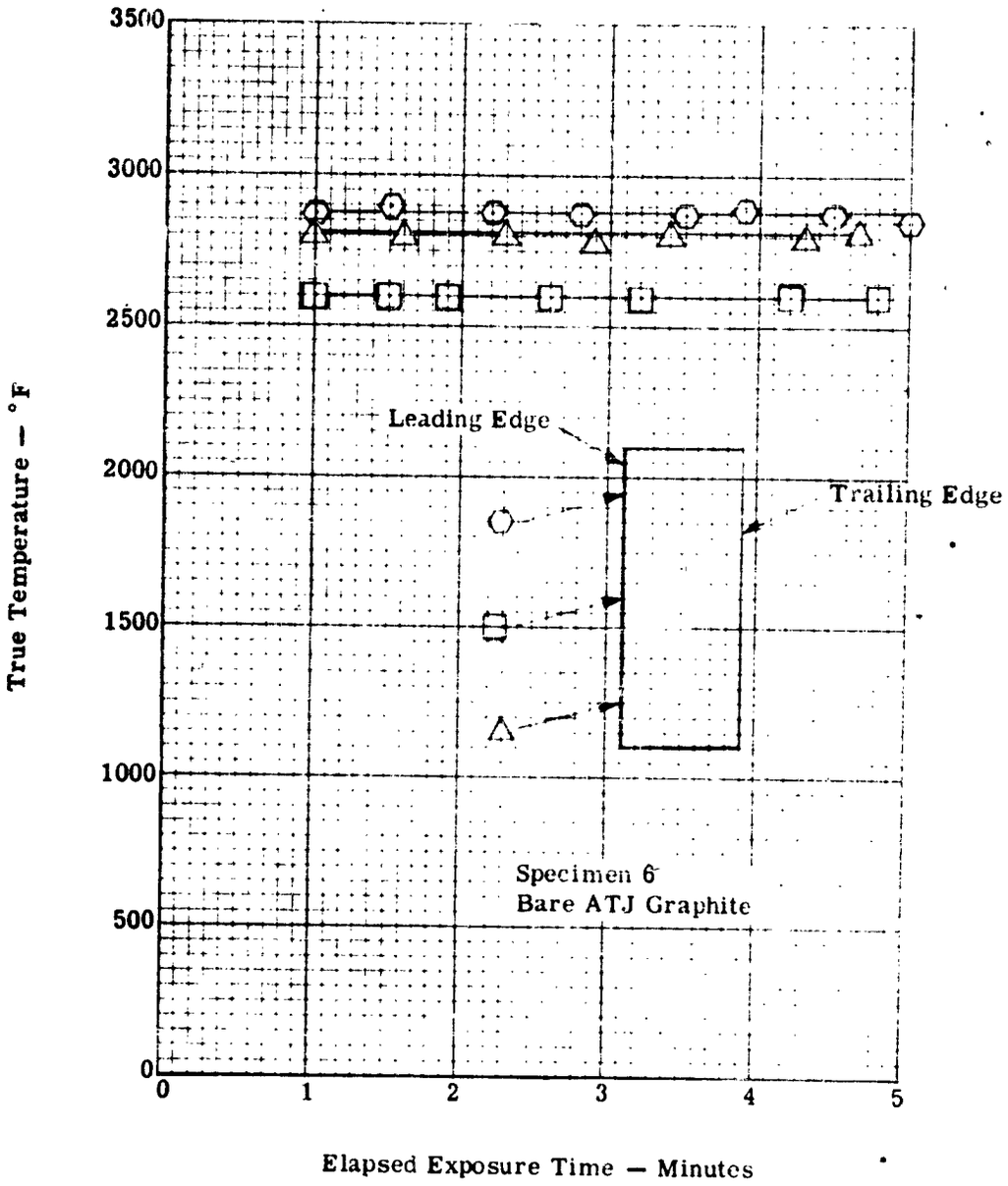

FIGURE 91. SPECIMEN 6 SURFACE TEMPERATURE VS TIME, PLASMADYNE CORPORATION

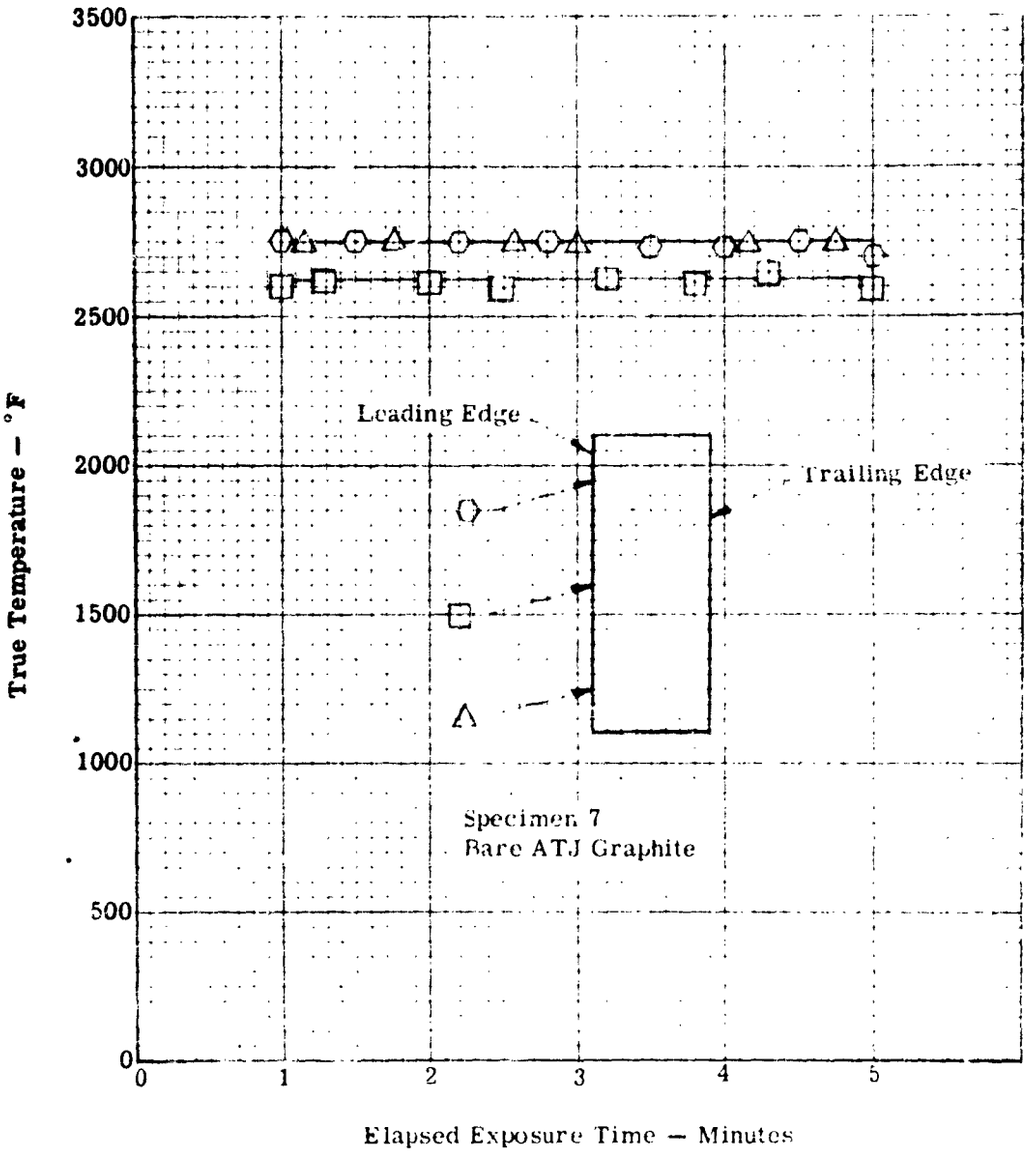

FIGURE 92. SPECIMEN 7 SURFACE TEMPERATURE VS TIME, PLASMADYNE CORPORATION

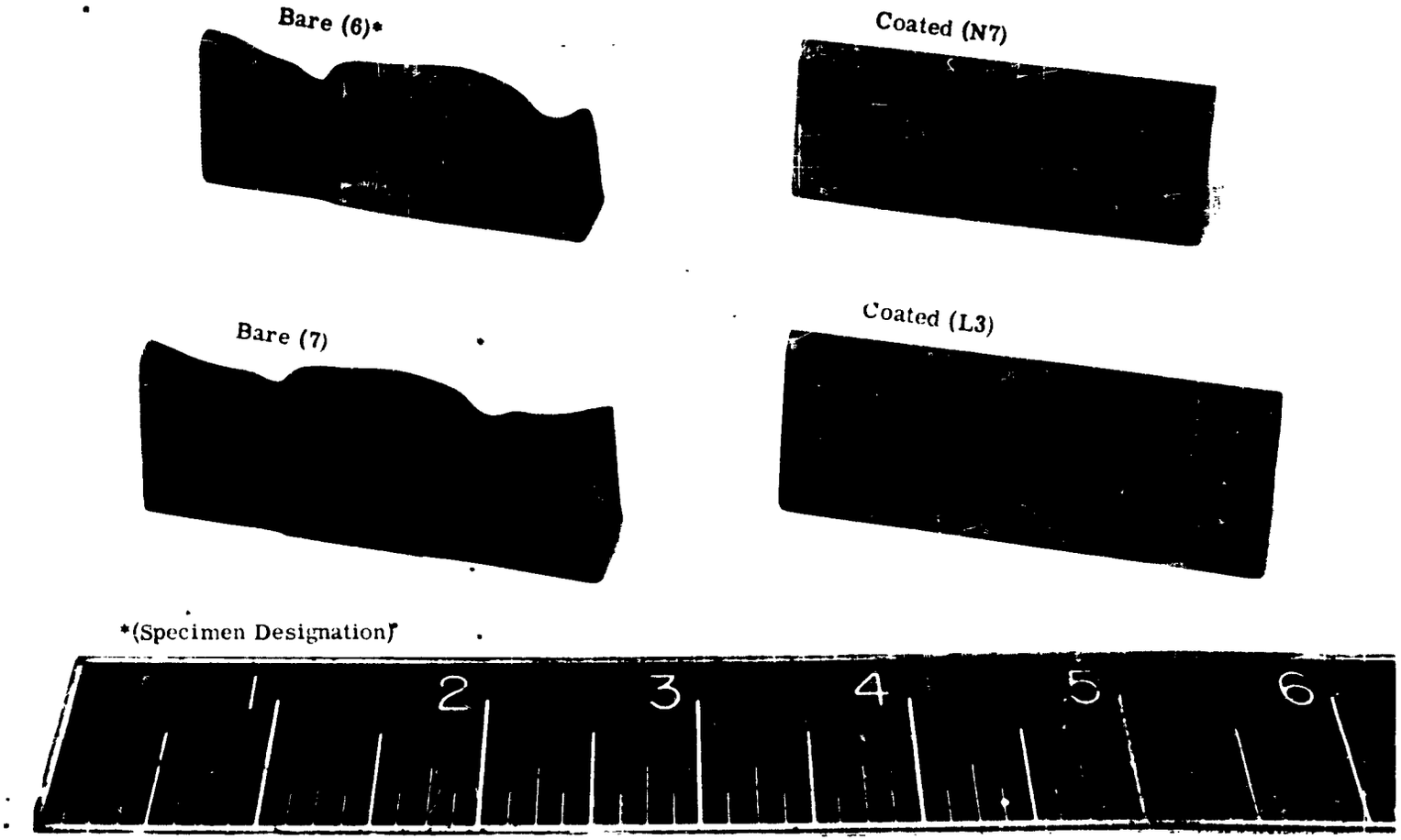

FIGURE 93. ALL BARE AND SILICONIZED ATJ GRAPHITE LEADING EDGE SPECIMENS TESTED AT PLASMADYNE CORPORATION

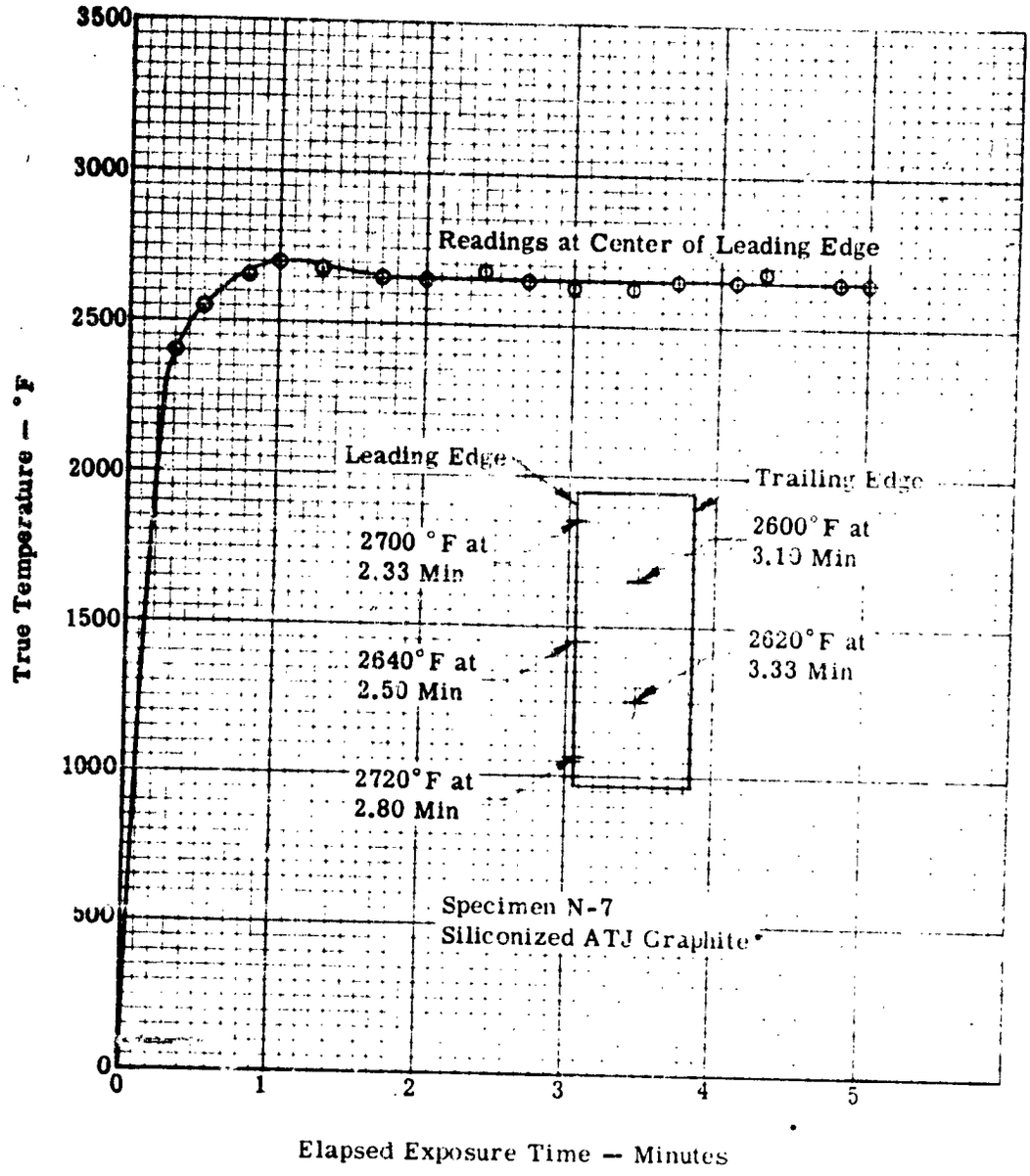

FIGURE 94. SPECIMEN N-7 SURFACE TEMPERATURE VS TIME, PLASMADYNE CORPORATION

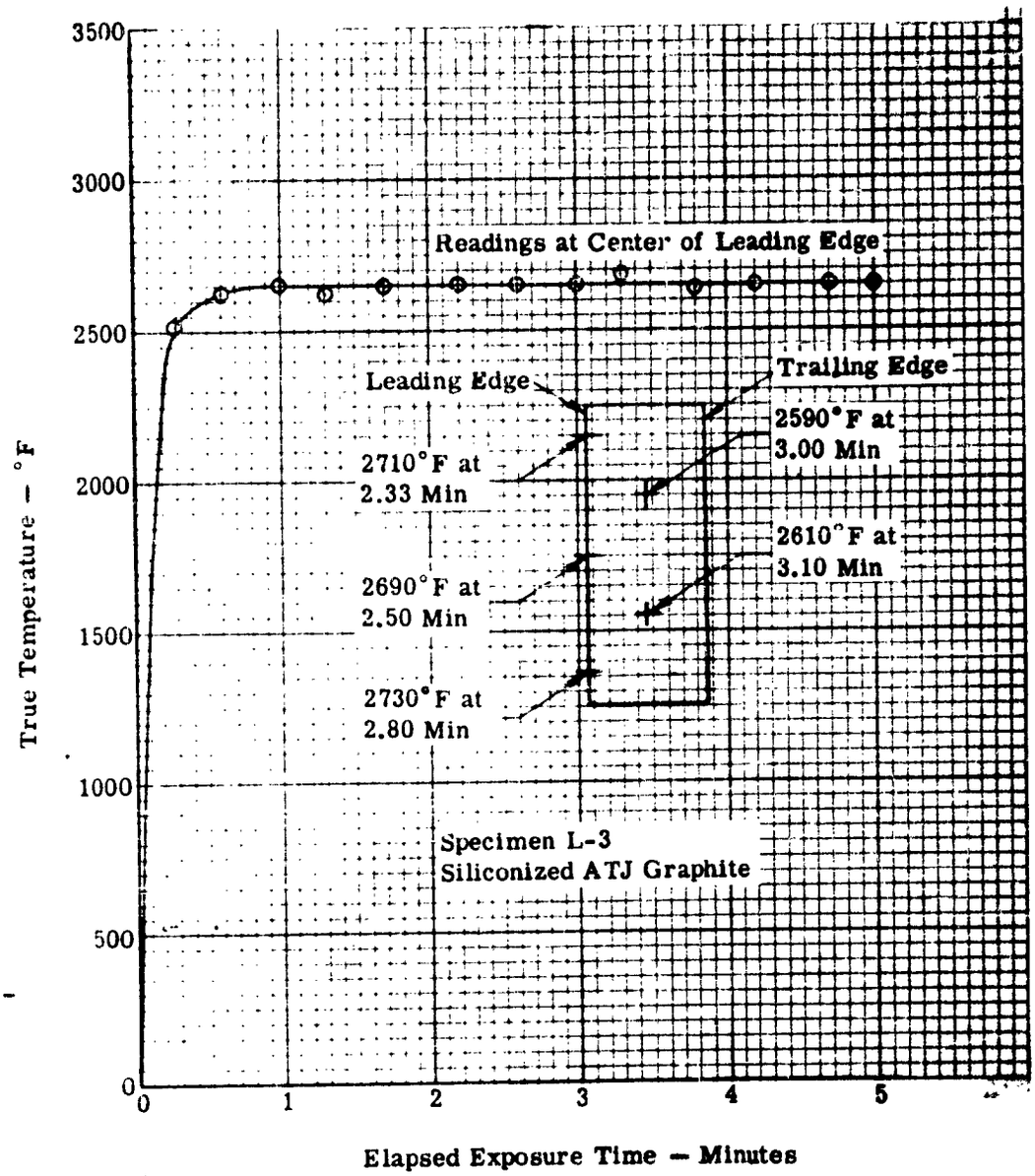

FIGURE 95. SPECIMEN L-3 SURFACE TEMPERATURE VS TIME, PLASMADYNE CORPORATION

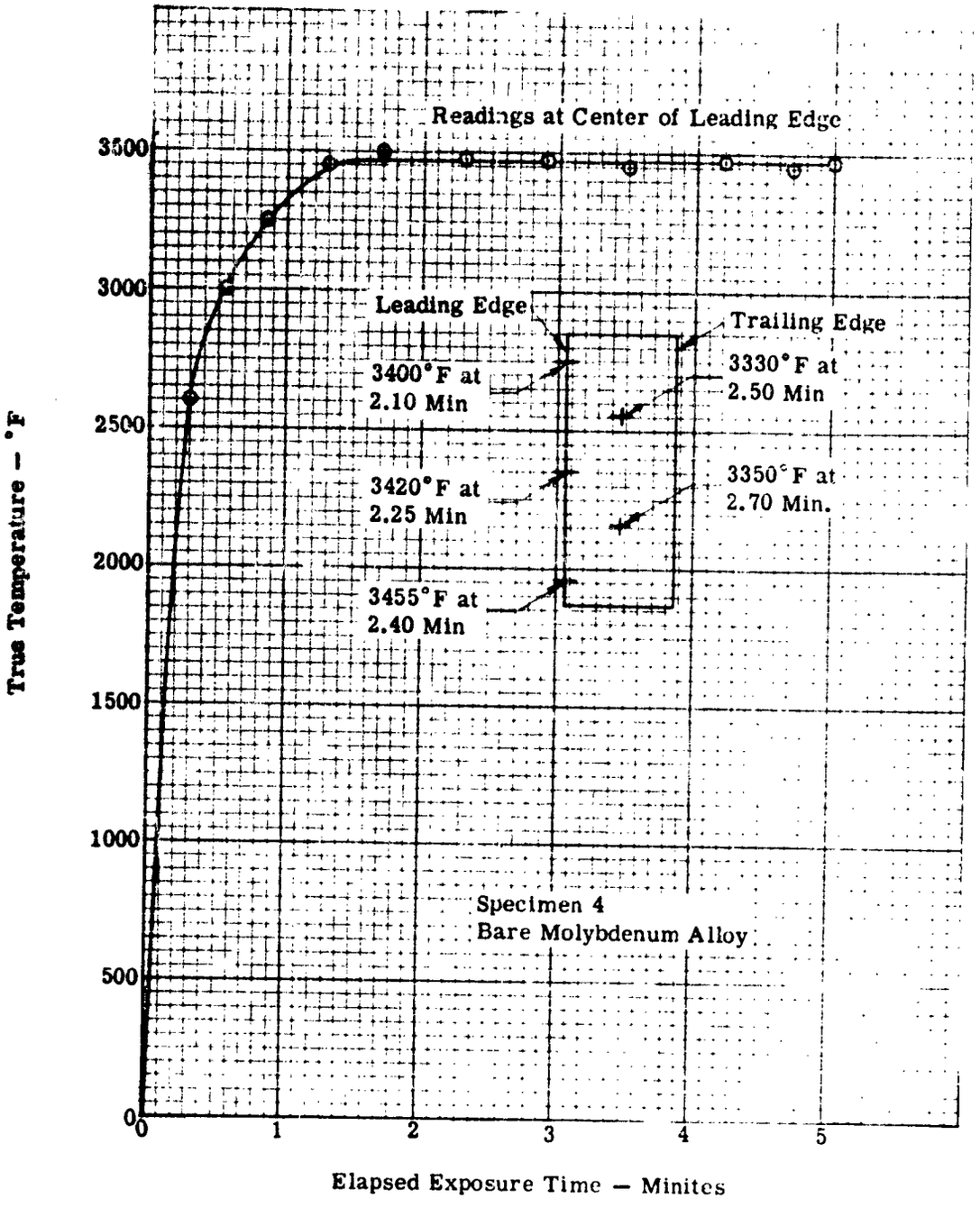

FIGURE 96. SPECIMEN 4 SURFACE TEMPERATURE VS TIME, PLASMADYNE CORPORATION

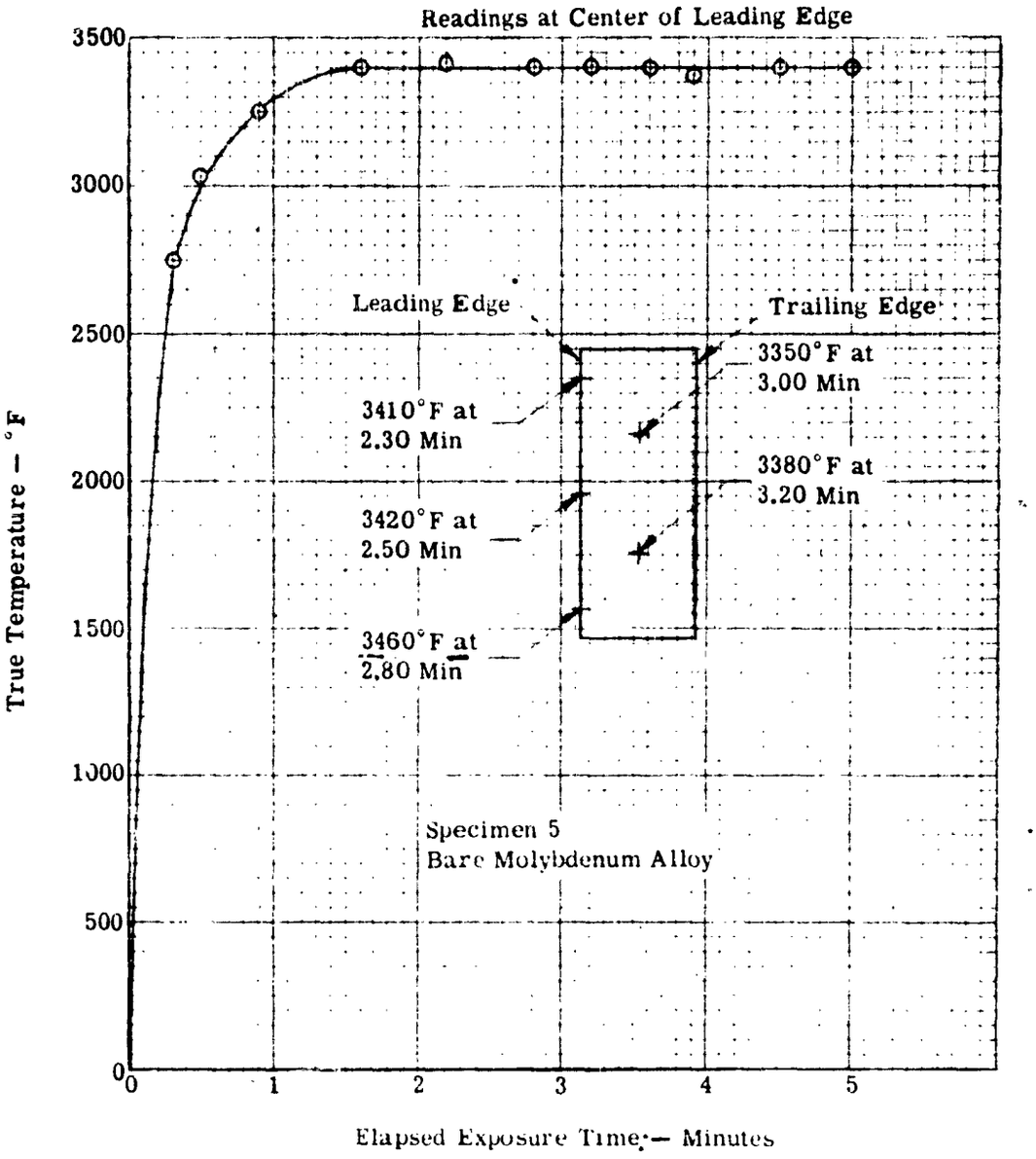

FIGURE 97. SPECIMEN 5 SURFACE TEMPERATURE VS TIME, PLASMADYNE CORPORATION

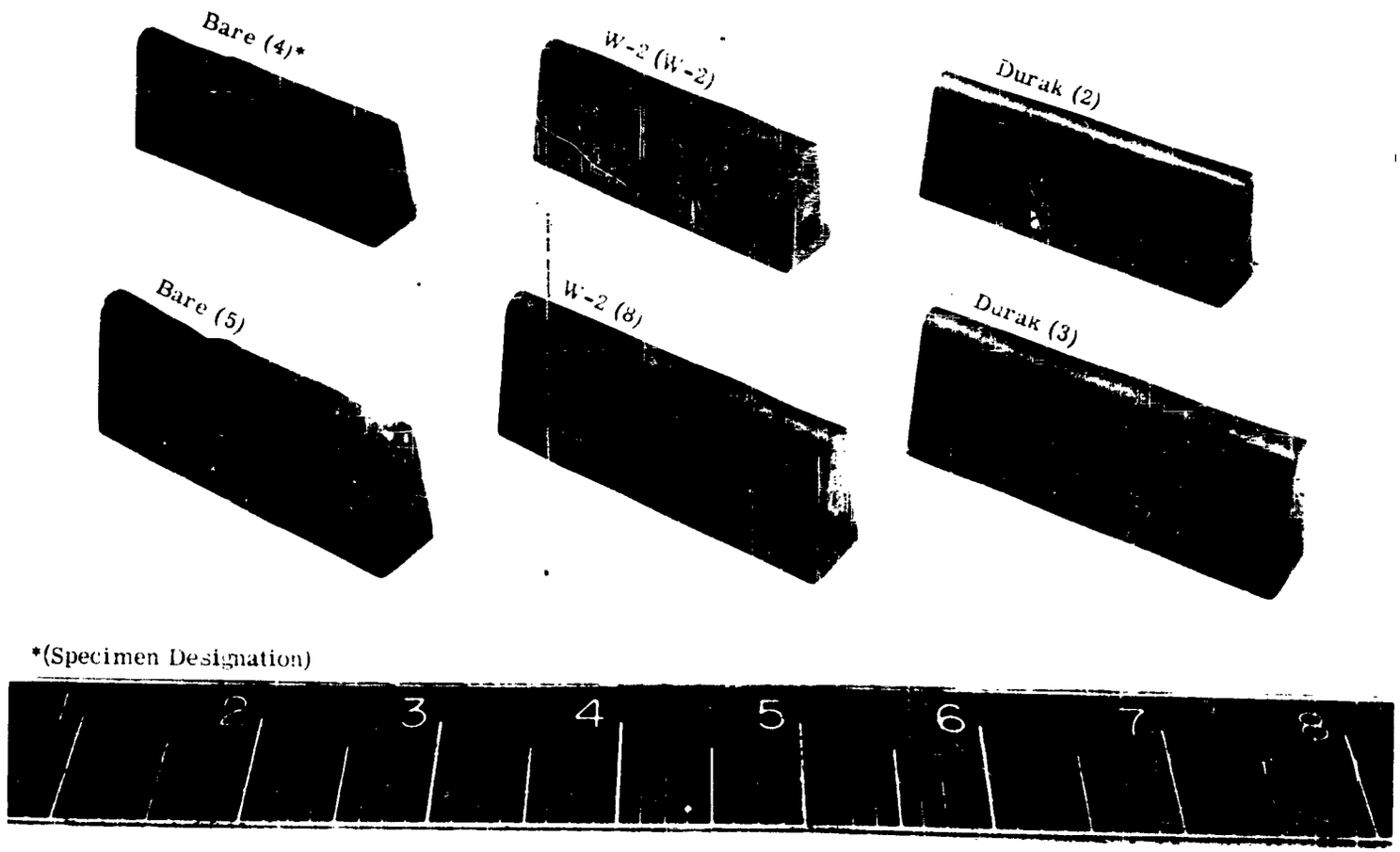

FIGURE 98. ALL BARE, W-2 COATED, AND DURAK MG COATED MOLYBDENUM ALLOY LEADING EDGE SPECIMENS TESTED AT PLASMADYNE CORPORATION

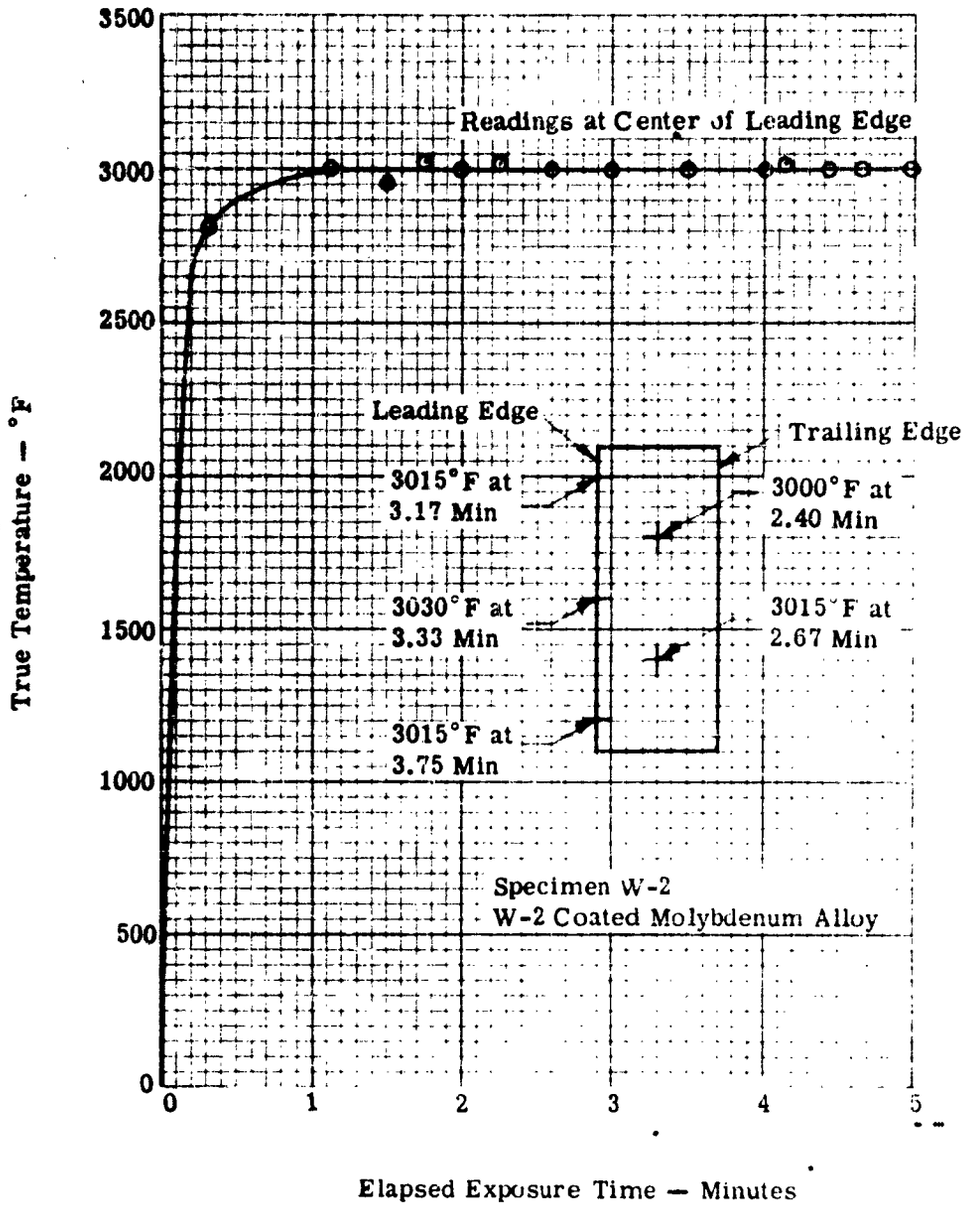

FIGURE 99. SPECIMEN W-2 SURFACE TEMPERATURE VS TIME, PLASMADYNE CORPORATION

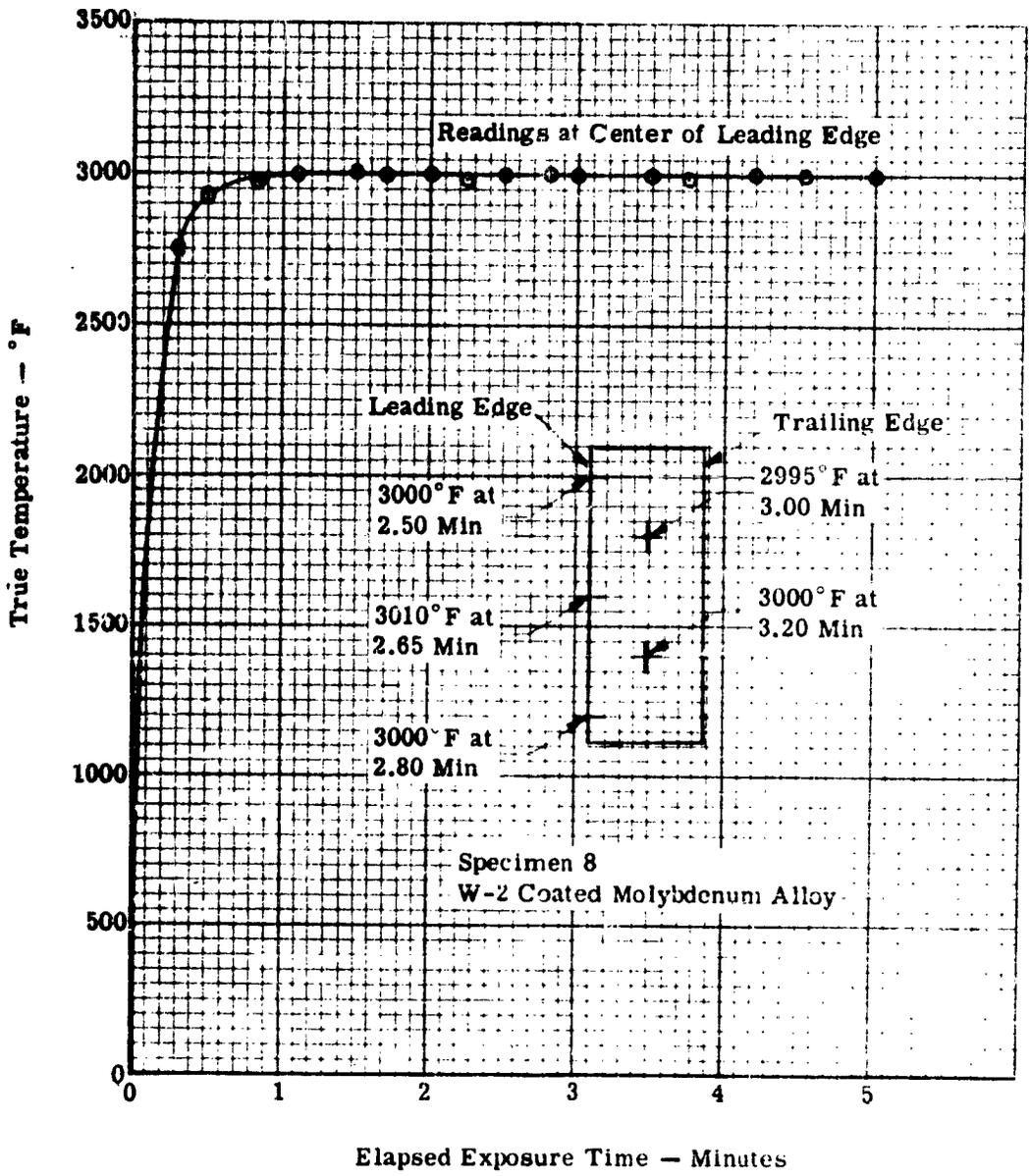

FIGURE 100. SPECIMEN 8 SURFACE TEMPERATURE VS TIME, PLASMADYNE CORPORATION

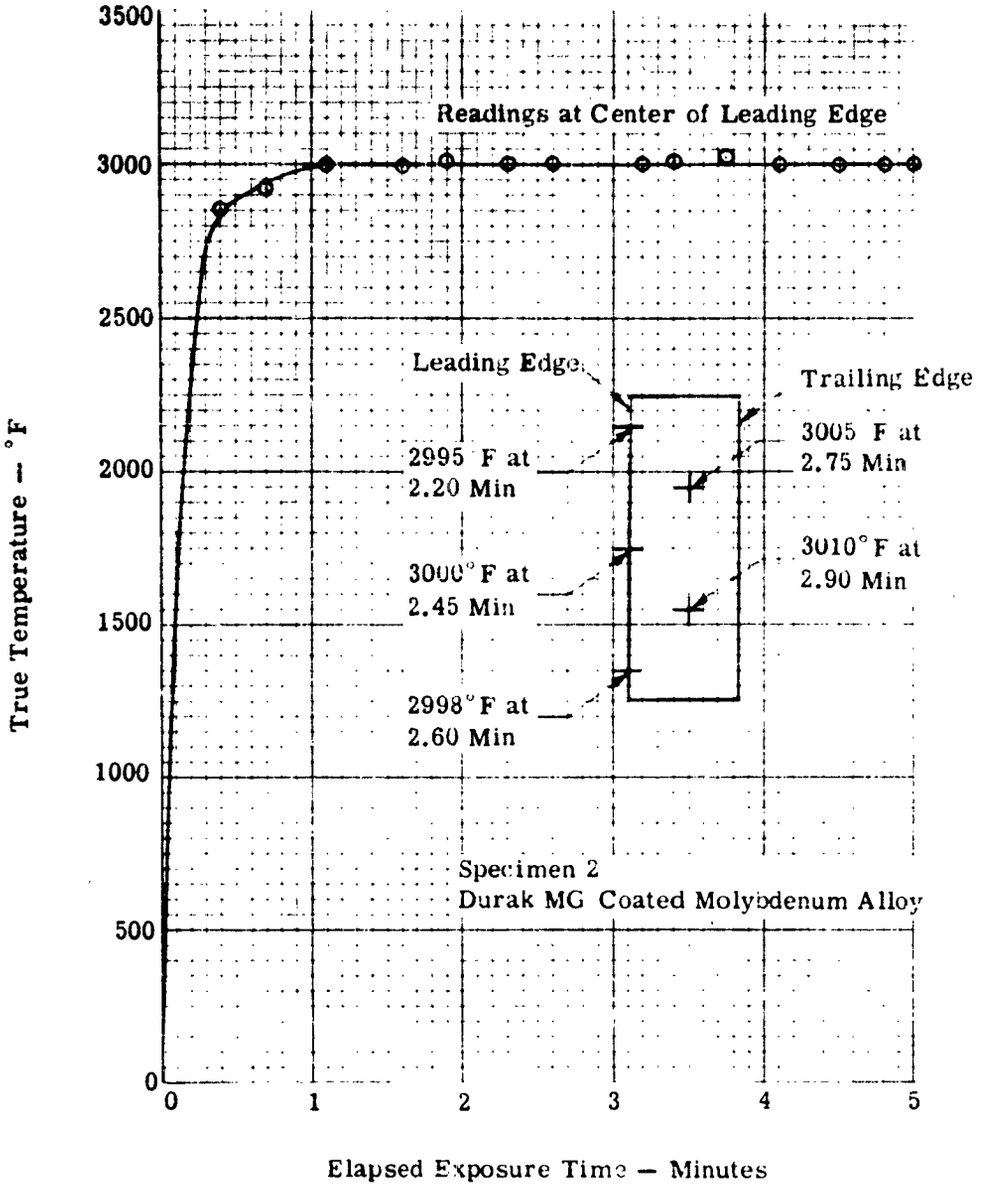

FIGURE 101. SPECIMEN 2 SURFACE TEMPERATURE VS TIME, PLASMADYNE CORPORATION

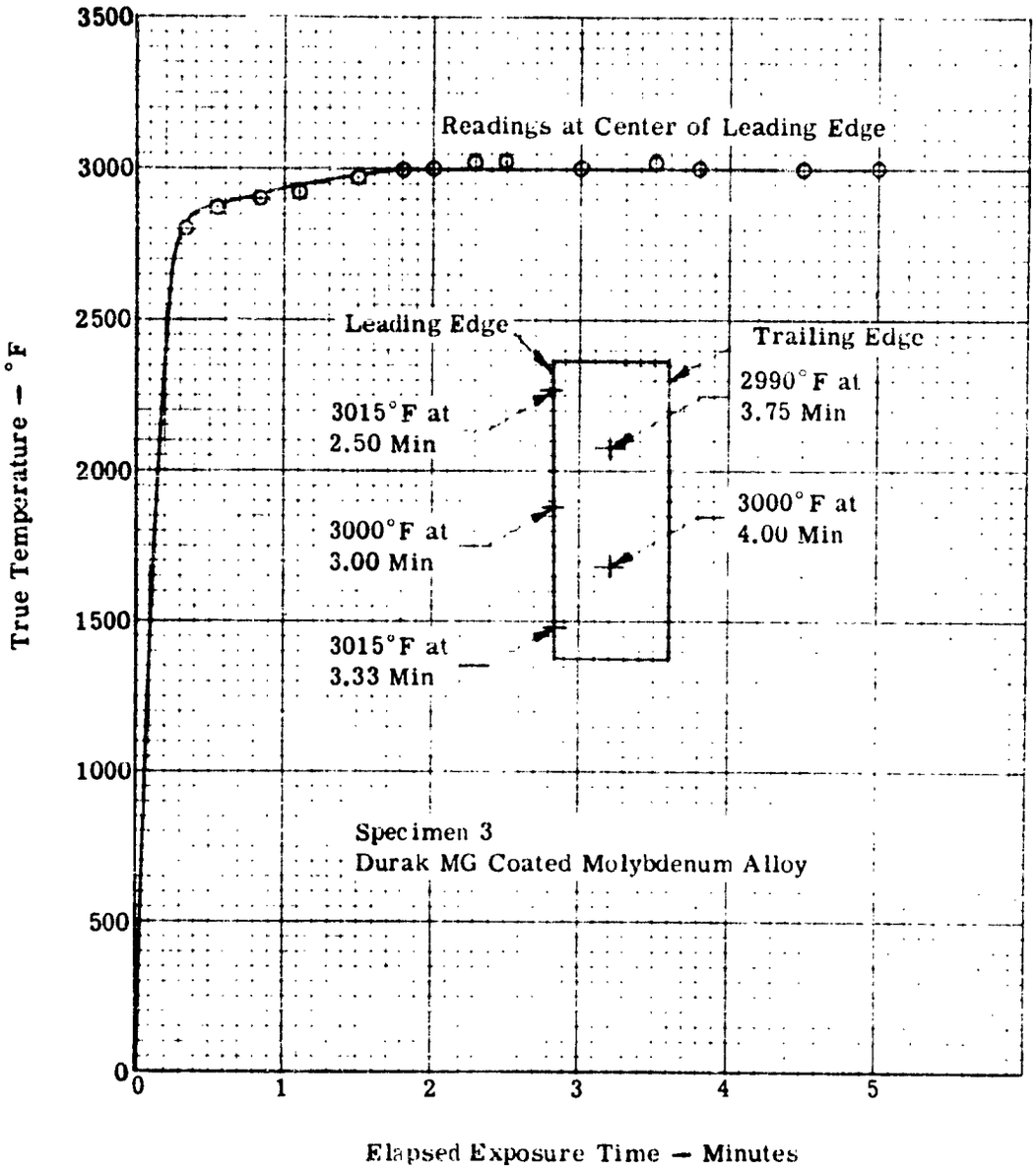

FIGURE 102. SPECIMEN 3 SURFACE TEMPERATURE VS TIME, PLASMADYNE CORPORATION

FIGURE 103. CLOSEUP VIEW OF W-2 COATED MOLYBDENUM ALLOY SPECIMEN, DESIGNATION W-2

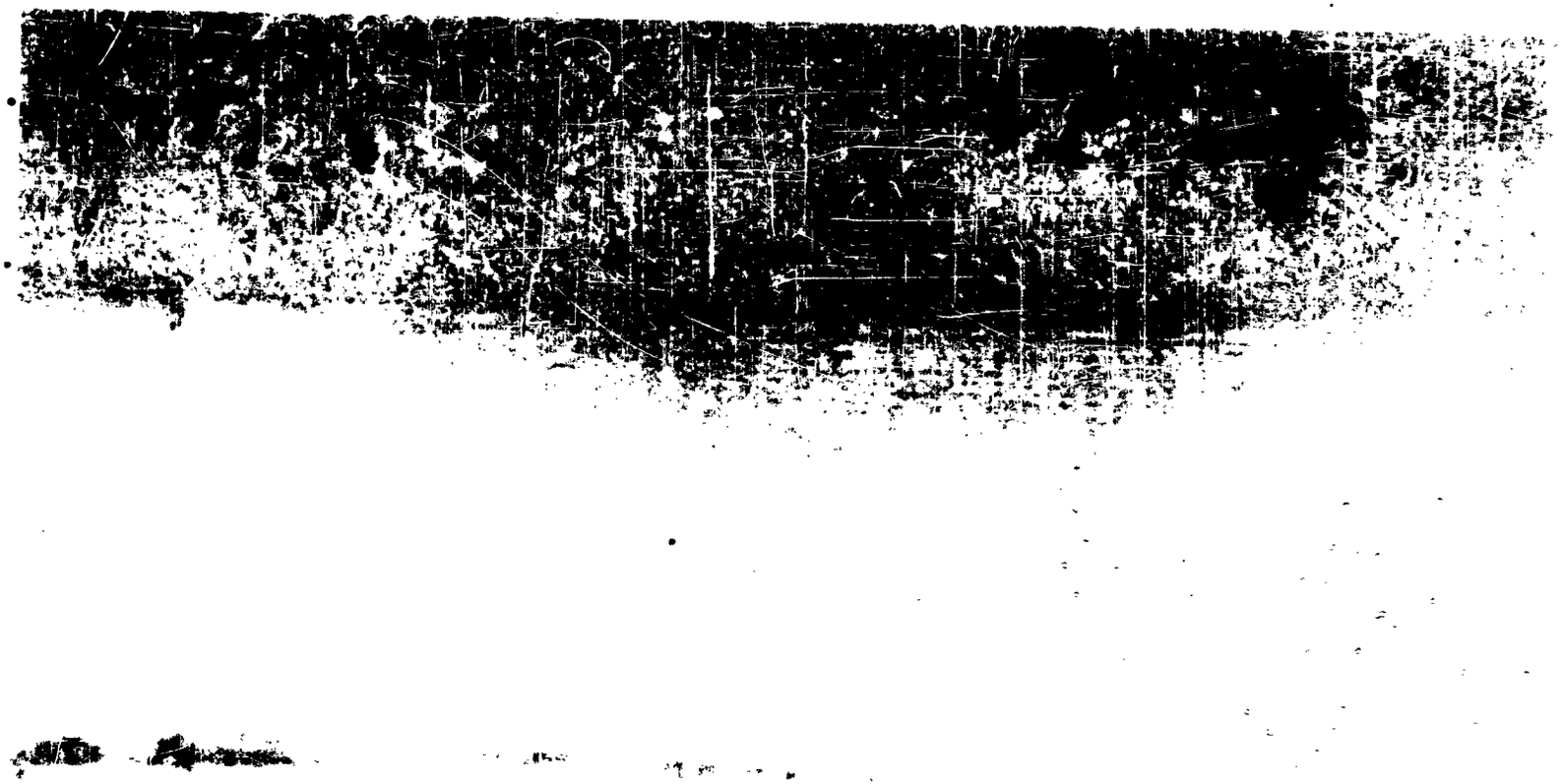

FIGURE 104. CLOSEUP VIEW OF PITTED REGION OF SPECIMEN W-2, W-2 COATED MOLYBDENUM ALLOY

V. COMPARISON OF RESULTS

In addition to the general evaluation of the materials of interest under different operating conditions, the results obtained and described in Sections II, III, and IV should be examined in an attempt to learn how test variables influence oxidation resistance. The test specimens used fall into three groups: (1) uncoated material, (2) coated material, and (3) coated material with intentional damage. Tests of the uncoated materials were conducted in flowing air arc plasma facilities at various temperatures, velocities and pressures. The coated materials were tested in flowing air, flowing oxy-acetylene combustion products and arc plasma jets, at various temperatures, velocities, and pressures. The intentionally damaged specimens were tested only in the preheated flowing air facility at two temperatures and two flow rates.

The effects of the following variables should be indicated:

Specimen temperature
Gas pressure
Gas velocity
Gas enthalpy
Degree of gas dissociation
Gas composition
Gas temperature

In addition, comparison is possible between the oxidation behavior of uncoated materials and the behavior of the same materials when the protective coatings are damaged.

This section of the report compares the data obtained from the tests in various facilities and investigates the possible effects of the test variables. Where possible, the data obtained from this portion of the material evaluation phase of the program are compared with data generated during the screening test phase; see Volume III, Section V.G.

A. UNCOATED MOLYBDENUM ALLOY

Figure 105 presents the loss rate of the 0.5% Ti molybdenum alloy in the various test facilities. The data are plotted as the log of surface recession versus reciprocal temperature. Also included are the data obtained during the screening tests.

Consider first the data obtained in the two preheated flowing air test series. Although test equipment was essentially the same in both series there is considerable disagreement between the oxidation behavior of the wedges, as reported in Section II, and the cylinders tested during the screening program.

From the 13 wedge shaped specimens tested in the temperature range from 2200F to 2700F the oxidation behavior as defined by a least squares fit of the data is

$$k = 57 \times 10^4 \, e^{-23860/RT}, \text{ mils/hr, at the nose}$$

$$k = 123 \times 10^4 \, e^{-29500/RT}, \text{ mils/hr/side, on the skirt}$$

The corresponding equation based on a least squares fit of the 16 cylinder tests at temperatures from 1950F to 2900F is

$$k = 9{,}222 \, e^{-12030/RT}, \text{ mils/hr/side}$$

At low temperature the cylinder data indicate the higher oxidation rates, while at higher temperature the wedge data indicate the higher loss rates. Since the wedge skirt recession data are essentially those for the entire specimen based on weight calculations it is appropriate to compare this line with the cylinder data. The intersection of the lines occurs at approximately 2700F, or a value of inverse temperature in Figure 105 of $5.7\ 10^{-4}/k$.

While the wedges were about seven times the weight of the cylinders, the surface area-to-volume ratios of the two geometrically different specimens were essentially the same; the ratio of nose surface area to total surface area was about 50% higher for the cylinders than for the wedges. The range of weight changes as a result of oxidation were also quite comparable with a range of approximately 20% to 50% loss for the wedges and 20% to 60% for the cylinders. Another similarity between the sets of data is the similarity in the incremental temperature rise which resulted from the exothermic reaction; these data are shown in Figure 106 and will be discussed later.

The major difference in the two series of tests conducted in preheated flowing air is the range of specimen temperatures investigated, as indicated previously. A layer of molybdenum trioxide may have been present at the lower temperatures but absent at the higher temperature since this oxide melts at 1470F and boils at 2335F at sea level pressure. The presence or absence of a molten oxide layer might influence the reaction kinetics and thus affect the surface recession rates. The cylinder test series contained 4 samples tested at temperatures below the lowest temperature of the wedge test series. If a change in reaction kinetics takes place at temperatures of approximately 2200F the Arrhenius equation assumed for the cylinder data, with its constant value of A, may be in error and the oxidation behavior could not be expressed by a single expression. The above reasoning is speculative, and the difference between the two sets of data cannot be resolved at this time. Additional testing is required at closely spaced temperature intervals.

Until the aforementioned differences are resolved, the use of the data obtained on the wedges is recommended for use. This choice is based primarily upon the fact that the data for temperatures of 3000+F in Arc Jet No. 20 agree with or fall below the resulting extrapolation of the surface recession curves from the tests of wedges. The Arc Jet No. 20 data which falls below the extrapolated wedge data might be explained as follows: Among the data obtained from the testing in Arc Jet No. 20, preference is given to those specimens which experienced the highest weight losses. It will be recalled that during some tests molten silica from the fused silica electrode spacing plate impinged on test specimens. These deposits are obvious on the coated samples tested but not on the uncoated materials. Nevertheless, the pressure of the molten silica in the gas stream, or intermittently on the specimen surface, may have reduced the oxidation rate. Additional reasons for choosing the wedge data are that the surface loss on the wedges was slightly more uniform, the wedges were larger, thus permitting measurements that should have greater accuracy, and both weight and dimensional measurements made for the wedges agreed quite well with each other.

An interesting feature of the oxidation tests of the wedges is the higher recession of the nose area as compared with the skirt. In the various facilities the ratio of nose loss to skirt loss has the following ranges:

Flowing Air	2 to 2.7
Arc Jet No. 20	2.6 to 3.3
Plasmadyne Jet	3.2 to 3.5

In other words, in the Plasmadyne jet, for example, the oxidation rate on the nose of the wedge specimen was from 3.2 to 3.5 times as great as the oxidation rate on the nose of the wedge specimen was from 3.2 to 3.5 times as great as the oxidation rate on the skirt. Data from Arc Jet No. 10 were incomplete and could not be compared. While the data are sufficient to indicate a definite trend, no specific reason can be given to explain this behavior. Two effects which might be influential are the thickening of the boundary layer aft of the nose region, which would reduce the diffusion of oxygen through the boundary layer and to the specimen surface, and the presence of combustion products, from the nose region, in the flow over the skirt, which would reduce the percentage of oxygen available to the specimen surface. The difference in the ratios among the three facilities is easier to explain. In the flowing air facility the specimen is within a furnace and the air passing over it is also at the test zone temperature. There is no convective heating of the specimen, in fact, since the temperature of the specimen rises above the test zone temperature as a result of the exothermic reaction; a small amount of convective cooling is more likely. In the arc jet tests heat was supplied convectively from a hot boundary layer. Thus the heating rate on the nose will be higher than that on the skirt and a slight temperature difference will exist from front to rear despite the high thermal conductivity of the molybdenum alloy. The higher temperature in the nose region would, naturally, increase the local oxidation rate. As operating pressure is reduced and as flow velocity is increased the heating rate on the skirt becomes a smaller percentage of the stagnation heat flux. Thus the higher relative temperature which would result from the conditions in the Plasmadyne jet should cause a relatively higher nose-to-skirt loss ratio, which it does.

As indicated previously in Volume III there appeared to be no direct correlation of oxidation rate with mass velocity but, rather, an indirect effect. The oxidation reaction of molybdenum is exothermic at the temperatures of interest. The heat generated results in an increase of specimen temperature which accelerates the reaction. As the flow of air over the specimen increases the incremental temperature rise also increases; see Figure 106. Therefore, the mass velocity of air does influence the oxidation rate. However, if the specimen temperature is measured and used for analysis purposes, rather than the test zone temperature, the effect of mass flow will not be apparent. Although two different mass flows were employed during the testing in Arc Jet No. 20, it was not possible to check for a mass flow effect. Since the temperature of a non-reacting specimen under operating conditions was not determined there was no base line from which to determine the incremental temperature rise due to the exothermic reaction.

Within the scatter of the data and considering the limited number of test points, no effect of gas velocity on oxidation behavior was observed. Calculated velocities in the various facilities were

Preheated flowing air	8 to 100 fps
Arc Jet No. 20	300 to 400 fps
Arc Jet No. 10	700 fps
Plasmadyne Jet	12,300 fps

Neither was it possible to detect effects of enthalpy of dissociation. Enthalpies range from about 700 BTU/lb in the flowing air facility to 6800 BTU/lb in the Plasmadyne arc tunnel. Both of the NASA jets are low enthalpy units. The low gas temperatures of the flowing air facility precluded any dissociation of the air. In the arc jets the primary constituents of the gas stream were N_2 and O, with slight amounts of NO, N and O_2. Because of the carbon electrodes in Arc Jet No. 20, CO_2 and CO were undoubtedly present also. More detailed investigations might reveal effects of velocity, enthalpy and dissociation, but these factors do not appear to be of major importance as far as oxidation is concerned.

The only factor, other than surface temperature, found to have a significant influence on the oxidation rate of the 0.5% Ti molybdenum alloy was pressure. While only a limited number of tests were conducted at reduced pressures, other data tend to confirm the trends of the present work. Figure 107 presents the relation between oxidation rate and pressure as a plot of oxidation rate ratio, $k_p/k_{p=1\ atm}$, versus pressure ratio, p/1 atm. Because of the limited amount of data obtained during this study the relationship is shown as a straight line on the log-log scales of the figure. More testing would be required to accurately define the relationship. The oxidation rate at one atmosphere was determined from the Arrhenius equation, based on the flowing air tests of the wedge specimens.

While the reduced pressure test results of this study were obtained at temperatures between 3000F and 3500F, the resulting relationship should be applicable from 1600F to 3500F, based on test results obtained at lower temperatures by other investigators. These additional data are also shown in Figure 107.

The primary purpose of conducting oxidation resistance tests of the uncoated 0.5% Ti molybdenum alloy was to obtain surface recession rates for use in establishing component wall thicknesses for implementation of the fail safe design concept. This concept requires that the wall of the leading edge shall be thick enough to avoid burn-through during a single flight despite the presence of an undetected defect or damage area in the protective coating. Part of the testing conducted during this program was designed to check the rate of oxidation at locations where damage was intentionally inflicted. These data can be compared with the surface recession data obtained using uncoated material.

Although the tests of the damaged specimens were conducted at two mass velocities, no temperature rise due to the exothermic reaction of the molybdenum alloy was detected. The maximum depths of penetration, after four hours of exposure, of all samples tested are

Test Temperature	Nose		Skirt	
	Penetration	Rate	Penetration	Rate
2000F	.19 inch	48 mils/hr	.16 inch	40 mils/hr
2450F	.38 inch	95 mils/hr	.22 inch	55 mils/hr

The recession rates, in mils/hour, for the uncoated material

Test Temperature	Nose	Skirt
2000F	99	38
2450F	355	160

With the exception of the loss on the skirt at 2000F, the maximum depths of penetration of the damaged specimens are only 1/3 to 1/2 the surface recession of the uncoated material. Hence, calculations of thickness loss based upon data obtained from uncoated 0.5% Ti molybdenum alloy should be conservative.

B. UNCOATED GRAPHITE

The results of the tests of uncoated ATJ graphite in the various facilities are presented in Figure 108. As was the case for the molybdenum alloy, the data obtained from the arc plasma jet tests of the graphite indicates lower surface recession rates than those predicted by the Arrhenius equations based upon the results of the tests in flowing air. This is true both on the skirt and in the nose region.

In reviewing available literature regarding the oxidation rate of carbon and graphite materials, activation energies are found to range from 20 to 30 K cal/mol above 1200C and up to 42 K cal/mol at approximately 800C. Gulbransen and Andrew* reported an activation energy of 36,700 cal/mol for Grade AUF graphite as a result of tests in pure oxygen at various pressures. These data are in good agreement with the work reported here which indicated activation energies of 30,466 cal/mol and 32,260 cal/mol based on nose and skirt data, respectively.

From the tests conducted, a higher recession rate was observed in the nose region. In the flowing air facility the ratio of nose to skirt recession ranged from 3.5 to 4.6:1, while this ratio ranged from 4.3 to 6.3:1 in the NASA jets. Because of the shock waves in the Plasmadyne tunnel the recession in the nose region was not uniform, and ratios could not be obtained. Explanations for the observations are the same as those presented previously for the molybdenum alloy.

For the uncoated ATJ graphite no direct effect of mass velocity changes was observed although there is an indirect effect. The oxidation reaction is exothermic at the temperatures of interest. The heat generated results in an increase of specimen temperature as presented in Figure 109. As the flow of air over the specimen increases, the incremental temperature rise also increases. Therefore, the mass velocity of air does influence the oxidation rate. However, if the specimen temperature is measured and used for analysis purposes, rather than the test zone temperature, the effect of mass flow will not be apparent. Although two different mass velocities were employed during the testing in Arc Jet No. 20, it was not possible to check for a mass flow effect. Since the temperature of a non-reacting specimen under operating conditions was not determined, there was no base line from which to determine the incremental temperature rise due to the exothermic reaction.

Within the scatter of the data and considering the limited number of test points, no effect of gas velocity was observed, nor was it possible to detect effects of enthalpy or dissociation. More detailed investigations might reveal effects of these variables, but the effects do not appear to be of major importance as far as oxidation is concerned.

Other than surface temperature, the only factor found to have a significant influence on the oxidation rate of ATJ graphite was pressure. While only a very limited number of tests were conducted at reduced pressures, there does appear to be a definite trend for the recession rate to decrease as pressure is reduced. This is presented graphically in Figure 107 which is a plot of oxidation rate ratio, $k_p/k_{p = 1\ ATM}$, versus pressure ratio, p/1 ATM. Because of the limited amount of data upon which this plot is based, a straight line, on log-log paper, has been used to approximate the relationship. More testing would be required to accurately define the relationship. The oxidation rate

---

* Gulbransen, E. A. and Andrew, K: "Reactions of Artificial Graphite" Industrial and Engineering Chemistry, Volume 44, Page 1034, 1952.

at one atmosphere was determined from the Arrhenius equation for the skirt region, based on the flowing air tests of the wedge specimens.

The primary purpose of conducting oxidation resistance tests of the uncoated ATJ graphite was to obtain surface recession rates for use in establishing wall thicknesses for implementing the fail safe design concept. This concept requires that the wall of the leading edge shell be thick enough to avoid burn-through during a single flight, despite the presence of an undetected defect or damaged area in the protective coating. Part of the testing conducted during this program was designed to check the rate of oxidation at locations where damage was intentionally inflicted. These data may be compared with the surface recession data obtained using uncoated material.

No indications of temperature increases due to the exothermic reaction of the damaged siliconized ATJ graphite were detected, despite the fact that the intentionally damaged specimens were tested at two mass velocities. The maximum depths of penetration, after four hours of exposure, of all specimens are

Test Temperature	Nose		Skirt	
	Penetration	Rate	Penetration	Rate
2000F	.19	48 mils/hr	.19	48 mils/hr
2450F	.35	88 mils/hr	.25	63 mils/hr

The recession rates, in mils/hour, for the uncoated graphite are

Test Temperature	Nose	Skirt
2000F	970	168
2450F	1400	305

In all cases the maximum depth of penetration of the damaged specimens are only a small fraction of the surface recession of the uncoated material. The ratio of measured penetration at a damaged area to the depth predicted using data from uncoated ATJ ranged from 1/20 to approximately 1/3. Hence, calculations of thickness loss based upon data obtained from uncoated ATJ graphite should be conservative.

C. COATED MOLYBDENUM ALLOY

In reviewing the data obtained in the five different test facilities for the W-2 and Durak MG coatings on the 0.5% Ti molybdenum alloy, the most dominant trend observed is the large variation in the performance of specimens protected by either coating. Because of the data and the limited number of tests, it is not possible to draw any detailed comparisons among the testing techniques employed. It would appear that the variability inherent in the protective coatings or the influence of the particular specimen geometry overshadows all testing variables with the possible exception of specimen temperature and exposure time. Such factors as gas temperature, gas composition, enthalpy, pressure, and mass velocity do not appear to have any major effect upon coating performance. As the coatings are improved to a higher level of reliability the effects of such factors may be found; however, the high degree of variability in the oxidation resistance of the specimens protected by the Durak MG and W-2 coatings precluded the observation of these effects during the present program.

From the information obtained it would appear that the best testing facility for the evaluation of oxidation resistance of protective coatings is one that

a. is inexpensive to assemble and operate,
b. can operate continuously for long periods of time with flowing gas,
c. can produce various specimen temperatures under oxidizing conditions,
d. can maintain reasonably constant operating conditions.

As protective coatings are improved to a higher degree of reliability, additional variables other than specimen temperature and exposure time should be introduced, and facilities can become more sophisticated.

Within the reservations imposed by the scatter of data it is possible to compare the relative performance of the W-2 and Durak MG coatings. Before making such a comparison, however, it must be remembered that these coatings were not designed for the specific application under consideration. Rather, they represent the two most promising protective coatings for molybdenum that were available during the present program. This promise was established on the basis of the screening tests of several coating systems as reported in Volume III. In fact, the W-2 and Durak MG coatings were, and still are, the most promising of approximately 30 coating systems evaluated at Bell Aircraft Corporation during the leading edge study and other programs.

Of the 25 W-2 coated specimens tested under various conditions, failures were detected on 14; of these three may have been influenced by the steel tongs used initially to insert and remove the test specimens. For the Durak MG specimens, failures were detected on 19 of the 25 tested. The following table compares the two coatings under the various test conditions.

	Average	Flowing Air 2000F	Flowing Air 2450F	Oxy-Acetylene 2750F	Oxy-Acetylene 3000F	Arc Plasma Jets #10	Arc Plasma Jets #20	Arc Plasma Jets Plasmadyne
W-2								
Failure Rate	14/35	0/3*	2/6	5/6	5/5	0/1	1/2	1/2
Percentage of Failures	56%	0%	34%	83%	100%	0%	50%	50%
Durak MG								
Failure Rate	10/25	3/3	4/6	5/5	5/5	0/1	2/3	0/2
Percentage of Failures	76%	100%	67%	100%	100%	0%	67%	0%

* Number of specimens that failed/total number of specimens tested.

Tests in the flowing air and oxy-acetylene facilities were to have been conducted for four hours; any specimen which did not remain completely protected for that duration was considered a failure. For the arc plasma jets the test times were: 70 seconds for No. 10, 300 and 600 seconds for No. 20, and 300 seconds for the Plasmadyne Jet.

From this rather gross comparison it appears that the W-2 coating is slightly superior to the Durak MG coating. This is further substantiated by comparing the appearance of the specimens tested, and the life curves presented in Figure 110. Examination of the photographs of the specimens after the flowing air and oxy-acetylene tests indicate the multiplicity of failures on the Durak MG coated samples. The photographs of the specimens after the testing is enlightening in another respect. Of the 33 specimens which failed from the total of 50 coated molybdenum alloy samples tested, 25 had failures occurring at edges and corners while only 12 had failures on the flat surface or nose areas. Of the 12 which had failures at locations other than edges or corners, in four cases this damage may have been due to reactions introduced by the initial use of steel tongs for insertion and removal of test specimens. Considering the total test results 33/50 or 66% of all specimens failed. If the edge protection had been adequate the percentage of failure may have been as low as 24%. The life curves indicate a longer average life for the W-2 coating at all test temperatures. The calculation of average life at any temperature is quite approximate since all test points were averaged. When a specimen had not failed even after four hours of exposure its life, for calculation purposes, was assumed to be one additional hour, that is, a total of five hours. Minimum lives for the two coatings, as indicated in previous sections, are essentially the same except at temperatures below 2450F. At the lower temperatures the W-2 appears to have the longer life.

D. SILICONIZED ATJ GRAPHITE

As in the case of the coated molybdenum alloy, the siliconized ATJ graphite specimens were tested in five different facilities. The dominant trend was also the same; the variability in the oxidation resistance afforded the specimens by the siliconizing process overshadowed all testing variables including temperature.

Of the 37 specimens tested under various conditions failures were detected on 20. In the long time tests employing the relatively low temperature gases, flowing air and oxy-acetylene facilities, 19 of the 20 samples failed in less than the four hour time duration set as a maximum. Performance in the three different arc plasma facilities was much better with only one specimen failing of the 8 tested. This superior performance in the arc plasma environments is attributed to the short time exposure, from approximately 70 to 600 seconds, rather than to differences in testing conditions or environments. The following tabulation illustrates the variability in performance and lack of correlation with test conditions.

		Flowing Air		Oxy-Acetylene		Arc Plasma Jet		
	Average	2000F	2450F	2750F	3000F	#10	#20	Plasmadyne
Failure Rate	20/37*	7/8	3/8	4/7	5/6	0/1	1/5	0/2
Percentage of Failures	54%	88%	38%	57%	83%	0	20%	0

* Number of specimens that failed/total number of specimens tested.

It is interesting to note that the percentage of failures at 2000F and 3000F are approximately the same. Despite the better performance at the intermediate temperatures the only conclusion that can be drawn logically is that coating variability obscures all testing parameters with the exception of exposure time. It is possible that optimum performance is obtained near 2450F; however, the high degree of variability in the data precludes any such conclusion.

Despite the high degree of scatter in the measured oxidation resistance afforded by the siliconized coating applied to the ATJ graphite specimens, an average life can be calculated at each test temperature. The calculation of average life is quite approximate since all tests conducted in the flowing air and oxy-acetylene facilities were included. When a specimen had not failed even after 4 hours of exposure its life, for calculation purposes, was assumed to be an additional hour; that is, a total of 5 hours. Furthermore, the specimens were examined after one hour exposure cycles. If a specimen failed between three and four hours the failure was assumed to have occurred just prior to removal from the furnace, and the life of the specimen would be recorded as four hours. The average performance of the siliconized ATJ graphite is plotted in Figure 110; minimum life is also shown.

Examination of the photographs of the siliconized ATJ graphite after testing indicates multiple failure locations on most specimens that failed. The majority of failures are on the flat surfaces of the specimen skirts. Compared with the coated molybdenum alloy samples, there were few edge or corner failures. In many cases the oxidation failures are associated with the unusual markings on the siliconized specimens. Studies of the mechanical properties of the siliconized ATJ material indicated that these markings were associated with micro-cracks. In the siliconizing procedure there is a treatment intended to seal such cracks but it would appear that this is not always completely adequate. It should be noted, however, that within the exposure times of the tests no failures were detected at many of the marked areas. Also, there were some failures at locations where there were no markings. It is impossible to decide, therefore, whether or not the markings on the specimens have any influence on the oxidation protection afforded by the siliconizing process. During the mechanical property testing reported in Volume VI, large variations in coating thickness were observed on a specific piece and from one piece to another. It is possible that the variation in thickness may be more significant than the markings.

Examination of the specimens after testing indicated a relatively large number of specimens had experienced failures on only one skirt. Of the 19 samples which failed during flowing air and oxy-acetylene testing 11 experienced single or multiple failures on one skirt only, 3 failed on both skirts, 1 failed only at the leading edge, 1 failed only at corners and edges, 2 had failures on one skirt and at the leading edge and 1 had failures on both sides as well as at the leading edge. This relatively high occurrence of failures on only one surface could possibly be an indication of the effect of the specimen's orientation in the siliconizing furnace. Unfortunately, no records are available to permit this speculation to be checked.

In the previous sections of this report the results of the oxidation tests on siliconized ATJ graphite specimens are discussed with respect to weight pick-up and graphite X-ray quality. The tests in preheated flowing air at 2000F and 2450F indicated a slight improvement in performance for the Grade AB samples as compared to the Grade C, but indicated no apparent correlation with weight gain during the coating process. The tests conducted in the oxy-acetylene facility showed no correlation with X-ray grade, due to the fact that only two Grade C samples were tested, and only the slightest indication of a trend with weight pick-up was demonstrated. A more comprehensive correlation might be expected if all samples tested were considered, except those exposed in the arc jets, since the exposure time was very short. All samples were processed during the same coating run so that processing is not a variable.

A total of 29 samples were tested in the two facilities and failures were detected on 19 of them. Of the 29 there were 20 Grade AB and 9 Grade C samples. The failure rates were 11 out of 20 and 8 out of 9 for Grades AB and C, respectively, or percentages of 55% and 89%. Even within the relatively large scatter in the data there appears to be a definitely higher performance from the Grade AB specimens. With regard to weight pick-up values ranged from 1.45 grams to 4.69 grams for the 29 samples tested. For the 10 samples which did not fail, the weight pickups ranged from 1.56 grams to 4.69 grams while for

the 19 specimens which failed the range was 1.45 grams to 3.02 grams. The average weight pick-up for the 10 specimens which did not fail is 2.32 grams and for the 19 which did fail it is 1.87 grams. The weight pick-up data just discussed is influenced quite strongly by one Grade C sample which had an unusually high weight pick-up of 4.69 grams. If this specimen is disregarded the picture is quite different. The range of weight pick-up for samples which did not fail becomes 1.56 grams to 2.53 grams, while for those that failed the range is still 1.45 grams to 3.02 grams. Thus, all specimens which did not fail are within the weight pick-up range of those which did fail. The average pick-ups also become much closer, 2.06 grams for those which did not fail and 1.87 grams for those which did fail. If only the Grade AB specimens are considered, the range of weight pick-up is 1.45 grams to 2.61 grams for the 20 specimens tested; 1.56 grams to 2.53 gramsfor those that did not fail; and 1.45 grams to 2.61 grams for those that experienced failure. The average weight pick-ups for the Grade AB specimens were 1.92 grams for those that failed and 2.06 grams for those that did not fail. In view of the scatter in the data the only conclusion that can be drawn with regard to weight pick-up is that this parameter does not correlate with oxidation resistance for the particular type of graphite investigated during this program.

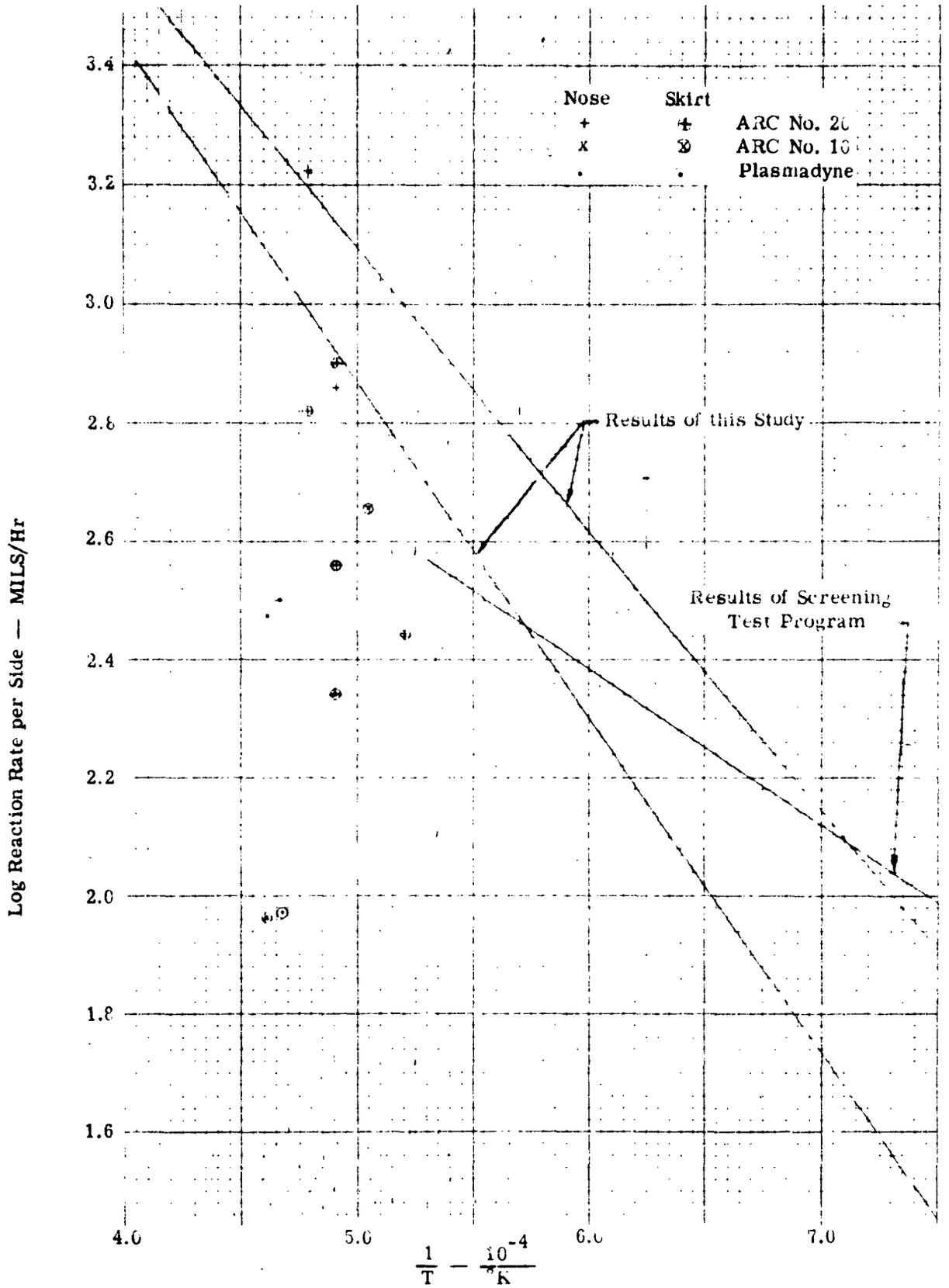

FIGURE 105. COMPARISON OF DATA FROM VARIOUS TEST FACILITIES, UNCOATED 0.5% TITANIUM MOLYBDENUM ALLOY

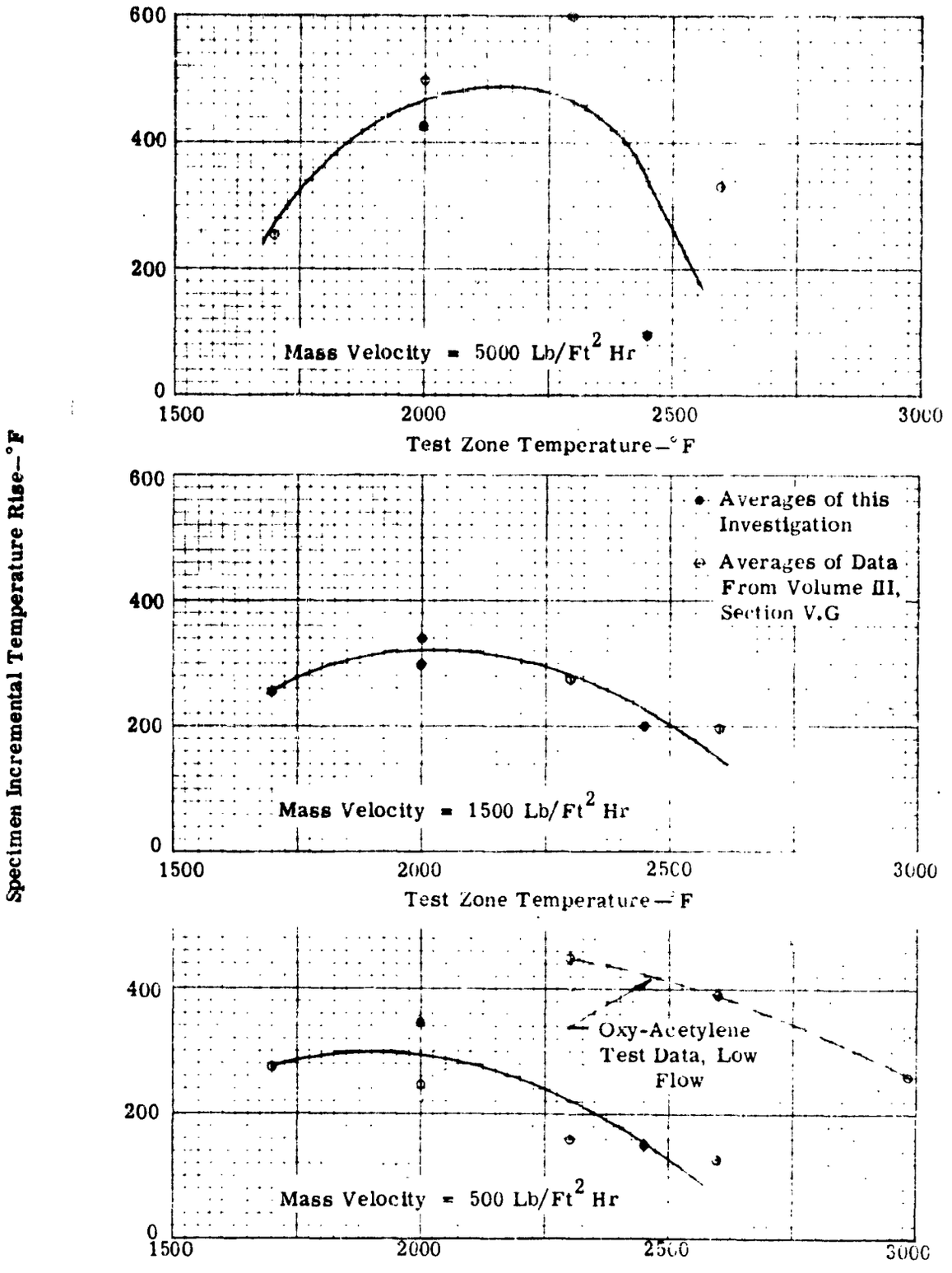

FIGURE 106. INCREMENTAL TEMPERATURE RISE DUE TO EXOTHERMIC REACTION, 0.5% TITANIUM MOLYBDENUM ALLOY

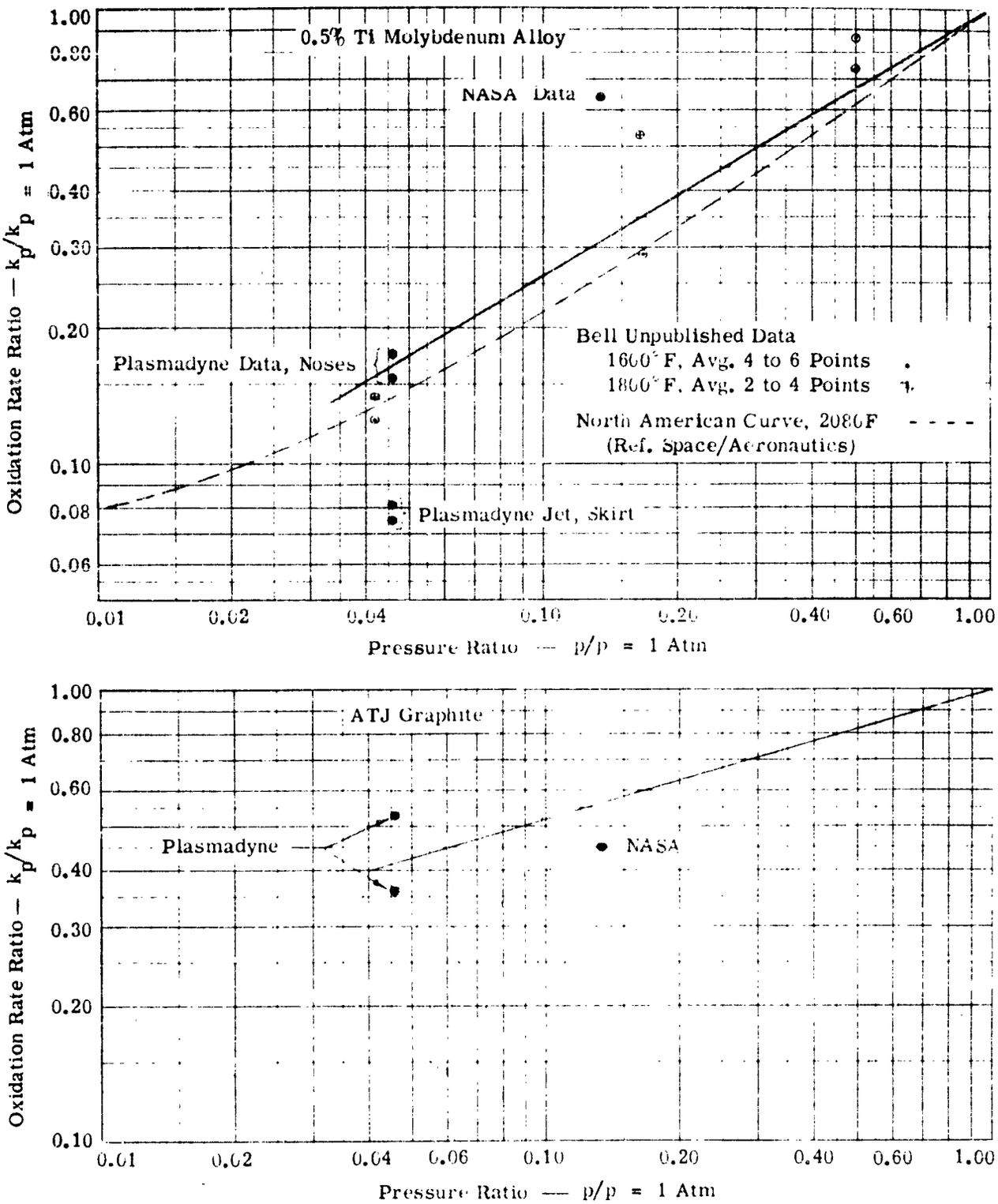

FIGURE 107. EFFECT OF PRESSURE ON THE OXIDATION BEHAVIOR OF 0.5% TITANIUM MOLYBDENUM ALLOY AND ATJ GRAPHITE

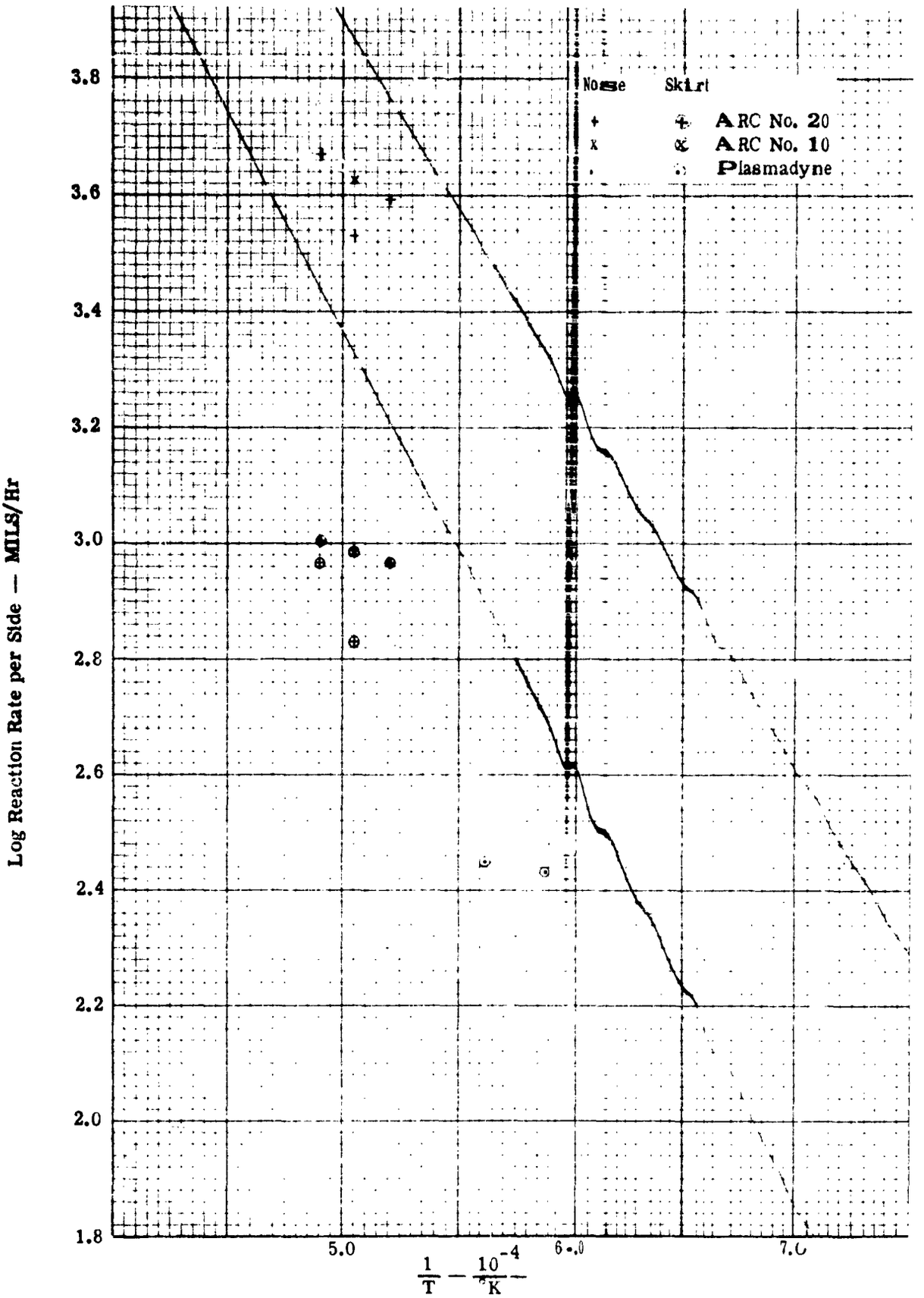

FIGURE 108. COMPARISON OF DATA FROM VARIOUS TEST FACILITIES, UNCOATED ATJ GRAPHITE

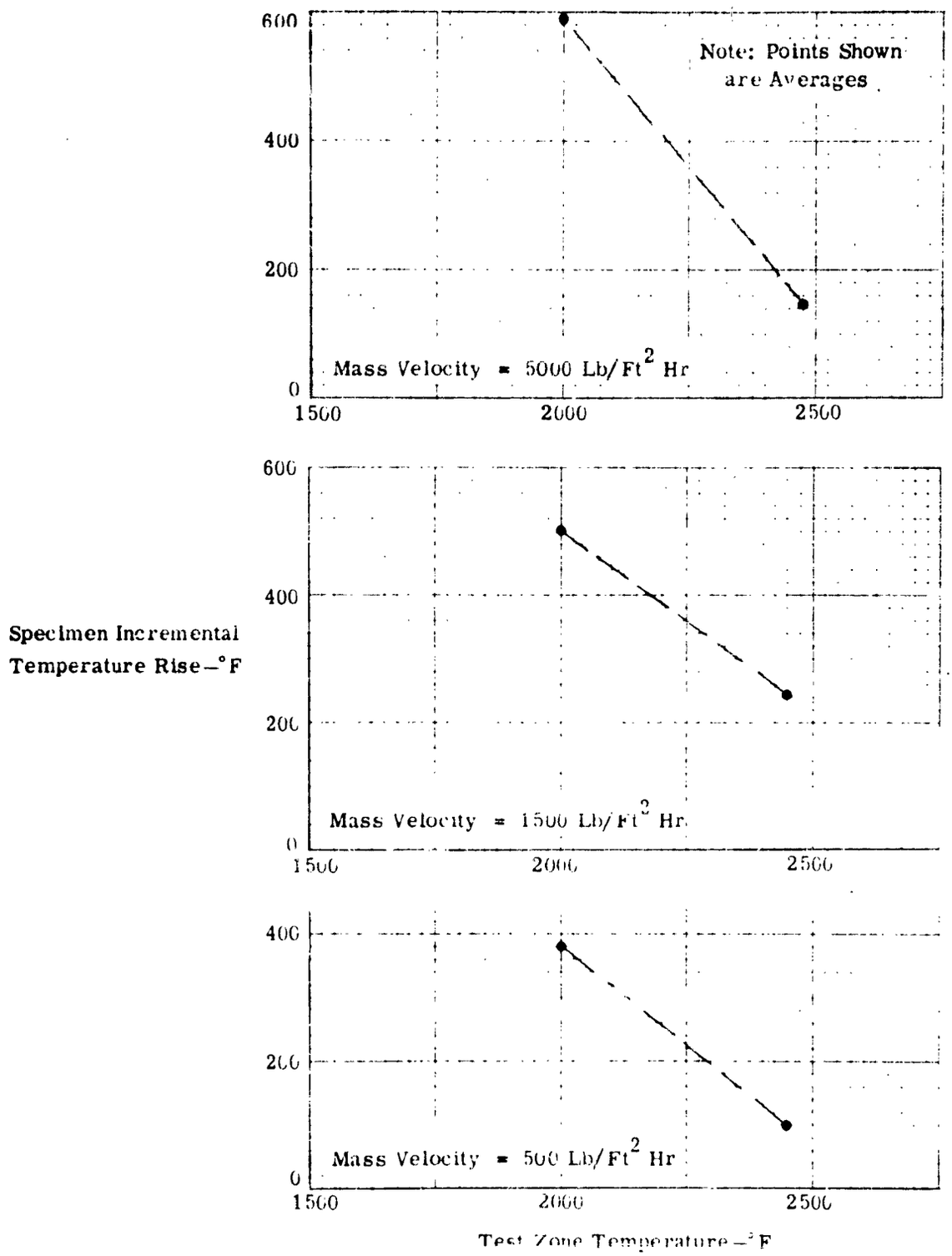

FIGURE 109. INCREMENTAL TEMPERATURE RISE DUE TO EXOTHERMIC REACTION, ATJ GRAPHITE

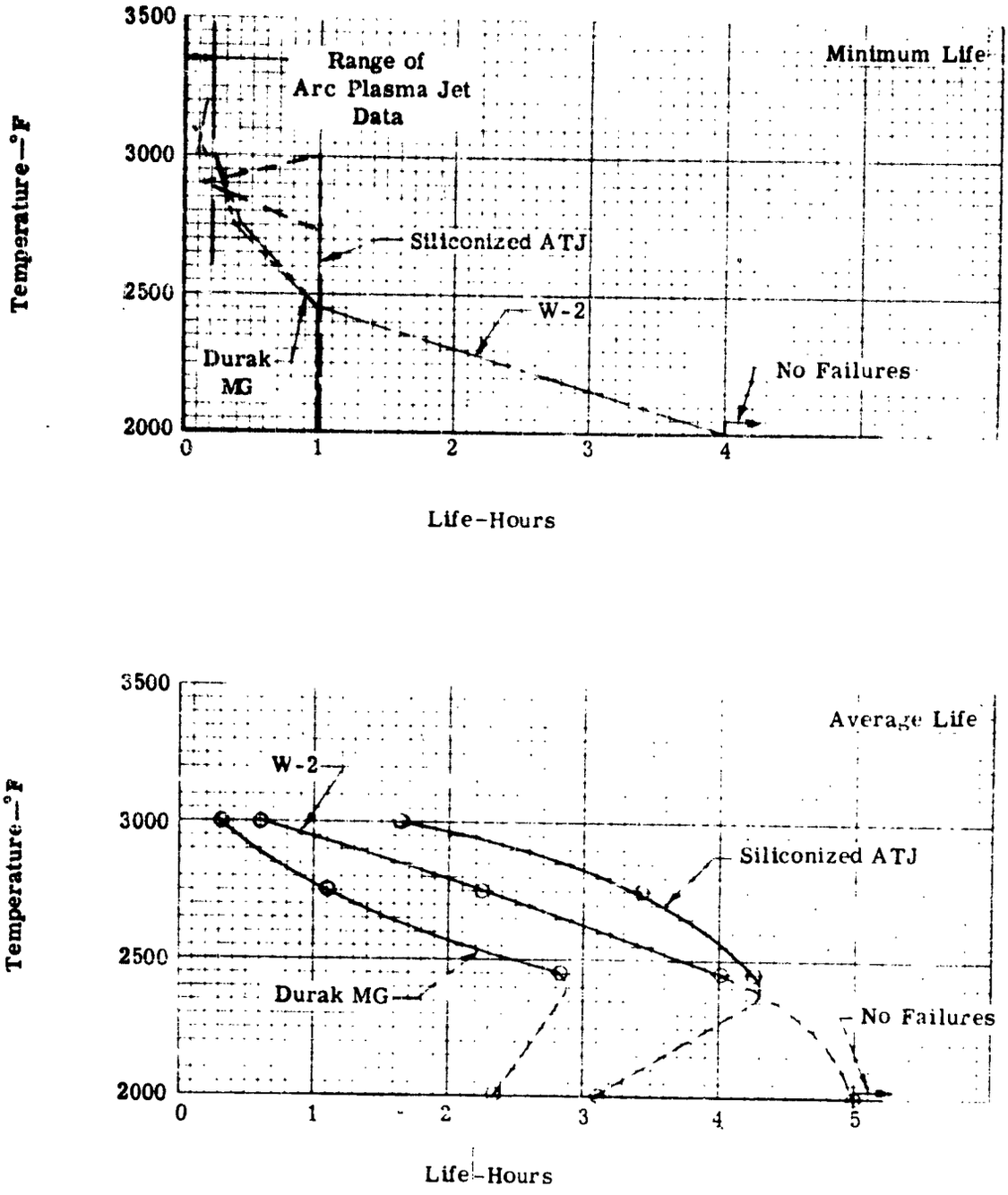

FIGURE 110. APPROXIMATE LIFE OF COATED MATERIALS

VI. CONCLUSIONS AND RECOMMENDATIONS

In the preceding sections of this report the oxidation resistance of uncoated and coated materials are discussed. The coatings employed to protect the 0.5% Ti molybdenum alloy and the ATJ graphite are among the most promising presently available. Conclusions based upon this work, therefore, represent the current state-of-the-art with regard to protective coating systems on these two materials. Since coating development is more advanced for molybdenum alloys than for other refractory metals the conclusions, in a broad sense, may be applicable to other coating-substrate combinations as well.

The most significant conclusions derived from the study reported herein are:

1. Not even the most promising of the presently available coating systems possess the high reliability required for use on critical components, such as leading edges, of manned, reusable hypersonic gliders.

2. Because of the limitations of presently available coating systems, a fail safe design concept, with regard to oxidation, should be incorporated in the design of critical refractory components that are not oxidation resistant. In this way components of high reliability can be produced.

These major conclusions naturally point to the need for more expenditure of effort on protective coating systems. The detailed conclusions which follow are more specific in nature and attempt to indicate significant findings having more immediate application.

1. The dominant factors affecting the behavior of the uncoated 0.5% Ti molybdenum alloy and ATJ graphite materials in a flowing, oxidizing environment, are surface temperature and pressure.

2. Gas stream parameters such as temperature, velocity, enthalpy, and degree of dissociation do not appear to be of major importance in the oxidation behavior of the two uncoated materials tested, at least at the level of refinement now possible in this type of testing.

3. The uniformity of oxidation and retention of shape of the two uncoated materials tested suggests their possible utilization, without protective coatings, for expendable components, particularly for short time applications.

4. Both the uncoated 0.5% Ti molybdenum alloy and the uncoated ATJ graphite react exothermically with oxygen. These reactions generate heat which increases the specimen temperature.

5. The surface recession at a point of small local coating damage is less than predicted on the basis of surface recession data for uncoated materials. The amount of heat generated at the damage areas on the specimen did not produce a detectable temperature rise.

6. Of the two protective coatings evaluated on the molybdenum alloy, Chromalloy W-2 and Chromizing Durak MG, the former appeared to offer superior protection.

7. A major problem in the protection of the molybdenum alloy by the two coatings is the adequate protection of edges and corners.

8. The oxidation protection afforded to the ATJ graphite by the siliconized coating appears to depend upon the quality of the graphite structure as defined by X-ray inspection.

9. Weight gain during the siliconizing process did not correlate with the oxidation protection of the ATJ graphite by the coating.

10. Presently available inspection techniques are inadequate for determining the acceptability of coated refractory materials investigated.

11. Until the reliability of available coating systems increases, simple test facilities which provide oxidizing flowing gas streams and reasonably constant test conditions, and are capable of long time operation at various temperature levels, would be adequate for the determination of protective coating performance.

Based on the work conducted, and the foregoing conclusions, the following recommendations are made:

1. Additional testing of uncoated and intentionally damaged coated specimens should be conducted to verify and/or modify the data presented herein. Such information would have a pronounced effect upon the weight of components designed with a fail safe concept. Effects on temperature and pressure should be investigated.

2. Detailed analytical and experimental studies of the protection problem at edges and corners should be conducted. A significant improvement in component reliability can be obtained if edge and corner protection were as good as protection afforded on flat surfaces or large curves.

3. Attempts should be made to improve the reliability of presently available coatings by conducting tests to investigate the effects of process and material variables.

4. Additional testing is required to investigate the possible effects of gas stream parameters, temperature, velocity, enthalpy, and degree of dissociation on the oxidation resistance of coated and uncoated refractory materials.

5. Inspection techniques should be developed which permit the determination of the protective quality of coatings applied to refractory components. Without adequate inspection methods, refractory components requiring protective coatings will not find effective service use.

6. As an aid in establishing the significance of oxidizing environments, correlations among data obtained from hypersonic flight tests and laboratory data should be made.

7. As the reliability of coated components is improved, either as a result of process refinements or better edge design, testing should be conducted to investigate oxidation resistance of such systems under known stress levels, and the cummulative degradation of the protective coatings under variable test conditions should be investigated.

In addition to these specific recommendations, efforts to develop new coating systems are desirable from the long range point of view. A continuing effort to evaluate new protective systems under similar test conditions is strongly recommended.

APPENDIX I

DESCRIPTION OF MATERIALS TESTED

The test specimens employed during the evaluations of the oxidation resistance of bare and protected graphite and molybdenum alloy are described in this appendix. A discussion of the protective coatings and the substrate materials is included. The fabrication procedures employed were similar to those which would be used for the production of actual leading edge components.

The same configuration was used for both the graphite and molybdenum alloy; this is shown in Figure 111. This configuration simulates the leading edge shape while recognizing the limitations of available test equipment and cost. The fabrication of these shapes did not require any special techniques other than those common to the fabrication of the specific materials. The molybdenum alloy specimens were fabricated by Custom Tool and Manufacturing Company of Minneapolis, Minnesota and the graphite specimens by the National Carbon Company at Cleveland, Ohio.

Two protective coatings were evaluated on the 0.5% titanium molybdenum alloy substrate plus the bare or unprotected alloy. The molybdenum alloy used for this investigation was recrystallized for 35 minutes at 2900F. An estimated grain size of approximately ASTM-2 and complete recrystallization were obtained from this treatment. The material used to fabricate these specimens was supplied by the General Electric Company, Cleveland, Ohio, and Climax Molybdenum Company, Coldwater, Michigan. The chemistry of the G.E. material was not supplied in detail, however, this material nominally contains 0.5% titanium and .010% minimum to .030% maximum carbon. The Climax material had the following range of alloying elements: carbon .018 to .027%, titanium .40 to .54%. The details of impurities were not furnished by the suppliers. A maximum total content of trace elements was .06% of which oxygen, nitrogen and hydrogen constituted .005% maximum.

The two coatings examined were the W-2 coating applied by the Chromalloy Corporation of White Plains, New York, and the Durak MG coating applied by Chromizing Company of Los Angeles, California. The processes for the two coatings are similar in that they both are pack deposition techniques. The uncoated parts are embedded in powdered compound containing elements to be deposited in a special retort. The retort is hermetically sealed, placed in the furnace and heated to approximately 2000F for a period of time. When heated the powdered compound generates a gas which is diffused into the parts resulting in a thin alloyed coating. The finish of the coated surface is approximately as smooth as the original base material.

Prior to processing, there was a visual inspection of the parts for edge defects, laminations, and sharp corners. After the initial inspection all parts were lightly etched in nitric acid in both processes; the W-2 processing differed in that the parts were also liquid honed. It had been the experience of the coating suppliers that some defects did not become apparent until after cleaning. After the cleaning procedure the specimens were again examined and found free of defects.

The full coating thickness, .002 inch, of the Durak coating is normally applied during a single operation. After coating, however, edge damage was noticed on several samples and the entire quantity were reprocessed. The initial coating was not removed. The W-2 process employed a double processing cycle to apply the desired coating thickness, .004 inch nominal. In the W-2 processing the parts were unpacked, cleaned and repacked in fresh compound for the second cycle.

After coating the specimens were all pre-oxidized in still air at 2000F to determine continuity of the coating. The exposure time for the Durak specimens was ten minutes while that for the W-2 specimens was one hour. All samples satisfactorily completed this inspection.

The samples coated with Durak MG were processed during December 1959. The specimens coated with the W-2 coating were processed during September 1959 and January 1960. A more detailed presentation of the substrate material and coating processes is given in Appendix I, Volume V. In this appendix is a table of processing dates, run numbers, quantities and remarks for each type of specimen coated with the W-2 coating.

The graphite evaluated was the National Carbon Company's Grade ATJ graphite. This is an extremely fine-grain premium quality molded graphite which is produced in blocks 9" x 20" x 24". This material has a maximum grain size of .006 inch and has an average ash content of approximately 0.20 percent. The stock used for the oxidation resistance evaluation specimens was taken from randomly selected material. The quality of the raw material was determined by X-ray inspection of the blocks and bulk density determinations. The majority of the specimens used were of the A or B quality material for both the coated and uncoated specimens. The significance of the quality grouping is discussed in Appendix IV of Volume VI. Group A denotes relatively uniform material, Group B is less uniform, etc.

The coating applied is essentially a diffusional deposit of silicon carbide-silicon nitride formed by the reaction of silicon containing compounds with the graphite surface. This siliconized coating was applied by the National Carbon Company by a proprietary procedure which cannot be disclosed. During the siliconizing the specimens are supported in the furnace on knife edges so that a maximum of the graphite surface was exposed to the silicon compounds. Experience gained during the coating of the screening test specimens showed that the spacing of the knife-edge supports should be relatively large. The quality of the coating was checked by weight measurements which were converted to weight gain per unit area. This weight gain was then compared with the standards established on the basis of previous experience. In addition to the quality control procedures followed by National Carbon Company for the normal production of the ATJ graphite and siliconized coating on X-ray inspection procedure, as outlined in Appendix IV of Volume VI, was conducted for further control. The ATJ graphite specimens were X-rayed after machining and after the coating was applied. After machining the specimens were graded as to uniformity at the internal structure of the graphite with Grade "A" denoting specimens of nearly perfect ATJ structure through Grade "C" which denotes the specimens with a mottled nonuniform structure. Since Grade "C" specimens had

indicated higher coating weight pickup the possibility existed that such specimens might possess superior oxidation resistance. Therefore, some Grade "C" oxidation specimens were accepted so that comparative evaluations could be made. The inspection requirements for bare and the siliconized ATJ graphite shapes were that all specimens were free of gross flaws or defects as determined by X-ray inspection. This inspection coupled with normal process control, was expected to result in a flaw-free product of the desired properties. More complete details of the processing are provided in Appendices III and IV of Volume VI. Weights of the specimens before and after coating as well as coating run numbers are presented in Table 25.

TABLE 25

PROCESSING HISTORY OF DELIVERED SPECIMENS

Specimen Type No.	C-3a Oxidation Specimen: Weight Change During Coating (grams) Before	After	Pickup	X-Ray Grade	Coating Run
B-2	23.64	24.94	1.30	AB	G-18
5	23.03	24.64	1.61	AB	G-18
6	23.13	24.58	1.45	AB	G-18
7	23.30	24.49	1.19	AB	G-18
10	23.06	24.61	1.55	AB	G-18
C-2	22.55	24.86	2.31	AB	G-18
5	22.97	25.00	2.03	AB	G-18
8	22.51	24.41	1.90	AB	G-18
9	22.89	25.12	2.23	AB	G-18
11	23.32	24.87	1.55	AB	G-18
12	22.67	24.38	1.71	AB	G-18
D-1	22.39	24.41	2.02	AB	G-18
2	23.09	24.34	1.25	AB	G-18
3	23.78	24.93	1.15	AB	G-18
4	22.42	24.66	2.24	AB	G-18
7	22.90	24.73	1.83	AB	G-18
8	22.60	24.78	2.18	AB	G-18
10	23.53	24.91	1.38	AB	G-18
12	22.89	24.53	1.64	AB	G-18
E-1	23.25	24.61	1.36	AB	G-18
3	23.04	23.90	.86	AB	G-18
6	22.60	24.45	1.85	AB	G-18
8	22.71	24.43	1.72	AB	G-18
9	23.00	24.43	1.43	AB	G-18
11	22.90	24.47	1.57	AB	G-18
F-1	22.93	23.99	.99	AB	G-16
2	22.23	24.06	1.29	AB	G-18
3	22.69	24.44	1.75	AB	G-18
4	22.75	24.39	1.64	AB	G-18
6	23.03	24.59	1.56	AB	G-18
7	22.95	24.52	1.57	AB	G-18

Specimen Type No.	C-3a Oxidation Specimen: Weight Change During Coating (grams) Before	After	Pickup	X-Ray Grade	Coating Run
J-12	23.05	25.44	2.39	AB	G-18
K-1	23.04	24.44	1.40	AB	G-18
3	22.65	24.55	1.90	AB	G-18
5	22.51	24.26	1.75	AB	G-18
7	22.73	24.44	1.71	AB	G-18
10	22.94	24.63	1.69	AB	G-18
11	22.12	24.37	2.25	AB	G-18
12	22.48	24.48	2.00	AB	G-18
L-2	22.59	24.66	2.07	AB	G-18
3	22.05	24.10	2.05	AB	G-18
5	23.21	24.32	1.11	AB	G-18
B-1	23.00	24.50	1.50	C	G-18
4	23.24	24.39	1.15	C	G-18
8	22.72	24.36	1.64	C	G-18
9	22.72	24.54	1.82	C	G-18
11	23.28	24.20	.92	C	G-18
12	22.61	25.02	2.41	C	G-18
C-3	22.78	24.36	1.58	C	G-16
6	23.00	24.70	1.70	C	G-18
7	23.00	24.80	1.80	C	G-18
D-6	22.01	25.17	3.16	C	G-18
11	22.17	25.19	3.02	C	G-18
E-2	23.50	24.99	1.49	C	G-18
4	22.74	24.57	1.83	C	G-18
7	22.91	24.58	1.67	C	G-18
10	22.64	24.76	2.12	C	G-18
12	22.30	25.01	2.71	C	G-18
G-4	22.82	24.64	1.82	C	G-18
5	22.91	24.70	1.79	C	G-18
H-9	22.83	24.25	1.42	C	G-18
10	22.46	24.42	1.96	C	G-18

TABLE 25 (CONT)

Specimen Type No.	C-3a Oxidation Specimen Weight Change During Coating (grams) Before	After	Pickup	X-Ray Grade	Coating Run
10	22.58	24.91	2.33	AB	G-18
11	22.93	24.99	2.06	AB	G-18
G-1	22.87	24.93	2.06	AB	G-18
2	23.04	24.30	1.26	AB	G-18
3	22.93	24.81	1.88	AB	G-18
7	23.38	25.04	1.66	AB	G-18
8	22.68	24.42	1.74	AB	G-18
9	22.55	24.69	2.14	AB	G-18
11	23.07	24.72	1.65	AB	G-18
12	22.87	24.68	1.81	AB	G-18
H-1	22.94	24.41	1.47	AB	G-18
2	22.91	24.64	1.73	AB	G-18
3	23.00	24.87	1.87	AB	G-18
4	23.23	25.32	2.09	AB	G-18
5	22.86	24.64	1.78	AB	G-18
6	22.81	24.73	1.92	AB	G-18
8	22.34	24.73	2.39	AB	G-18
12	23.24	25.03	1.79	AB	G-18
I-1	22.73	24.39	1.66	AB	G-18
2	22.94	24.84	1.90	AB	G-18
3	22.39	24.40	2.01	AB	G-18
5	22.99	24.72	1.73	AB	G-18
7	22.83	24.38	1.55	AB	G-18
8	23.43	24.96	1.53	AB	G-18
12	22.23	24.84	2.61	AB	G-18
J-1	22.91	25.19	2.28	AB	G-18
2	22.38	24.69	2.31	AB	G-18
3	22.52	25.05	2.53	AB	G-18
4	23.10	25.15	2.05	AB	G-18
7	23.40	25.08	1.68	AB	G-18
8	22.54	25.00	2.46	AB	G-18
11	23.26	25.02	1.76	AB	G-18
11	22.28	24.15	1.87	C	G-18
I-4	22.92	27.81	4.89	C	G-18
6	23.62	27.74	4.12	C	G-18
9	23.14	27.16	4.02	C	G-18
10	22.92	26.45	3.53	C	G-18
11	23.24	26.05	2.81	C	G-18
J-5	23.26	24.90	1.64	C	G-18
6	22.80	24.63	1.83	C	G-18
9	22.56	25.51	2.95	C	G-18
10	22.72	25.50	2.78	C	G-18
K-2	23.22	26.64	3.42	C	G-18
4	22.79	27.48	4.69	C	G-18
6	22.89	27.62	4.73	C	G-18
8	22.53	27.99	5.46	C	G-18
9	22.77	30.08	7.31	C	G-18
L-4	22.53	28.98	6.45	C	G-18
M-1	23.09	24.63	1.54	C	G-18
2	22.85	24.13	1.28	C	G-18
3	22.78	24.32	1.54	C	G-18
4	22.48	24.32	1.84	C	G-18
N-1	22.98	24.88	1.90	C	G-18
2	23.33	25.02	1.69	C	G-18
3	22.99	24.46	1.47	C	G-18
4	23.15	24.60	1.45	C	G-18
5	23.03	24.65	1.62	C	G-18
6	23.00	24.47	1.47	C	G-18
7	22.32	25.31	2.99	C	G-18
8	23.41	24.37	.96	C	G-18
9	23.41	24.38	.97	C	G-18
10	23.08	24.46	1.38	C	G-18
11	22.71	24.22	1.51	C	G-18

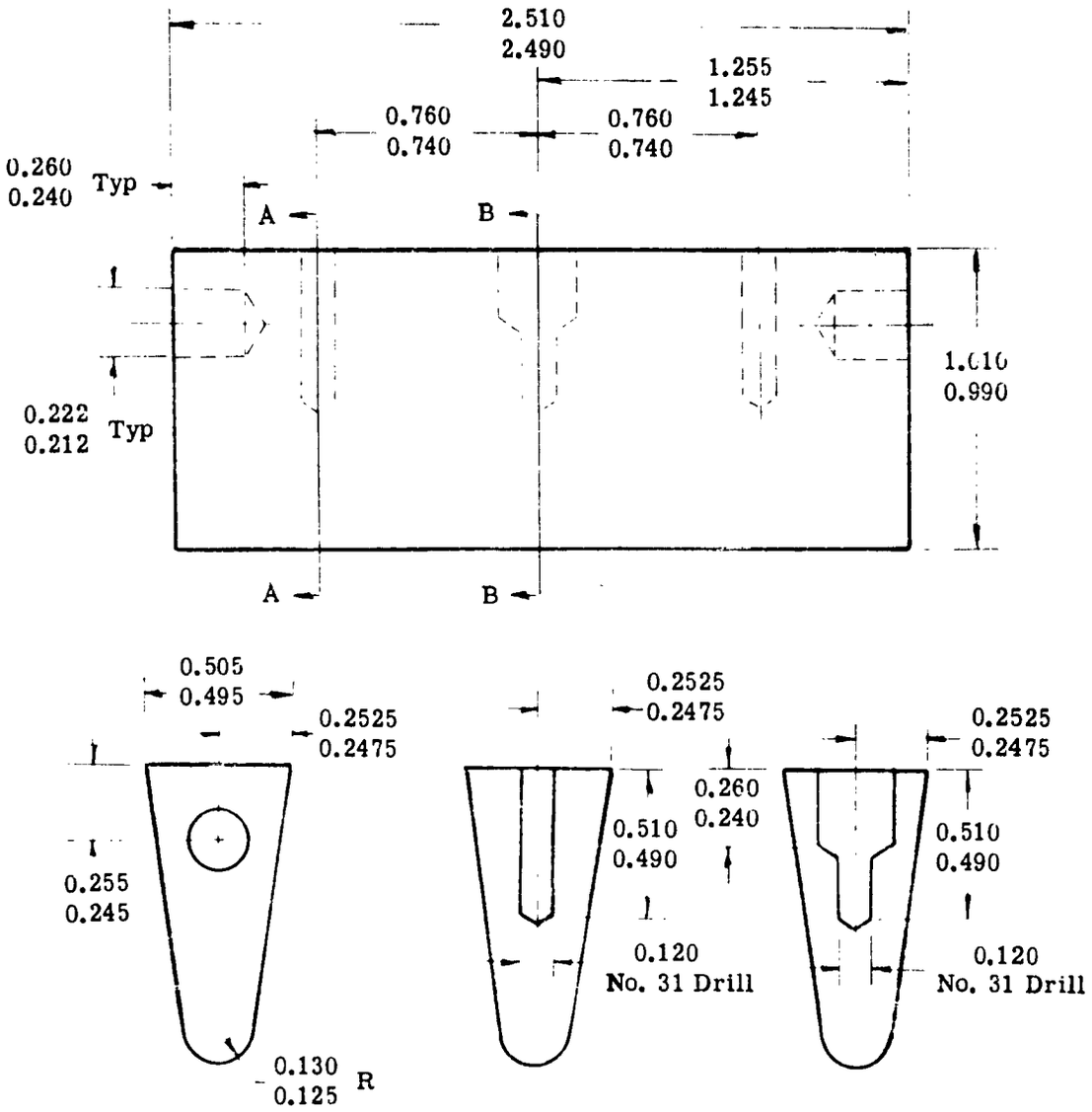

Notes: Surface Finish 63
Break all Edges and Holes
0.020-0.030

FIGURE 111. OXIDATION TEST SPECIMEN

UNCLASSIFIED

BELL AEROSYSTEMS COMPANY, Buffalo, N. Y. INVESTIGATION OF FEASIBILITY OF UTILIZING AVAILABLE HEAT RESISTANT MATERIALS FOR HYPERSONIC LEADING EDGE APPLICATIONS, Volume VII Oxidation Resistance of Bare and Coated Molybdenum Alloy and Graphite by Donald J. Powers, John A. Dickson, Joseph C. Conti and Frank M. Anthony. December 1960 (WADC TR 59-744, Volume VII)(Project Nos. 7350 & 1368; Task Nos. 73500 & 13719). (Contract No. AF 33(616)-6034.

Unclassified Report

The purpose of this contract was to investigate the feasibility of utilizing available heat resistant materials in the fabrication of leading edges for hypersonic gliders.

(over)

UNCLASSIFIED

UNCLASSIFIED

BELL AEROSYSTEMS COMPANY, Buffalo, N. Y. INVESTIGATION OF FEASIBILITY OF UTILIZING AVAILABLE HEAT RESISTANT MATERIALS FOR HYPERSONIC LEADING EDGE APPLICATIONS, Volume VII Oxidation Resistance of Bare and Coated Molybdenum Alloy and Graphite by Donald J. Powers, John A. Dickson, Joseph C. Conti and Frank M. Anthony. December 1960 (WADC TR 59-744, Volume VII)(Project Nos. 7350 & 1368; Task Nos. 73500 & 13719). (Contract No. AF 33(616)-6034.

Unclassified Report

The purpose of this contract was to investigate the feasibility of utilizing available heat resistant materials in the fabrication of leading edges for hypersonic gliders.

(over)

UNCLASSIFIED

UNCLASSIFIED

This particular volume presents the results of oxidation resistance tests of bare and coated 0.5% Ti molybdenum alloy and ATJ graphite. Chromalloy W-2 and Durak MG coatings were evaluated on the molybdenum alloy while the ATJ graphite was coated by the National Carbon Company's siliconizing process. Tests were conducted in five different facilities including three arc plasma jets. Specimen temperatures ranged from 2000°F to 3400°F. Test times ranged from approximately 1 minute to 4 hours.

UNCLASSIFIED

UNCLASSIFIED

This particular volume presents the results of oxidation resistance tests of bare and coated 0.5% Ti molybdenum alloy and ATJ graphite. Chromalloy W-2 and Durak MG coatings were evaluated on the molybdenum alloy while the ATJ graphite was coated by the National Carbon Company's siliconizing process. Tests were conducted in five different facilities including three arc plasma jets. Specimen temperatures ranged from 2000°F to 3400°F. Test times ranged from approximately 1 minute to 4 hours.

UNCLASSIFIED